Application to Food Standards Australia New Zealand
for the Inclusion of Corn MON 87429
in *Standard 1.5.2 - Food Derived from Gene Technology*

TABLE OF CONTENTS

LIST OF FIGURES

LIST OF TABLES

UNPUBLISHED REPORTS BEING SUBMITTED

Appendix 1. ██ 2018. Amended from MSL0028866: Molecular Characterization of Herbicide Tolerant Maize (MON 87429). **MSL0030619.** Monsanto Company.

Appendix 2. ███████. 2019. Amended Report for MSL0029498: Demonstration of the Presence of CP4 EPSPS, DMO, PAT and FT_T Proteins in Maize Grain Samples across Multiple Generations of MON 87429. **MSL0030646.** Monsanto Company.

Appendix 3. ████████████████████████████████ 2018 . Bioinformatics Evaluation of the Transfer DNA Insert in MON 87429 Utilizing the AD_2018, TOX_2018, and PRT_2018 Databases. **MSL0029454.** Monsanto Company.

Appendix 4. ████████████████████████████ 2018. Bioinformatics Evaluation of the DNA Sequences Flanking the 5′ and 3′ Junctions of the MON 87429 Insert: Assessment of Putative Peptides. **MSL0029453.** Monsanto Company.

Appendix 5. ██████████████████████. 2018. Amended from MSL0029565: Segregation Analysis of the T-DNA Insert in Herbicide Tolerant Maize MON 87429 Across Three Generations. **MSL0029841.** Monsanto Company.

Appendix 6. ███████████████████████ 2018. Characterization of the Dicamba Mono-Oxygenase Protein Purified from the Maize Grain of MON 87429 and Comparison of the Physicochemical and Functional Properties of the Plant-Produced and *Escherichia coli* (*E. coli*)-Produced Dicamba Mono-Oxygenase Proteins. **MSL0029510.** Monsanto Company.

Appendix 7. █████████████████████████████ 2018. Characterization of the PAT Protein Purified from the Maize Grain of MON 87429 and Comparison of the Physicochemical and Functional Properties of the Plant-Produced and *Escherichia coli* (*E. coli*)-Produced PAT Proteins. **MSL0029659.** Monsanto Company.

Appendix 8. ██████████████████████████ 2018. Amended Report for MSL0029897: Characterization of the FT_T Protein Purified from the Maize Grain of MON 87429 and Comparison of the Physicochemical and Functional Properties of the Plant-Produced and *Escherichia coli* (*E. coli*)-Produced FT_T Proteins. **MSL0030056.** Monsanto Company.

Appendix 9. ███████████████████████ 2018. Characterization of the CP4 EPSPS Protein Purified from the Maize Grain of MON 87429 and Comparison of the Physicochemical and Functional Properties of the Plant-Produced and *Escherichia coli* (*E. coli*)-Produced CP4 EPSPS Proteins. **MSL0029463.** Monsanto Company.

Appendix 10. █████████████ 2019. Amended Report for MSL0029693: Assessment of DMO, PAT (*pat*), FT_T and CP4 EPSPS Protein Levels in Maize Tissues

Collected from MON 87429 Produced in United States Field Trials During 2017. **MSL0030257.** Monsanto Company.

Appendix 11. ████████████████████████████ 2018. Bioinformatics Evaluation of the DMO and FT_T Proteins in MON 87429 Utilizing the AD_2018, TOX_2018, and PRT_2018 Databases. **MSL0029452**. Monsanto Company.

Appendix 12. ████████████████████ 2018. Bioinformatics Evaluation of the PAT Protein Utilizing the AD_2018, TOX_2018, and PRT_2018 Databases. **RAR-2018-0231**. Monsanto Company.

Appendix 13. ████████████████████████. 2018. Updated Bioinformatics Evaluation of the CP4 EPSPS Protein Utilizing the AD_2018, TOX_2018, and PRT_2018 Databases. **RAR-2018-0126**. Monsanto Company.

Appendix 14. ██████ 2018. Assessment of the *in vitro* Digestibility of *Escherichia coli*-produced Dicamba Mono-oxygenase Protein by Pepsin and Pancreatin. **MSL0029822**. Monsanto Company.

Appendix 15. ████████████████ 2019. Assessment of the *in vitro* Digestibility of Phosphinothricin N-Acetyltransferase Protein by Pepsin and Pancreatin. **MSL0030203**. Monsanto Company.

Appendix 16. █████████████ 2018. Assessment of the *in vitro* Digestibility of *Escherichia coli (E. coli)*-produced FT_T Protein by Pepsin and Pancreatin. **MSL0029802.** Monsanto Company.

Appendix 17. ████████████████████████████ ████████ 1993. Assessment of the *in vitro* Digestive Fate of CP4 EPSP Synthase. **MSL12949**. Monsanto Company.

Appendix 18. ████████████████████████████ ████████ 2002. Assessment of the *in vitro* Digestibility of Purified *E. coli*-Produced CP4 EPSPS Protein in Simulated Gastric Fluid. **MSL17566**. Monsanto Company.

Appendix 19. █████████████ 2018. The Effect of Heat Treatment on the Functional Activity of *Escherichia coli (E. coli)*-produced MON 87429 DMO Protein. **MSL0029818**.Monsanto Company.

Appendix 20. █████████ 2019. Effect of Heat Treatment on the Functional Activity of *Escherichia coli*-Produced Phosphinothricin N-acetyltransferase Protein. **SCR-2019-0110**. Monsanto Company.

Appendix 21. █████████████ 2018. The Effect of Heat Treatment on the Functional Activity of *Escherichia coli (E. coli)*-produced FT_T Protein. **MSL0029688**. Monsanto Company.

Appendix 22. ████████████████████████ 2011. Amended Report for MSL0022432: Effect of Temperature Treatment on the Functional Activity of CP4 EPSPS. **MSL0023307**. Monsanto Company.

*This report is the property of BASF.

CHECKLIST

General Requirements (3.1)	**Reference**
3.1.1 Form of application	
☑ Executive Summary	*Executive Summary*
☑ Relevant sections of Part 3 identified	
☑ Pages sequentially numbered	
☑ Electronic copy	
☑ All references available upon request	
3.1.2 Applicant details	*Page 1*
3.1.3 Purpose of the application	*Page 1*
3.1.4 Justification for the application	*Page 2*
3.1.5 Information to support the application	*Appendices 1 - 30*
3.1.6 Assessment procedure	*Page 4*
☑ General	
☐ Major	
☐ Minor	
3.1.7 Confidential Commercial Information	
☑ Confidential material separated in electronic copies	
☑ Justification provided	
3.1.8 Exclusive Capturable Commercial Benefit	*Page 4*
3.1.9 International and Other National Standards	*Page 4*
3.1.10 Statutory Declaration	*Page 238*
3.1.11 Checklist/s provided with Application	
☑ Checklist	
☑ Any other relevant checklists for Sections 3.2 – 3.7	*Checklist 3.5.1*

Foods Produced using Gene Technology (3.5.1)

ABBREVIATIONS AND DEFINITIONS[1]

2,4-D	2,4-Dichlorophenoxyacetic Acid
AA	Amino Acid
ACCase	Acetyl Coenzyme A Carboxylase
ADF	Acid Detergent Fiber
APHIS	Animal and Plant Health Inspection Service
CAB	Chlorophyll a/b-Binding
CaMV	Cauliflower Mosaic Virus
CFR	Code of Federal Regulations
COMPARE	COMprehensive Protein Allergen REsource
CP4 EPSPS	*Agrobacterium tumefaciens* strain CP4, 5-enolpyruvlshikimate-3-phosphate synthase protein
CTP	Chloroplast Transit Peptide
CTAB	Hexadecyltrimethylammonium Bromide
DCSA	3,6-Dichlorosalycilic Acid
DMO	Dicamba Mono-Oxygenase
DNA	Deoxyribonucleic Acid
dw	Dry Weight
E. coli	*Escherichia coli*
ELISA	Enzyme-linked Immunosorbent Assay
EPA	Environmental Protection Agency
E-score	Expectation Score
ETS	Excellence Through Stewardship
FA	Fatty Acid
FDA	Food and Drug Administration (U.S.)
FT_T	FOPs and 2,4-D Dioxygenase Protein
fw	Fresh Weight
GLP	Good Laboratory Practice
GRAS	Generally Recognized as Safe
HESI	Health and Environmental Sciences Institute
HPLC	High-Performance Liquid Chromatography
ILSI	International Life Sciences Institute
kb	Kilobase
LOQ	Limit of Quantitation
MOA	Mode of Action
mRNA	Messenger RNA
mts-siRNA	Male Tissue Specific Small Interfering RNA
MW	Molecular Weight
NGS	Next Generation Sequencing
OECD	Organization for Economic Co-operation and Development
ORF	Open Reading Frame
OSL	Over Season Leaf
PAT	Phosphinothricin N–Acetyltransferase
PCR	Polymerase Chain Reaction

---

[1] Alred, G.J., C.T. Brusaw, and W.E. Oliu. 2003. Handbook of Technical Writing, 7th edn., pp. 2-7. Bedford/St. Martin's, Boston, MA.

RdpA	R-2,4-Dichlorophenoxypropionate Dioxygenase
RHS	Roundup® Hybridization System
SDS-PAGE	Sodium Dodecyl Sulfate–Polyacrylamide Gel Electrophoresis
SE	Standard Error
siRNA	Small Interfering RNA
SOP	Standard Operating Procedure
USDA	United States Department of Agriculture
WT	Wildtype

PART 1   GENERAL INFORMATION

1.1   Applicant Details

(a) Applicant's name/s   ███████████, Ph.D.

(b) Company/organisation name   Monsanto Australia Proprietary Limited

(c) Address (street and postal)   Level 1, 8 Redfern Road, Hawthorn East, Victoria
3123

(d) Telephone number   ████████████

(e) Email address   ██████████████████

(f) Nature of applicant's business   Technology Provider to the Agricultural and Food
Industries

**(g) Details of other individuals,
companies or organisations
associated with the application**

1.2   Purpose of the Application

This application is submitted to Food Standards Australia New Zealand by Monsanto
Australia Proprietary Limited on behalf of Monsanto Company.

The purpose of this submission is to make an application to vary **Standard 1.5.2** – *Food
Produced Using Gene Technology* of the *Australia New Zealand Food Standards Code* to
seek the addition of maize line MON 87429 and products containing maize line MON 87429
(hereafter referred to as MON 87429) to the Table to Clause 2 (see below).

Food derived from gene technology	Special requirements
Food derived from maize line MON 87429	None

1.3   Justification for the Application

1.3(a)   The need for the proposed change

Monsanto Company has developed herbicide tolerant MON 87429 maize, which is tolerant to the herbicides dicamba, glufosinate, aryloxyphenoxypropionate (AOPP) acetyl coenzyme A carboxylase (ACCase) inhibitors (so called "FOPs" herbicides such as quizalofop) and 2,4-dichlorophenoxyacetic acid (2,4-D).   In addition, it provides tissue-specific glyphosate tolerance to facilitate the production of hybrid maize seeds.

MON 87429 contains a demethylase gene from *Stenotrophomonas maltophilia* that expresses a dicamba mono-oxygenase (DMO) protein to confer tolerance to dicamba herbicide, the phosphinothricin-N-acetyltransferase (*pat*) gene from *Streptomyces viridochromogenes* that expresses the PAT protein to confer tolerance to glufosinate herbicide and the *ft_t* gene, a modified version of the R-2,4-dichlorophenoxypropionate dioxygenase *(Rdpa)* gene from *Sphingobium herbicidovorans*, that expresses a FOPs and 2,4-D dioxygenase protein (FT_T) that confers tolerance to FOPs and 2,4-D herbicides.

MON 87429 maize also produces the 5-enolpyruvylshikimate-3-phosphate synthase protein from *Agrobacterium* sp. strain CP4 (CP4 EPSPS). MON 87429 maize utilizes an endogenous maize regulatory element to target CP4 EPSPS mRNA for degradation in tassel tissues, resulting in reduced CP4 EPSPS protein expression in pollen. Appropriately timed glyphosate applications produce a non-viable pollen phenotype and allow for desirable cross pollinations to be made in maize without using mechanical or manual detasseling methods to control self-pollination in female inbred parents.

1.3(b)   The advantages of the proposed change over the status quo, taking into account any disadvantages

MON 87429 maize will offer growers multiple choices for effective weed management including tough-to-control and herbicide-resistant broadleaf and grass weeds.   The flexibility to use combinations of any of these four herbicides representing multiple mechanisms-of-action provides an effective weed management system for maize production.   Dicamba provides effective control of over 95 annual and biennial broadleaf weed species, and suppression of over 100 perennial broadleaf and woody plant species.   Glufosinate, a broad-spectrum contact herbicide, provides effective control of approximately 70 broadleaf and 60 grass weeds. Quizalofop, a selective postemergence herbicide, provides effective control of approximately 35 annual and perennial grass weeds including glyphosate-resistant grasses. 2,4-D provides effective control of over 70 annual and biennial broadleaf weed species, and suppression of over 30 perennial broadleaf species. Additionally, dicamba, glufosinate, and 2,4-D individually or in certain combinations provide control of herbicide-resistant weeds, including glyphosate-resistant biotypes of Palmer amaranth (*Amaranthus palmeri*), marestail (*Conyza canadensis*), common ragweed (*Ambrosia artemisiifolia*), giant ragweed (*Ambrosia trifida*) and waterhemp (*Amaranthus tuberculatus*).

MON 87429 maize will likely be combined, through traditional breeding methods, with other deregulated events (e.g. glyphosate-tolerant).   MON 87429 maize combined with glyphosate-tolerant maize systems through traditional breeding will provide: 1) an

opportunity for an efficient, effective weed management system for hard-to-control and herbicide-resistant weeds; 2) a flexible system with multiple herbicide mechanisms-of-action for in-crop application in current maize production systems; 3) an opportunity to delay selection for further resistance to glyphosate and other herbicides that are important in crop production; 4) excellent crop tolerance to dicamba, glufosinate, quizalofop, 2,4-D and glyphosate; and 5) additional weed management tools to enhance weed management systems necessary to maintain or improve maize yield and quality to meet the growing needs of the food, feed, and industrial markets.

1.4   Regulatory Impact Information

1.4(a)   Costs and benefits

If the draft variation to permit the sale and use of food derived from MON 87429 is approved, possible affected parties may include consumers, industry sectors and government.   The consumers who may be affected are those that consume food containing ingredients derived from maize.   Industry sectors affected may be food importers and exporters, distributors, processors and manufacturers.   Lastly, government enforcement agencies may be affected.

A cost/benefit analysis quantified in monetary terms is difficult to determine.   In fact, most of the impacts that need to be considered cannot be assigned a dollar value.   Criteria would need to be deliberately limited to those involving broad areas such as trade, consumer information and compliance.   If the draft variation is approved:

Consumers:

- There would be benefits in the broader availability of corn products.

- There is unlikely to be any significant increase in the prices of foods if manufacturers are able to use comingled corn products.

- Consumers wishing to do so will be able to avoid GM corn products as a result of labeling requirements and marketing activities.

Government:

- Benefit that if corn MON 87429 was detected in food products, approval would ensure compliance of those products with the Code.   This would ensure no potential for trade disruption on regulatory grounds.

- Approval of corn MON 87429 would ensure no potential conflict with WTO responsibilities.

- In the case of approved GM foods, monitoring is required to ensure compliance with the labeling requirements, and in the case of GM foods that have not been approved, monitoring is required to ensure they are not illegally entering the food supply.   The costs of monitoring are thus expected to be comparable, whether a GM food is approved or not.

Industry:

- Sellers of processed foods containing corn derivatives would benefit as foods derived from corn MON 87429 would be compliant with the Code, allowing broader market access and increased choice in raw materials. Retailers may be able to offer a broader range of corn products or imported foods manufactured using corn derivatives.

- Possible cost to food industry as some food ingredients derived from corn MON 87429 would be required to be labelled

1.4(b) Impact on international trade

If the draft variation to permit the sale and use of food derived from MON 87429 was rejected it would result in the requirement for segregation of any corn derived products containing MON 87429 from those containing approved corn, which would be likely to increase the costs of imported corn derived foods.

It is important to note that if the draft variation is approved, corn MON 87429 will not have a mandatory introduction. The consumer will always have the right to choose not to use/consume this product.

1.5 Assessment Procedure

Monsanto Australia is submitting this application in anticipation that it will fall within the General Procedure category.

1.6 Exclusive Capturable Commercial Benefit

This application is likely to result in an amendment to the Code that provides exclusive benefits and therefore Monsanto intends to pay the full cost of processing the application.

1.7 International and Other National Standards

1.7(a) International standards

Monsanto makes all efforts to ensure that safety assessments are aligned, as closely as possible, with relevant international standards such as the Codex Alimentarius Commission's *Principles for the Risk Analysis of Foods Derived from Modern Biotechnology* and supporting *Guideline for the Conduct of Food Safety Assessment of Foods Derived from Recombinant-DNA Plants* (Codex Alimentarius, 2009).

In addition, the composition analysis is conducted in accordance with OECD guidelines and includes the measurement of OECD-defined corn nutrients and anti-nutrients based on conventional commercial corn varieties (OECD, 2002b).

1.7(b) Other national standards or regulations

Monsanto has submitted a food and feed safety and nutritional assessment summary for MON 87429 to the United States Food and Drug Administration (FDA) and has also requested a Determination of Nonregulated Status for MON 87429, including all progenies derived from crosses between MON 87429 and other corn, from the Animal and Plant Health Inspection Service (APHIS) of the U.S. Department of Agriculture (USDA).

Consistent with our commitments to the Excellence Through Stewardship® (ETS) Program[2], regulatory submissions have been or will be made to countries that import significant maize or food and feed products derived from U.S. maize and have functional regulatory review processes in place.

---

[2] Excellence Through Stewardship is a registered trademark of Excellence Through Stewardship, Washington, DC.   (http://www.excellencethroughstewardship.org)

PART 2 SPECIFIC DATA REQUIREMENTS FOR SAFETY ASSESSMENT

A. TECHNICAL INFORMATION ON THE GM FOOD

A1 Nature and Identity of the Genetically Modified Food

A1(a) A description of the new GM organism

MON 87429 is tolerant to the herbicides dicamba, glufosinate, aryloxyphenoxypropionate (AOPP) acetyl coenzyme A carboxylase (ACCase) inhibitors (so-called "FOPs" herbicides such as quizalofop) and 2,4-dichlorophenoxyacetic acid (2,4-D). MON 87429 contains a demethylase gene from *Stenotrophomonas maltophilia* that expresses a dicamba mono-oxygenase (DMO) protein to confer tolerance to dicamba herbicide, the phosphinothricin-N-acetyltransferase (*pat*) gene from *Streptomyces viridochromogenes* that expresses the PAT protein to confer tolerance to glufosinate herbicide and the *ft_t* gene, a modified version of the R-2,4-dichlorophenoxypropionate dioxygenase *(Rdpa)* gene from *Sphingobium herbicidovorans*, that expresses a FOPs and 2,4-D dioxygenase protein (FT_T) that confers tolerance to FOPs and 2,4-D herbicides. MON 87429 also produces the 5-enolpyruvylshikimate-3-phosphate synthase protein from *Agrobacterium* sp. strain CP4 (CP4 EPSPS) to provide maize lines with tissue specific glyphosate tolerance to facilitate the production of hybrid maize seed. MON 87429 utilizes an endogenous maize regulatory element to target CP4 EPSPS mRNA for degradation in tassel tissues, resulting in reduced CP4 EPSPS protein expression in pollen. Appropriately timed glyphosate applications produce a non-viable pollen phenotype and allow for desired cross-pollinations to be made in maize without using traditional methods to control self-pollination in female inbred parents.

MON 87429 maize will offer growers multiple choices for effective weed management including tough-to-control and herbicide-resistant broadleaf and grass weeds. The flexibility to use combinations of any of these four herbicides representing multiple mechanisms-of-action provides an effective weed management system for maize production. Dicamba provides effective control of over 95 annual and biennial broadleaf weed species, and suppression of over 100 perennial broadleaf and woody plant species. Glufosinate, a broad-spectrum contact herbicide, provides effective control of approximately 70 broadleaf and 60 grass weeds. Quizalofop, a selective postemergence herbicide, provides effective control of approximately 35 annual and perennial grass weeds including glyphosate-resistant grasses. 2,4-D provides effective control of over 70 annual and biennial broadleaf weed species, and suppression of over 30 perennial broadleaf species. Additionally, dicamba, glufosinate, and 2,4-D herbicides individually or in certain combination, provide control of herbicide-resistant weeds, including glyphosate-resistant biotypes of Palmer amaranth (*Amaranthus palmeri*), marestail (*Conyza canadensis*), common ragweed (*Ambrosia artemisiifolia*), giant ragweed (*Ambrosia trifida*) and waterhemp (*Amaranthus tuberculatus*).

MON 87429 maize will likely be combined, through traditional breeding methods, with other deregulated events (e.g. glyphosate tolerant events for whole plant tolerance and insect protected traits). MON 87429 maize combined with glyphosate-tolerant maize systems through traditional breeding will provide: 1) an opportunity for an efficient, effective weed management system for hard-to-control and herbicide-resistant weeds; 2) a flexible system with multiple herbicide mechanisms-of-action for in-crop application in current maize

production systems; 3) an opportunity to delay selection for further resistance to glyphosate and other herbicides that are important in crop production; 4) excellent crop tolerance to dicamba, glufosinate, quizalofop, 2,4-D and glyphosate; and 5) additional weed management tools to enhance weed management systems necessary to maintain or improve maize yield and quality to meet the growing needs of the food, feed, and industrial markets. MON 87429 maize also allows inbreds to be treated with glyphosate (between V8 to V13), in place of detasseling, providing flexibility to hybrid maize seed producers as well as reducing the cost of hybrid seed production by removing the reliance on costly, labor intensive manual/mechanical detasseling.

MON 87429 Roundup® Hybridization System (RHS) Mechanism of Action

Expression of CP4 EPSPS in MON 87429 plants is driven by the *CaMV 35S* promoter, a known constitutive promoter (Holtorf *et al.*, 1995; Terada and Shimamoto, 1990). In maize and other monocot plants, *CaMV 35S* has been shown to drive weak gene expression in pollen tissue (Hamilton *et al.*, 1992; Heck *et al.*, 2005). Additionally, MON 87429 maize utilizes an endogenous maize regulatory element to target CP4 EPSPS mRNA for degradation specifically in tassel tissues, resulting in reduced CP4 EPSPS protein expression in pollen.

RNA interference (RNAi) is a natural process in eukaryotic organisms for the regulation of endogenous gene expression (Fire *et al.*, 1998; Jones-Rhoades *et al.*, 2006). Both microRNAs (miRNAs) and small interfering RNAs (siRNAs) can trigger RNAi (Carthew and Sontheimer, 2009). Endogenous maize male tissue specific small interfering RNAs (mts-siRNA) described in Yang *et al.* (2018), are expected to be involved in regulation of endogenous gene expression in male tissue such as the tassel. MON 87429 takes advantage of endogenous mts-siRNAs to degrade the CP4 EPSPS mRNA in male tissue. MON 87429 CP4 EPSPS mRNA contains a 201 bp siRNA Target Sequence in the 3' UTR (Figure 1) which is recognized by the mts-siRNAs resulting in degradation of the CP4 EPSPS mRNA, and reduced expression of CP4 EPSPS protein in male tissue.
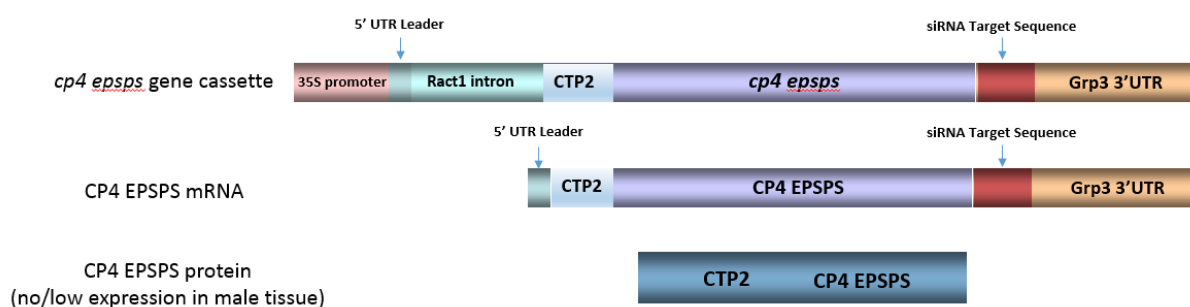
Figure 1.   Schematic Diagram of *cp4 epsps* Gene Cassette, CP4 EPSPS mRNA and CP4 EPSPS Protein

(Note: DNA, RNA and polypeptide lengths cannot be equated; this image is not drawn to scale).

The identification, cloning and testing of the 201 bp siRNA Target Sequence in MON 87429 is described in detail in Yang *et al.* (2018).   The process is summarized as follows: 1) Identification of male tissue specific small interfering RNAs (mts-siRNA) primarily expressed in tassel, 2) Identification of Target Sequences corresponding to these endogenous mts-siRNAs present in maize, 3) Identification and selection of the target gene, EU974548, based on the 3' UTR region of this gene contains clustered, overlapping alignments of multiple siRNA Target Sequences, 4) Confirmation that the endogenous target, EU974548, is conserved across a wide range of maize germplasms, 5) Selection of the 201 bp siRNA Target Sequence, derived from EU974548, based on the intended non-viable pollen phenotype under glyphosate treatment.

The model representing the mechanism of action by which mts-siRNAs trigger degradation of the CP4 EPSPS mRNA in MON 87429 tassel tissue is summarized below and shown in Figure 2.   The first five steps represent the endogenous mts-siRNA pathway in conventional maize, based on current knowledge of siRNA driven RNAi systems (Gorski *et al.*, 2017):

- Step 1: mts-siRNA precursor(s) RNA is produced from endogenous mts-siRNA gene.
- Step 2: The mts-siRNA precursor RNA is cleaved by the Dicer (DCL4) complex to produce mts-siRNAs.
- Step 3: Independently, endogenous target genes are transcribed that contain siRNA Target Sequences (shown as red line in the endogenous target gene double helix).
- Step 4: The resulting mts-siRNA molecules, from step 2, are then incorporated into multiprotein RNA-induced silencing complexes (RISC), which facilitate siRNA Target Sequence recognition and mRNA cleavage which leads to specific suppression of the target mRNA.
- Step 5: It is expected that endogenous mRNAs containing siRNA Target Sequences are cleaved by the RISC complex and then subjected to further degradation by 3'-5' and 5'-3' exoribonucleases due to the lack of a 3' poly adenine

tail or a 5' cap structure at the cleavage site, inhibiting mRNA translation into protein.

The following three steps occur only in MON 87429 male tassel tissue as MON 87429 uses the endogenous siRNA machinery to specifically target CP4 EPSPS mRNA for degradation:

- Step 6: Upon CP4 EPSPS mRNA transcription, endogenous mts-siRNAs trigger cleavage of CP4 EPSPS mRNA via recognition of the 201bp siRNA Target Sequence in the 3' UTR of the CP4 EPSPS mRNA.
- Step 7: The CP4 EPSPS mRNA cleavage products are then subjected to degradation by 3'-5' and 5'-3' exoribonucleases due to the lack of a 3' poly adenine tail or a 5' cap structure at the cleavage site.
- Step 8: As a result of above processes, translation of the CP4 EPSPS mRNA into protein is reduced. Thus, little to no CP4 EPSPS protein is expressed in male tissue resulting in glyphosate sensitivity.

The same CP4 EPSPS mRNA is expressed throughout MON 87429 maize tissue (e.g., root, leaf, ear and tassel), however due to the male tissue specific expression of the mtssiRNAs, the CP4 EPSPS mRNA is only targeted for degradation in tassel tissue resulting in little to no expression of CP4 EPSPS protein in pollen (Please see Section B3(e)).
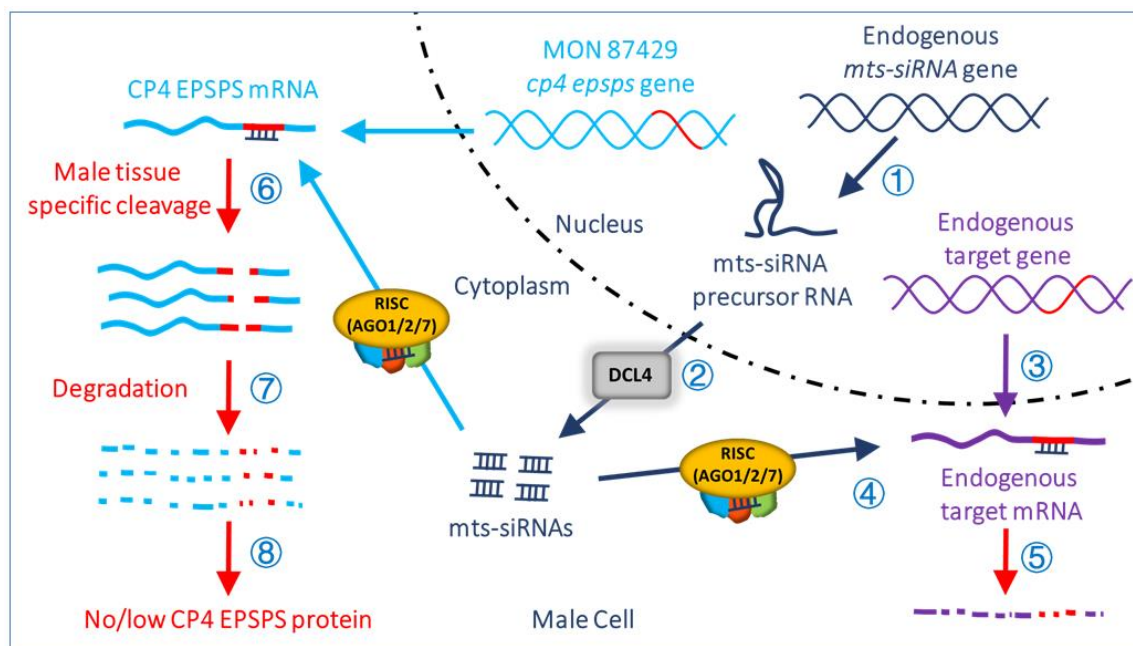
Figure 2.   MON 87429 CP4 EPSPS siRNA Target Sequence Molecular Mechanism of Action

A1(b)   Name, number or other identifier of each new line or strain

In accordance with OECD's "Guidance for the Designation of a Unique Identifier for Transgenic Plants" MON 87429 has been assigned the unique identifier MON-87429-9.

A1(c)   The name the food will be marketed under (if known)

Maize containing the transformation event MON 87429 will be produced in North America. There are currently no plans to produce this product in Australia and New Zealand.   A commercial trade name for the product has not been determined at the time of this submission and will be available prior to commercial launch of the product in North America.

A1(d)   The types of products likely to include the food or food ingredient

Maize is widely used for a variety of food and feed purposes, and it is intended that MON 87429 will be utilized in the same manner and for the same uses as conventional maize.   Maize grain and its processed products are consumed in a multitude of human food and animal feed products.   Maize forage (as silage) is extensively consumed as an animal feed by ruminants.

A2   History of Use of the Host and Donor Organisms

A2(a)   Description of all donor organism(s)

A2(a)(i)   Common and scientific names and taxonomic classification

The *dmo* gene is derived from the bacterium *S. maltophilia* strain DI-6, isolated from soil at a dicamba manufacturing plant (Krueger *et al.*, 1989).   *S. maltophilia* was originally named *Pseudomonas maltophilia*, and then transferred to the genus *Xanthomonas* before it was given its own genus (Palleroni and Bradbury, 1993).   The taxonomy of *S. maltophilia* is (Palleroni and Bradbury, 1993; Ryan *et al.*, 2009):

> Kingdom: Bacteria
>
> Phylum: Proteobacteria
>
> Class: Gammaproteobacteria
>
> Order: Xanthomonadales
>
> Family: Xanthomonadaceae
>
> Genus: *Stenotrophomonas*

The *pat* gene is derived from the bacterium *S. viridochromogenes* .   The taxonomy of *S. viridochromogenes* is (Waksman and Henrici, 1943):

> Kingdom: Bacteria
>
> Phylum: Actinobacteria
>
> Class: Actinobacteria
>
> Order: Actinomycetales
>
> Family: Streptomycetaceae
>
> Genus: *Streptomyces*

MON 87429 contains the *ft_t* gene, a modified version of the *Rdpa* gene from *Sphingobium herbicidovorans*, that expresses the FT_T protein. FT_T is a modified version of the R-2,4-dichlorophenoxypropionate dioxygenase (RdpA) protein (Müller *et al.*, 2006). *S. herbicidovorans* is a common gram-negative, rod-shaped, non-motile, non-spore-forming soil bacterium (Takeuchi *et al.*, 2001; Zipper *et al.*, 1996), which is strictly aerobic and chemo-organotrophic, and not known to be associated with human disease. The taxonomy of *S. herbicidovorans* is:

> Kingdom: Bacteria
>
> Phylum: Proteobacteria
>
> Class: Alphaproteobacteria
>
> Order: Sphingomonadales
>
> Family: Sphingomonadaceae
>
> Genus: *Sphingobium*

The donor organism for *cp4 epsps* is *Agrobacterium* sp. strain CP4 (Padgette *et al.*, 1996). *Agrobacterium* species are not known for human or animal pathogenicity and are not commonly allergenic (FAO-WHO, 1991; Mehrotra and Goyal, 2012; Nester, 2015). The taxonomy of *Agrobacterium* sp is:

> Kingdom: Bacteria
>
> Phylum: Proteobacteria
>
> Class: Alphaproteobacteria
>
> Order: Rhizobiales
>
> Family: Rhizobiaceae
>
> Genus: *Agrobacterium*

A2(a)(ii)   Information on pathogenicity, toxicity, allergenicity

dmo gene

S. maltophilia is an aerobic, environmentally ubiquitous, gram-negative bacterium commonly present in aquatic environments, soil and plants. *S. maltophilia* is ubiquitously associated with plants and has been isolated from the rhizosphere of wheat, maize, grasses, beet, cucumber, potato, strawberry, sugarcane, and rapeseed (Berg *et al.*, 1996; Berg *et al.*, 1999; Berg *et al.*, 2002; Denton *et al.*, 1998; Echemendia, 2010; Juhnke and des Jardin, 1989; Juhnke *et al.*, 1987; Lambert *et al.*, 1987). *S. maltophilia* has also been isolated from cottonseed, bean pods, and coffee (Nunes and de Melo, 2006; Swings *et al.*, 1983); thus, *S. maltophilia* can be found in a variety of foods and feeds. *S. maltophilia* is also widespread in the home environment and can be found around sponges, flowers, plants, fruits, vegetables, frozen fish, milk and poultry (Berg *et al.*, 1999; Denton and Kerr, 1998; Echemendia, 2010). Strains of *S. maltophilia* have been found in the transient flora of hospitalized patients as a commensal organism (Echemendia, 2010). *S. maltophilia* can be found in healthy individuals without causing any harm to human health (Denton *et al.*, 1998) and infections in humans caused by *S. maltophilia* are extremely uncommon (Cunha, 2009). Similar to the indigenous bacteria of the gastrointestinal tract, *S. maltophilia* can be an opportunistic pathogen (Berg, 1996).   As such, *S. maltophilia* is of low virulence in immuno-compromised patients where a series of risk factors (severe debilitation, the presence of indwelling devices such as ventilator tubes or catheters, for prolonged periods of time and prolonged courses of antibiotics) must occur for colonization by *S. maltophilia* in humans (Ryan *et al.*, 2009). Therefore, infections by *S. maltophilia* almost exclusively occur in hospital settings, in which case they are only present in a minimal percentage of infections (Ryan *et al.*, 2009).   Finally, *S. maltophilia* has not been reported to be a source of allergens.

pat gene

S. viridochromogenes is a saprophytic, soil-borne bacterium with no known safety issues. *Streptomyces* species are widespread in the environment and present no known allergenic or toxicity issues (Kämpfer, 2006; Kutzner, 1981), though human exposure is quite common (Goodfellow and Williams, 1983). *S. viridochromogenes* is not considered pathogenic to

plants, humans or other animals (Cross, 1989; Goodfellow and Williams, 1983; Locci, 1989). *S. viridochromogenes* history of safe use is discussed in Hérouet *et al*., (2005) and this organism has been extensively reviewed during the evaluation of several glufosinate-tolerant events with no safety or allergenicity issues identified by FDA or other regulatory agencies.

ft_t gene

Members of the *Sphingobium* have been isolated from a wide variety of habitats including soil and freshwater (Chaudhary *et al.*, 2017). *Sphingobium* species have also been isolated from food products such as corn (Rijavec *et al.*, 2007), papaya (Thomas *et al.*, 2007) and tomato (Enya *et al.*, 2007). The biosythesis and biodegrading properties of this genus have been exploited in the food industry (Fialho *et al.*, 2008; Pozo *et al.*, 2007), bioremediation (Alarcón *et al.*, 2008; Jin *et al.*, 2013), and biofuel industry (Varman *et al.*, 2016). The ubiquitous presence of *Sphingobium* species in the environment has resulted in widespread human and animal exposure without any known adverse safety or allergenicity reports.

cp4 epsps gene

The donor organism for *cp4 epsps* is *Agrobacterium* sp. strain CP4 (Padgette *et al.*, 1996). *Agrobacterium* species are not known for human or animal pathogenicity and are not commonly allergenic (FAO-WHO, 1991; Mehrotra and Goyal, 2012; Nester, 2015). The history of safe use of the CP4 EPSPS protein from *Agrobacterium* sp. strain CP4 has been previously reviewed regarding Roundup Ready® events of soybean, canola , maize, sugar beet, alfalfa, and cotton.

A2(a)(iii)   History of use of the organism in food supply or human exposure

The ubiquitous presence of *S. maltophilia* in the environment, the presence in healthy individuals without any harm to human health, the incidental presence in foods without any adverse safety reports, and the lack of reported allergenicity establish the safety of the donor organism.

The ubiquitous presence of *S. viridochromogenes* in the environment, the widespread human exposure without any adverse safety or allergenicity reports, and the successive reviews of several glufosinate-tolerant events by regulators that have not identified particular safety or allergenicity issues further establishes the safety of the donor organism.

The ubiquitous presence of *Sphingobium* species in the environment has resulted in widespread human and animal exposure without any known adverse safety or allergenicity reports.

The history of safe use of the CP4 EPSPS protein from *Agrobacterium* sp. strain CP4 has been previously reviewed regarding Roundup Ready® events of soybean, canola , maize, sugar beet, alfalfa, and cotton.

A2(b)   Description of the host organism

A2(b)(i)   Phenotypic information

Maize (*Zea mays* L.) is a member of the genus *Zea* within the tribe Maydeae, which is included in the subfamily Panicoideae of the grass family Poaceae. The following taxonomic information is condensed from OECD (2003).

Family: Poaceae
Subfamily: Panicoideae
Tribe: Maydeae
Genus *Zea*
Section *ZEA*
       Zea mays L. (maize)
       Zea mays subsp. *mays* (L.) (maize, 2n = 20)
       Zea mays subsp. *mexicana* (Schrader) (teosinte, 2n = 20)
       Zea mays subsp. *parviglumis* (teosinte, 2n = 20)
Section *LUXURIANTES*
       Zea diploperennis (perennial teosinte, 2n = 20)
       Zea luxurians (Durieu) (teosinte, 2n = 20)
       Zea nicaraguensis (2n = 20?)
       Zea perennis (Hitchc.) (2n = 40)

The genera included in the tribe Maydeae include *Zea* and *Tripsacum* in the Western Hemisphere, and *Coix*, *Chionachne*, *Polytoca*, *Schlerachne*, and *Trilobachne* in Asia or Australia (OECD, 2003; Russell and Hallauer, 1980).

As reviewed by OECD (2003), maize may be considered a subspecies of *Zea mays* L., with annual teosintes forming additional subspecies.   However, until recently, the teosinte species were included in the genus *Euchlaena* rather than the genus *Zea* (Goodman, 1988).

Maize has been a staple of the human diet for centuries, and its processed fractions are consumed in a multitude of food and animal feed products. For the 2016/2017 market year, values for U.S. domestic maize usage were 37% for feed and residual uses; 37% for alcohol for fuel; 10% for food, seed, and industrial uses other than alcohol for fuel; and 16% for exports (Capehart *et al.*, 2019). Global demand for maize has increased due to greater meat consumption in emerging economic countries including China, and biofuels production (Edgerton, 2009).

Food uses of maize include processed products from field maize and direct consumption of sweet maize and popcorn. Food products derived from the wet milling process include starch and sweetener products (e.g. high fructose maize syrup) (May, 1987). Food products derived from the dry milling process include maize grits, maize meal, and maize flour (Watson, 1988). Maize oil may be derived from either milling process (Watson, 1988).

Maize is used extensively as a livestock feed for reasons that include its palatability, digestibility, and metabolizable energy (Loy and Lundy, 2019) and its relatively low cost (OECD, 2002b). Maize grain may be fed whole (Watson, 1988), but in many cases it is

ground and mixed with other ingredients to provide a balanced ration (Leath and Hill, 1987). As reviewed by Loy and Lundy (2019), animal feed products from the wet milling process include maize gluten feed and maize gluten meal. Animal feed products from the dry milling process include hominy feed (Loy and Lundy, 2019). Ethanol production from dry milled maize provides distillers grains, another source of animal feed (Loy and Lundy, 2019). Maize can also be fed as a whole plant silage.

A2(b)(ii)   How the organism is propagated for food use

Maize is a wind pollinated species with plant morphology that facilitates relatively high levels of cross pollination at short distances. Agitation of the anthers by wind encourages release of pollen (Kiesselbach, 1949), and the physical separation of the tassel and the ear allows wind to move pollen toward other plants as it settles through the air to the level of the silks. Outcrossing at short distances is not limited by the time that pollen and silks remain viable. As reviewed by OGTR (2008), pollen released from the tassel may be viable for approximately 20 minutes to 24 hours depending on environmental conditions. Bassetti and Westgate (1994) found evidence that unpollinated silks were viable for five days following first silk emergence. These factors, combined with close proximity of plants in maize fields, may contribute to the high outcrossing rates in maize. Poehlman and Sleper (1995) indicate that typical outcrossing rates are 95%.

In older hybrids and varieties, it was common for individual plants to initiate pollen shed before silking. This pattern further favors outcrossing (Galinat, 1988), especially if the interval between pollen shed and silking is large. However, breeders have selected for a reduced interval between pollen shed and silking in more recent maize hybrids (Duvick, 2005).

A2(b)(iii)   What part of the organism is used for food

Maize has been a staple of the human diet for centuries, and its processed fractions are consumed in a multitude of food and animal feed products. For the 2016/2017 market year, values for U.S. domestic maize usage were 37% for feed and residual uses; 37% for alcohol for fuel; 10% for food, seed, and industrial uses other than alcohol for fuel; and 16% for exports (Capehart *et al.*, 2019). Global demand for maize has increased due to greater meat consumption in emerging economic countries, including China, and biofuels production (Edgerton, 2009).

Food uses of maize include processed products from field maize and direct consumption of sweet maize and popcorn. Food products derived from the wet milling process include starch and sweetener products (e.g. high fructose maize syrup) (May, 1987). Food products derived from the dry milling process include maize grits, maize meal, and maize flour (Watson, 1988). Maize oil may be derived from either milling process (Watson, 1988).

Maize is used extensively as a livestock feed for reasons that include its palatability, digestibility, and metabolizable energy (Loy and Lundy, 2019) and its relatively low cost (OECD, 2002b). Maize grain may be fed whole (Watson, 1988), but in many cases it is ground and mixed with other ingredients to provide a balanced ration (Leath and Hill, 1987).

As reviewed by (Loy and Lundy, 2019), animal feed products from the wet milling process include maize gluten feed and maize gluten meal. Animal feed products from the dry milling process include hominy feed (Loy and Lundy, 2019). Ethanol production from dry milled maize provides distillers grains, another source of animal feed (Loy and Lundy, 2019). Maize can also be fed as a whole plant silage.

A2(b)(iv)   Whether special processing is required to render food safe to eat

Food uses of maize include processed products from field maize and direct consumption of sweet maize and popcorn. Maize grain processing has been reviewed by Watson (1988). On a dry weight basis, the main components of maize kernels are endosperm (83%), germ (11%), and pericarp (bran) (5%) (Watson, 1988). Milling separates the grain into these components, with subsequent products dependent on the milling type (Watson, 1988).

Products from wet milling: As reviewed by (Rausch *et al.*, 2019), the products of the wet milling include starch and sweeteners used in foodstuffs. Native or modified maize starch is used in a wide range of foods, including bakery products, puddings and custards, snack foods, salad dressings, meat products, prepared soups, and many others (Rausch *et al.*, 2019). Starch is also converted into a variety of sweetener products including high fructose maize syrup (Watson, 1988). The various sweeteners are also used in a wide range of foods, including bakery products, breakfast foods, desserts, prepared soups, canned fruits and juices and many others (Rausch *et al.*, 2019). In addition to starch and sweeteners, oil is obtained from the germ fraction that is separated during the wet milling process (Rausch *et al.*, 2019).

Products from dry milling: The products of the dry milling process include maize grits, maize meal, and maize flours, each of which is derived from the endosperm (Watson, 1988). The food uses of these products have been reviewed by (Rooney and Serna-Saldivar, 2003). Maize grits have the largest particles and have less than 1% oil content (Rooney and Serna-Saldivar, 2003). Grits are used in making breakfast cereals and snacks (Rooney and Serna-Saldivar, 2003), and are eaten in the U.S. as side dish (Watson, 1988). Maize meal has smaller particles than maize grits (Rooney and Serna-Saldivar, 2003). It is used in baked products like maize bread and muffins, and may be enriched with vitamins and minerals like thiamine, riboflavin, niacin, and iron (Rooney and Serna-Saldivar, 2003). Maize flour is made up of fine endosperm particles and has many uses as a food ingredient (e.g. in ready to eat snacks or pancake mixes) or binder (e.g. in processed meats) (Rooney and Serna-Saldivar, 2003). In addition to endosperm products, oil is obtained from the germ faction that is separated during the dry milling process (Watson, 1988).

Products from fermentation: Products from the wet and dry milling processes (e.g. corn syrups, grits) can also be used in producing distilled beverages through fermentation (Rooney and Serna-Saldivar, 2003; Watson, 1988).

A2(b)(v)   The significance to the diet in Australia and New Zealand of the host organism

Maize has been a staple of the human diet for centuries, and its processed fractions are consumed in a multitude of food. Estimates of maize consumption are available from the

WHO Global Environmental Monitoring System - Food Contamination Monitoring and Assessment Programme (GEMS/Food) (www.who.int/foodsafety/chem/gems). The GEMS/Food programme has developed 13 Cluster Diets which are considered to be representative of the major food consumption patterns exhibited by regional and cultural groups around the world. Australia is included in Cluster M, along with United States and Canada and several other countries.

A3   The Nature of the Genetic Modification

A3(a)   Method used to transform host organism

For details, please refer to ████████████, 2018 (MSL0030619).

MON 87429 was developed through *Agrobacterium tumefaciens* mediated transformation of immature maize embryos based on the method described by (Sidorov and Duncan, 2009) utilizing PV-ZMHT519224.   Immature embryos were excised from a post-pollinated maize ear of LH244.   After co-culturing the excised immature embryos with *Agrobacterium* carrying the plasmid vector, the immature embryos were placed on selection medium containing glyphosate and carbenicillin disodium salt in order to inhibit the growth of untransformed plant cells and excess *Agrobacterium*, respectively.   Once transformed callus developed, the callus was placed on media conducive to shoot and root development.   The rooted plants (R0) with normal phenotypic characteristics were selected and transferred to soil for growth and further assessment.

The R0 plants generated through the transformation process described above had already been exposed to glyphosate in the selection medium and demonstrated glyphosate tolerance. The R0 plants were self-pollinated to produce R1 seed.   Subsequently, the R1 population was screened for the presence of T-DNA and absence of vector backbone sequences by construct-level PCR assay and Southern blot analysis.   Only plants that were homozygous positive for T-DNA and negative for vector backbone were selected for further development and their progenies were subjected to further molecular and phenotypic assessments.   As is typical of a commercial event production and selection process, hundreds of different transformation events (regenerants) were generated in the laboratory using PV-ZMHT519224. After careful selection and evaluation of these events in the laboratory, greenhouse and field, MON 87429 was selected as the lead event based on superior trait efficacy, agronomic, phenotypic, and molecular characteristics (Prado *et al.*, 2014).   Studies on MON 87429 were initiated to further characterise the genetic insertion and the expressed product, and to establish the food, feed, and environmental safety relative to conventional maize.   The major steps involved in the development of MON 87429 are depicted in Figure 3.   The result of this process was the production of MON 87429 maize with the *pat, dmo, ft_t* and *cp4 epsps* expression cassettes.

Assembled *Agrobacterium* binary plasmid vector PV-ZMHT519224 and transferred to *Agrobacterium tumefaciens* strain ABI

↓

Transformed LH244 (a maize line for more efficient transformation) immature embryos with PV-ZMHT519224 in *Agrobacterium tumefaciens*

↓

Selected transformants containing the selectable marker (*cp4 epsps* expression cassette) and generated rooted shoots from the transformed callus tissues

↓

Evaluated by PCR and selected the transformed plants for the homozygous presence of the T-DNA

↓

Evaluated plants for insert integrity using molecular analyses

↓

Identified MON 87429 as lead event and further evaluated its progeny in laboratory and field assessments for T-DNA insert integrity, dicamba-, glufosinate-, quizalofop-, 2,4-D-, and tissue-specific glyphosate-tolerance, absence of all other vector DNA, and superior agronomic/phenotypic characteristics

Figure 3.   Schematic of the Development of MON 87429

A3(b)   Intermediate hosts (*e.g.* bacteria)

A disarmed strain of *Agrobacterium tumefaciens* was the intermediate host used to transfer the plasmid PV-ZMHT519224 into maize cells.   PV-ZMHT519224 contains one T-DNA containing the *dmo, pat, ft_t and cp4 epsps* expression cassettes.   Following transformation, self-pollination, breeding, and segregation methods were used to produce MON 87429.

A3(c)   Gene construct including size, source and function of all elements

A3(c)(i)   The size, source and function of all the genetic components including marker genes, regulatory and other elements

MON 87429 was developed through *Agrobacterium tumefaciens*-mediated transformation of maize immature embryos from line LH244 utilizing PV-ZMHT519224.

PV-ZMHT519224

Plasmid vector PV-ZMHT519224 was used in the transformation of maize to produce MON 87429 and its plasmid map is shown in Figure 8.   A detailed description of the genetic elements and their prefixes (e.g, B, P, L, I, TS, CS, T, and OR) in PVZMHT519224 is provided in Table 1.   Plasmid vector PV-ZMHT519224 is approximately 17.8 kb in length and contains a single T-DNA that is delineated by Right and Left Border regions.   The T-DNA contains the *pat*, *dmo*, *ft_t*, and *cp4 epsps* expression cassettes.   During transformation, the T-DNA was inserted into the maize genome. Following transformation, traditional breeding, segregation, selection and screening were used to isolate those plants that contained the *pat*, *dmo*, *ft_t*, and *cp4 epsps* expression cassettes and did not contain the backbone sequences.

The *pat* expression cassette contains the following genetic elements: promoter, 5' UTR, and intron sequences for a ubiquitin gene (*Ubq*) from *Erianthus ravennae* (plume grass), and the 3' UTR sequence of the *fructose-bisphosphate aldolase* (*Fba*) gene from *Setaria italica* (foxtail millet). The *dmo* expression cassette contains the following genetic elements: Promoter, 5' UTR, and intron sequences for a ubiquitin gene (*Ubq*) from *Coix lacryma-jobi* (adlay millet), chloroplast-targeting sequence of the *Albino and pale green 6* (*Apg6)* gene from *Arabidopsis thaliana*, and the 3' UTR sequence of the *OsMt* gene from *Oryza sativa* (rice).   The *ft_t* expression cassette contains the following genetic elements: promoter, 5' UTR, and intron sequences for a *ubiquitin* gene (*Ubq*) from *Arundo donax* (giant reed), chloroplast-targeting sequence from *Arabidopsis thaliana Mdh* gene, and the 3' UTR sequence from the gene coding for a no apical meristem (*Nam*) protein domain from *Oryza sativa* (rice).   The *cp4 epsps* expression cassette contains the following genetic elements: promoter and leader sequence from the 35S RNA of cauliflower mosaic virus (CaMV), 5' UTR leader sequence from the gene coding for chlorophyll a/b-binding (*CAB*) protein of *Triticum aestivum* (wheat), intron and flanking UTR sequence of the *act1* gene from *Oryza sativa* (rice), chloroplast-targeting sequence of the *ShkG* gene from *Arabidopsis thaliana*, 3' UTR sequence of *Zea mays* cDNA (Genbank Accession: EU974548) that contains male tissue specific siRNA target sequence, and 3' UTR sequence of the glycine-rich RNA binding protein (*Grp3*) gene from *Oryza sativa* (rice).

The backbone region of PV-ZMHT519224 contains two origins of replication for maintenance of the plasmid vector in bacteria (*ori V, ori pBR322*), and a bacterial selectable marker gene (*aadA*).

The *pat* Coding Sequence and PAT Protein

The *pat* expression cassette contains the *pat* gene encoding a protein of 183 amino acids. MON 87429 expresses a 25.5 kDa PAT protein, which consists of a single polypeptide of 182 amino acids after the removal of the lead methionine that is cleaved during a co-translational process in MON 87429 (Figure 4) (Wehrmann *et al.*, 1996; Wohlleben *et al.*, 1988). The *pat* open reading frame in the expression cassette includes sequence from *S. viridochromogenes* that encodes the PAT protein. The expression of PAT protein confers glufosinate tolerance.

PAT

1   MSPERRPVEI RPATAADMAA VCDIVNHYIE TSTVNFRTEP QTPQEWIDDL

51   ERLQDRYPWL VAEVEGVVAG IAYAGPWKAR NAYDWTVEST VYVSHRHQRL

101   GLGSTLYTHL LKSMEAQGFK SVVAVIGLPN DPSVRLHEAL GYTARGTLRA

151   AGYKHGGWHD VGFWQRDFEL PAPPRPVRPV TQI

Figure 4.   Deduced Amino Acid Sequence of the PAT Protein

The amino acid sequence of the MON 87429 PAT protein was deduced from the full-length coding nucleotide sequence present in PV-ZMHT519224 (see Table 1 for more detail). The lead methionine (boxed with solid line) of the PAT protein produced in MON 87429 is cleaved during a co-translational process in MON 87429.

The *dmo* Coding Sequence and the DMO Protein

The *dmo* expression cassette contains the *dmo* gene encoding a precursor protein of 408 amino acids (340 amino acids encoded by the *dmo* gene and 68 amino acids encoded by the *APG6* gene for targeting the DMO protein into chloroplasts). MON 87429 expresses two forms of mature DMO protein due to alternative processing of the chloroplast transit peptide (CTP) (Figure 5). One form consists of 341 amino acids, which includes 340 amino acids encoded by the *dmo* gene and 1 amino acid (cysteine) encoded by the *APG6* gene. The other form of the DMO protein consists of 340 amino acids encoded by the *dmo* gene. The two forms of mature DMO protein expressed in MON 87429 are indistinguishable by Coomassie stain of SDS-PAGE and Western blot analysis because the difference in molecular weight between these two forms is very small. Therefore, only a ~38.4 kDa DMO protein band is observed by Coomassie stain of SDS-PAGE and Western blot analysis. The *dmo* open reading frame in the expression cassette includes a codon optimized sequence from *S. maltophilia* that encodes the DMO protein (Herman *et al.*, 2005; Wang *et al.*, 1997). The expression of the DMO protein confers tolerance to dicamba herbicide.

```
DMO

1     MATATTTATA AFSGVVSVGT ETRRIYSFSH LQPSAAFPAK PSSFKSLKLK

51    QSARLTRRLD HRPFVVRCML TFVRNAWYVA ALPEELSEKP LGRTILDTPL

101   ALYRQPDGVV AALLDICPHR FAPLSDGILV NGHLQCPYHG LEFDGGGQCV

151   HNPHGNGARP ASLNVRSFPV VERDALIWIW PGDPALADPG AIPDFGCRVD

201   PAYRTVGGYG HVDCNYKLLV DNLMDLGHAQ YVHRANAQTD AFDRLEREVI

251   VGDGEIQALM KIPGGTPSVL MAKFLRGANT PVDAWNDIRW NKVSAMLNFI

301   AVAPEGTPKE QSIHSRGTHI LTPETEASCH YFFGSSRNFG IDDPEMDGVL

351   RSWQAQALVK EDKVVVEAIE RRRAYVEANG IRPAMLSCDE AAVRVSREIE

401   KLEQLEAA
```

Figure 5. Deduced Amino Acid Sequence of APG6 Chloroplast Targeting Sequence and the DMO Protein

The amino acid sequence of the MON 87429 DMO precursor protein was deduced from the full-length coding nucleotide sequence present in PV-ZMHT519224 (See Table 1 for more detail). The first 68 amino acids of the precursor protein (underlined) are the CTP from *APG6* gene. The CTP targets MON 87429 DMO precursor protein to the chloroplast and is partially cleaved in the chloroplast producing the mature 341 amino acid and 340 amino acid DMO proteins that begin with the cysteine at position 68 and methionine at position 69, respectively. The double underline shows the cysteine amino acid from APG6 that is in one form of the fully mature DMO protein (DMO+1).

The *ft_t* Coding Sequence and FT_T Protein

The *ft_t* expression cassette contains the *ft_t* gene encoding a precursor protein of 376 amino acids (295 amino acids encoded by the *ft_t* gene and 81 amino acids encoded by the *MDH* gene for targeting the FT_T protein into chloroplasts) (Figure 6). MON 87429 expresses a ~36 kDa mature FT_T protein, which consists of a single polypeptide of 296 amino acids, 295 amino acids are encoded by the *ft_t* gene and 1 amino acid (alanine) is encoded by *MDH* gene due to the processing of the chloroplast transit peptide (CTP). The *ft_t* open reading frame in the expression cassette is the modified version of R-2,4-dichlorophenoxypropionate dioxygenase (*Rdpa)* gene from *Sphingobium herbicidovorans* that encodes a FOPs and 2,4-D dioxygenase protein (FT_T) (Müller *et al.*, 2006). The expression of FT_T protein confers tolerance to FOPs and 2,4-D herbicides.

```
FT_T

1     MATATSASLF STVSSSYSKA SSIPHSRLQS VKFNSVPSFT GLKSTSLISG

51    SDSSSLAKTL RGSVTKAQTS DKKPYGFKIN AMHAALTPLT NKYRFIDVQP

101   LTGVLGAEIT GVDLREPLDD STWNEILDAF HTYQVIYFPG QAITNEQHIA

151   FSRRFGPVDP VPILKSIEGY PEVQMIRREA NESSRFIGDD WHTDSTFLDA

201   PPAAVVMRAI EVPEYGGDTG FLSMYSAWET LSPTMQATIE GLNVVHSATK

251   VFGSLYQATN WRFSNTSVKV MDVDAGDRET VHPLVVTHPV TGRRALYCNQ

301   VYCQKIQGMT DAESKSLLQF LYEHATKFDF TCRVRWKKDQ VLVWDNLCTM

351   HRAVPDYAGK FRYLTRTTVA GDKPSR
```

Figure 6. Deduced Amino Acid Sequence of MDH Chloroplast Targeting Sequence and the FT_T Protein

The amino acid sequence of the MON 87429 FT_T precursor protein was deduced from the full-length coding nucleotide sequence present in PV-ZMHT519224 (See Table 1 for more detail). The first 81 amino acids of the precursor protein (underlined) are the CTP from *MDH* gene. MDH targets FT_T protein to the chloroplast and is cleaved in the chloroplast producing the mature 296 amino acid FT_T protein that begins with the alanine at position 81. The double underline shows the alanine amino acid from MDH that is the N-terminus of the mature FT_T protein.

The *cp4 epsps* Coding Sequence and CP4 EPSPS Protein

The *cp4 epsps* expression cassette contains the *cp4 epsps* gene encoding a precursor protein of 531 amino acids (455 amino acids encoded by the *cp4 epsps* gene and 76 amino acids encoded by the *CTP2* gene for targeting the CP4 EPSPS protein into chloroplasts). MON 87429 expresses a 44 kDa CP4 EPSPS protein (Figure 7), consisting of a single polypeptide of 455 amino acids starting at the methionine position 77 (Padgette *et al.*, 1996) after a complete cleavage of the chloroplast transit peptide (CTP2). The *cp4 epsps* coding sequence is the codon optimized coding sequence of the *aroA* gene from *Agrobacterium* sp. strain CP4 encoding CP4 EPSPS (Barry *et al.*, 2001; Padgette *et al.*, 1996). The CP4 EPSPS protein is similar and functionally equivalent to endogenous plant EPSPS enzymes, but has a much-reduced affinity for glyphosate, the active ingredient in Roundup agricultural herbicides, relative to endogenous plant EPSPS (Barry *et al.*, 2001; Padgette *et al.*, 1996). The presence of this protein renders the plant tolerant to glyphosate.

```
CP4 EPSPS

1     MLHGASSRPA TARKSSGLSG TVRIPGDKSI SHRSFMFGGL ASGETRITGL

51    LEGEDVINTG KAMQAMGARI RKEGDTWIID GVGNGGLLAP EAPLDFGNAA

101   TGCRLTMGLV GVYDFDSTFI GDASLTKRPM GRVLNPLREM GVQVKSEDGD

151   RLPVTLRGPK TPTPITYRVP MASAQVKSAV LLAGLNTPGI TTVIEPIMTR

201   DHTEKMLQGF GANLTVETDA DGVRTIRLEG RGKLTGQVID VPGDPSSTAF

251   PLVAALLVPG SDVTILNVLM NPTRTGLILT LQEMGADIEV INPRLAGGED

301   VADLRVRSST LKGVTVPEDR APSMIDEYPI LAVAAAFAEG ATVMNGLEEL

351   RVKESDRLSA VANGLKLNGV DCDEGETSLV VRGRPDGKGL GNASGAAVAT

401   HLDHRIAMSF LVMGLVSENP VTVDDATMIA TSFPEFMDLM AGLGAKIELS

451   DTKAA
```

Figure 7. Deduced Amino Acid Sequence of the CP4 EPSPS Protein

The amino acid sequence of the MON 87429 CP4 EPSPS protein was deduced from the full-length coding nucleotide sequence present in PV-ZMHT519224 (See Table 1 for more detail). Another mature form of CP4 EPSPS protein containing 454 amino acids, resulting from the cleavage of the lead methionine (boxed with dash line) was also observed.

Regulatory Sequences

The *pat* coding sequence in MON 87429 is under the regulation of the promoter, 5' untranslated region (UTR) and intron for a ubiquitin gene (*Ubq*) from *Erianthus ravennae* (plume grass) that direct transcription in plant cells (Cornejo *et al.*, 1993). The *pat* coding sequence also utilizes the 3′ UTR sequence of the *fructose-bisphosphate aldolase* (*Fba*) gene from *Setaria italica* (foxtail millet) that directs polyadenylation of mRNA (Hunt, 1994).

The *dmo* coding sequence in MON 87429 is under the regulation of the promoter, 5' UTR and intron for a ubiquitin gene (*Ubq*) from *Coix lacryma-jobi* (adlay millet) that direct transcription in plant cells (Cornejo *et al.*, 1993). The *dmo* coding sequence utilizes a codon optimized targeting sequence of the *Albino and pale green 6* (*Apg6)* gene from *Arabidopsis thaliana* encoding a chloroplast-targeted Hsp101 homologue transit peptide region that directs transport of the DMO protein to the chloroplast (GenBank Accession: NM_121549). The *dmo* coding sequence also utilizes the 3' UTR sequence of the *OsMt* gene from *Oryza sativa* (rice) encoding metallothionein-like protein that directs polyadenylation of mRNA (Hunt, 1994).

The *ft_t* coding sequence in MON 87429 is under the regulation of the promoter, 5' UTR, and intron for a *ubiquitin* gene (*Ubq*) from *Arundo donax* (giant reed) that directs transcription in plant cells (Cornejo *et al.*, 1993). The *ft_t* coding sequence utilizes a chloroplast targeting sequence from *Arabidopsis thaliana Mdh* gene encoding the malate dehydrogenase transit peptide region that directs transport of the FT_T protein to the chloroplast (GenBank Accession: BT000621). The *ft_t* coding sequence also utilizes the 3' UTR sequence from the gene coding for a no apical meristem (*Nam*) protein domain containing protein from *Oryza sativa* (rice) that directs polyadenylation of mRNA (Hunt, 1994).

The *cp4 epsps* coding sequence in MON 87429 is under the regulation of the promoter and leader from the 35S RNA of cauliflower mosaic virus (CaMV) (Odell *et al.*, 1985) that direct transcription in plant cells. The *cp4 epsps* coding sequence also utilizes the 5' UTR leader sequence from the gene coding for chlorophyll a/b-binding (CAB) protein of *Triticum aestivum* (wheat) that is involved in regulating gene expression (Lamppa *et al.*, 1985), and the intron and flanking UTR sequence of the *act1* gene from *Oryza sativa* (rice) encoding rice Actin 1 (*Ract1*) protein that is also involved in regulating gene expression (McElroy *et al.*, 1990). The *cp4 epsps* coding sequence utilizes a chloroplast targeting sequence of the *ShkG* gene from *Arabidopsis thaliana* encoding the EPSPS transit peptide region that directs transport of the CP4 EPSPS protein to the chloroplast (Klee *et al.*, 1987; Herrmann, 1995). The *cp4 epsps* coding sequence is regulated by a modified partial 3' UTR sequence of *Zea mays* cDNA (Genbank Accession: EU974548) that contains a target sequence recognized by endogenous male tissue specific siRNAs (Brodersen and Voinnet, 2006), which suppresses *cp4 epsps* gene expression in maize male tissue (Yang *et al.*, 2018). The *cp4 epsps* coding sequence also utilizes a 3' UTR sequence of the glycine-rich RNA-binding protein (*Grp3*) gene from *Oryza sativa* (rice) encoding the GRP3 protein that directs polyadenylation of mRNA (Hunt, 1994).

T-DNA Border Regions

PV-ZMHT519224 contains Left and Right Border regions (Figure 8 and Table 1) that were derived from *A. tumefaciens* plasmids. The border regions each contain a nick site that is the site of DNA exchange during transformation (Barker *et al.*, 1983; Depicker *et al.*, 1982; Zambryski *et al.*, 1982). The border regions separate the T-DNA from the plasmid backbone region and are involved in the efficient transfer of T-DNA into the maize genome.

Genetic Elements Outside of the T-DNA Border Regions

Genetic elements that exist outside of the T-DNA border regions are those that are essential for the maintenance or selection of PV-ZMHT519224 in bacteria and are referred to as plasmid backbone. The selectable marker, *aadA* is the coding sequence for an aminoglycoside-modifying enzyme, 3"(9)–*O*–nucleotidyltransferase from the transposon Tn*7* (Fling *et al.*, 1985) that confers spectinomycin and streptomycin resistance in *E. coli* and *Agrobacterium* for use in molecular cloning. The origin of replication, *ori-pBR322*, is required for the maintenance of the plasmid in *E. coli* and is derived from the plasmid vector pBR322 (Sutcliffe, 1979). The origin of replication, *ori V*, is required for the maintenance of the plasmid in *Agrobacterium* and is derived from the broad host range plasmid RK2 from *Agrobacterium* (Stalker *et al.*, 1981). Because these elements are outside the T-DNA border regions, they are not expected to be transferred into the maize genome. The absence of the backbone and other unintended plasmid sequence in MON 87429 was confirmed by sequencing and bioinformatic analyses (see Section A3(d)(ii)).

Table 1.   Summary of Genetic Elements in PV-ZMHT519224

Genetic Element	Location in Plasmid Vector	Function (Reference)
T-DNA		
B[1]-Left Border Region	1-442	DNA region from *Agrobacterium tumefaciens* containing the left border sequence used for transfer of the T–DNA (Barker *et al.*, 1983)
Intervening Sequence	443-513	Sequence used in DNA cloning
P[2]-*Ea.Ubq*	514-2695	Promoter, 5' UTR, and intron sequences for a ubiquitin gene (*Ubq*) from *Erianthus ravennae* (plume grass) that directs transcription in plant cells (Cornejo *et al.*, 1993)
Intervening Sequence	2696-2700	Sequence used in DNA cloning
CS[3]-*pat*	2701-3252	Coding sequence for the phosphinothricin N–acetyltransferase (PAT) protein of *Streptomyces viridochromogenes* that confers tolerance to glufosinate (Wehrmann *et al.*, 1996; Wohlleben *et al.*, 1988)
T[4]-*Fba*	3253-3629	3' UTR sequence of the *fructose-bisphosphate aldolase* (*Fba*) gene from *Setaria italica* (foxtail millet) that directs polyadenylation of mRNA (Hunt, 1994)
Intervening Sequence	3630-3691	Sequence used in DNA cloning
P-*Clj.Ubq*	3692-5617	Promoter, 5' UTR, and intron sequences for a ubiquitin gene (*Ubq*) from *Coix lacryma-jobi* (adlay millet) that directs transcription in plant cells (Cornejo *et al.*, 1993)
Intervening Sequence	5618-5627	Sequence used in DNA cloning

Table 1.   Summary of Genetic Elements in PV-ZMHT519224 (continued)

Genetic Element	Location in Plasmid Vector	Function (Reference)
TS[5]-*APG6*	5628-5831	Codon optimized targeting sequence of the *Albino and pale green 6* (*Apg6)* gene from *Arabidopsis thaliana* encoding a chloroplast-targeted Hsp101 homologue transit peptide region that directs the protein to the chloroplast (GenBank Accession: NM_121549)
CS-*dmo*	5832-6854	Codon optimized coding sequence for the dicamba mono–oxygenase (DMO) protein of *Stenotrophomonas maltophilia* that confers dicamba resistance (Herman *et al.*, 2005; Wang *et al.*, 1997)
Intervening Sequence	6855-6862	Sequence used in DNA cloning
T-*Mt*	6863-7162	3' UTR sequence of the *OsMt* gene from *Oryza sativa* (rice) encoding metallothionein-like protein that directs polyadenylation of mRNA (Hunt, 1994)
Intervening Sequence	7163-7170	Sequence used in DNA cloning
P-*Ad.Ubq*	7171-9127	Promoter, 5' UTR, and intron sequences for a *ubiquitin* gene (*Ubq*) from *Arundo donax* (giant reed) that directs transcription in plant cells (Cornejo *et al.*, 1993)
Intervening Sequence	9128-9140	Sequence used in DNA cloning
TS-*MDH*	9141-9383	Targeting sequence from *Arabidopsis thaliana Mdh* gene encoding the malate dehydrogenase transit peptide region that directs the protein to the chloroplast (GenBank Accession: BT000621)
CS-*ft_t*	9384-10271	Modified version of R-2,4-dichlorophenoxypropionate dioxygenase (*Rdpa)* gene from *Sphingobium herbicidovorans* that expresses a FOPs and 2,4-D dioxygenase protein (FT_T) that confers tolerance to FOPs and 2,4-D herbicides (Müller *et al.*, 2006)
Intervening Sequence	10272-10286	Sequence used in DNA cloning

Table 1.   Summary of Genetic Elements in PV-ZMHT519224 (continued)

Genetic Element	Location in Plasmid Vector	Function (Reference)
T-*Nam*	10287-10803	3' UTR sequence from the gene coding for a no apical meristem (*Nam*) protein domain containing protein from *Oryza sativa* (rice) (Hunt, 1994)
Intervening Sequence	10804-10809	Sequence used in DNA cloning
P-*35S*	10810-11133	Promoter and leader from the 35S RNA of cauliflower mosaic virus (CaMV) (Odell *et al.*, 1985) that directs transcription in plant cells
Intervening Sequence	11134-11155	Sequence used in DNA cloning
L⁶-*Cab*	11156-11216	5' UTR leader sequence from the gene coding for chlorophyll a/b-binding (*CAB*) protein of *Triticum aestivum* (wheat) that is involved in regulating gene expression (Lamppa *et al.*, 1985)
Intervening Sequence	11217-11232	Sequence used in DNA cloning
I⁷-*Ract1*	11233-11712	Intron and flanking UTR sequence of the *act1* gene from *Oryza sativa* (rice) encoding rice Actin 1 protein (McElroy *et al.*, 1990) that is involved in regulating gene expression.
Intervening Sequence	11713-11721	Sequence used in DNA cloning
TS-*CTP2*	11722-11949	Targeting sequence of the *ShkG* gene from *Arabidopsis thaliana* encoding the EPSPS transit peptide region that directs transport of the protein to the chloroplast (Herrmann, 1995; Klee *et al.*, 1987)
CS-*cp4 epsps*	11950-13317	Codon optimized coding sequence of the *aroA* gene from the *Agrobacterium* sp. strain CP4 encoding the CP4 EPSPS protein that provides glyphosate tolerance (Barry *et al.*, 2001; Padgette *et al.*, 1996)
Intervening Sequence	13318-13323	Sequence used in DNA cloning
siRNA Target Sequence	13324-13524	Modified partial 3' UTR sequence of *Zea mays* cDNA (Genbank Accession: EU974548) that contains male tissue specific siRNA target sequence (Brodersen and Voinnet, 2006; Yang *et al.*, 2018)
Intervening Sequence	13525-13532	Sequence used in DNA cloning

Table 1.   Summary of Genetic Elements in PV-ZMHT519224 (continued)

Genetic Element	Location in Plasmid Vector	Function (Reference)
T-*Grp3*	13533-14143	3' UTR sequence of the glycine-rich RNA binding- protein (*Grp3*) gene from *Oryza sativa* (rice) encoding the GRP3 protein that directs polyadenylation of mRNA (Hunt, 1994)
Intervening Sequence	14144-14184	Sequence used in DNA cloning
B-Right Border Region	14185-14515	DNA region from *Agrobacterium tumefaciens* containing the right border sequence used for transfer of the T–DNA (Depicker *et al.*, 1982; Zambryski *et al.*, 1982)
Vector Backbone		
Intervening Sequence	14516-14659	Sequence used in DNA cloning
aadA	14660-15548	Bacterial promoter, coding sequence, and 3' UTR for an aminoglycoside-modifying enzyme, 3"(9) –*O*–nucleotidyltransferase from the transposon Tn*7* (Fling *et al.*, 1985) that confers spectinomycin and streptomycin resistance
Intervening Sequence	15549-16082	Sequence used in DNA cloning
OR[8]-*ori-pBR322*	16083-16671	Origin of replication from plasmid pBR322 for maintenance of plasmid in *E. coli* (Sutcliffe, 1979)
Intervening Sequence	16672-17293	Sequence used in DNA cloning
OR-*ori V*	17294-17690	Origin of replication from the broad host range plasmid RK2 for maintenance of plasmid in *Agrobacterium* (Stalker *et al.*, 1981)
Intervening Sequence	17691-17776	Sequence used in DNA cloning

[1] B, Border
[2] P, Promoter
[3] CS, Coding Sequence
[4] T, Transcription Termination Sequence
[5] TS, Targeting Sequence
[6] L, Leader
[7] I, Intron
[8] OR, Origin of Replication

A3(c)(ii)   Detailed map of the location and orientation of all genetic elements
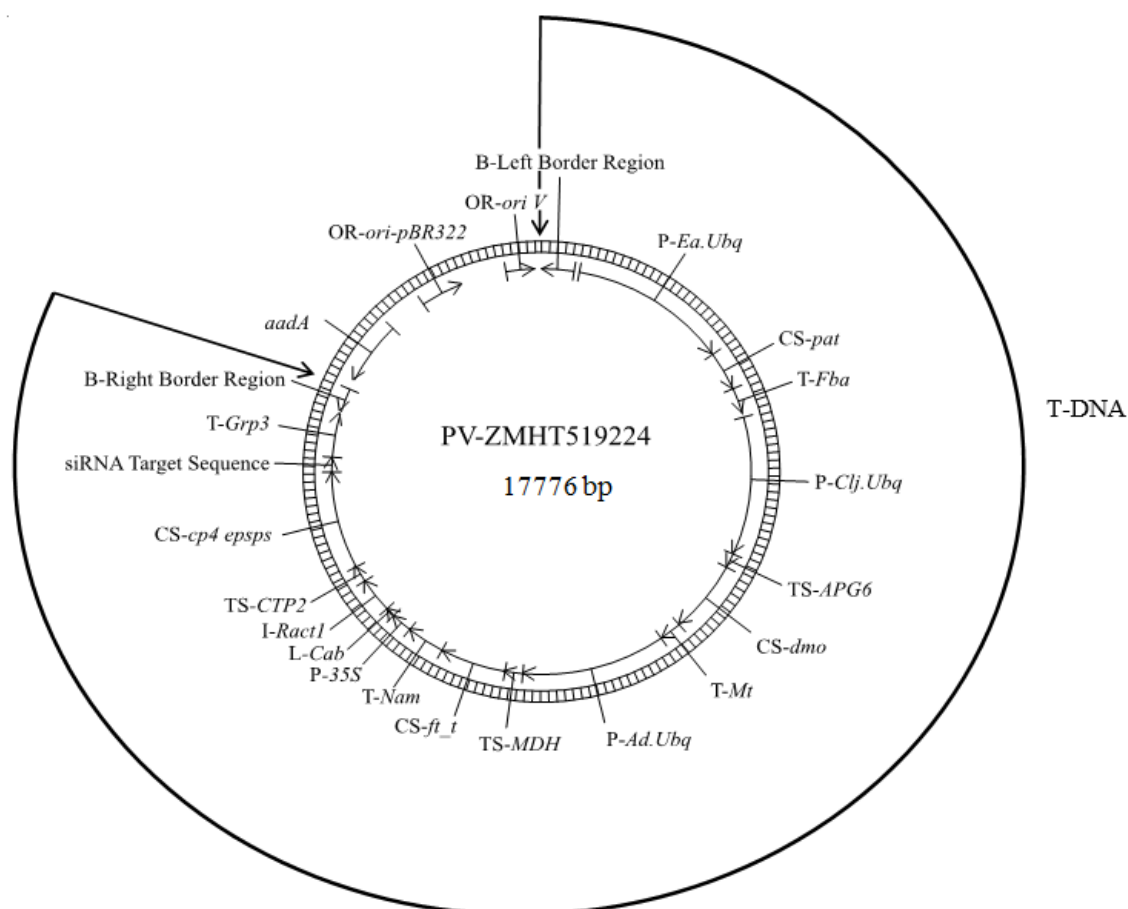
Figure 8.   Circular Map of PV-ZMHT519224

A circular map of PV-ZMHT519224 used to develop MON 87429 is shown.   PV ZMHT519224 contains one T–DNA.   Genetic elements are shown on the exterior of the map.

A3(d)   Full characterisation of the genetic modification in the new organism, including:

A3(d)(i)   Identification of all transferred genetic material and whether it has undergone any rearrangements

This section describes the methods and results of a comprehensive molecular characterisation of the genetic modification present in MON 87429. It provides information on the DNA insertion(s) into the plant genome of MON 87429, and additional information regarding the arrangement and stability of the introduced genetic material. The information provided in this section addresses the relevant factors in Codex Plant Guidelines, Section 4, paragraphs 30, 31, 32, and 33 (Codex Alimentarius, 2009).

A schematic representation of the next generation sequencing (NGS) methodology and the basis of the characterisation using NGS and PCR sequencing are illustrated in Figure 9 below. Appendix 1 (███████████, 2018) defines the test, control and reference substances, and provides an additional overview of these techniques, their use in DNA characterisation in maize plants and the materials and methods.

Experimental Stage   **Resultant Molecular Characterization**

NGS

Step 1: Next Generation Sequencing (NGS) of genomic DNA samples. A collection of read sequences are generated which comprehensively cover the test and control sample genomes

Step 2: Selection of the reads containing sequence significantly similar to that of the transformation plasmid

Step 3: Bioinformatic analysis to detect and characterize all read sequences originating from the transgenic insertion(s)

1. Presence or absence of backbone insertions: No unintended backbone or T-DNA sequences detected (Read Mapping)
2. Insert and copy number determined: Junctions located and characterized

Directed Sequencing

Step 4: Directed sequencing across the insertion from the 5' flank to the 3' flank

3. Exact sequence of insert(s)
4. Organization and intactness of genetic elements in the insert sequence is confirmed

Step 5: Directed sequencing across the wild type insertion site

5. Integrity and organization of insertion site(s)

Figure 9.   Molecular Characterisation using Sequencing and Bioinformatics

Genomic DNA from MON 87429 (Test) and the conventional control was sequenced using technology that produces a set of short, randomly distributed sequence reads that comprehensively cover test and control genomes (Step 1). Utilizing these genomic sequence reads, bioinformatics searches are conducted to identify all sequence reads that are significantly similar to the transformation plasmid (Step 2). These identified captured reads are then mapped and analyzed to determine the presence/absence of transformation plasmid backbone sequences, identify insert junctions, and to determine the insert and copy number (Step 3). Using directed sequencing, overlapping PCR products are also produced which span any insert and the wild type insertion locus (Step 4 and Step 5 respectively); these overlapping PCR products are sequenced to allow for detailed characterisation of the inserted DNA and insertion site.

The NGS method was used to characterise the genomic DNA from MON 87429 and the conventional control by generating short (~150 bp) randomly distributed sequence fragments (sequencing reads) generated in sufficient number to ensure comprehensive coverage of the sample genomes. It has been previously demonstrated that whole genome sequencing at $75\times$ depth of coverage is adequate to provide comprehensive coverage and ensure detection of inserted DNA (Kovalic *et al.*, 2012). To confirm sufficient sequence coverage of the genome, the 150 bp sequence reads are analyzed to determine the coverage of a known single-copy endogenous maize gene. This establishes the depth of coverage (the median number of times each base of the genome is independently sequenced). The level of sensitivity of this method was demonstrated by detection of a positive control plasmid DNA spiked at 1 and 1/10th copy-per-genome equivalent. This confirms the method's ability to detect any sequences derived from the transformation plasmid. Bioinformatics analysis was then used to select sequencing reads that contained sequences similar to the transformation plasmid, and these were analyzed in depth to determine the number of DNA inserts. NGS was run on five breeding generations of MON 87429 and the appropriate conventional controls. Results of NGS are shown in Sections A3(d) and A3(f).

The DNA inserts of MON 87429 were characterised by mapping of sequencing reads to the transformation plasmid and identifying junctions and unpaired read mappings adjacent to the junctions. Examples of five types of NGS reads are shown in Figure 10. The junctions of the DNA insert and the flanking DNA are unique for each insertion (Kovalic *et al.*, 2012). Therefore, insertion sites can be recognized by analyzing for sequence reads containing such junctions.

Directed sequencing (locus-specific PCR and DNA sequencing analyses, Figure 9, Step 4) complements the NGS method. It assesses the sequence identity of the insert relative to the corresponding sequence from the T-DNA in PV-ZMHT519224, and demonstrates that each genetic element in the insert was intact without rearrangement. It also characterises the flank sequence beyond the insert corresponding to the genomic DNA of MON 87429. Directed sequencing results are described in Sections A3(d)(i) and A3(d)(ii).

The stability of the T-DNA present in MON 87429 across multiple breeding generations was evaluated by NGS as described above by determining the number and identity of the DNA inserts in each generation. For a single copy T-DNA insert, two junction sequence classes are expected. In the case of an event where a single insertion locus is stably inherited over multiple breeding generations, two identical junction sequence classes would be detected in all the breeding generations tested. Results are described in Section A3(f)(i).

Segregation analysis of the T-DNA was conducted to determine the inheritance and generational stability of the insert in maize. Segregation analysis corroborates the insert stability demonstrated by NGS and independently establishes the genetic behavior of the T-DNA. Results are described in Section A3(f)(i).

Mapping of Plasmid Sequence Alignments
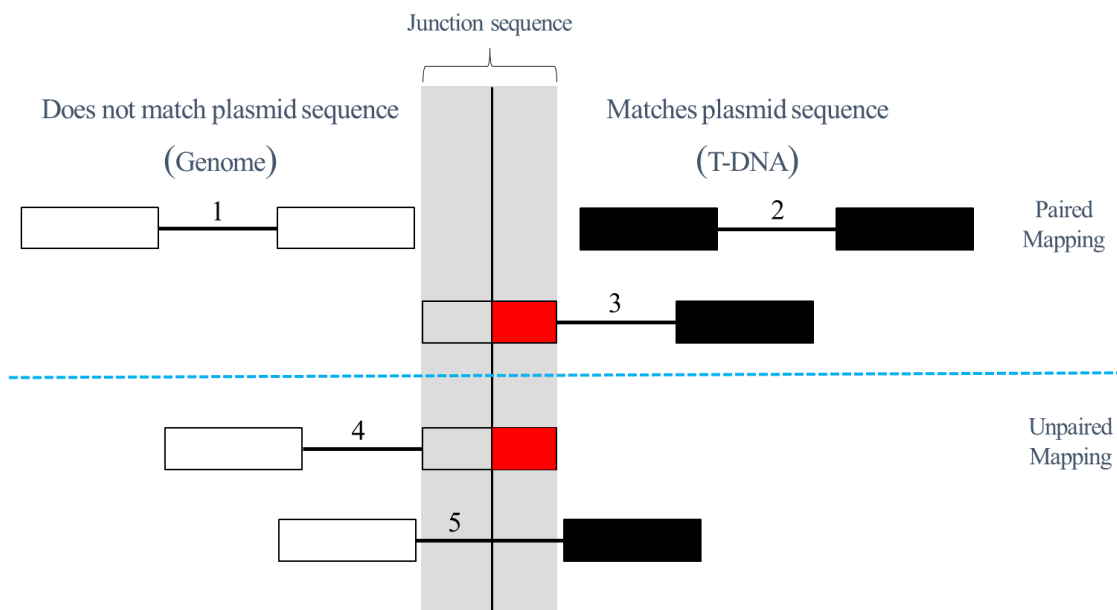
Figure 10.   Five Types of NGS Reads

NGS yields data in the form of read pairs where sequence from each end of a size selected DNA fragment is returned.   Depicted above are five types of sequencing reads/read pairs generated by NGS sequencing which can be found spanning or outside of junction points.   Sequence boxes are filled red or black if it matches with plasmid sequence, and empty if it matches with genomic sequence.   Grey highlighting indicates sequence reads spanning the junction.   Junctions are detected by examining the NGS data for reads having portions of plasmid sequences that span less than the full read, as well as reads mapping adjacent to the junction points where their mate pair does not map to the plasmid sequence.   The five types of sequencing reads/read pairs being (1) Paired and unpaired reads mapping to genomic sequence outside of the insert, greater than 99.999% of collected reads fall into this category and are not evaluated in this analysis, (2) Paired reads mapping entirely to the transformation plasmid sequence, such reads reveal the presence of transformation related sequence *in planta*, (3) Paired reads where one read maps entirely within the inserted DNA and the other read maps partially to the insert (indicating a junction point), (4) Single read mapping partially to the transformation plasmid DNA sequence (indicating a junction point) where its mate maps entirely to the genomic flanking sequence and (5) Single read mapping entirely to the transformation plasmid DNA sequence where its mate maps entirely to genomic flanking sequence, such reads are part of the junction signature.

A3(d)(ii)   Determination of number and identity of DNA inserts in MON 87429

The number of inserted DNA sequences from PV-ZMHT519224 in MON 87429 was assessed by generating a comprehensive collection of reads via NGS of MON 87429 genomic DNA using the R3 generation. A plasmid map of PV-ZMHT519224 is shown in Figure 8. Table 2 provides descriptions of the genetic elements present in MON 87429.   A schematic representation of the insert and flanking sequences in MON 87429 is shown in Figure 11.

Next Generation Sequencing for MON 87429 and Conventional Control Genomic DNA

Genomic DNA from five breeding generations of MON 87429 (Figure 12) and conventional controls were isolated from seed and prepared for sequencing   These genomic DNA libraries were used to generate short (~150 bp) randomly distributed sequencing reads of the maize genome (Figure 9, Step 1).

To demonstrate sufficient sequence coverage the 150 bp sequence reads were analyzed by mapping all reads to a known single copy endogenous gene (*Zea mays* pyruvate decarboxylase (*pdc3*), GenBank Accession: AF370006.2) in each of the five breeding generations.   The analysis of sequence coverage plots showed that the depth of coverage (i.e., the median number of times any base of the genome is expected to be independently sequenced) was 86× or greater for the five generations of MON 87429 (R3, R3F1, R4, R4F1, and R5) and the conventional control.   It has been previously demonstrated that whole genome sequencing at 75× depth of coverage provides comprehensive coverage and ensures detection of inserted DNA (Kovalic *et al.*, 2012).

To demonstrate the method's ability to detect any sequences derived from the PV-ZMHT519224 transformation plasmid, a sample of conventional control genomic DNA spiked with PV-ZMHT519224 DNA was analyzed by NGS and bioinformatics.   The level of sensitivity of this method was demonstrated to a level of one genome equivalent and $1/10^{th}$ genome equivalent, 100% nucleotide identity was observed over 100% of PV-ZMHT519224. This result demonstrates that all nucleotides of PV-ZMHT519224 are observed by the sequencing and bioinformatic assessments performed and that a detection level of at least $1/10^{th}$ genome equivalent was achieved for the plasmid DNA sequence assessment.

Table 2.   Summary of Genetic Elements in MON 87429

Genetic Element[1]	Location in Sequence[2]	Function (Reference)
5' Flanking DNA	**1-1029**	DNA sequence flanking the 5' end of the insert
B[3]-Left Border Region[r1]	**1030-1288**	DNA region from *Agrobacterium tumefaciens* containing the left border sequence used for transfer of the T–DNA (Barker *et al.*, 1983)
Intervening Sequence	**1289-1359**	Sequence used in DNA cloning
P[4]-*Ea.Ubq*	**1360-3541**	Promoter, 5' UTR, and intron sequences for a ubiquitin gene (*Ubq*) from *Erianthus ravennae* (plume grass) that directs transcription in plant cells (Cornejo *et al.*, 1993)
Intervening Sequence	**3542-3546**	Sequence used in DNA cloning
CS[5]-*pat*	**3547-4098**	Coding sequence for the phosphinothricin N–acetyltransferase (PAT) protein of *Streptomyces viridochromogenes* that confers tolerance to glufosinate (Wehrmann *et al.*, 1996; Wohlleben *et al.*, 1988)
T[6]-*Fba*	**4099-4475**	3' UTR sequence of the *fructose-bisphosphate aldolase* (*Fba*) gene from *Setaria italica* (foxtail millet) that directs polyadenylation of mRNA (Hunt, 1994)
Intervening Sequence	**4476-4537**	Sequence used in DNA cloning
P-*Clj.Ubq*	**4538-6463**	Promoter, 5' UTR, and intron sequences for a ubiquitin gene (*Ubq*) from *Coix lacryma-jobi* (adlay millet) that directs transcription in plant cells (Cornejo *et al.*, 1993)
Intervening Sequence	**6464-6473**	Sequence used in DNA cloning
TS[7]-*APG6*	**6474-6677**	Codon optimized targeting sequence of the *Albino and pale green 6 (Apg6)* gene from *Arabidopsis thaliana* encoding a chloroplast-targeted Hsp101 homologue transit peptide region that directs the protein to the chloroplast (GenBank Accession: NM_121549)
CS-*dmo*	**6678-7700**	Codon optimized coding sequence for the dicamba mono–oxygenase (DMO) protein of *Stenotrophomonas maltophilia* that confers dicamba resistance (Herman *et al.*, 2005; Wang *et al.*, 1997)

Table 2. Summary of Genetic Elements in MON 87429 (continued)

Intervening Sequence	**7701-7708**	Sequence used in DNA cloning
T-*Mt*	**7709-8008**	3' UTR sequence of the *OsMt* gene from *Oryza sativa* (rice) encoding metallothionein-like protein that directs polyadenylation of mRNA (Hunt, 1994)
Intervening Sequence	**8009-8016**	Sequence used in DNA cloning
P-*Ad.Ubq*	**8017-9973**	Promoter, 5' UTR, and intron sequences for a *ubiquitin* gene (*Ubq*) from *Arundo donax* (giant reed) that directs transcription in plant cells (Cornejo *et al.*, 1993)
Intervening Sequence	**9974-9986**	Sequence used in DNA cloning
TS-*MDH*	**9987-10229**	Targeting sequence from *Arabidopsis thaliana Mdh* gene encoding the malate dehydrogenase transit peptide region that directs the protein to the chloroplast (GenBank Accession: BT000621)
CS-*ft_t*	**10230-11117**	Modified version of R-2,4-dichlorophenoxypropionate dioxygenase (*Rdpa)* gene from *Sphingobium herbicidovorans* that expresses a FOPs and 2,4-D dioxygenase protein (FT_T) that confers tolerance to FOPs and 2,4-D herbicides (Müller *et al.*, 2006)
Intervening Sequence	**11118-11132**	Sequence used in DNA cloning
T-*Nam*	**11133-11649**	3' UTR sequence from the gene coding for a no apical meristem (*Nam*) protein domain containing protein from *Oryza sativa* (rice) (Hunt, 1994)
Intervening Sequence	**11650-11655**	Sequence used in DNA cloning
P-*35S*	**11656-11979**	Promoter and leader from the 35S RNA of cauliflower mosaic virus (CaMV) (Odell *et al.*, 1985) that directs transcription in plant cells
Intervening Sequence	**11980-12001**	Sequence used in DNA cloning
L^8-*Cab*	**12002-12062**	5' UTR leader sequence from the gene coding for chlorophyll a/b-binding (*CAB*) protein of *Triticum aestivum* (wheat) that is involved in regulating gene expression (Lamppa *et al.*, 1985)
Intervening Sequence	**12063-12078**	Sequence used in DNA cloning
I^9-*Ract1*	**12079-12558**	Intron and flanking UTR sequence of the *act1* gene from *Oryza sativa* (rice) encoding rice Actin 1 protein (McElroy *et al.*, 1990) that is involved in regulating gene expression.

Table 2.   Summary of Genetic Elements in MON 87429 (continued)

Intervening Sequence	12559-12567	Sequence used in DNA cloning
TS-*CTP2*	12568-12795	Targeting sequence of the *ShkG* gene from *Arabidopsis thaliana* encoding the EPSPS transit peptide region that directs transport of the protein to the chloroplast (Herrmann, 1995; Klee *et al.*, 1987)
CS-*cp4 epsps*	12796-14163	Codon optimized coding sequence of the *aroA* gene from the *Agrobacterium* sp. strain CP4 encoding the CP4 EPSPS protein that provides glyphosate tolerance (Barry *et al.*, 2001; Padgette *et al.*, 1996)
Intervening Sequence	14164-14169	Sequence used in DNA cloning
siRNA Target Sequence	14170-14370	Modified partial 3' UTR sequence of *Zea mays* cDNA (Genbank Accession: EU974548) that contains male tissue specific siRNA Target Sequence (Brodersen and Voinnet, 2006; Yang *et al.*, 2018)
Intervening Sequence	14371-14378	Sequence used in DNA cloning
T-*Grp3*	14379-14989	3' UTR sequence of the glycine-rich RNA binding- protein (*Grp3*) gene from *Oryza sativa* (rice) encoding the GRP3 protein that directs polyadenylation of mRNA (Hunt, 1994)
Intervening Sequence	14990-15030	Sequence used in DNA cloning
B-Right Border Region[r1]	15031-15037	DNA region from *Agrobacterium tumefaciens* containing the right border sequence used for transfer of the T–DNA (Depicker *et al.*, 1982; Zambryski *et al.*, 1982)
3' Flanking DNA	15038-16068	Flanking DNA

[1] Although flanking sequences and intervening sequences are not functional genetic elements, they comprise a portion of the sequence.

[2] Numbering refers to the sequence of the insert in MON 87429 and adjacent DNA

[3] B, Border

[4] P, Promoter

[5] CS, Coding Sequence

[6] T, Transcription Termination Sequence

[7] TS, Targeting Sequence

[8] L, Leader

[9] I, Intron

[r1] Superscript in Left and Right Border Regions indicate that the sequence in MON 87429 was truncated compared to the sequences in PV-ZMHT519224
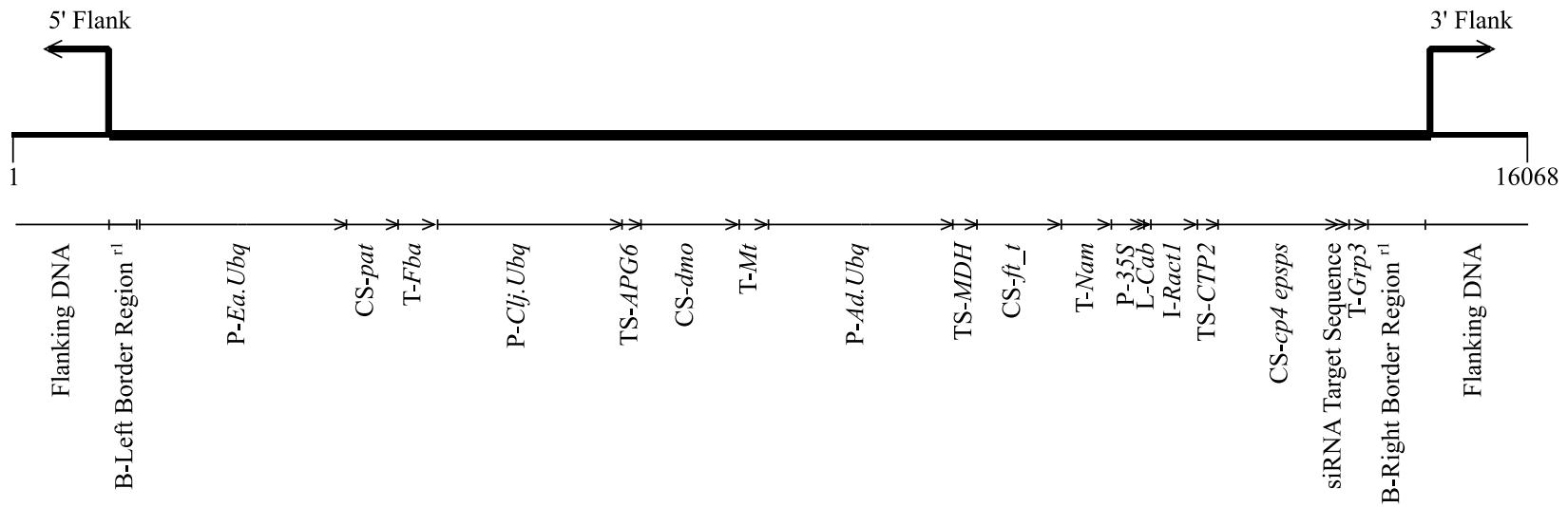
Figure 11.   Schematic Representation of the Insert and Flanking Sequences in MON 87429

DNA derived from T-DNA of PV-ZMHT519224 integrated in MON 87429.   Right-angled arrows indicate the ends of the integrated T-DNA and the beginning of the flanking sequence.   Identified on the map are genetic elements within the insert.   This schematic diagram may not be drawn to scale.

[r1] Superscript in Left and Right Border Regions indicate that the sequence in MON 87429 was truncated compared to the sequences in PV-ZMHT519224.

R0

$\otimes$

R1

$\otimes$

R2

$\otimes$

R3[1, 2, 3] ———— × HCL617 ————→ **R3F1**[1]

$\otimes$

R4[1] ———— × L7126Z ————→ **R4F1**[1]

$\otimes$

R5[1]
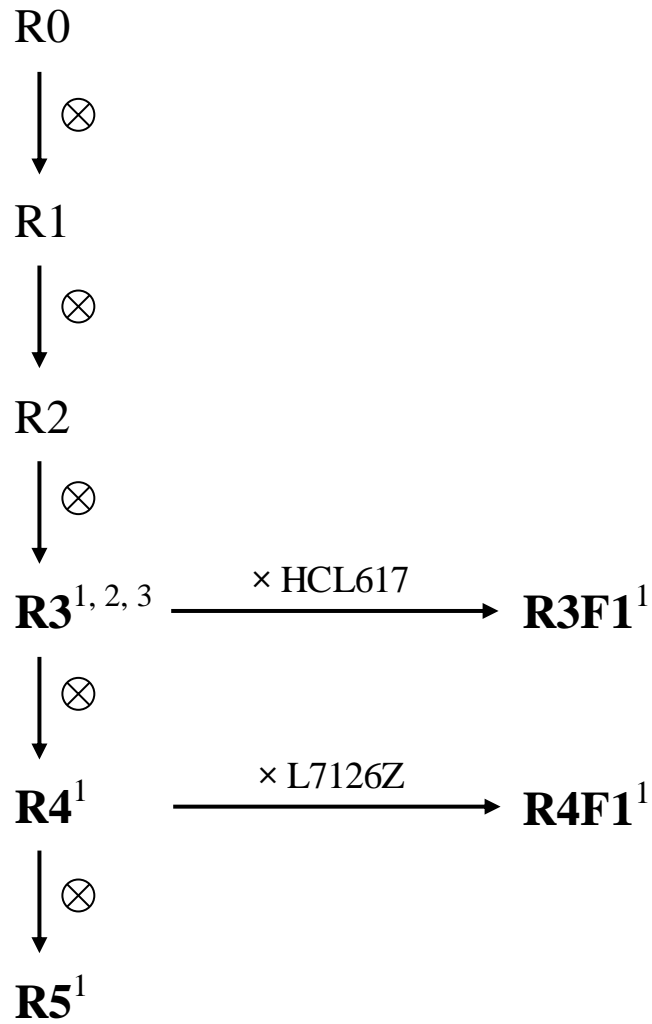
Figure 12.   Breeding History of MON 87429

The generations used for molecular characterisation and insert stability analyses are indicated in bold text.   R0 (LH244) corresponds to the transformed plant, $\otimes$ designates self-pollination.

[1] Generations used to confirm insert stability
[2] Generation used for molecular characterisation
[3] Generation used for commercial development of MON 87429

Selection of Sequence Reads Containing Sequence of the PV-ZMHT519224

The transformation plasmid, PV-ZMHT519224 was transformed into the parental variety LH244 to produce MON 87429. Consequently, any DNA inserted into MON 87429 will consist of sequences that are similar to the PV-ZMHT519224 DNA sequence. Therefore, to fully characterise the DNA from PV-ZMHT519224 inserted in MON 87429, it is sufficient to analyze only the sequence reads that have significant similarity to PV-ZMHT519224 (Figure 9, Step 2).

Using established criteria, sequence reads similar to PV-ZMHT519224 were selected from MON 87429 sequence datasets and were then used as input data for bioinformatic junction sequence analysis. PV-ZMHT519224 sequences were also compared against the conventional control sequence dataset.

Determination of T-DNA Copy Number and Presence or Absence of Plasmid Vector Backbone

By mapping sequence reads to the transformation plasmid sequence and identifying junction signatures, the presence or absence of backbone sequence and the number of T-DNA insertions can be determined. For a single copy T-DNA insert sequence at a single genomic locus, a single junction signature pair and few if any reads aligning with the transformation plasmid backbone sequences are expected.

When reads from conventional maize LH244 were aligned with the transformation plasmid sequence, a number of reads mapped to the T-DNA element siRNA Target Sequence (Figure 13, see Panels 1 and 2; Panel 3 illustrates the read depth). The sequence alignments were expected since the siRNA Target Sequence in the T-DNA is derived from endogenous maize genomic sequence. Notably, the sequence alignment is isolated to that element alone and does not cross the element boundaries. No other sequence reads from LH244 conventional maize mapped to the transformation plasmid. Additional conventional controls (LH244 × HCL617 was the control for R3F1, and LH244 × L7126Z was the control for R4F1) evaluated in the generational stability analysis (see Table 4) produced comparable read maps.

When reads from the MON 87429 (R3) dataset were aligned with the transformation plasmid sequence, large numbers of reads mapped to T-DNA, and no reads were identified which aligned to the transformation plasmid backbone (Figure 14).

The mapping of a large number of sequencing reads from the MON 87429 (R3) dataset to the T-DNA was expected and fully consistent with the presence of the inserted DNA MON 87429. Since these sequences are identical, the mapped read mate pairs were used to distinguish their true mapping location. Also, no reads in the MON 87429 (R3) generation dataset were identified that align with the plasmid backbone. As a result, it is concluded that MON 87429 (R3) does not contain inserted sequence from the transformation plasmid backbone.

To determine the insert number in MON 87429 (R3), selected reads mapping to T-DNA as described above were analysed to identify junctions. This bioinformatic analysis is used to

find and classify partially matched reads characteristic of the ends of insertions. The number of unique junctions determined by this analysis are shown in Table 3.

Table 3.   Unique Junction Sequence Class Results

Sample	Junctions Detected
MON 87429 (R3)	2
LH244	0
LH244 × HCL617	0
LH244 × L7126Z	0

Detailed mapping information of the junction sequences is shown in Figure 14. The location and orientation of the junction sequences relative to the T-DNA insert determined for MON 87429 are illustrated in Figure 14, panels 1 and 2. As shown in the figure, there are two junctions identified in MON 87429. Both junctions contain the T-DNA border sequence joined to flanking genomic sequence, indicating that they represent the sequences at the junctions of the intended T-DNA insert and the maize genome. As described earlier, no junctions were detected in any of the conventional maize control samples.

Considered together, the absence of plasmid backbone and the presence of two junctions (joining T-DNA borders and flanking sequences) indicate a single intended T-DNA at a single locus in the genome of MON 87429. Both of these junctions originate from the same locus of the MON 87429 genome and are linked by contiguous, known and expected DNA sequence. This is demonstrated by complete coverage of the sequenced reads spanning the interval between the junctions and the directed sequencing of overlapping PCR products described in Section A.3.

Based on the comprehensive NGS and junction identification it is concluded that MON 87429 contains one copy of the T-DNA inserted into a single locus. This conclusion is confirmed by the sequencing and analysis of overlapping PCR products from this locus as described below.
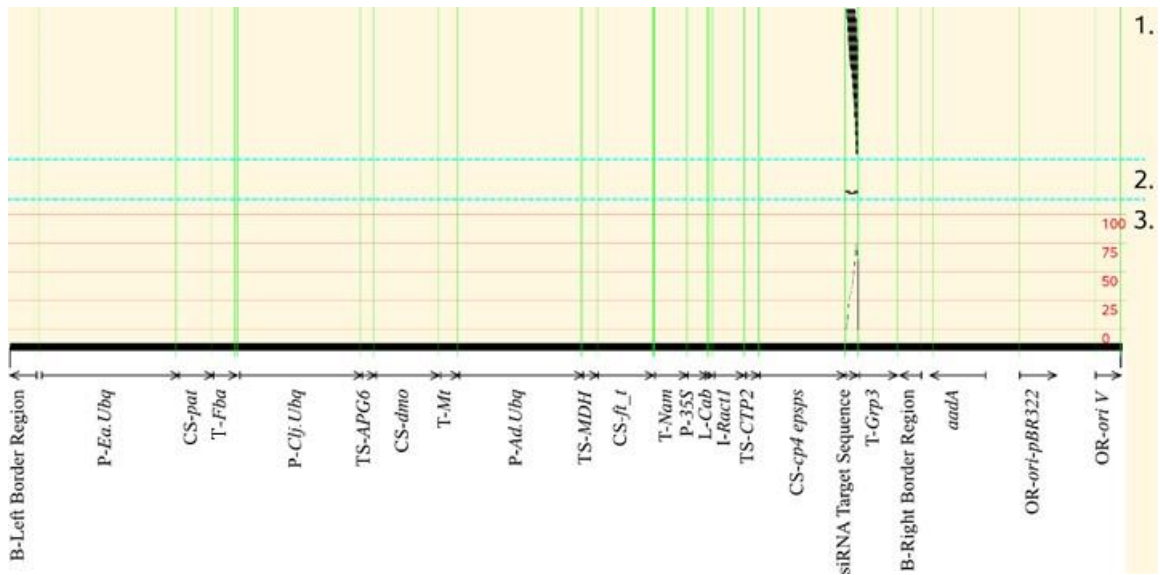
Figure 13.   Read Mapping of Conventional Maize LH244 Versus PV-ZMHT519224

Panel 1 shows the location of unpaired mapped reads, Panel 2 shows paired mapped reads, and Panel 3 shows a representation of combined read depth for unpaired and paired reads.   Vertical lines, in green, show genetic element boundaries. Comparable results were observed when read mapping LH244 × HCL617 versus PV-ZMHT519224, or read mapping LH244 × L7126Z versus PV-ZMHT519224. These additional conventional controls were used for the generational stability analysis (see Table 4).
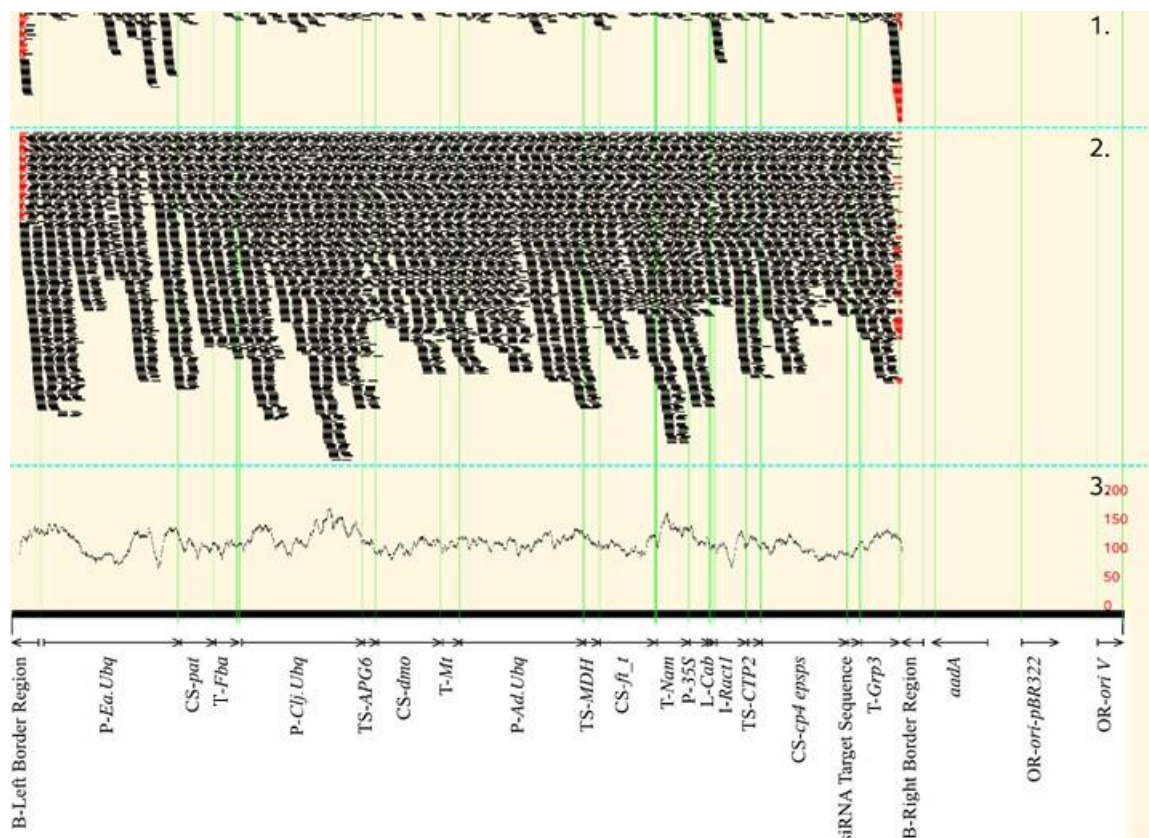
Figure 14.   Read Mapping of MON 87429 (R3) Versus PV-ZMHT519224

Panel 1 shows the location of unpaired mapped reads.   Panel 2 shows paired mapped reads and Panel 3 shows a representation of combined read depth for unpaired and paired reads.   Vertical lines, in green, show genetic element boundaries.   The region of flank junction sequences that aligns with transformation plasmid is shown in red. Comparable results were observed when read mapping the R3F1, R4, R4F1, and R5 generations of MON 87429 versus PV-ZMHT519224 (see Table 4 for the generational stability analysis).

A3(d)(iii)   Full DNA sequence, including junction regions

Organisation and Sequence of the Insert and Adjacent DNA in MON 87429

The organisation of the elements within the DNA insert and the adjacent genomic DNA was assessed using directed DNA sequence analysis (refer to Figure 9, Step 4).   PCR primers were designed to amplify two overlapping regions of the MON 87429 genomic DNA that span the entire length of the insert and the adjacent DNA flanking the insert (Figure 15). The amplified PCR products were subjected to DNA sequencing analyses.   The results of this analysis confirm that the MON 87429 insert is 14,008 bp and that each genetic element within the T-DNA is intact compared to PV-ZMHT519224.   The border regions both contain small terminal deletions with the remainder of the inserted border regions being identical to the sequence in PV-ZMHT519224.   The sequence and organisation of the insert was also shown to be identical to the corresponding T-DNA of PV-ZMHT519224 as intended.   This analysis also shows that only T-DNA elements (described in Table 2) were present within the inserted DNA. In addition, 1,029 base pairs flanking the 5′ end of the MON 87429 insert (Table 2, bases 1-1029) and 1031 base pairs flanking the 3′ end of the MON 87429 insert (Table 2, bases 15038-16068) were determined.
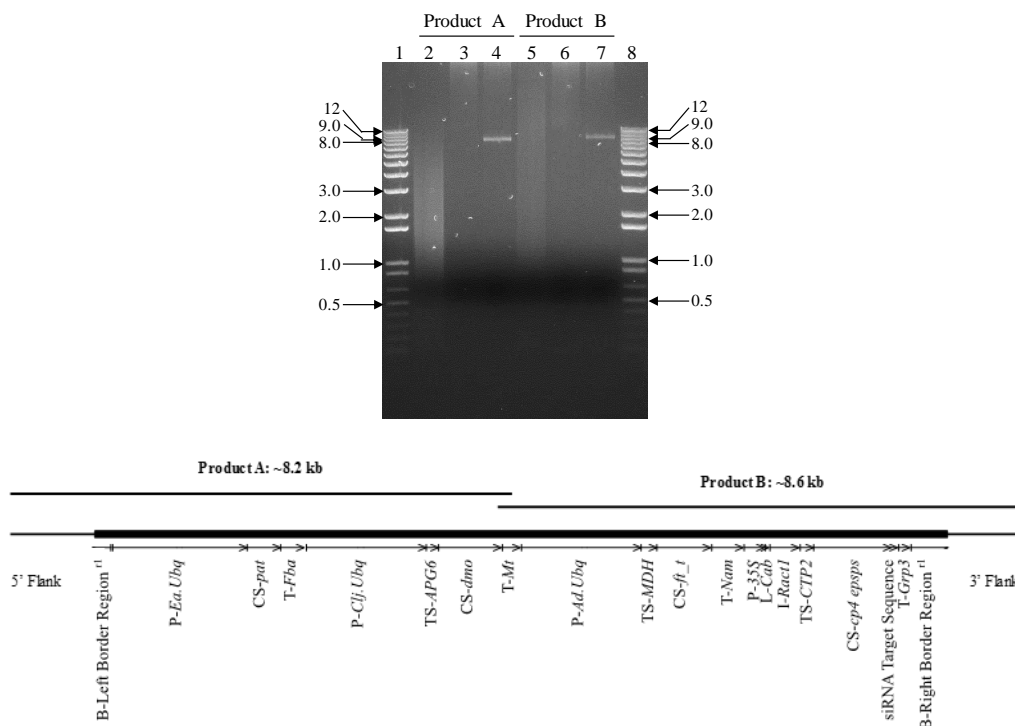
Figure 15.   Overlapping PCR Analysis across the Insert in MON 87429

PCR was performed on both conventional control genomic DNA and genomic DNA of the R3 generation of MON 87429 using two pairs of primers to generate overlapping PCR fragments from MON 87429 for sequencing analysis.   To verify size and specificity of the PCR products, 12 µl of each of the PCR reactions was loaded on the gel.   The expected product size for each amplicon is provided in the illustration of the insert in MON 87429 that appears at the bottom of the figure.   This figure is a representative of the data generated in the study.   Lane designations are as follows:

Lane	
1	1 Kb Plus DNA Ladder
2	No template control
3	LH244 Conventional Control
4	MON 87429
5	No template control
6	LH244 Conventional Control
7	MON 87429
8	1 Kb Plus DNA Ladder

Arrows on the agarose gel photograph denote the size of the DNA, in kilobase pairs, obtained from the 1 Kb Plus DNA Ladder (Invitrogen) on the ethidium bromide stained gel.
[rl] Superscript in Left and Right Border Regions indicate that the sequence in MON 87429 was truncated compared to the sequences in PV-ZMHT519224

Sequencing of the MON 87429 Insertion Site

PCR and sequence analysis were performed on genomic DNA extracted from the conventional control to examine the insertion site in conventional maize (see Figure 9, Step 5). The PCR was performed with one primer specific to the genomic DNA sequence flanking the 5' end of the MON 87429 insert paired with a second primer specific to the genomic DNA sequence flanking the 3' end of the insert (Figure 16). A sequence comparison between the PCR product generated from the conventional control and the sequence generated from the 5' and 3' flanking sequences of MON 87429 indicates that 54 bases of maize genomic DNA were deleted during integration of the T-DNA. There also was a 29 base insertion in the MON 87429 5′ flanking sequence and a 31 base insertion in the MON 87429 3' flanking sequence. Such changes are common during plant transformation (Anderson *et al.*, 2016) and these changes presumably resulted from double stranded break repair mechanisms in the plant during *Agrobacterium*-mediated transformation process (Salomon and Puchta, 1998).
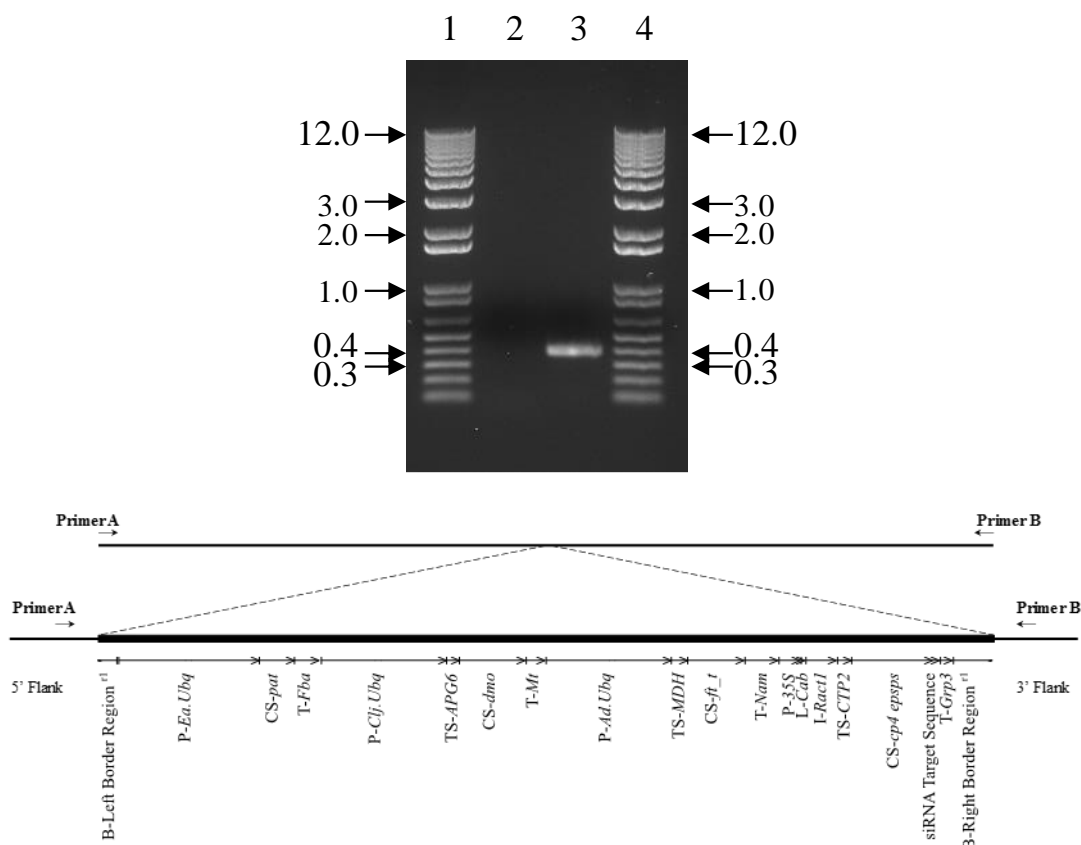
Figure 16.   PCR Amplification of the MON 87429 Insertion Site

PCR analysis was performed to evaluate the insertion site.   PCR was performed on conventional control genomic DNA using Primer A, specific to the 5′ flanking sequence, and Primer B, specific to the 3′ flanking sequence of the insert in MON 87429.   The DNA generated from the conventional control PCR was used for sequencing analysis.   This illustration depicts the MON 87429 insertion site in the conventional control (upper panel) and the MON 87429 insert (lower panel). Approximately 5 µl of each of the PCR reactions was loaded on the gel.   This figure is representative of the data generated.   Lane designations are as follows:

Lane
1   1 Kb Plus DNA Ladder
2   No template control
3   LH244 Conventional Control
4   1 Kb Plus DNA Ladder

Arrows on the agarose gel photograph denote the size of the DNA, in kilobase pairs, obtained from the 1 Kb Plus DNA Ladder (Invitrogen) on the ethidium bromide stained gel.

[r1] Superscript in Left and Right Border Regions indicate that the sequence in MON 87429 was truncated compared to the sequences in PV-ZMHT519224.

A3(d)(iv) Map of the organisation of the inserted DNA (each site)

PCR and DNA sequence analyses performed on MON 87429 and the conventional control determined the organisation of the genetic elements within the insert as given in Figure 15.

A3(d)(v) Identification and characterisation of unexpected ORFs

Unlike the previous section where prior safety assessments can be applied due to identical coding regions, each unique transformation (MON 87429) must be assessed with bioinformatic analyses to confirm a lack of allergenic or toxic effects due to the specific location in which the transformation occurred.

The 2009 Codex Alimentarius Commission guidelines for the safety assessment of food derived from biotechnology crops (Codex Alimentarius, 2009) includes an assessment element on the identification and evaluation of "*open reading frames within the inserted DNA or created by the insertion with contiguous plant genomic DNA*." These assessments examine the potential homology of any putative polypeptides or proteins that could be produced from open reading frames (ORFs) in the insert or at the plant-insert junction to known toxins or allergens. These analyses are conducted even if there is no evidence that such alternative reading frames in the insert or such ORFs at the plant-insert junction are capable of being transcribed or translated into a protein. Bioinformatic analyses were performed on the MON 87429 insert and flanking genomic DNA sequences to assess the potential for allergenicity, toxicity, or biological activity of putative polypeptides encoded by all six reading frames present in the MON 87429 insert DNA, as well as ORFs spanning the 5' and 3' insert DNA-flanking sequence junctions. The results from these bioinformatics analyses demonstrate that any putative polypeptides encoded by the MON 87429 event sequence are unlikely to exhibit allergenic, toxic or otherwise biologically adverse properties.

In addition to the bioinformatic analyses conducted on MON 87429 DMO, PAT, CP4 EPSPS and FT_T protein sequences (Sections B4(a) and B5(b), bioinformatic analyses were also performed on the MON 87429 insert to assess the potential for allergenicity, toxicity, or biological activity of putative polypeptides encoded by all six reading frames present in the MON 87429 insert DNA, as well as ORFs present in the 5' and 3' flanking sequence junctions. These various bioinformatic evaluations are depicted in Figure 17. ORFs spanning the 5' and 3' maize genomic DNA-inserted DNA junctions were translated from stop codon to stop codon in all six reading frames (three forward reading frames and three reading frames in reverse orientation)[3]. Polypeptides of eight amino acids or greater from each reading frame were then compared to toxin, allergen and all proteins databases using bioinformatic tools.   Similarly, the entire T-DNA sequence was translated in all six reading frames and the resulting deduced amino acid sequence was subjected to bioinformatic analyses. The data generated from these analyses confirm that even in the highly unlikely occurrence that a translation product other than MON 87429 DMO, PAT, CP4 EPSPS and

---

[3] An evaluation of sequence translated from stop codon to stop codon represents the most conservative approach possible for flank junction analysis as it does not take into consideration that a start codon is necessary for the production of a protein sequence.

FT_T proteins were derived from frames one to six of the insert DNA or the ORFs spanning the insert junctions, they would not share a sufficient degree of sequence similarity with other proteins to indicate they would be potentially allergenic, toxic, or have other safety implications. Therefore, there is no evidence for concern regarding the relatedness of the putative polypeptides for MON 87429 to known toxins, allergens, or biologically active putative peptides.

Bioinformatics Evaluation of the T-DNA Insert in MON 87429

For details, please refer to ▉▉▉▉▉, 2018 (MSL0029454).

Bioinformatic analyses were performed to assess the potential of toxicity, allergenicity or biological activity of any putative peptides encoded by translation of reading frames 1 through 6 of the inserted DNA in MON 87429 (Figure 17).

The FASTA sequence alignment tool was used to assess structural relatedness between the query sequences and any protein sequences in the AD_2018, TOX_2018, and PRT_2018 databases. Structural similarities shared between each putative polypeptide with each sequence in the database were examined. The extent of structural relatedness was evaluated by detailed visual inspection of the alignment, the calculated percent identity and alignment length to ascertain if alignments exceeded Codex (Codex Alimentarius, 2009) thresholds for FASTA searches of the AD_2018 database, and the *E*-score. Alignments having an *E*-score-less than 1×10^{-5} are deemed significant because they may reflect shared structure and function among sequences. In addition to structural similarity, each putative polypeptide was screened for short polypeptide matches using a pair-wise comparison algorithm. In these analyses, eight contiguous and identical amino acids were defined as immunologically relevant, where eight represents the typical minimum sequence length likely to represent an immunological epitope (Silvanovich *et al.*, 2006) and evaluated against the AD_2018 database.

The results of the search comparisons showed that no relevant structural similarity to known allergens and toxins were observed for any of the putative polypeptides when compared to proteins in the allergen (AD_2018) or toxin (TOX_2018) databases. Furthermore, no short (eight amino acid) polypeptide matches were shared between any of the putative polypeptides and proteins in the allergen database.

When the frames were used to query the PRT_2018 database, the results of these analyses positively identified the following genetic elements within the MON 87429 T-DNA: (1) frame 1 was observed to contain the non-coding T-*Grp3* element that directs polyadenylation of mRNA; (2) frame 2 was observed to contain the TS-*APG6* chloroplast targeting peptide and DMO protein, and the TS-*MDH* targeting peptide and FT_T protein, the non-coding P-*35S* RNA of cauliflower mosaic virus that directs transcription in plant cells, and siRNA Target Sequence; (3) frame 3 was observed to contain the CP4 EPSPS protein and associated chloroplast targeting peptide, the PAT protein, the siRNA Target Sequence, and the non-coding T-*Grp3* element that directs polyadenylation of mRNA; and (4) frames 4, 5, and 6 were not observed to define genetic elements within the MON 87429 T-DNA. Each of the genetic elements are described and expected based on the known sequence of the

MON 87429 T-DNA.   The positive identification of these elements does not indicate potential for adverse biological activity.   No other relevant sequence similarities between the 6 reading frames translated from the MON 87429 T-DNA were observed with allergens, toxins, or other biologically active proteins of concern.

Taken together, these data demonstrate the lack of relevant similarities between known allergens or toxins for putative peptides derived from all six reading frames from the inserted DNA sequence of MON 87429.   As a result, in the unlikely event that a translation product other than DMO, PAT, CP4 EPSPS and FT_T proteins was derived from reading frames 1 to 6, these putative polypeptides are not expected to be cross-reactive allergens, toxins, or display adverse biological activity.

Bioinformatics Evaluation of the DNA Sequences Flanking the 5′ and 3′ Junctions of the MON 87429 Insert: Assessment of Putative Peptides

For details please refer to ▮▮▮▮▮., 2018 (MSL0029453).

Analyses of putative polypeptides encoded by DNA spanning the 5' and 3' genomic junctions of the MON 87429 inserted DNA were performed using a bioinformatic comparison strategy. The purpose of the assessment is to evaluate the potential for novel open reading frames (ORFs) that may have homology to known allergens, toxins, or proteins that display adverse biological activity.   Sequences spanning the 5' and 3' genomic DNA-insert DNA junctions, (Figure 17) were translated from stop codon (TGA, TAG, TAA) to stop codon in all six reading frames.   Putative polypeptides from each reading frame, that were eight amino acids or greater in length, were compared to AD_2018, TOX_2018, and PRT_2018 databases using FASTA and to the AD_2018 database using an eight amino acid sliding window search.   A total of 14 putative peptides were compared to allergen (AD_2018), toxin (TOX_2018), and all protein (PRT_2018) databases using bioinformatic tools.

The FASTA sequence alignment tool was used to assess the relatedness between the query sequences and any protein sequence in the AD_2018, TOX_2018, and PRT_2018 databases. Similarities shared between the sequence with each sequence in the database were examined. The extent of relatedness was evaluated by detailed visual inspection of the alignment, the calculated percent identity, and the *E*-score.   Alignments having *E*-scores of $\leq$1e-5 (1×10^{-5}) are deemed significant because they may reflect shared structure and function among sequences.   In addition to sequence similarity, sequences were screened for short peptide matches using a pair-wise comparison algorithm.   In these analyses, eight contiguous and identical amino acids were defined as immunologically relevant, where eight represents the typical minimum sequence length likely to represent an immunological epitope (Silvanovich *et al.*, 2006).

The bioinformatic analysis performed using the 14 putative peptide sequences translated from junctions is theoretical as there is no reason to suspect, or evidence to indicate, the presence of transcripts spanning the flank junctions.   The results of these bioinformatic analyses indicate that no structurally relevant sequence similarities were observed between the 14 putative flank junction derived sequences and allergens, toxins, or biologically active proteins.   As a result, in the unlikely occurrence that any of the 14 peptides analysed herein

is found *in planta*, none would share significant similarity or identity to known allergens, toxins, or other biologically active proteins that could affect human or animal health.
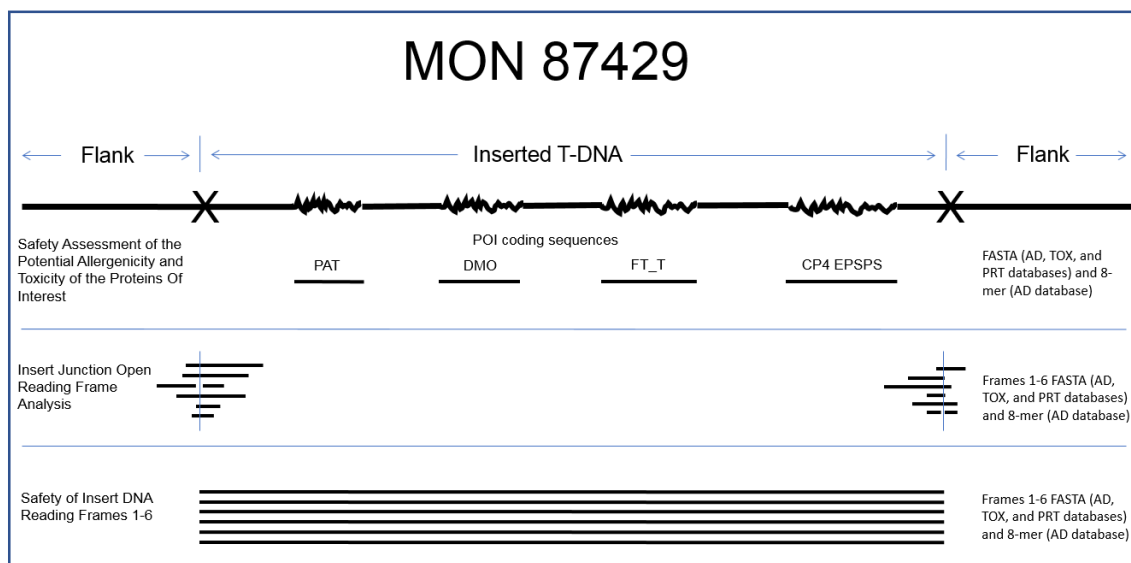
AD= AD_2018, TOX= TOX_2018 and PRT= PRT_2018 (GenBank Release #223); 8-mer= the eight amino acid sliding window search

Figure 17.   Schematic Summary of MON 87429 Bioinformatic Analyses

Bioinformatic Evaluation of Putative Open Reading Frames of MON 87429 Insert and Flanking Sequences Summary and Conclusions

A conservative bioinformatic assessment of potential allergenicity, toxicity and adverse biological activity for putative polypeptides derived from different reading frames of the entire insert MON 87429 or that span the 5' and 3' insert junctions was conducted.   There are no analytical data that indicate any putative polypeptides subjected to bioinformatic evaluation are produced by MON 87429.   Moreover, the data generated from these analyses confirm that even in the highly unlikely occurrence that a translation product other than DMO, PAT, CP4 EPSPS and FT_T proteins was derived from frames 1 to 6 of the insert DNA, or the ORFs spanning the insert junctions; they would not share a sufficient degree of sequence similarity with other proteins to indicate they would be potentially allergenic, toxic, or have other safety implications.   Therefore, there is no evidence for concern regarding the putative polypeptides for MON 87429 relatedness to known toxins, allergens, or biologically active putative peptides.

A3(e)   Family tree or breeding process

The MON 87429 transformation was conducted with inbred maize line LH244, a patented maize line assigned to Holden's Foundation Seeds LLC in 2001 (U.S. Patent #6,252,148). LH244 is a medium season yellow dent maize line with a Stiff Stalk background that is best adapted to the central regions of the U.S. corn belt.

Following transformation of immature LH244 embryos, a single transformed plant was selected and self-crossed to increase seed supplies. A homozygous inbred line was developed through further self-crossing and selection and was then used to produce other MON 87429 lines that were used for product testing, safety assessment studies, and commercial hybrid development. The non-transformed LH244 was used as a conventional maize comparator (hereafter referred to as the conventional control) in the safety assessment of MON 87429. For more details, see MON 87429 breeding history, Figure 12.

Please also refer to Section A3(f)(i).

A3(f)   Evidence of the stability of the genetic changes

A3(f)(i)   Pattern of inheritance of insert and number of generations monitored

Determination of Insert Stability over Multiple Generations of MON 87429

In order to demonstrate the genetic stability of the T-DNA present in MON 87429 through multiple breeding generations, NGS reads from five breeding generations of MON 87429 were mapped to the transformation plasmid for junction identification. The breeding history of MON 87429 is presented in Figure 12, and the specific generations tested are indicated in the figure legend. The MON 87429 (R3) generation was used for the molecular characterisation analyses discussed in Section A3(3)(ii) and shown in Figure 12. To assess stability, four additional generations were evaluated by NGS (Section A3(d)(i)), and compared to the fully characterised MON 87429 R3 generation. The conventional controls used for the generational stability analysis included LH244, LH244 × HCL617 and LH244 × L7126Z which represent similar background genetics to each of the analyzed MON 87429 breeding generations. Genomic DNA isolated from each of the selected generations of MON 87429 and conventional controls were used for mapping and subsequent junction identification (Table 4).

To determine the insert number in the MON 87429 samples, the sequences generated and selected as described above in Section A3(d)(ii) were analyzed to identify junctions. The number of any resultant unique junctions containing the PV-ZMHT519224 DNA sequence determined by this analysis is shown in the table below.

Table 4.   Junction Sequence Classes Detected

Sample	Junction Sequences Detected
MON 87429 (R3)	2
MON 87429 (R3F1)	2
MON 87429 (R4)	2
MON 87429 (R4F1)	2
MON 87429 (R5)	2
LH244	0
LH244 × HCL617	0
LH244 × L7126Z	0

As shown by alignment to the full flank/insert sequence obtained from directed sequencing, a single conserved pair of junctions linked by contiguous known and expected DNA sequence is present in MON 87429 (R3). Two identical junctions are found in each of the breeding generations (R3, R3F1, R4, R4F1, and R5), confirming the insertion of a single copy of PV-ZMHT519224 T-DNA at a single locus in the genome of MON 87429, and the consistency of these junctions in the mapping data across all generations tested demonstrates that this single locus is stably maintained throughout the MON 87429 breeding process.

These results demonstrate that the single locus of integration characterised in the R3 generation of MON 87429 is found in five breeding generations of MON 87429, confirming the stability of the insert. This comprehensive NGS and bioinformatic analysis of NGS data from multiple generations supports the conclusion that MON 87429 contains a single, stable, inserted T-DNA.

Inheritance of the Genetic Insert in MON 87429

The MON 87429 T-DNA resides at a single locus within the maize genome and therefore should be inherited according to Mendelian principles of inheritance. During development of lines containing MON 87429, phenotypic and genotypic segregation data were recorded to assess the inheritance and stability of the MON 87429 T-DNA using Chi square (χ^2) analysis over several generations. The χ^2 analysis is based on comparing the observed segregation ratio to the expected segregation ratio according to Mendelian principles.

The MON 87429 breeding path for generating segregation data is described in Figure 18. The transformed R0 plant was self-pollinated to generate R1 seed. An individual plant homozygous for the MON 87429 T-DNA was identified in the R1 segregating population via a Real-Time TaqMan® PCR assay.

The homozygous positive R1 plant was self-pollinated to give rise to R2 seed. The R2 plants were self-pollinated to produce R3 seed. R3 plants homozygous for the MON 87429 T-DNA were crossed via traditional breeding techniques to a Monsanto proprietary elite inbred parent that did not contain the *dmo*, *pat*, *ft_t*, or *cp4 epsps* coding sequences to produce hemizygous R3F1 seed. The R3F1 plants were crossed again with a Monsanto proprietary elite inbred parent to produce BC1 seed. The BC1 generation was tested for the presence of the MON 87429 T-DNA by Real-Time TaqMan® PCR assay to select for hemizygous MON 87429 plants. At the BC1 generation, the MON 87429 T-DNA was predicted to segregate at a 1:1 ratio (hemizygous positive: homozygous negative) according to Mendelian inheritance principles.

Selection of hemizygous BC1 plants, followed by crossing with the Monsanto proprietary elite inbred parent, followed by testing for the presence of the T-DNA was repeated for two additional generations, to produce hemizygous BC2 seed and hemizygous BC3 seed, each at a predicted 1:1 (hemizygous positive: homozygous negative) segregation ratio according to Mendelian inheritance principles.

A Pearson's chi-square (χ^2) analysis was used to compare the observed segregation ratios of the MON 87429 T-DNA to the expected ratios. The χ^2 analysis was performed using the statistical program R Version 3.3.1 (2016-06-21).

The Chi-square was calculated as:

$$\chi^2 = \sum [(\,|\,o - e\,|\,)^2 / e]$$

where o = observed frequency of the genotype or phenotype and e = expected frequency of the genotype or phenotype. The level of statistical significance was predetermined to be 5% ($\alpha = 0.05$).

The results of the χ^2 analysis of the segregating progeny of MON 87429 are presented in Table 5. The χ^2 value in the BC1, BC2, and BC3 generations indicated no statistically significant difference between the observed and expected segregation ratios of MON 87429 T-DNA. These results support the conclusion that the MON 87429 T-DNA resides at a single locus within the maize genome and is inherited according to Mendelian principles. These results are also consistent with the molecular characterisation data indicating that MON 87429 contains a single intact copy of the T-DNA inserted at a single locus in the maize genome (Sections A3(a)-A3(d)).
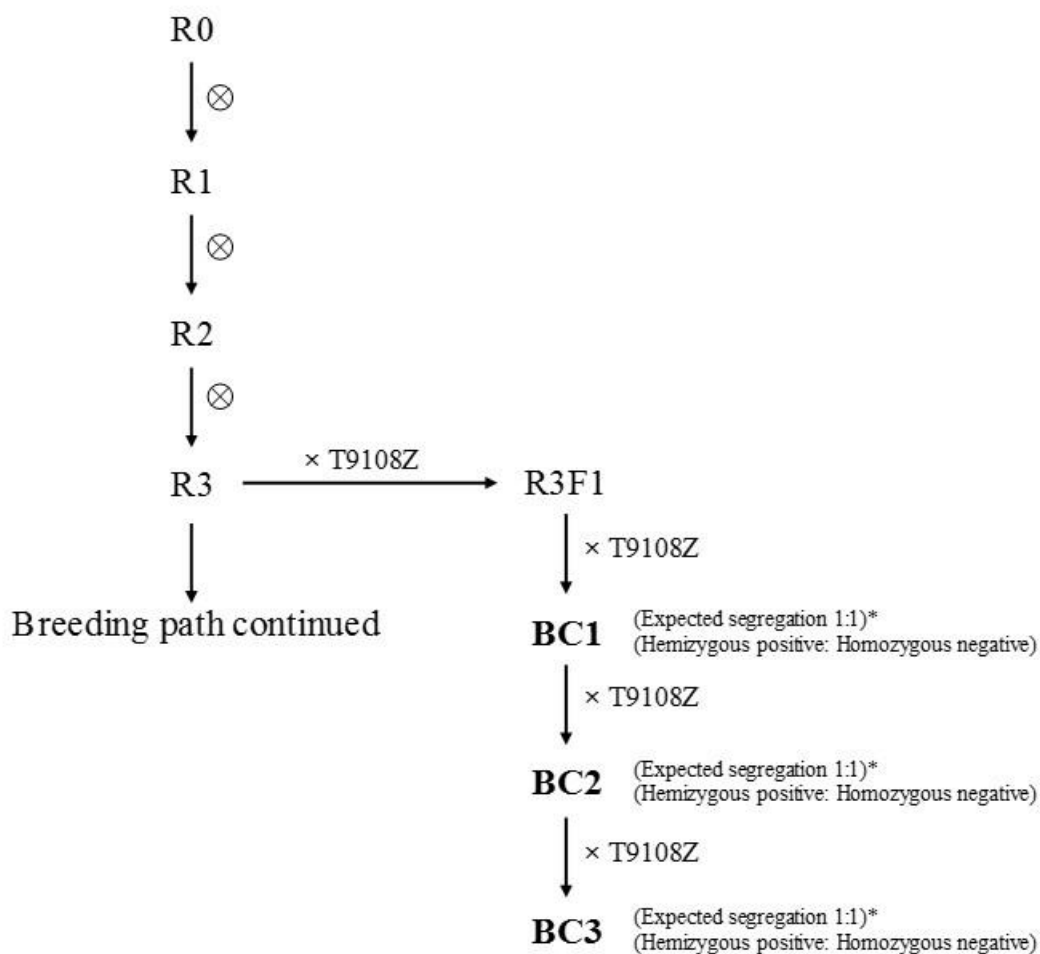
Figure 18.   Breeding Path for Generating Segregation Data for MON 87429

*Chi-square analysis was conducted on segregation data from BC1, BC2, and BC3 generations (bolded text).
Genetic background of R0-R3 generations: LH244
⊗:   Self-Pollinated
BC: Back Cross

Table 5.   Segregation of the Expression Cassette During the Development of MON 87429

Generation	Total Plants	Observed # Plant Positive	Observed # Plant Negative	1:1 Segregation		χ^2	Probability
				Expected # Plant Positive	Expected # Plant Negative		
BC1	309	148	161	154.50	154.50	0.55	0.460
BC2	236	112	124	118.00	118.00	0.61	0.435
BC3	216	97	119	108.00	108.00	2.24	0.134

Characterisation of the Genetic Modification Summary and Conclusion

As described above, characterisation of the genetic modification in MON 87429 was conducted using a combination of sequencing, PCR, and bioinformatics. The results of this characterisation demonstrate that MON 87429 contains a single copy of the intended T-DNA containing the *pat, dmo, ft_t,* and *cp4 epsps* expression cassettes that is stably integrated at a single locus and is inherited according to Mendelian principles over multiple generations. These conclusions are based on the following:

- Molecular characterisation of MON 87429 by NGS demonstrated that MON 87429 contained a single DNA insert. These whole-genome sequence analyses provided a comprehensive assessment of MON 87429 to determine the presence of sequences derived from PV-ZMHT519224 (Kovalic *et al.*, 2012) and demonstrated that MON 87429 contained a single DNA insert with no detectable backbone sequences.

- Directed sequencing (locus-specific PCR, DNA sequencing and analyses) of MON 87429, characterises the complete sequence of the single DNA insert from PV-ZMHT519224, the adjacent flanking DNA, and the 5' and 3' insert-to-flank junctions. This analysis confirmed that the sequence and organisation of the DNA is identical to the corresponding region in the PV-ZMHT519224 T-DNA. Furthermore, the genomic organisation at the insertion site was assessed by comparing the sequences flanking the T-DNA insert in MON 87429 to the sequence of the insertion site in conventional maize.

- Generational stability analysis by NGS demonstrated that the single PV-ZMHT519224 T-DNA insert in MON 87429 has been maintained through five breeding generations, thereby confirming the stability of the T-DNA in MON 87429.

- Segregation data confirm that the inserted T-DNA segregated following Mendelian inheritance patterns, which corroborates the insert stability demonstrated by NGS and independently establishes the nature of the T-DNA at a single chromosomal locus.

Taken together, the characterisation of the genetic modification in MON 87429 demonstrates that a single copy of the intended T-DNA was stably integrated at a single locus of the maize genome and that no plasmid backbone sequences were present in MON 87429.

A3(f)(ii) Pattern of expression of phenotype over several generations

For details, please also refer to ▇▇ 2019 (MSL0030646).

In order to assess the presence of the DMO, PAT (*pat*), FT_T and CP4 EPSPS protein in MON 87429 across multiple breeding generations, Western blot analysis of MON 87419 was conducted on seed tissue collected from generations R3, R3F1, R4, R4F1, and R5 of MON 87429, using seed tissue of the conventional control (LH244) as negative control.

The presence of the DMO protein was demonstrated in five breeding generations of MON 87429 using Western blot analysis. The *E. coli*-produced DMO protein reference

standard (10 ng) was used as a reference for the positive identification of the DMO protein Figure 19, lane 2). The presence of the DMO protein in grain tissue samples of MON 87429 was determined by visual comparison of the bands detected in five breeding generations (Figure 19, lanes 4-8) to the *E. coli*-produced DMO protein reference standard. The MON 87429-produced DMO protein migrated indistinguishably from that of the *E. coli*-produced protein standard analyzed on the same Western blot. As expected, the DMO protein was not detected in the conventional control grain extract (Figure 19, lane 9).

The presence of the PAT (*pat*) protein was demonstrated in five breeding generations of MON 87429 using Western blot analysis. The *E. coli*-produced PAT protein reference standard (10 ng) was used as a reference for the positive identification of the PAT (*pat*) protein (Figure 20, lane 2). The presence of the PAT (*pat*) protein in grain tissue samples of MON 87429 was determined by visual comparison of the bands detected in five breeding generations (Figure 20, lanes 4-8) to the *E. coli*-produced PAT (*pat*) protein reference standard. The MON 87429-produced PAT (*pat*) protein migrated indistinguishably from that of the *E. coli*-produced protein standard analyzed on the same Western blot. As expected, the PAT (*pat*) protein was not detected in the conventional control grain extract (Figure 20, lane 9).

The presence of the FT_T protein was demonstrated in five breeding generations of MON 87429 using Western blot analysis. The *E. coli*-produced FT_T protein reference standard (10 ng) was used as a reference for the positive identification of the FT_T protein (Figure 21, lane 2). The presence of the FT_T protein in grain tissue samples of MON 87429 was determined by visual comparison of the bands detected in five breeding generations (Figure 21, lanes 4-8) to the *E. coli*-produced FT_T protein reference standard. The MON 87429-produced FT_T protein migrated indistinguishably from that of the *E. coli*-produced protein standard analyzed on the same Western blot. As expected, the FT_T protein was not detected in the conventional control grain extract (Figure 21, lane 9).

The presence of the CP4 EPSPS protein was demonstrated in five breeding generations of MON 87429 using Western blot analysis. The *E. coli*-produced CP4 EPSPS protein reference standard (10 ng) was used as a reference for the positive identification of the CP4 EPSPS protein (Figure 22, lane 2). The presence of the CP4 EPSPS protein in grain tissue samples of MON 87429 was determined by visual comparison of the bands detected in five breeding generations (Figure 22, lanes 4-8) to the *E. coli*-produced CP4 EPSPS protein reference standard. The MON 87429-produced CP4 EPSPS protein migrated indistinguishably from that of the *E. coli*-produced protein standard analyzed on the same Western blot. As expected, the CP4 EPSPS protein was not detected in the conventional control grain extract (Figure 22, lane 9).

Lane 1 2 3 4 5 6 7 8 9 10
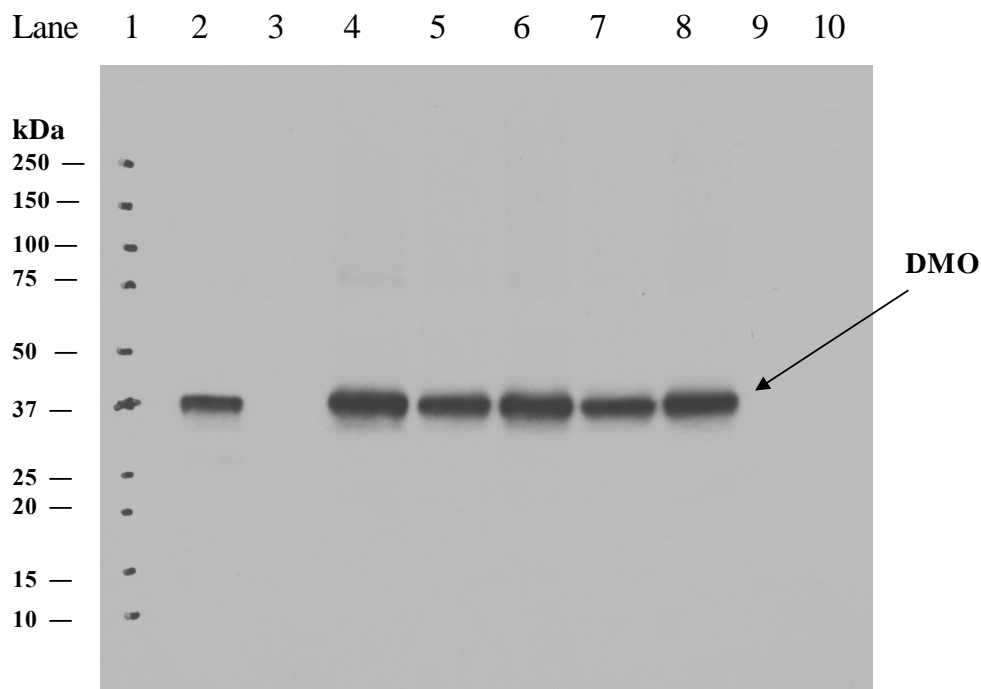
Figure 19.   Presence of DMO Protein in Multiple Generations of MON 87429

Blot probed with monoclonal anti-DMO primary antibodies and HRP conjugated anti-mouse IgG secondary antibodies. Exposure time was 10 seconds. The approximate MWs (kDa) of the Precision Plus Protein Standards were shown on the left.

Lane	Description	Amount Loaded
1	Precision Plus Protein Standards	5 µl
2	*E. coli*-produced DMO protein	10 ng
3	Empty	0
4	MON 87429, R3, 11464932	10 µl
5	MON 87429, R3F1, 11464934	10 µl
6	MON 87429, R4, 11464931	10 µl
7	MON 87429, R4F1, 11465707	10 µl
8	MON 87429, R5, 11465738	10 µl
9	Conventional Control, 11464930	10 µl
10	Empty	0
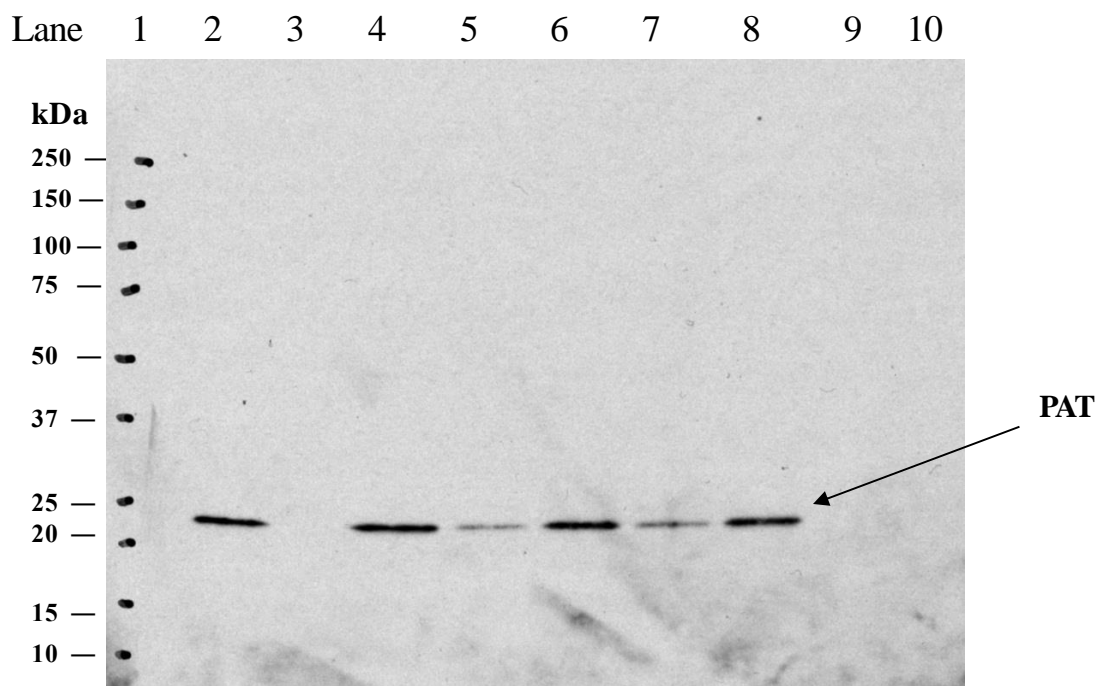
Figure 20.   Presence of PAT (*pat*) Protein in Multiple Generations of MON 87429

Blot probed with monoclonal anti-PAT primary antibodies and HRP conjugated anti-mouse IgG secondary antibodies. Exposure time was 15 seconds. The approximate MWs (kDa) of the Precision Plus Protein Standards were shown on the left.

Lane	Description	Amount Loaded
1	Precision Plus Protein Standards	5 µl
2	*E. coli*-produced PAT (*pat*) protein	10 ng
3	Empty	0
4	MON 87429, R3, 11464932	10 µl
5	MON 87429, R3F1, 11464934	10 µl
6	MON 87429, R4, 11464931	10 µl
7	MON 87429, R4F1, 11465707	10 µl
8	MON 87429, R5, 11465738	10 µl
9	Conventional Control, 11464930	10 µl
10	Empty	0
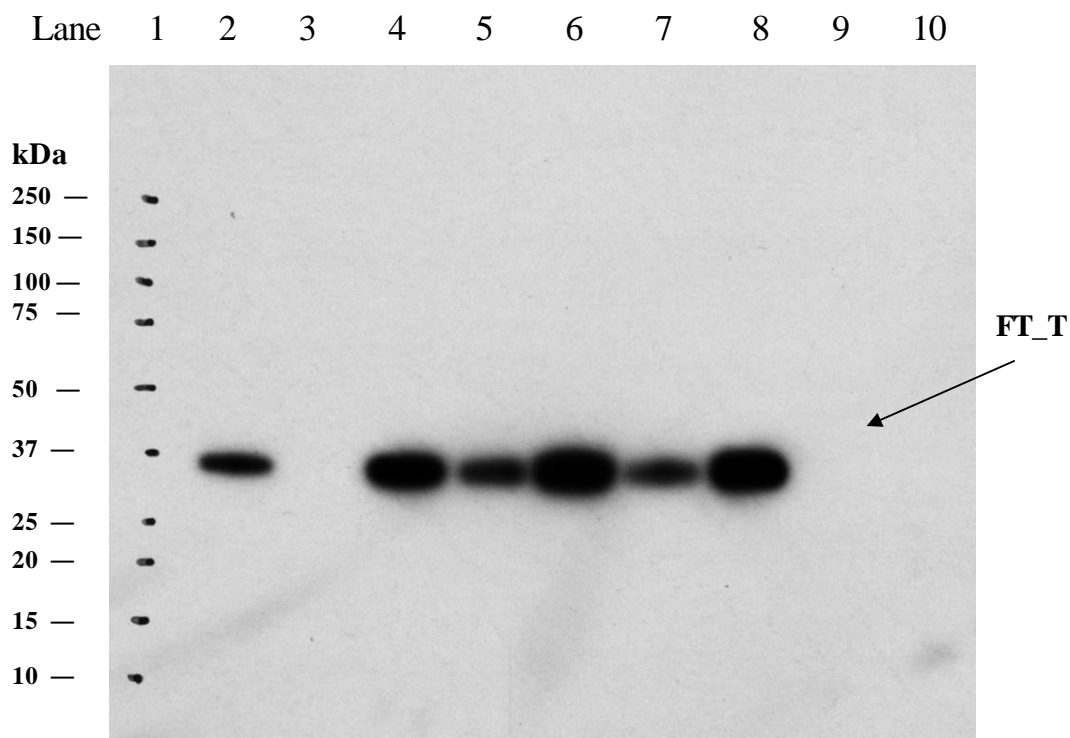
Figure 21.   Presence of FT_T Protein in Multiple Generations of MON 87429

Blot probed with monoclonal anti-FT_T primary antibodies and HRP conjugated anti-mouse IgG secondary antibodies. Exposure time was 15 seconds. The approximate MWs (kDa) of the Precision Plus Protein Standards were shown on the left.

Lane	Description	Amount Loaded
1	Precision Plus Protein Standards	5 µl
2	*E. coli*-produced FT_T protein	10 ng
3	Empty	0
4	MON 87429, R3, 11464932	10 µl
5	MON 87429, R3F1, 11464934	10 µl
6	MON 87429, R4, 11464931	10 µl
7	MON 87429, R4F1, 11465707	10 µl
8	MON 87429, R5, 11465738	10 µl
9	Conventional Control, 11464930	10 µl
10	Empty	0
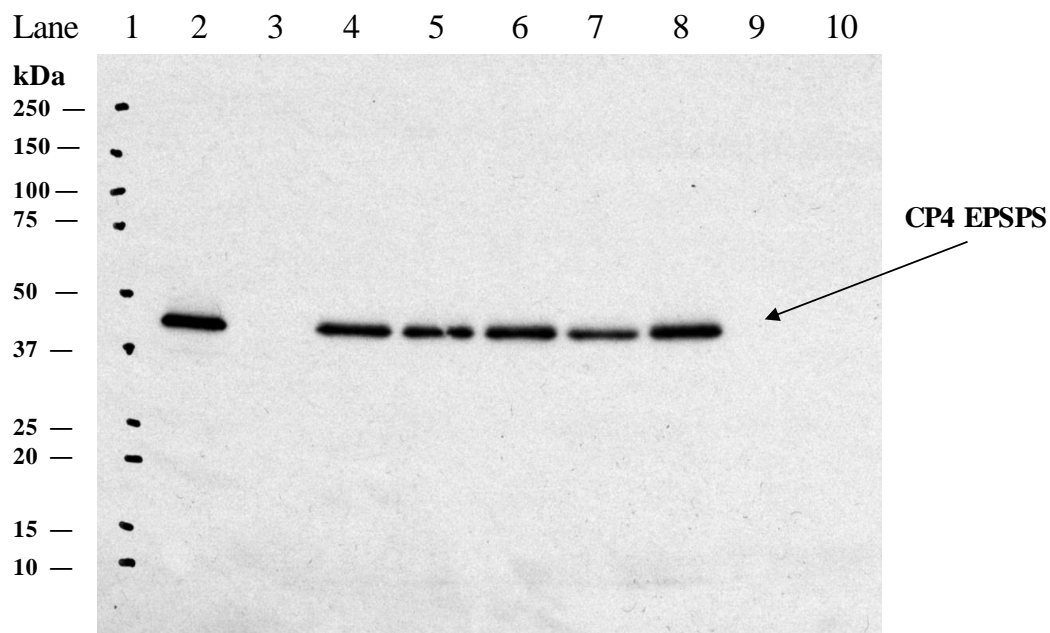
Figure 22.   Presence of CP4 EPSPS Protein in Multiple Generations of MON 87429

Blot probed with goat anti-CP4 EPSPS primary antibodies and HRP conjugated anti-goat IgG secondary antibodies. Exposure time was 30 seconds. The approximate MWs (kDa) of the Precision Plus Protein Standards were shown on the left.

Lane	Description	Amount Loaded
1	Precision Plus Protein Standards	5 µl
2	*E. coli*-produced CP4 EPSPS protein	10 ng
3	Empty	0
4	MON 87429, R3, 11464932	10 µl
5	MON 87429, R3F1, 11464934	10 µl
6	MON 87429, R4, 11464931	10 µl
7	MON 87429, R4F1, 11465707	10 µl
8	MON 87429, R5, 11465738	10 µl
9	Conventional control, 11464930	10 µl
10	Empty	0

A4   Analytical Method for Detection

The event-specific DNA-based detection methods such as PCR can be used as the monitoring tool to determine the presence of MON 87429 in a collected sample.

B.   INFORMATION RELATED TO THE SAFETY OF THE GM FOOD

B1   Equivalence Studies

B1(a)   Characterisation and equivalence of MON 87429-produced DMO protein

For details, please also refer to ████████, 2018 (MSL0029510).

Identity and Function of the DMO Protein

DMO proteins have been isolated from the bacterium *S. maltophilia* strain DI-6 (Herman *et al.*, 2005; Krueger *et al.*, 1989; Palleroni and Bradbury, 1993).   MON 87429 expresses the DMO protein to confer tolerance to dicamba herbicide.   DMO is an enzyme that catalyzes the demethylation of dicamba to the non-herbicidal compounds 3,6-dichlorosalicylic acid (DCSA) and formaldehyde (Chakraborty *et al.*, 2005).   DCSA is a known metabolite of dicamba in cotton, soybean, soil, and livestock, whose safety has been evaluated by the FAO-WHO and EPA (FAO-WHO, 2011a; U.S. EPA, 2009).   The other reaction product, formaldehyde, is found naturally in many plants at levels up to several hundred ppm (Adrian-Romero *et al.*, 1999).

MON 87429 DMO is targeted to chloroplasts by a chloroplast transit peptide (CTP) to allow co-localization with the endogenous reductase and ferredoxin enzymes that supply electrons for the DMO demethylation reaction as described by Behrens *et al.* (2007).   In the construction of the plasmid vector used in the development of MON 87429, PV-ZMHT519224, the *Albino and pale green 6* (*Apg6)* chloroplast transit peptide coding sequence from *Arabidopsis thaliana* (*APG6*, Table 2) was joined to the *dmo* coding sequence; this coding sequence results in the production of a precursor protein consisting of the DMO protein and a N-terminal 68 amino acid chloroplast transit peptide APG6, which is utilized to target the precursor protein to the chloroplast (Herrmann, 1995; Klee *et al.*, 1987). Typically, transit peptides are precisely removed from the precursor protein following delivery to the targeted plastid (della-Cioppa *et al.*, 1986) resulting in the full length protein. However, there are examples in the literature of alternatively processed forms of a protein targeted to a plant's chloroplast (Behrens *et al.*, 2007; Clark and Lamppa, 1992).   Data from N-terminal sequencing analysis of the MON 87429-produced DMO indicate that processing of the DMO precursor protein expressed in MON 87429 produced two isoforms of the mature MON 87429 DMO protein that differ by a single, additional amino acid at the N-terminus that is derived from the chloroplast transit peptide APG6. Because the single amino difference between the two isoforms of the DMO protein expressed in MON 87429 (designated DMO+1 and DMO+0) is minor and indistinguiable by Coomassie stain and Western blot analysis of SDS-PAGE gels, MON 87429 DMO protein will be used to refer to both forms of the protein collectively and distinctions will only be made, where necessary.

Except for the single amino acid derived from the chloroplast transit peptide APG6 at the N-terminus for MON 87429 DMO+1 and an additional leucine at position two, the MON 87429 DMO protein has an identical sequence to the wild-type DMO protein from the DI-6 strain of *S. maltophilia* (Herman *et al.*, 2005) (Figure 23).   The MON 87429 DMO proteins are identical to MON 88701 DMO (FSANZ approval A1080), except for the amino acid encoded by the *AGP6* gene at the N-terminus, and 9 amino acids encoded by the *CTP2* gene for

MON 88701 DMO. The MON 87429 DMO proteins are also identical to MON 87708 DMO (fully processed; FSANZ approval A1063), except for an addition of the single amino acid encoded by the *APG6* gene at the N-terminus for MON 87429 DMO+1, a methionine that remained at the N-terminus from the *dmo* gene, and two single amino acid changes at positions 2 and 112 (Figure 23). The differences in the amino acid sequence between the wild-type DMO, MON 88701 DMO, MON 87708 DMO and MON 87429 DMO proteins are not anticipated to have an effect on the structure of the catalytic site, functional activity, immunoreactivity or specificity because the N-terminus and position two are sterically distant from the catalytic site (D'Ordine *et al.*, 2009; Dumitru *et al.*, 2009).

In order to confirm that the minor differences in amino acid sequences observed in the MON 87429 DMO protein do not impact the selectivity for dicamba herbicide as compared to potential endogenous substrates, the potential for MON 87429 DMO to catabolize *o*-anisic acid was evaluated using the same qualitative assay used to evaluate the selectivity of MON 87708 DMO (A1063). Although *o*-anisic acid is not known to be present in corn, this substance was chosen for this confirmatory experiment since, among the five substrates used in the original study supporting MON 87708 A1063, which included ferulic acid, *o*-anisic acid, sinapic acid, syringic acid, and vanillic acid; *o*-anisic acid is the substrate that is most structurally similar to dicamba. The results were similar to the previously reported results for MON 87708 DMO, in that no new peaks indicative of the predicted demethylated product were observed, confirming that the MON 87429 DMO did not catabolize *o*-anisic acid. Taken together with the previously reported results, these data demonstrate that MON 87429 DMO has a high specificity for dicamba as a substrate.
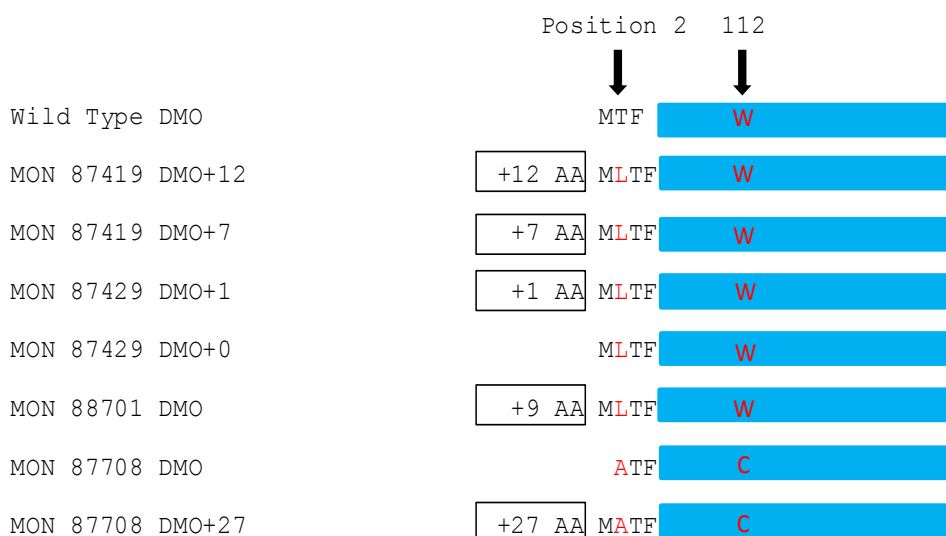
Figure 23.   Forms of DMO Protein and Their Relation to the Wild-Type DMO Protein

The diagram represents the various DMO forms discussed in this section.   The blue regions indicate regions of 100% amino acid identity.   The wild-type DMO form isolated from *S. maltophilia* was the first form sequenced (Herman *et al.*, 2005).   The MON 87419 DMO proteins are identical to wild-type DMO, except for the insertion of a leucine at position 2 and the amino acids derived from the C-terminal transit peptides at the N-terminus, which are 12 and 7 amino acids encoded by the *CTP4* gene at the N-terminus for MON 87419 DMO+12 and MON 87419 DMO+7, respectively.   The MON 87429 DMO proteins are identical to wild-type DMO, except for the insertion of a leucine at position 2 and an addition of 1 amino acid encoded by the *AGP6* gene at the N-terminus for MON 87429 DMO+1.   The MON 88701 DMO protein is identical to wild-type DMO, except for an insertion of a leucine at position 2, and an addition of 9 amino acids encoded by the *CTP2* gene at the N-terminus.   The MON 87708 DMO proteins are identical to wild-type DMO, except for the insertion of an alanine at position 2, a single amino acid change at position 112 (tryptophan to cysteine) and an additional 27 amino acids encoded by the *RbcS* gene at the N-terminus for MON 87708 DMO+27.   The MON 87708 DMO (fully processed) protein additionally lacks a lead methionine residue.   Position refers to amino acid residues as wild type DMO and boxed regions correspond to C-terminal transit peptides.

Equivalence Studies of the DMO Protein

The safety assessment of crops derived through biotechnology includes characterisation of the physicochemical and functional properties of and confirmation of the safety of the introduced protein(s). For the safety data generated using *E. coli*-produced DMO to be applicable to MON 87429 DMO protein (plant-produced DMO), the equivalence of the plant- and *E. coli*-produced proteins must first be demonstrated. To assess the equivalence between MON 87429-produced DMO and *E. coli*-produced DMO proteins, a small quantity of the MON 87429 DMO protein was purified from grain of MON 87429 maize. The MON 87429-produced DMO protein was characterised and the equivalence of the physicochemical characteristics and functional activity between the MON 87429-produced DMO and the *E. coli*-produced DMO proteins was assessed using a panel of six analytical tests as shown in Table 6. Taken together, these data provide a detailed characterisation of the MON 87429-produced DMO protein and establish the equivalence of MON 87429-produced DMO and *E. coli*-produced DMO proteins.

Table 6.   Summary of MON 87429 DMO Protein Identity and Equivalence

Analytical Test Assessment	Section Cross Reference	Analytical Test Outcome
1. N-terminal sequence	B1 (a)(i)	The N-terminal sequences of two forms of DMO proteins were identified, referred to as MON 87429 DMO+1 and MON 87429 DMO+0
2. Nano LC-MS/MS[1]	B1 (a)(ii)	Nano LC-MS/MS[1] analysis yielded peptide masses consistent with the peptide masses from the theoretical trypsin digest of the MON 87429-produced DMO sequence
3. Western blot analysis	B1 (a)(iii)	MON 87429-produced DMO protein identity was confirmed using a Western blot probed with an antibody specific for DMO proteins Immunoreactive properties of the MON 87429-produced DMO and the *E. coli*-produced DMO proteins were shown to be equivalent
4. Apparent molecular weight (MW)	B1 (a)(iv)	Electrophoretic mobility and apparent molecular weight of the MON 87429-produced DMO and the *E. coli*-produced DMO proteins were shown to be equivalent
5. Glycosylation analysis	B1 (a)(v)	MON 87429-produced DMO and the *E. coli*-produced DMO proteins were both shown to not be glycosylated
6. Functional activity	B1 (a)(vi)	Functional activity of the MON 87429-produced DMO and the *E. coli*-produced DMO proteins were shown to be equivalent

[1] Nano LC-MS/MS = Nanoscale liquid chromatography coupled to tandem mass spectrometry
[2] SDS-PAGE = sodium dodecyl sulfate-polyacrylamide gel electrophoresis

A summary of the data obtained to support the characterisation of the MON 87429-produced DMO and a conclusion of protein equivalence is below.

B1(a)(i)   Results of the N-terminal sequencing analysis

The expected N-terminal sequence for the DMO protein deduced from the *dmo* gene present in maize of MON 87429 was observed by LC-MS/MS.   The experimentally determined sequence corresponds to the deduced DMO protein beginning at the initial cysteine position (DMO+1) (Figure 24).   The cysteine is derived from a chloroplast transit peptide (CTP).   In addition, the mature form of the DMO protein without the cysteine (DMO+0) was also observed (data not shown).   Two forms are indistinguishable by SDS-PAGE due to only one amino acid difference (Figure 24).   Alternative cleavage of CTP from DMO in *planta* by a general stromal processing peptidase is common (Richter and Lamppa, 1998).   The N-terminal sequencing results for MON 87429-produced DMO protein were consistent with the sequencing results for the *E. coli*-produced DMO protein (Figure 24).   Hence, the sequence information confirms the identity of the DMO protein isolated from the grain of MON 87429.

DMO + 1

Amino Acid Residue # from the N-terminus →	1	2	3	4	5	6	7	8	9	10	11	12	13	14	15
E. coli-produced DMO+1 Sequence →	C	M	L	T	F	V	R	N	A	W	Y	V	A	A	L
	|	|	|	|	|	|	|	|	|	|	|	|	|	|	|
Expected DMO+1 Sequence →	C	M	L	T	F	V	R	N	A	W	Y	V	A	A	L
	|	|	|	|	|	|	|	|	|	|	|	|	|	|	|
MON 87429 Experimental Sequence →	C	M	L	T	F	V	R	N	A	W	Y	V	A	A	L

DMO+0

Amino Acid Residue # from the N-terminus →	1	2	3	4	5	6	7	8	9	10	11	12	13	14	15
E. coli-produced DMO+0 Sequence →	M	L	T	F	V	R	N	A	W	Y	V	A	A	L	P
	|	|	|	|	|	|	|	|	|	|	|	|	|	|	|
Expected DMO+0 Sequence →	M	L	T	F	V	R	N	A	W	Y	V	A	A	L	P
	|	|	|	|	|	|	|	|	|	|	|	|	|	|	|
MON 87429 Experimental Sequence →	M	L	T	F	V	R	N	A	W	Y	V	A	A	L	P

Figure 24.   N-Terminal Sequence of the MON 87429-Produced DMO Protein

The experimental sequence obtained from the MON 87429 produced DMO was compared to the expected sequence deduced from the *dmo* gene present in MON 87429.   The N-terminal sequence of the *E. coli*-produced MON 87429 DMO protein was also obtained by Nano LC-MS/MS peptide analysis.   The single letter International Union of Pure and Applied Chemistry International Union of Biochemistry (IUPAC-IUB) amino acid code is C, cysteine; M, methionine; L, leucine; T, threonine; F, phenylalanine; V, valine: R, arginine; N, asparagine; A, alanine; W, tryptophan; Y, tyrosine.

B1(a)(ii)   Results of nano LC-MS/MS mass fingerprint analysis

Peptide mass fingerprint analysis is a standard technique used for confirming the identity of proteins. The ability to identify a protein using this method is dependent upon matching a sufficient number of observed tryptic peptide fragment masses with predicted tryptic peptide fragment masses. In general, protein identification made by peptide mapping is considered to be reliable if >40% of the protein sequence was identified by matching experimental masses observed for the tryptic peptide fragments to the expected masses for the fragments (Biron *et al.*, 2006; Krause *et al.*, 1999). The identity of the MON 87429-produced DMO protein was confirmed by LC-MS/MS analysis of peptide fragments produced by the trypsin digestion of the MON 87429 produced DMO protein.

There were 39 unique peptides identified that corresponded to the masses expected to be produced by trypsin digestion of the MON 87429-produced DMO protein, including two N-terminal peptides with and without the N-terminal cysteine (Table 7).   The identified masses were used to assemble a coverage map of the MON 87429-produced DMO protein (Figure 25).   The experimentally determined coverage of the MON 87429 produced DMO substance was 86% (294 out of 341 amino acids, Figure 25A).   This analysis further confirms the identity of MON 87429 produced DMO protein.

There were 47 unique peptides identified that corresponded to the masses expected to be produced by trypsin digestion of the *E. coli*-produced DMO protein (Table 8).   Similar to the MON 87429-produced DMO, two N-terminal peptides with and without the N-terminal cysteine were also detected.   The identified masses were used to assemble a coverage map of the *E. coli*-produced DMO protein (Figure 25).   The experimentally determined coverage of the *E. coli*-produced DMO protein was 100% (341 out of 341 amino acids, Figure 25B). This analysis further confirms the identity of the *E. coli*-produced DMO protein.

Table 7. Summary of the Tryptic Masses Identified for the MON 87429-Produced DMO Using Nano LC-MS/MS[1]

Experimental Mass[2]	Calculated Mass[3]	Difference[4]	Fragment[5]	Sequence[6]
925.4512	925.4514	-0.0002	1 - 7	CMLTFVR
3049.5488	3049.5517	-0.0029	1 - 26	CMLT...PLGR
765.4206	765.4207	-0.0001	2 -7	MLTFVR
2889.5200	2889.5211	-0.0011	2 - 26	MLTF...PLGR
2142.1107	2142.1109	-0.0002	8 - 26	NAWY...PLGR
1274.7243	1274.7234	0.0009	27 - 37	TILD...ALYR
3016.6267	3016.6168	0.0099	27 - 53	TILD...CPHR
1759.9029	1759.9039	-0.001	38 - 53	QPDG...CPHR
832.4452	832.4443	0.0009	100 - 106	SFPVVER
3536.7581	3536.7551	0.003	100 - 131	SFPV...FGCR
2722.3238	2722.3214	0.0024	107 - 131	DALI...FGCR
719.3598	719.3602	-0.0004	132 - 137	VDPAYR
1468.6416	1468.6405	0.0011	138 - 150	TVGG...CNYK
1993.0196	1993.0204	-0.0008	151 - 167	LLVD...YVHR
1107.4957	1107.4945	0.0012	168 - 177	ANAQ...AFDR
1505.7230	1505.7222	0.0008	168- 180	ANAQ...RLER
1500.7884	1500.7858	0.0026	181 - 194	EVIV...ALMK
2652.4222	2652.423	-0.0008	181 - 206	EVIV...LMAK
1169.6487	1169.6478	0.0009	195 - 206	IPGG...LMAK
1585.9010	1585.9014	-0.0004	195 - 209	IPGG...KFLR
1427.6803	1427.6793	0.001	210 - 222	GANT...NDIR
1855.8986	1855.8965	0.0021	210 - 225	GANT...RWNK
3581.8085	3581.8089	-0.0004	210 - 242	GANT...GTPK
2172.1385	2172.1401	-0.0016	223 - 242	WNKV...GTPK
1743.9221	1743.9229	-0.0008	226 - 242	VSAM...GTPK
2581.3288	2581.3322	-0.0034	226 - 249	VSAM...IHSR
855.4198	855.4199	-0.0001	243 - 249	EQSIHSR

Table 7. **Summary of the Tryptic Masses Identified for the MON 87429-Produced DMO Using Nano LC-MS/MS[1] (continued)**

Experimental Mass[2]	Calculated Mass[3]	Difference[4]	Fragment[5]	Sequence[6]
2396.0846	2396.0856	-0.001	250 - 270	GTHI...GSSR
1576.7219	1576.7192	0.0027	271 - 284	NFGI...GVLR
1029.5611	1029.5607	0.0004	285 - 293	SWQA...ALVK
1401.7202	1401.7252	-0.005	285 - 296	SWQA...KEDK
2297.2394	2297.2379	0.0015	285 - 304	SWQA...AIER
1285.6876	1285.6878	-0.0002	294 - 304	EDKV...AIER
1441.7905	1441.7889	0.0016	294 - 305	EDKV...IERR
913.5241	913.5233	0.0008	297 - 304	VVVEAIER
2292.0954	2292.099	-0.0036	307 - 327	AYVE...AAVR
1613.8628	1613.8624	0.0004	328 - 341	VSRE...LEAA
1271.6611	1271.6608	0.0003	331 - 341	EIEK...LEAA
772.3963	772.3967	-0.0004	335 - 341	LEQLEAA

[1] All imported values were rounded to 4 decimal places.

[2] Only experimental masses that matched calculated masses with the highest scores (Mascot ion score) are listed in the table.

[3] The calculated mass is the relative molecular mass calculated from the matched peptide sequence.

[4] The calculated difference = experimental mass – calculated mass.

[5] Position refers to amino acid residues within the predicted MON 87429-produced DMO sequence as depicted in Figure 25.

[6] For peptide matching greater than nine amino acids in length, the first 4 residues and last 4 residues are shown separated by three dots (...).

Table 8. Summary of the Tryptic Masses Identified for *E. coli*-produced DMO Protein Using Nano LC-MS/MS[1]

Experimental Mass[2]	Calculated Mass[3]	Difference[4]	Fragment[5]	Sequence[6]
925.4522	925.4514	0.0008	1 –7	CMLTFVR
3049.5500	3049.5517	-0.0017	1- 26	CMLT…PLGR
765.4209	765.4207	0.0002	2 - 7	MLTFVR
2889.5170	2889.5211	-0.0041	2 - 26	MLTF…PLGR
2142.1156	2142.1109	0.0047	8 - 26	NAWY…PLGR
1274.7236	1274.7234	0.0002	27 - 37	TILD...ALYR
3016.6182	3016.6168	0.0014	27 - 53	TILD...CPHR
1759.9029	1759.9039	-0.001	38- 53	QPDG...CPHR
4934.3514	4934.3631	-0.0117	54 - 99	FAPL…LNVR
832.4435	832.4443	-0.0008	100 - 106	SFPVVER
3536.7529	3536.7551	-0.0022	100 - 131	SFPV...FGCR
4238.1071	4238.1048	0.0023	100 - 137	SFPV…PAYR
2722.3236	2722.3214	0.0022	107 - 131	DALI…FGCR
3423.6708	3423.6710	-0.0002	107 - 137	DALI…PAYR
719.3601	719.3602	-0.0001	132 - 137	VDPAYR
1468.6413	1468.6405	0.0008	138 - 150	TVGG…CNYK
1993.0178	1993.0204	-0.0026	151 - 167	LLVD…YVHR
1107.4948	1107.4945	0.0003	168 - 177	ANAQ…AFDR
1505.7237	1505.7222	0.0015	168 - 180	ANAQ...RLER
2988.5012	2988.4975	0.0037	168 - 194	ANAQ...ALMK
1500.7854	1500.7858	-0.0004	181 - 194	EVIV…ALMK
2652.4213	2652.4230	-0.0017	181 - 206	EVIV…LMAK
1169.6488	1169.6478	0.001	195 - 206	IPGG…LMAK
1585.9000	1585.9014	-0.0014	195 - 209	IPGG…KFLR
1843.9330	1843.9329	0.0001	207 - 222	FLRG…NDIR
1427.6800	1427.6793	0.0005	210 - 222	GANT…NDIR
1855.8976	1855.8965	0.0011	210 - 225	GANT…RWNK
3581.7984	3581.8089	-0.0105	210 - 242	GANT…GTPK
2172.1410	2172.1401	0.0009	223 - 242	WNKV…GTPK
1743.9255	1743.9229	0.0026	226- 242	VSAM…GTPK
2581.3328	2581.3322	0.0006	226 - 249	VSAM…IHSR
855.4197	855.4199	-0.0002	243 - 249	EQSIHSR
3233.4929	3233.4949	-0.002	243 - 270	EQSI…GSSR
2396.0873	2396.0856	0.0017	250 - 270	GTHI…GSSR
1576.7197	1576.7192	0.0005	271 - 284	NFGI…GVLR
1029.5610	1029.5607	0.0003	285 - 293	SWQA…ALVK
1401.7267	1401.7252	0.0015	285 - 296	SWQA…KEDK
2297.2359	2297.2379	-0.002	285 - 304	SWQA…AIER

Table 8.   Summary of the Tryptic Masses Identified for *E. coli*-produced DMO Protein Using Nano LC-MS/MS[1] (continued)

Experimental Mass[2]	Calculated Mass[3]	Difference[4]	Fragment[5]	Sequence[6]
1285.6884	1285.6878	0.0006	294 - 304	EDKV...AIER
1441.7903	1441.7889	0.0014	294 - 305	EDKV…IERR
913.5239	913.5233	0.0006	297 - 304	VVVEAIER
1069.6250	1069.6244	0.0006	297 - 305	VVVE…IERR
2448.2041	2448.2002	0.0039	306 - 327	RAYV…AAVR
2292.1065	2292.0990	0.0075	307 - 327	AYVE…AAVR
859.4771	859.4763	0.0008	328 - 334	VSREIEK
1613.8626	1613.8624	0.0002	328 - 341	VSRE…LEAA
1271.6614	1271.6608	0.0006	331 - 341	EIEK…LEAA

[1] All imported values were rounded to 4 decimal places.

[2] Only experimental masses that matched calculated masses with the highest scores (Mascot ion score) are listed in the table.

[3] The calculated mass is the relative molecular mass calculated from the matched peptide sequence.

[4] The calculated difference = experimental mass – calculated mass.

[5] Position refers to amino acid residues within the predicted *E. coli*-produced DMO sequence as depicted in Figure 25.

[6] For peptide matching greater than nine amino acids in length, the first 4 residues and last 4 residues are shown separated by three dots (...).

(A)

1 CMLTFVRNAW YVAALPEELS EKPLGRTILD TPLALYRQPD GVVAALLDIC

51 PHRFAPLSDG ILVNGHLQCP YHGLEFDGGG QCVHNPHGNG ARPASLNVRS

101 FPVVERDALI WIWPGDPALA DPGAIPDFGC RVDPAYRTVG GYGHVDCNYK

151 LLVDNLMDLG HAQYVHRANA QTDAFDRLER EVIVGDGEIQ ALMKIPGGTP

201 SVLMAKFLRG ANTPVDAWND IRWNKVSAML NFIAVAPEGT PKEQSIHSRG

251 THILTPETEA SCHYFFGSSR NFGIDDPEMD GVLRSWQAQA LVKEDKVVVE

301 AIERRRAYVE ANGIRPAMLS CDEAAVRVSR EIEKLEQLEA A

(B)

1 CMLTFVRNAW YVAALPEELS EKPLGRTILD TPLALYRQPD GVVAALLDIC

51 PHRFAPLSDG ILVNGHLQCP YHGLEFDGGG QCVHNPHGNG ARPASLNVRS

101 FPVVERDALI WIWPGDPALA DPGAIPDFGC RVDPAYRTVG GYGHVDCNYK

151 LLVDNLMDLG HAQYVHRANA QTDAFDRLER EVIVGDGEIQ ALMKIPGGTP

201 SVLMAKFLRG ANTPVDAWND IRWNKVSAML NFIAVAPEGT PKEQSIHSRG

251 THILTPETEA SCHYFFGSSR NFGIDDPEMD GVLRSWQAQA LVKEDKVVVE

301 AIERRRAYVE ANGIRPAMLS CDEAAVRVSR EIEKLEQLEA A

Figure 25.   Peptide Map of the MON 87429-Produced DMO and *E. coli*-Produced DMO

(A)   The amino acid sequence of the MON 87429-produced DMO protein was deduced from the *dmo* gene present in MON 87429.   Boxed regions correspond to peptides that were identified from the MON 87429-produced DMO protein sample using Nano LC-MS/MS.   In total, 86% coverage (294 out of 341 amino acids) of the expected protein sequence was covered by the identified peptides.

(B) The amino acid sequence of the *E. coli*-produced DMO protein was deduced from the *dmo* gene that is contained on the expression plasmid.   Boxed regions correspond to peptides that were identified from the test substance sample using Nano LC-MS/MS.   In total, 100% (341 out of 341 amino acids) of the expected protein sequence was identified.

B1(a)(iii) Results of Western blot analysis of the MON 87429 DMO protein isolated from the grain of MON 87429 and immunoreactivity comparison to *E. coli*-produced DMO

Western blot analysis was conducted using goat anti-DMO polyclonal antibody as additional means to confirm the identity of the DMO protein isolated from the grain of MON 87429 and to assess the equivalence of the immunoreactivity of the MON 87429-produced and *E. coli*-produced DMO proteins.

The results showed that immunoreactive bands with the same electrophoretic mobility were present in all lanes loaded with the MON 87429-produced and *E. coli*-produced DMO proteins (Figure 26). For each amount loaded, comparable signal intensity was observed between the MON 87429-produced and *E. coli*-produced DMO protein bands. As expected, the signal intensity increased with increasing load amounts of the MON 87429-produced and *E. coli*-produced DMO proteins, thus, supporting identification of the MON 87429-produced DMO protein.

To compare the immunoreactivity of the MON 87429-produced and the *E. coli*-produced DMO proteins, densitometric analysis was conducted on the bands that migrated at the expected apparent MW for DMO proteins (~ 38 kDa). The signal intensity (reported in $OD \times mm^2$) of the band of interest in lanes loaded with MON 87429-produced and the *E. coli*-produced DMO proteins was measured (Table 9). Because the mean signal intensity of the MON 87429-produced DMO protein band was within ± 35% of the mean signal of the *E. coli*-produced DMO protein, the MON 87429-produced DMO and *E. coli*-produced DMO proteins were determined to have equivalent immunoreactivity.
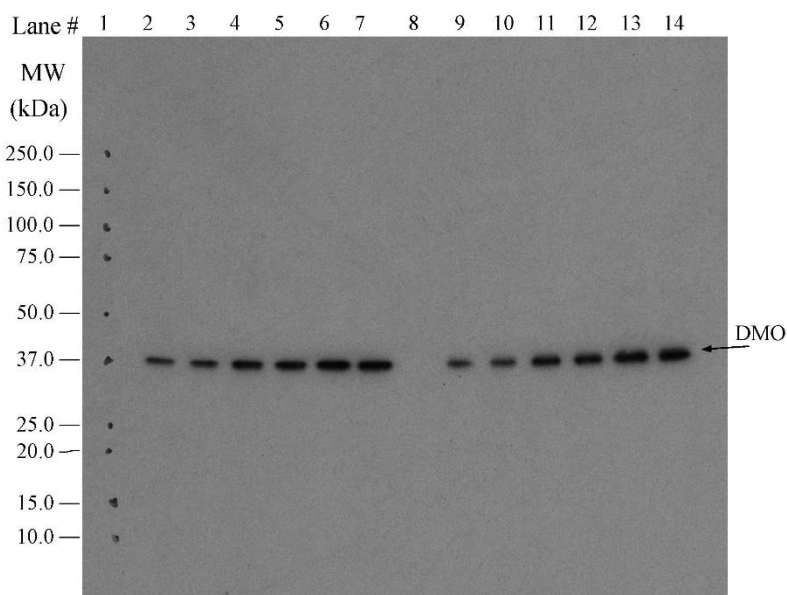
Figure 26. **Western Blot Analysis of MON 87429-Produced and *E. coli*-Produced DMO**

Aliquots of the MON 87429-produced DMO protein and the *E. coli*-produced DMO protein were subjected to SDS-PAGE and electrotransferred to a nitrocellulose membrane. Proteins were detected using goat anti-DMO polyclonal antibody and then horse anti-goat polyclonal antibody conjugated with peroxidase. Immunoreactive bands were visualized using an ECL system. The approximate MW (kDa) of the standards are shown on the left. Lane 15 was cropped from the image. The 5 second image is shown. Lane designations are as follows:

Lane	Sample	Amount (ng)
1	Precision Plus Protein™ Standards	-
2	*E. coli*-produced DMO	5
3	*E. coli*-produced DMO	5
4	*E. coli*-produced DMO	10
5	*E. coli*-produced DMO	10
6	*E. coli*-produced DMO	20
7	*E. coli*-produced DMO	20
8	Blank	-
9	MON 87429-produced DMO	5
10	MON 87429-produced DMO	5
11	MON 87429-produced DMO	10
12	MON 87429-produced DMO	10
13	MON 87429-produced DMO	20
14	MON 87429-produced DMO	20
15	Blank	-

Table 9. Immunoreactivity of the MON 87429-Produced DMO Protein and *E. coli*-Produced DMO Protein

Mean Signal Intensity from MON 87429-Produced DMO[1] (OD x mm²)	Mean Signal Intensity from *E. coli*-Produced DMO[1] (OD x mm²)	Acceptance Limits[2] (OD x mm²)
27,035.71	28,803.92	18722.55 -38885.29

[1] Each value represents the mean of six values (n = 6).

[2] The acceptance limits are for the MON 87429-produced DMO protein and are based on the interval between -35% (28803.92 x 0.65=18722.55) and +35% (28803.92 x 1.35=38885.29) of the mean of the *E. coli*-produced DMO signal intensity across all loads.

B1(a)(iv)   Results of MON 87429 DMO protein molecular weight and purity analysis

For apparent MW and purity determination, the MON 87429-produced DMO and the *E. coli*-produced DMO proteins were subjected to SDS-PAGE.   Following electrophoresis, the gel was stained with Brilliant Blue G-Colloidal stain and analyzed by densitometry.   The MON 87429-produced DMO protein (Figure 27, lanes 3-8) migrated to the same position on the gel as the *E. coli*-produced DMO protein (Figure 27, lane 2) and the apparent MW was calculated to be 38.4 kDa (Table 10).   Because the experimentally determined apparent MW of the MON 87429-produced DMO protein was within the acceptance limits for equivalence (Table 11), the MON 87429-produced DMO and *E. coli*-produced DMO proteins were determined to have equivalent apparent molecular weights.

The purity of the MON 87429-produced DMO protein was calculated based on the six lanes loaded on the gel (Figure 27, lanes 3-8).   The average purity was determined to be 98% (Table 10).
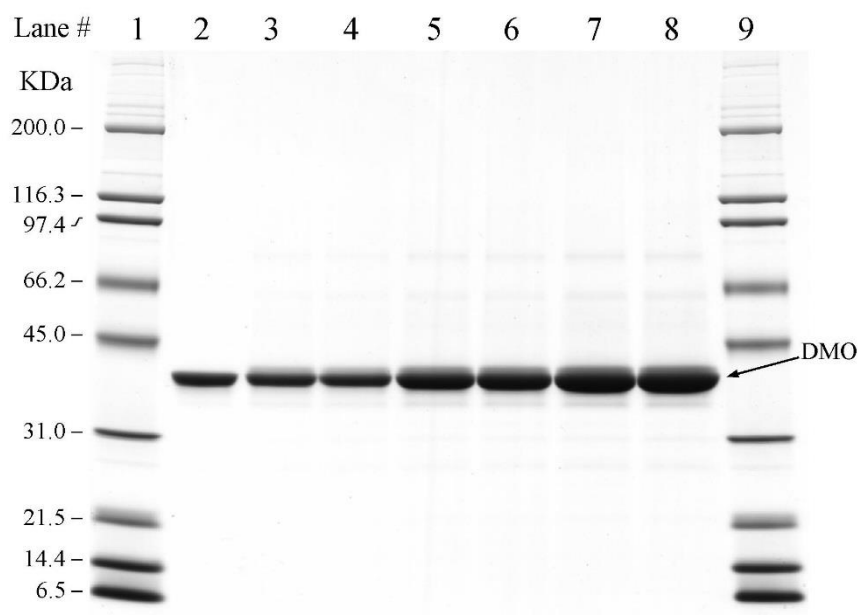
Figure 27. **Purity and Apparent Molecular Weight Analysis of the MON 87429-Produced DMO Protein**

Aliquots of the *E. coli*-produced and the MON 87429-produced DMO proteins were subjected to SDS-PAGE and the gel was stained with Brilliant Blue G-Colloidal stain.   The MWs (kDa) are shown on the left and correspond to the standards loaded in lanes 1 and 9.   Lane 10 was cropped from the image.   Lane designations are as follows:

Lane	Sample	Amount (µg)
1	Broad Range MW Standard	5.0
2	*E. coli*-produced DMO	1.0
3	MON 87429-produced DMO	1.0
4	MON 87429-produced DMO	1.0
5	MON 87429-produced DMO	2.0
6	MON 87429-produced DMO	2.0
7	MON 87429-produced DMO	3.0
8	MON 87429-produced DMO	3.0
9	Broad Range MW Standard	5.0
10	Blank	

Table 10.   Apparent Molecular Weight and Purity Analysis of the MON 87429-Produced DMO Protein

	Apparent MW[1] (kDa)	Purity[2] (%)
Average (n=6)	38.4	98

[1]Final MW was rounded to one decimal place.
[2]Average % purity was rounded to the nearest whole number.

Table 11.   Apparent Molecular Weight Comparison Between the MON 87429-Produced DMO and *E. coli*-Produced DMO Proteins

Apparent MW of MON 87429-Produced DMO Protein (kDa)[1]	Apparent MW of *E. coli*-Produced DMO Protein (kDa)	Acceptance Limits[2] (kDa)
38.4	38.0	36.0 – 40.0

[1] Value refers to mean calculated based on n=6
[2]Data obtained for the *E. coli*-produced DMO protein was used to generate the prediction interval.

B1(a)(v)   MON 87429 DMO glycosylation analysis

Eukaryotic proteins can be post-translationally modified with carbohydrate moieties (Rademacher *et al.*, 1988). To test whether the MON 87429 DMO protein was glycosylated when expressed in the grain of MON 87429, the MON 87429-produced DMO protein was analysed using an ECL™ glycoprotein detection method. To assess equivalence of the MON 87429-produced to *E. coli*-produced DMO proteins, both the MON 87429- and *E. coli*-produced DMO proteins were analysed.

In the lanes containing the positive control (transferrin), a clear glycosylation signal was observed at the expected molecular weight (~ 80 kDa) and the band intensity increased with increasing concentration (Figure 28A). In contrast, no glycosylation signal was observed in the lanes containing the *E. coli*-produced DMO protein or MON 87429-produced DMO protein (Figure 28A).

To confirm that MON 87429-produced DMO and *E. coli*-produced DMO proteins were appropriately loaded for glycosylation analysis, a second membrane with identical loadings and transfer time was stained with Coomassie Blue R250 for protein detection. Both the MON 87429-produced and *E. coli*-produced DMO proteins were detected (Figure 28B). These data indicate that the glycosylation status of MON 87429-produced DMO protein is equivalent to that of the *E. coli*-produced DMO protein and that neither is glycosylated.

A.   B.
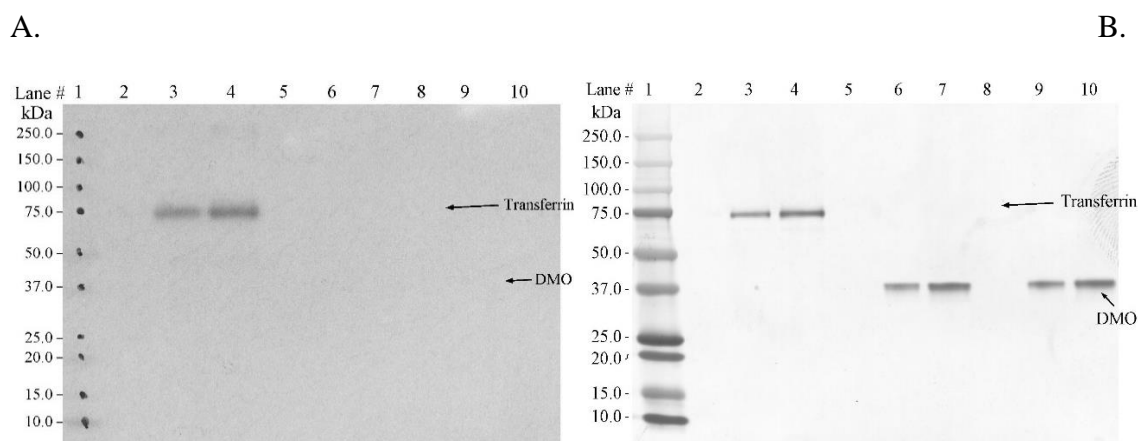
Figure 28.   Glycosylation Analysis of the MON 87429-Produced DMO Protein and *E. coli*-Produced DMO Protein

Aliquots of the transferrin (positive control), *E. coli*-produced DMO and MON 87429-produced DMO were subjected to SDS-PAGE and electrotransferred to a PVDF membrane.   The MWs (kDa) correspond to the Precision Plus Protein™ Standards.   The arrows show the expected migration of the MON 87429-produced and *E. coli*-produced DMO proteins and transferrin.   (A) Where present, the labeled carbohydrate moieties were detected by addition of streptavidin conjugated to HRP followed by a luminol-based the detection using ECL reagents and exposure to Hyperfilm®.   The 90-second exposure is shown.   (B) An equivalent blot was stained with Coomassie Blue R250 to confirm the presence of proteins.   Lane designations are as follows:

Lane	Sample	Amount (ng)
1	Precision Plus Protein™ Standards	-
2	Blank	-
3	Transferrin (positive control)	100
4	Transferrin (positive control)	200
5	Blank	-
6	*E. coli*-produced DMO	100
7	*E. coli*-produced DMO	200
8	Blank	-
9	MON 87429-produced DMO	100
10	MON 87429-produced DMO	200

B1(a)(vi)   MON 87429 DMO functional activity

The functional activity of the MON 87429-produced and *E. coli*-produced DMO proteins was determined by measuring the amount of dicamba that was converted to DCSA via HPLC separation and fluorescence detection.   In this assay, activity is expressed as specific activity (nmol $\times$ minute^{-1} $\times$ mg^{-1}).   The MON 87429-produced DMO and *E. coli*-produced DMO proteins were considered functionally equivalent if the specific activity of both were within acceptance limits of 143.0 to 748.8 (the prediction interval calculated from data obtained for the *E. coli*-produced DMO protein activity).

The specific activity of the MON 87429-produced and *E. coli*-produced DMO proteins were determined to be 400.3 and 589.3 nmol $\times$ minute^{-1} $\times$ mg^{-1} respectively (Table 12).   Because the specific activity of MON 87429-produced and *E. coli*-produced DMO proteins were within the acceptance limits, the proteins were determined to have equivalent functional activity.

Table 12.   Functional Activity Comparison of MON 87429-Produced DMO and *E. coli*-Produced DMO Proteins

MON 87429-Produced DMO[1] (nmol $\times$ minute^{-1} $\times$ mg^{-1})	*E. coli*-Produced DMO[1] (nmol $\times$ minute^{-1} $\times$ mg^{-1})	Acceptance Limits[2] (nmol $\times$ minute^{-1} $\times$ mg^{-1})
400.3	589.3	143.0 - 748.8

[1] Value refers to mean calculated based on n = 3.

[2] Data obtained for the *E. coli*-produced DMO was used to generate a prediction interval for setting the acceptance limits

B1(a)(vii)   MON 87429 DMO protein identity and equivalence - Conclusion

The MON 87429-produced DMO protein purified from MON 87429 grain was characterised, and a comparison of the physicochemical and functional properties between the MON 87429-produced and the *E. coli*-produced DMO proteins was conducted following a panel of analytical tests: 1) the N-terminal sequence of the MON 87429-produced DMO protein was confirmed by Nano LC-MS/MS analysis; 2) Nano LC-MS/MS analysis yielded peptide masses consistent with the expected peptide masses from the theoretical trypsin digest of the *dmo* gene product present in MON 87429; 3) the MON 87429-produced and the *E. coli*-produced DMO proteins were both detected on a Western blot probed with antibodies specific for DMO protein and the immunoreactive properties of both proteins was shown to be equivalent; 4) the electrophoretic mobility and apparent molecular weight of the MON 87429-produced and *E. coli*-produced DMO proteins were shown to be equivalent; 5) the glycosylation status of MON 87429-produced and *E. coli*-produced DMO proteins was determined to be equivalent and neither to be glycosylated; and 6) the functional activity of the MON 87429-produced and *E. coli*-produced DMO was demonstrated to be equivalent. These results demonstrate that the MON 87429-produced DMO protein and the *E. coli*-

produced DMO protein are equivalent. This demonstration of protein equivalence confirms that the *E. coli*-produced DMO protein is appropriate for use in the evaluation of the safety of the MON 87429-produced DMO protein.

B1(b) Characterisation and equivalence of MON 87429-produced PAT (*pat*) protein

For details, please also refer to ████████., 2018 (MSL0029659).

Identity and Function of the PAT Protein

PAT proteins have been isolated from two separate species of *Streptomyces*, *S. hygroscopicus* (Thompson *et al.*, 1987) and *S. viridochromogenes* (Wohlleben *et al.*, 1988). The PAT protein isolated from *S. hygroscopicus* is encoded by the *bar* gene, and the PAT protein isolated from *S. viridochromogenes* is encoded by the *pat* gene. These PAT proteins are made up of 183 amino acids with 85% identity at the amino acid level (Wohlleben *et al.*, 1988). Based on previous studies (Wehrmann *et al.*, 1996) that have extensively characterised PAT proteins produced from *bar* and *pat* genes, OECD recognizes both proteins to be equivalent with regard to function and safety (OECD, 1999). The PAT protein produced in MON 87429 is encoded by the *pat* gene and is identical to the wild type PAT protein encoded by *S. viridochromogenes* except for the first methionine, which is removed due to co-translational processing in MON 87429, which results in a single polypeptide of 182 amino acids that has an apparent molecular weight of ~25.5 kDa. N-terminal methionine cleavage is common and naturally occurs in the vast majority of proteins (Meinnel and Giglione, 2008). The PAT protein in MON 87429 is also produced in several commercially available glufosinate tolerant products including T25, TC1507, A5547-127 and DAS-59122-7, and therefore has an extensive history of safe use (Hérouet *et al.*, 2005; ILSI-CERA, 2011). Thus, these prior safety assessments for the PAT protein are directly applicable to the PAT protein expressed in MON 87429.

The mode-of-action for PAT protein has been extensively assessed, as numerous glufosinate-tolerant products including oilseed rape, corn, canola, sugarbeet, soybean, rice, and cotton have been reviewed by the FSANZ (A372, A375, A481, A589 and A533) and many other regulatory agencies (ILSI-CERA, 2011; OECD, 1999; OECD, 2002a). PAT is an enzyme classified as an acetyltransferase which acetylates glufosinate to produce non-herbicidal N-acetyl glufosinate. The PAT protein is specific for glufosinate.

Identity and Equivalence Studies of the PAT (*pat*) Protein

As previously described, the safety assessment of crops derived through biotechnology includes characterisation of the physicochemical and functional properties of and confirmation of the safety of the introduced protein(s). For the safety data generated using *E. coli*-produced PAT (*pat*) to be applied to PAT (*pat*) protein produced in MON 87429, the equivalence of the plant- and *E. coli*-produced proteins must be estabilished. To assess the equivalence between MON 87429-produced and *E. coli*-produced PAT (*pat*) proteins, a small quantity of the PAT (*pat*) protein was purified from grain of MON 87429 maize. The MON 87429-produced PAT (*pat*) protein was characterised and the equivalence of the physicochemical characteristics and functional activity between the MON 87429-produced

and the *E. coli*-produced PAT (*pat*) proteins was assessed using a panel of six analytical tests as shown in Table 13. Taken together, these data provide a detailed characterisation of the MON 87429-produced PAT (*pat*) protein and establish the equivalence of MON 87429-produced PAT (*pat*) and *E. coli*-produced PAT (*pat*) proteins.

Table 13. Summary of MON 87429 PAT (*pat*) Protein Identity and Equivalence

Analytical Test Assessment	Section Cross Reference	Analytical Test Outcome
1. N-terminal sequence	B1 (b)(i)	The expected N-terminal sequence was confirmed
2. Nano LC-MS/MS[1]	B1 (b)(ii)	Nano LC-MS/MS[1] analysis yielded peptide masses consistent with the expected peptide masses from the theoretical AspN digest of the MON 87429-produced PAT (*pat*) sequence
3. Western blot analysis	B1 (b)(iii)	MON 87429-produced PAT (*pat*) protein identity was confirmed using a Western blot probed with an antibody specific for PAT (*pat*) proteins Immunoreactive properties of the MON 87429-produced PAT (*pat*)and the *E. coli*-produced PAT (*pat*) proteins were shown to be equivalent
4. Apparent molecular weight (MW)	B1 (b)(iv)	Electrophoretic mobility and apparent molecular weight of the MON 87429-produced PAT (*pat*) and the *E. coli*-produced PAT (*pat*) proteins were shown to be equivalent
5. Glycosylation analysis	B1 (b)(v)	MON 87429-produced PAT (*pat*) and the *E. coli*-produced PAT (*pat*) proteins were each shown to not be glycosylated
6. Functional activity	B1 (b)(vi)	Functional activity of the MON 87429-produced PAT (*pat*) and the *E. coli*-produced PAT (*pat*) proteins were shown to be equivalent

[1] Nano LC-MS/MS = Nanoscale liquid chromatography coupled to tandem mass spectrometry
[2] SDS-PAGE = sodium dodecyl sulfate-polyacrylamide gel electrophoresis

A summary of the data obtained to support a conclusion of protein equivalence is below.

B1(b)(i)   Results of the N-terminal sequencing analysis

The expected N-terminal sequence for the PAT (*pat*) protein deduced from the *pat* gene present in maize of MON 87429 was observed by Nano LC-MS/MS minus the initiator methionine (Figure 29, MON 87429 experimental sequence). The removal of the initiator methionine (M) was expected for the MON 87429-produced PAT (*pat*) protein which is expressed in the cytoplasm. The cleavage of the N-terminal methionine from proteins *in vivo* by methionine aminopeptidase is thought to occur in all organisms (Bradshaw *et al.*, 1998; Giglione *et al.*, 2004) and is observed with high frequency when the penultimate amino acid residue is a serine (Frottin *et al.*, 2006) as is the case for the PAT protein. The N-terminal sequencing results for MON 87429-produced PAT (*pat*) protein were consistent with the sequencing results for the *E. coli*-produced PAT (*pat*) protein observed by fifteen cycles of Edman sequence analysis (Figure 29).   Hence, the sequence information confirms the identity of the PAT protein isolated from the grain of MON 87429.

Amino Acids Residue # from the N-terminus	→	1	2	3	4	5	6	7	8	9	10	11	12	13	14	15
E. coli-produced PAT sequence	→	M	S	P	E	R	R	P	V	E	I	R	P	A	T	A
		|	|	|	|	|	|	|	|	|	|	|	|	|	|	|
Expected PAT sequence	→	M	S	P	E	R	R	P	V	E	I	R	P	A	T	A
		|	|	|	|	|	|	|	|	|	|	|	|	|	|	|
MON 87429-produced PAT Experimental Sequence	→	-	S	P	E	R	R	P	V	E	I	R	P	A	T	A

Figure 29.   N-Terminal Sequence of the MON 87429-Produced PAT (*pat*) Protein

The experimental sequence obtained from the MON 87429-produced PAT (*pat*) was compared to the expected sequence deduced from the *pat* gene present in MON 87429.   The *E. coli*-produced PAT (*pat*) protein was N-terminally sequenced sequentially through 15 cycles using Edman Degradation chemistry, whereas the sequence of the N-terminus of the MON 87429-produced PAT (*pat*) protein was obtained by Nano LC-MS/MS peptide analysis (AspN digest). The single letter International Union of Pure and Applied Chemistry- International Union of Biochemistry (IUPAC-IUB) amino acid code is M, methionine; S; serine; P, proline; E, glutamic acid; R, arginine; V, valine; I, isoleucine; A, alanine; T, threonine.

B1(b)(ii)   Results nano LC-MS/MS mass fingerprint analysis

Peptide mass fingerprint analysis is a standard technique used for confirming the identity of proteins. The ability to identify a protein using this method is dependent upon matching a sufficient number of observed tryptic peptide fragment masses with predicted tryptic peptide fragment masses. In general, protein identification made by peptide mapping is considered to be reliable if >40% of the protein sequence was identified by matching experimental masses observed for the tryptic peptide fragments to the expected masses for the fragments (Biron *et al.*, 2006; Krause *et al.*, 1999). The identity of the MON 87429-produced PAT (*pat*) protein was confirmed by Nano LC-MS/MS analysis of peptide fragments produced by the AspN digestion of the MON 87429-produced PAT (*pat*) protein. A trypsin digest of the MON 87429-produced PAT (*pat*) protein was also conducted. Because the AspN digest provided the required coverage, including coverage of the intact N-terminus, the results of the trypsin digest are not reported here.

There were 16 unique peptides identified that corresponded to the masses expected to be produced by AspN digestion of the MON 87429-produced PAT (*pat*) protein (Table 14). The identified masses were used to assemble a coverage map of the entire PAT (*pat*) protein (Figure 30A). The experimentally determined coverage of the PAT (*pat*) protein was 100% (Figure 30A, 182 out of 182 amino acids, the lead methionine is cleaved during a co-translational process in MON 87429). This analysis further confirms the identity of MON 87429-produced PAT (*pat*) protein.

There were 11 unique peptides identified that corresponded to the masses expected to be produced by trypsin digestion of the *E. coli*-produced PAT (*pat*) protein (Table 15) by MALDI-TOF MS analysis during the protein characterisation. The identified masses were used to assemble a coverage map of the entire PAT (*pat*) protein (Figure 30B). The experimentally determined coverage of the *E. coli*-produced PAT (*pat*) protein was 86% (Figure 30B, 159 out of 183 amino acids). This analysis further confirms the identity of *E. coli*-produced PAT (*pat*) protein.

Table 14.   Summary of the AspN Masses Identified for the MON 87429-Produced PAT (*pat*) Using Nano LC-MS/MS[1]

Experimental Mass[2]	Calculated Mass[3]	Difference[4]	Fragment[5]	Sequence[6]
1648.9026	1648.9009	0.0017	2 - 16	SPER...ATAA
1690.9114	1690.9114	0	2 - 16	*SPER…ATAA
5294.6029	5294.5877	0.0152	2 - 47	SPER...QEWI
3663.7121	3663.6974	0.0147	17 - 47	DMAA...QEWI
3016.4586	3016.4567	0.0019	23 - 47	DIVN...QEWI
3131.4757	3131.4836	-0.0079	23 - 48	DIVN...EWID
3885.8842	3885.881	0.0032	23 - 54	DIVN...ERLQ
887.4350	887.4348	0.0002	48 - 54	DDLERLQ
4090.0717	4090.0701	0.0016	48 - 83	DDLE...RNAY
772.4078	772.4079	-0.0001	49 - 54	DLERLQ
3220.6467	3220.6458	0.0009	55 - 83	DRYP...RNAY
5223.7313	5223.7292	0.0021	84 - 130	DWTV...GLPN
3175.6208	3175.6176	0.0032	131 - 159	DPSV...GGWH
906.4358	906.4348	0.001	160 - 166	DVGFWQR
2819.4884	2819.4871	0.0013	160 - 183	DVGF...VTQI
1931.0632	1931.0629	0.0003	167 - 183	DFEL...VTQI

[1]All imported values were rounded to 4 decimal places.

[2]Only experimental masses that matched calculated masses with the highest scores (Mascot ion score) are listed in the table.

[3]The calculated mass is the exact molecular mass calculated from the matched peptide sequence.

[4]The calculated difference = experimental mass – calculated mass.

[5]Position refers to amino acid residues within the predicted MON 87429-produced PAT (*pat*) sequence as depicted in Figure 30A.

[6]For peptide matches greater than nine amino acids in length the first 4 residues and last 4 residues are shown separated by dots (…).

*acetylation of serine (S) was observed.

Table 15.   Summary of the Tryptic Masses Identified for the *E. coli*-Produced PAT (*pat*) Using MALDI-TOF MS[1]

Experimental Mass[2]	Calculated Mass[3]	Difference[5]	Fragment[5]	Sequence[6]
3616.7368	3616.7766	-0.0398	6 - 37	RPVE…VNFR
1855.8205	1855.8588	-0.0383	38 - 52	TEPQ…DLER
2886.4400	2886.5068	-0.0668	53 - 78	LQDR…GPWK
2374.1822	2374.2361	-0.0539	57 - 78	YPWL…GPWK
1925.8546	1925.8908	-0.0362	81 - 96	NAYD…VSHR
2347.1682	2347.1094	0.0588	81 - 99	NAYD…RHQR
1414.7882	1414.8184	-0.0302	100 - 112	LGLG…HLLK
1521.8238	1521.8515	-0.0277	121 - 135	SVVA…PSVR
1129.5744	1129.5880	-0.0136	136 - 145	LHEA…YTAR
1480.6502	1480.6749	-0.0247	155 - 166	HGGW…FWQR
1931.0281	1931.0629	-0.0348	167 - 183	DFEL…VTQI

[1] All imported values were rounded to 4 decimal places.

[2] Only experimental masses that matched calculated PAT (*pat*) trypsin digested masses are listed in the table.

[3] The calculated mass is the exact molecular mass calculated from the matched peptide sequence.

[4] The calculated difference = experimental mass - calculated mass.

[5] Position refers to amino acid residues within the predicted *E. coli*-produced PAT (*pat*) sequence as depicted in Figure 30B.

[6] For peptide matches greater than nine amino acids in length, the first 4 residues and last 4 residues are show separated by three dots (...).

(A)

```
001 MSPERRPVEI RPATAADMAA VCDIVNHYIE TSTVNFRTEP QTPQEWIDDL
051 ERLQDRYPWL VAEVEGVVAG IAYAGPWKAR NAYDWTVEST VYVSHRHQRL
101 GLGSTLYTHL LKSMEAQGFK SVVAVIGLPN DPSVRLHEAL GYTARGTLRA
151 AGYKHGGWHD VGFWQRDFEL PAPPRPVRPV TQI
```

(B)

```
001 MSPERRPVEI RPATAADMAA VCDIVNHYIE TSTVNFRTEP QTPQEWIDDL
051 ERLQDRYPWL VAEVEGVVAG IAYAGPWKAR NAYDWTVEST VYVSHRHQRL
101 GLGSTLYTHL LKSMEAQGFK SVVAVIGLPN DPSVRLHEAL GYTARGTLRA
151 AGYKHGGWHD VGFWQRDFEL PAPPRPVRPV TQI
```

Figure 30.   Peptide Maps of the MON 87429-Produced PAT (*pat*) and *E. coli*-Produced PAT (*pat*) Proteins

(A). The amino acid sequence of the MON 87429-produced PAT (*pat*) protein was deduced from the *pat* gene present in MON 87429.   Boxed regions correspond to peptides that were identified from the MON 87429-produced PAT (*pat*) protein sample (AspN digest) using Nano LC-MS/MS.   In total, 100% (182 out of 182 amino acids) of the MON 87429-produced PAT (*pat*) protein sequence was covered by the identified peptides.   Note that it was experimentally determined that the N-terminus of the MON 87429-produced PAT (*pat*) starts at position 2 of the expected sequence.   Therefore, the calculation of 100% sequence coverage takes the removal of the initiator methionine into consideration.

(B). The amino acid sequence of the *E. coli*-produced PAT (*pat*) protein was deduced from the *pat* gene that is contained on the expression plasmid pMON282887.   Boxed regions correspond to peptides that were identified from the *E. coli*-produced PAT (*pat*) protein sample using MALDI-TOF MS.   In total, 86% coverage (159 out of 183 amino acids) of the expected protein sequence was covered by the identified peptides

B1(b)(iii)   Results of Western blot analysis of the PAT (*pat*) protein isolated from the grain of MON 87429 and immunoreactivity comparison to *E. coli*-produced MON 87429 PAT (*pat*) protein

Western blot analysis was conducted using a mouse anti-PAT (*pat*) monoclonal antibody as additional means to confirm the identity of the PAT protein isolated from the grain of MON 87429 and to assess the equivalence of the immunoreactivity of the MON 87429-produced and *E. coli*-produced PAT (*pat*) proteins.

The results showed that immunoreactive bands with the same electrophoretic mobility were present in all lanes loaded with the MON 87429-produced and *E. coli*-produced PAT (*pat*) proteins (Figure 31). At the higher loadings of MON 87429-produced PAT (*pat*), a weak band corresponding to the expected position of the PAT dimer was observed on the blot films. For each amount loaded, comparable signal intensity for the principal bands at ~ 20-25 kDa was observed between the MON 87429-produced and *E. coli*-produced PAT protein bands. As expected, the signal intensity increased with increasing load amounts of the MON 87429-produced and *E. coli*-produced PAT (*pat*) proteins, thus, supporting identification of MON 87429-produced PAT (*pat*) protein.

To compare the immunoreactivity of the MON 87429-produced and the *E. coli*-produced PAT (*pat*) proteins, densitometric analysis was conducted on the bands that migrated at the expected apparent MW for PAT proteins (~ 25 kDa). The signal intensity (reported in $OD \times mm^2$) of the band of interest in lanes loaded with MON 87429-produced and the *E. coli*-produced PAT (*pat*) proteins was measured (Table 16). Because the mean signal intensity of the MON 87429-produced PAT protein band was within $\pm$ 35% of the mean signal of the *E. coli*-produced PAT protein, the MON 87429-produced PAT (*pat*) and *E. coli*-produced PAT (*pat*) proteins were determined to have equivalent immunoreactivity.
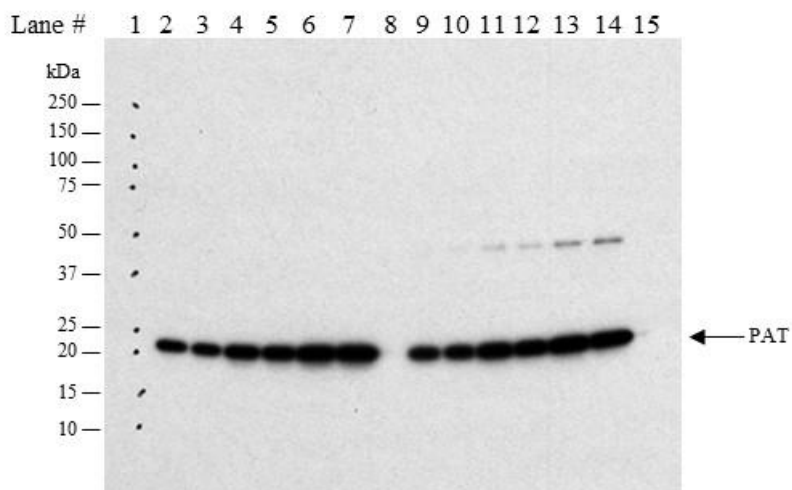
Figure 31.   Western Blot Analysis and Immunoreactivity of MON 87429-Produced and *E. coli*-Produced PAT (*pat*)

Aliquots of the MON 87429-produced PAT (*pat*) protein and the *E. coli*-produced PAT (*pat*) protein were subjected to SDS-PAGE and electro-transferred to a PVDF membrane.   Proteins bound to the PVDF membrane were initially probed using a mouse anti-PAT monoclonal antibody.   The presence of bound mAb was detected using a peroxidase conjugated anti-mouse IgG (H+L) affinity purified polyclonal antibody raised in horses.   Immunoreactive bands were visualized using an ECL system. The approximate MW (kDa) of the standards are shown on the left.   The 10-second image is shown. Lane designations are as follows:

Lane	Sample	Amount (ng)
1	Precision Plus Protein™ Standards	-
2	*E. coli*-produced PAT	5
3	*E. coli*-produced PAT	5
4	*E. coli*-produced PAT	10
5	*E. coli*-produced PAT	10
6	*E. coli*-produced PAT	20
7	*E. coli*-produced PAT	20
8	Blank	-
9	MON 87429-produced PAT	5
10	MON 87429-produced PAT	5
11	MON 87429-produced PAT	10
12	MON 87429-produced PAT	10
13	MON 87429-produced PAT	20
14	MON 87429-produced PAT	20
15	Blank	-

Table 16.   Immunoreactivity of the MON 87429-Produced PAT (*pat*) Protein and *E. coli*-Produced PAT (*pat*) Protein

Mean Signal Intensity from MON 87429-Produced PAT [1] (OD × mm²)	Mean Signal Intensity from *E. coli*-Produced PAT [1] (OD × mm²)	Acceptance Limits[2] (OD × mm²)
142602.12	123785.04	80460.28 – 167109.80

[1] Each value represents the mean of six values (n = 6).
[2] The acceptance limits are for the MON 87429-produced PAT (*pat*) protein and are based on the interval between -35% (123785.04 × 0.65 = 80460.28) and +35 % (123785.04 × 1.35 = 167109.80) of the mean of the *E. coli*-produced PAT (*pat*) signal intensity across all loads.

B1(b)(iv)   Results of the MON 87429-produced PAT (*pat*) protein molecular weight analysis

For apparent MW and purity determination, the MON 87429-produced PAT (*pat*) and the *E. coli*-produced PAT (*pat*) proteins were subjected to SDS-PAGE.   Following electrophoresis, the gel was stained with Brilliant Blue G-Colloidal stain and analysed by densitometry.   The MON 87429-produced PAT (*pat*) protein (Figure 32, lanes 3-8) migrated to the same position on the gel as the *E. coli*-produced PAT (*pat*) protein (Figure 32, lane 2) and the apparent MW was calculated to be 25.5 kDa (Table 17).   Because the experimentally determined apparent MW of the MON 87429-produced PAT (*pat*) protein was within the acceptance limits for equivalence (Table 18), the MON 87429-produced PAT(*pat*) and *E. coli*-produced PAT (*pat*) proteins were determined to have equivalent apparent molecular weights.

The purity of the MON 87429-produced PAT (*pat*) protein was calculated based on the six lanes loaded on the gel (Figure 32, lanes 3-8).   The average purity was determined to be 93% (Table 17).
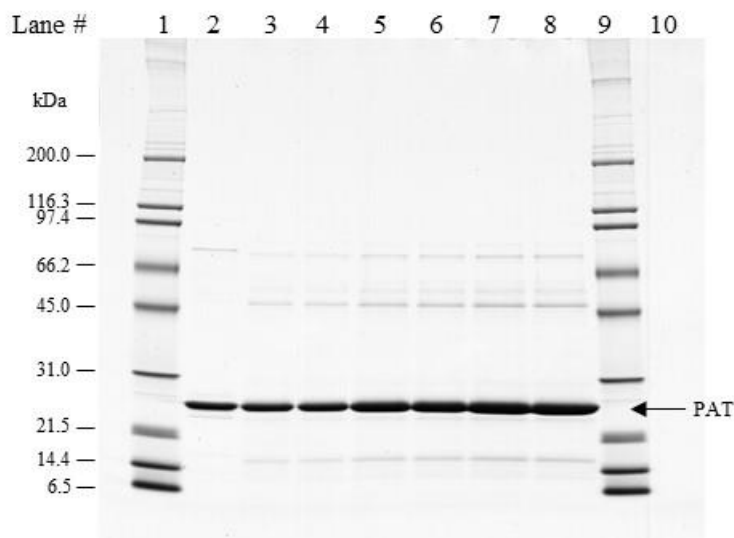
Figure 32.   Purity and Apparent Molecular Weight Analysis of the MON 87429-Produced PAT (*pat*) Protein

Aliquots of the MON 87429-produced and the *E. coli*-produced PAT (*pat*) proteins were subjected to SDS-PAGE and the gel was stained with Brilliant Blue G Colloidal stain.   The MWs (kDa) are shown on the left and correspond to the standards loaded in lanes 1 and 9. Lane designations are as follows:

Lane	Sample	Amount (µg)
1	Broad Range MW Standard	5.0
2	*E. coli*-produced PAT	1.0
3	MON 87429-produced PAT	1.0
4	MON 87429-produced PAT	1.0
5	MON 87429-produced PAT	2.0
6	MON 87429-produced PAT	2.0
7	MON 87429-produced PAT	3.0
8	MON 87429-produced PAT	3.0
9	Broad Range MW Standard	5.0
10	Blank	-

Table 17. Apparent Molecular Weight and Purity Analysis of the MON 87429-Produced PAT (*pat*) Protein

	Apparent MW[1] (kDa)	Purity[2] (%)
Average (n=6)	25.5	93

[1]Final MW was rounded to one decimal place.

[2]Average % purity was rounded to the nearest whole number.

Table 18. Apparent Molecular Weight Comparison Between the MON 87429-Produced PAT (*pat*) and *E. coli*-Produced PAT (*pat*) Proteins

Apparent MW of MON 87429-Produced PAT Protein (kDa)	Apparent MW of *E. coli*-Produced PAT Protein (kDa)	Acceptance Limits[1] (kDa)
25.5	24.8	24.0 – 25.7

[1] Data obtained for the *E. coli*-produced PAT (*pat*) protein was used to generate the prediction interval.

B1(b)(v) MON 87429 PAT (*pat*) glycosylation analysis

Some eukaryotic proteins are post-translationally modified by the addition of carbohydrate moieties (Rademacher *et al.*, 1988). To test whether the PAT (*pat*) protein was glycosylated when expressed in the maize grain of MON 87429, the MON 87429-produced PAT (*pat*) protein was analyzed using an ECL™ glycoprotein detection method. Transferrin, a glycosylated protein, was used as a positive control in the assay. To assess equivalence of the MON 87429-produced and *E. coli*-produced PAT (*pat*) proteins, the *E. coli*-produced PAT (*pat*) protein, previously shown to be free of glycosylation in another equivalence assessment, was also analyzed.

A clear glycosylation signal was observed at the expected molecular weight (~80 kDa) in the lanes containing the positive control (transferrin) and the band intensity increased with increasing concentration (Figure 33A). In contrast, no glycosylation signal was observed in the lanes containing the *E. coli*-produced PAT (*pat*) protein or MON 87429-produced PAT (*pat*) protein (Figure 33A).

To confirm that MON 87429-produced PAT (*pat*) and *E. coli*-produced PAT (*pat*) proteins were appropriately loaded for glycosylation analysis, a second membrane with identical loadings and transfer time was stained with Coomassie Blue R-250 for protein detection. Both the MON 87429-produced and *E. coli*-produced PAT (*pat*) proteins were detected (Figure 33B). These data indicate that the glycosylation status of MON 87429-produced PAT (*pat*) protein is equivalent to that of the *E. coli*-produced PAT (*pat*) protein and that neither is glycosylated.
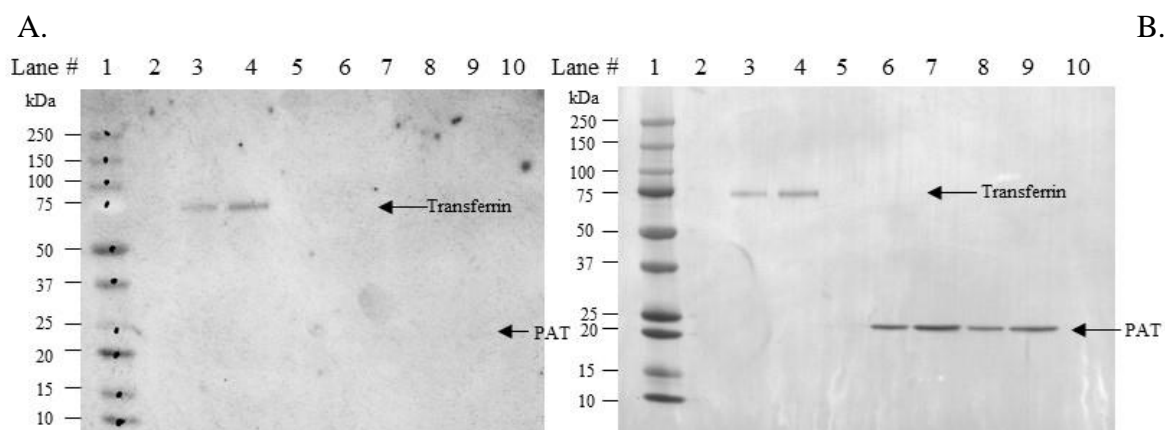
Figure 33.   Glycosylation Analysis of the MON 87429-Produced PAT (*pat*) Protein

Aliquots of the transferrin (positive control), *E. coli*-produced PAT (*pat*) and MON 87429-produced PAT (*pat*) were subjected to SDS-PAGE and electro-transferred to a PVDF membrane.   The MWs (kDa) correspond to the Precision Plus Dual Color Protein™ Standards.   The arrows show the expected migration of the MON 87429-produced and *E. coli*-produced PAT (*pat*) proteins and transferrin.   (A) Where present, the labeled carbohydrate moieties were detected by addition of streptavidin conjugated to HRP followed by a luminol-based detection using ECL reagents and exposure to Hyperfilm®.   The 2.5-minute exposure is shown. (B) An equivalent blot was stained with Coomassie Blue R250 to confirm the presence of proteins.   Lane designations are as follows:

Lane	Sample	Amount (ng)
1	Precision Plus Protein™ Standards	-
2	Blank	-
3	Transferrin (positive control)	100
4	Transferrin (positive control)	200
5	Blank	-
6	*E. coli*-produced MON 87429 PAT	100
7	*E. coli*-produced MON 87429 PAT	200
8	MON 87429-produced PAT	100
9	MON 87429-produced PAT	200
10	Blank	-

B1(b)(vi)   PAT (*pat*) functional activity

The functional activity of the MON 87429-produced and *E. coli*-produced PAT (*pat*) proteins was assessed using a coenzyme A (CoA) release assay (Wehrmann *et al.*, 1996) .   PAT catalyzes the reaction of phosphinothricin (PPT) with acetyl-CoA to form acetyl-PPT and free CoA.   CoA released during the reaction can be monitored using the reduction of 5,5'-dithio-bis-(2-nitrobenzoic acid) (DTNB) by CoA to form the colorimetric reagent 5-thio-nitrobenzoate (TNB).   In this assay, protein-specific activity is expressed as μmoles TNB released per minute at 30 °C per milligram of PAT protein. The MON 87429-produced PAT (*pat*) and *E. coli*-produced PAT (*pat*) proteins were considered to have equivalent functional activity if the specific activity of both were within acceptance limits of 18.3 to 67.7 μmoles $\times$ min^{-1} $\times$ mg^{-1} (the prediction interval calculated from a data set based on assays conducted for the *E. coli*-produced PAT (*pat*) protein).

The experimentally determined specific activity for the MON 87429-produced and *E. coli*-produced PAT (*pat*) proteins are presented in Table 19.   The specific activities of MON 87429-produced and *E. coli*-produced PAT (*pat*) proteins were 40 and 54 μmoles $\times$ min^{-1} $\times$ mg^{-1} PAT protein, respectively. Because the specific activities of MON 87429-produced and *E. coli*-produced PAT (*pat*) proteins fall within the preset acceptance limits (Table 19), the MON 87429-produced PAT (*pat*) protein was considered to have equivalent functional activity to that of the *E. coli*-produced PAT (*pat*) protein.

Table 19.   Functional Activity of MON 87429-Produced PAT (*pat*) and *E. coli*-Produced PAT (*pat*) Proteins

MON 87429-Produced PAT (*pat*) [1] (μmoles × min^{-1} × mg^{-1})	*E. coli*-Produced PAT (*pat*) [1] (μmoles × min^{-1} × mg^{-1})	Acceptance Limits[2] (μmoles × min^{-1} × mg^{-1})
40	54	18.3 – 67.7

[1] Value refers to mean calculated based on 5 data points (n = 5) within each assay.
[2] Data obtained for the *E. coli*-produced PAT(pat) protein were used to generate a prediction interval for setting the acceptance limits   .

B1(b)(vii)   MON 87429 PAT (*pat*) protein identity and equivalence – Conclusion

The PAT (*pat*) protein purified from grain of MON 87429 maize was characterised and the equivalence of the immunoreactive and physicochemical characteristics and functional activity between the MON 87429-produced and the *E. coli*-produced PAT (*pat*) proteins was established using a panel of analytical tests: 1) the N-terminal sequence of the MON 87429-produced PAT (*pat*) protein was confirmed by Nano LC-MS/MS analysis; 2) Nano LC-MS/MS analysis yielded peptide masses consistent with the expected peptide masses from the theoretical AspN digest of the MON 87429-produced PAT (*pat*) sequence; 3) MON 87429-produced PAT (*pat*) protein was detected on a Western blot probed with antibodies specific for PAT protein and the immunoreactive properties of the MON 87429-produced and *E. coli*-produced PAT (*pat*) proteins were shown to be equivalent; 4) the electrophoretic mobility and apparent molecular weight of the MON 87429-produced and *E. coli*-produced PAT (*pat*) proteins were shown to be equivalent; 5) MON 87429-produced and *E. coli*-produced PAT (*pat*) proteins were determined to not be glycosylated; and 6) functional activities of the MON 87429-produced and *E. coli*-produced PAT (*pat*) proteins were demonstrated to be equivalent.

Taken together, these data provide a detailed characterisation of the MON 87429-produced PAT (*pat*) protein and establish the equivalence of the MON 87429-produced and the *E. coli*-produced PAT (*pat*) proteins.   This equivalence justifies the use of the *E. coli*-produced PAT (*pat*) protein in studies to establish the safety of the PAT (*pat*) protein expressed in MON 87429.

B1(c)   Characterisation and equivalence of MON 87429-produced FT_T protein

For details, please also refer to ▮▮▮▮▮▮▮▮, 2018 (MSL0030056).

Identity and Function of the FT_T Protein

MON 87429 produces the FT_T protein encoded by the *ft_t* gene that provides tolerance to aryloxyalkanoate herbicides. The *ft_t* gene in MON 87429 is a modified version of the R-2,4-dichlorophenoxypropionate dioxygenase (*Rdp*a) gene from a soil bacteria, *Sphingobium herbicidovorans*.   Aryloxyalkanoate herbicides include the aryloxyphenoxypropionate acetyl coenzyme A carboxylase (ACCase) inhibitors (so called "FOPs" herbicides such as quizalofop) and some synthetic auxins, such as 2,4-D.   The amino acid sequence of the FT_T protein shares ~ 89% sequence identity with wild type RdpA protein.   A total of 30 amino acid substitutions throughout the protein sequence resulted in FT_T protein displaying improved enzyme kinetics (increased V_{max}) and substrate affinity (reduced K_m) for 2,4-D, relative to RdpA protein.   The amino acid substitutions also resulted in FT_T protein displaying retained activity at temperatures experienced during the summer months in maize growing areas compared to RdpA protein.

Identity and Equivalence Studies of the FT_T Protein

The safety assessment of crops derived through biotechnology includes characterisation of the physicochemical and functional properties and confirmation of the safety of the

introduced protein(s). For the safety data generated using the *E. coli*-produced FT_T protein to be applied to the MON 87429-produced FT_T protein (plant-produced FT_T), the equivalence of the plant- and *E. coli*-produced proteins must first be demonstrated. To assess the equivalence between the MON 87429-produced FT_T and *E. coli*-produced FT_T proteins, a small quantity of the MON 87429-produced FT_T protein was purified from MON 87429 grain. The MON 87429-produced FT_T protein was characterised and the equivalence of the physicochemical characteristics and functional activity between the MON 87429-produced and *E. coli*-produced FT_T proteins was assessed using a panel of six analytical tests; as shown in Table 20. Taken together, these data provide a detailed characterisation of the MON 87429-produced FT_T protein and establish the equivalence of the MON 87429-produced FT_T and *E. coli*-produced FT_T proteins. Based on this established equivalence, conclusions derived from digestibility, heat susceptibility and oral acute toxiciology studies conducted with *E. coli*-produced FT_T protein are applicable to MON 87429-produced FT_T protein.

Table 20. Summary of MON 87429 FT_T Protein Identity and Equivalence

Analytical Test	Section Cross Reference	Analytical Test Outcome
1. N-terminal sequence	B1(c)(i)	The expected N-terminal sequence for MON 87429-produced FT_T was observed by Nano LC-MS/MS[1]
2. Nano LC-MS/MS[1]	B1(c)(ii)	Nano LC-MS/MS[1] analysis of trypsin digested peptides from for MON 87429-produced FT_T protein yielded peptide masses consistent with expected peptide masses from the theoretical trypsin digest of the amino acid sequence
3. Western blot analysis	B1(c)(iii)	MON 87429-produced FT_T protein identity was confirmed using a Western blot probed with antibodies specific for FT_T protein Immunoreactive properties of the MON 87429-produced FT_T and the *E. coli*-produced FT_T proteins were shown to be equivalent
4. Apparent molecular weight (MW)	B1(c)(iv)	Electrophoretic mobility and apparent molecular weight of the MON 87429-produced FT_T and the *E. coli*-produced FT_T proteins were shown to be equivalent
5. Glycosylation analysis	B1(c)(v)	Glycosylation status of MON 87429-produced FT_T and *E. coli*-produced FT_T proteins were shown to be equivalent and not glycosylated
6. Functional activity	B1(c)(vi)	Functional activity of the MON 87429-produced FT_T and the *E. coli*-produced FT_T proteins were shown to be equivalent

[1] Nano LC-MS/MS = Nanoscale liquid chromatography-tandem mass spectrometry

A summary of the data obtained to support a conclusion of protein equivalence is below.

B1(c)(i)   Results of the N-terminal sequencing analysis

The expected N-terminal sequence for the FT_T protein deduced from the *ft_t* gene present in maize of MON 87429 was confirmed by Nano LC-MS/MS. The experimentally determined sequence corresponds to the deduced FT_T protein beginning at the initial alanine position (Figure 34).   The alanine is derived from the MDH gene due to the incomplete processing of the chloroplast transit peptide. Alternative cleavage of CTP from FT_T in *planta* by a general stromal processing peptidase is common (Richter and Lamppa, 1998).   The N-terminal sequencing results for MON 87429-produced FT_T protein were consistent with the sequencing results for the *E. coli*-produced FT_T protein (Figure 34).   The expression plasmid designed to express the mature FT_T protein in *E. coli* included an N-terminal

methionine residue that was likely cleaved by methionine aminopeptidase and other aminopeptidases. Therefore, the *E. coli*-produced FT_T sequence begins at position 2 of the expected sequence deduced from the *E. coli* expression plasmid, which corresponds to position 1 of the mature FT_T protein present in MON 87429. The cleavage of the N-terminal methionine from proteins *in vivo* by methionine aminopeptidase is common in many organisms (Bradshaw *et al.*, 1998). Hence, the sequence information confirms the identity of the FT_T protein isolated from the grain of MON 87429.

Amino Acids Residue # from the N-terminus	→	1	2	3	4	5	6	7	8	9	10	11	12	13	14	15
E. coli-produced FT_T sequence	→	A	M	H	A	A	L	T	P	L	T	N	K	Y	R	F
		|	|	|	|	|	|	|	|	|	|	|	|	|	|	|
Expected FT_T Sequence	→	A	M	H	A	A	L	T	P	L	T	N	K	Y	R	F
		|	|	|	|	|	|	|	|	|	|	|	|	|	|	|
MON 87429-produced FT_T Experimental Sequence	→	A	M	H	A	A	L	T	P	L	T	N	K	Y	R	F

Figure 34.   N-Terminal Sequence of the MON 87429-Produced FT_T Protein

The experimental sequence obtained from the MON 87429-produced FT_T was compared to the expected sequence of the mature protein deduced from the *ft_t* gene, a modified version of the R-2,4-dichlorophenoxypropionate dioxygenase (*Rdpa*) gene, present in MON 87429. The *E. coli*-produced FT_T sequence begins at position 2 of the expected sequence deduced from the *E. coli* expression plasmid, which corresponds to position 1 of the mature FT_T protein present in MON 87429. The single letter International Union of Pure and Applied Chemistry- International Union of Biochemistry (IUPAC-IUB) amino acid code is A, alanine; M, methionine; H, histidine; L, leucine; T, threonine; P, proline; N, asparagine; K, lysine; Y, tyrosine; R, arginine; F, phelyalanine.

B1(c)(ii)   Results of mass fingerprint analysis

Peptide mass fingerprint analysis is a standard technique used for confirming the identity of proteins. The ability to identify a protein using this method is dependent upon matching a sufficient number of observed tryptic peptide fragment masses with predicted tryptic peptide fragment masses. In general, protein identification made by peptide mapping is considered to be reliable if >40% of the protein sequence was identified by matching experimental masses observed for the tryptic peptide fragments to the expected masses for the fragments (Biron *et al.*, 2006; Krause *et al.*, 1999). The identity of the MON 87429-produced FT_T protein was confirmed by Nano LC-MS/MS analysis of peptide fragments produced by the trypsin digestion of the MON 87429-produced FT_T protein.

There were 34 unique peptides identified that corresponded to the masses expected to be produced by trypsin digestion of the MON 87429-produced FT_T protein (Table 21). The identified masses were used to assemble a coverage map of the entire FT_T protein (Figure 35A). The experimentally determined coverage of the FT_T protein was 97% (Figure 35A 288 out of 296 amino acids). This analysis further confirms the identity of MON 87429-produced FT_T protein.

There were 20 unique peptides identified that corresponded to the masses expected to be produced by trypsin digestion of the *E. coli*-produced FT_T protein (Table 22) by MALDI-TOF MS analysis during the protein characterisation. The identified masses were used to assemble a coverage map of the entire FT_T protein (Figure 35B). The experimentally determined coverage of the *E. coli*-produced FT_T protein was 65% (Figure 35B, 194 out of 297 amino acids). This analysis further confirms the identity of *E. coli*-produced FT_T protein.

Table 21. Summary of the Tryptic Masses Identified for the MON 87429-Produced FT_T Using Nano LC-MS/MS

[1]Experimental Mass[2]	Calculated Mass[3]	Diff[4]	Fragment[5]	Sequence[6]
1266.6764	1266.6754	0.001	1 – 12	AMHA...LTNK
1308.6891	1308.686	0.0031	1 - 12	*AMHA…LTNK
2531.3715	2531.3748	-0.0033	13 - 35	YRFI...VDLR
2212.2081	2212.2104	-0.0023	15 - 35	FIDV...VDLR
6659.3313	6659.3289	0.0024	15 - 73	FIDV...AFSR
4465.1336	4465.1291	0.0045	36 - 73	EPLD...AFSR
1336.7871	1336.7867	0.0004	74 - 85	RFGP...PILK
1180.6852	1180.6856	-0.0004	75 - 85	FGPV...PILK
2583.3786	2583.3771	0.0015	75 - 97	FGPV...QMIR
1420.7026	1420.702	0.0006	86 - 97	SIEG...QMIR
947.4422	947.442	0.0002	98 - 105	REANESSR
791.3409	791.3409	0	99 - 105	EANESSR
2560.2049	2560.2057	-0.0008	106 - 128	FIGD...VVMR
4500.1576	4500.1505	0.0071	129 - 170	AIEV...SATK
5922.8591	5922.8549	0.0042	129 - 182	AIEV...TNWR
1440.7149	1440.715	-0.0001	171 - 182	VFGS...TNWR
2204.1021	2204.1015	0.0006	171 - 189	VFGS...TSVK
781.3974	781.397	0.0004	183 - 189	FSNTSVK
3362.7007	3362.7042	-0.0035	183 - 213	FSNT...VTGR
976.4284	976.4284	0	190 - 198	VMDV...AGDR
2599.3170	2599.3177	-0.0007	190 - 213	VMDV...VTGR
1640.8988	1640.8999	-0.0011	199 - 213	ETVH...VTGR
1796.9998	1797.001	-0.0012	199 - 214	ETVH...TGRR
1601.7407	1601.7442	-0.0035	214 - 225	RALY...YCQK
1445.6441	1445.6431	0.001	215 - 225	ALYC...YCQK
1078.4969	1078.4965	0.0004	226 - 235	IQGM...AESK
1448.7651	1448.7663	-0.0012	236 - 247	SLLQ...HATK

[1] All imported values were rounded to 4 decimal places.

[2] Only experimental masses that matched calculated masses with the highest scores are listed.

[3] The calculated mass is the relative molecular mass calculated from the matched peptide sequence.

[4] The calculated difference = (experimental mass − calculated mass).

[5] Position refers to amino acid residues within the predicted MON 87429-produced FT_T sequence as depicted in Figure 35.

[6] For peptide matches greater than nine amino acids in length the first 4 residues and last 4 residues are shown separated by dots (…).

* acetylation and oxidation of alanine (A) observed.

Table 21.   Summary of the Tryptic Masses Identified for the MON 87429-Produced FT_T Using Nano LC-MS/MS (continued)

[1]Experimental Mass[2]	Calculated Mass[3]	Diff[4]	Fragment[5]	Sequence[6]
2275.1126	2275.1096	0.003	236 - 253	SLLQ...FTCR
844.3548	844.3538	0.001	248 - 253	FDFTCR
1913.9253	1913.924	0.0013	258 - 272	KDQV...TMHR
1785.8299	1785.8291	0.0008	259 - 272	DQVL...TMHR
819.4129	819.4127	0.0002	273 - 280	AVPDYAGK
1122.5821	1122.5822	-0.0001	273 - 282	AVPD...GKFR
1030.5409	1030.5407	0.0002	288 - 296	TTVA...KPSR

[1] All imported values were rounded to 4 decimal places.

[2] Only experimental masses that matched calculated masses with the highest scores are listed.

[3] The calculated mass is the relative molecular mass calculated from the matched peptide sequence.

[4] The calculated difference = (experimental mass – calculated mass).

[5] Position refers to amino acid residues within the predicted MON 87429-produced FT_T sequence as depicted in Figure 34.

[6] For peptide matches greater than nine amino acids in length the first 4 residues and last 4 residues are shown separated by dots (…).

[*] acetylation and oxidation observed.

Table 22. Summary of the Tryptic Masses Identified for *E. coli*-produced FT_T using MALDI-TOF MS[1]

Experimental Mass[2]	Calculated Mass[3]	Diff.[4]	Fragment[5]	Sequence[6]
1266.5457	1266.6754	-0.1297	2 - 13	AMHA…LTNK
2211.9397	2212.2104	-0.2706	16 - 36	FIDV…VDLR
1336.6551	1336.7867	-0.1316	75 - 86	RFGP...PILK
1180.5685	1180.6856	-0.1171	76 - 86	FGPV...PILK
1420.5619	1420.7020	-0.0792	87 - 98	SIEG...QMIR
791.2727	791.3409	-0.0682	99 - 106	REANESSR
2559.8802	2560.2057	-0.3255	107 - 129	FIGD…VVMR
1440.5745	1440.7150	-0.1405	172 - 183	VFGS...TNWR
781.3226	781.3970	-0.0744	184 - 190	FSNTSVK
2598.9771	2599.3177	-0.3406	191 - 214	VMDV…VTGR
1640.7249	1640.8999	-0.1749	200 - 214	ETVH…VTGR
1603.5482	1603.7123	-0.1640	215 - 226	RALY…YCQK
1447.4541	1447.6112	-0.1570	216 - 226	ALYC…YCQK
1448.6154	1448.7663	-0.1509	237 - 248	SLLQ…HATK
2275.8086	2276.0936	-0.2850	237 - 254	SLLQ…FTCR
845.2653	845.3378	0.0725	249 - 254	FDFTCR
1786.6216	1786.8131	-0.1915	260 - 273	DQVL…TMHR
819.3327	819.4127	-0.0799	274 - 281	AVPDYAGK
1030.4390	1030.5407	-0.1017	288 - 297	TTVAGDKPSR

[1] All imported values were rounded to 4 decimal places.

[2] Only experimental masses that matched calculated FT_T trypsin digested masses are listed in the table.

[3] The calculated mass is the exact molecular mass calculated from the matched peptide sequence.

[4] The calculated difference = experimental mass - calculated mass.

[5] Position refers to amino acid residues within the predicted *E. coli*-produced FT_T sequence.

[6] For peptide matches greater than nine amino acids in length, the first 4 residues and last 4 residues are show separated by three dots (...).

(A)

001 AMHAALTPLT NKYRFIDVQP LTGVLGAEIT GVDLREPLDD STWNEILDAF

051 HTYQVIYFPG QAITNEQHIA FSRRFGPVDP VPILKSIEGY PEVQMIRREA

101 NESSRFIGDD WHTDSTFLDA PPAAVVMRAI EVPEYGGDTG FLSMYSAWET

151 LSPTMQATIE GLNVVHSATK VFGSLYQATN WRFSNTSVKV MDVDAGDRET

201 VHPLVVTHPV TGRRALYCNQ VYCQKIQGMT DAESKSLLQF LYEHATKFDF

251 TCR VRWK KDQ VLVWDNLCTM HRAVPDYAGK FR YLTR TTVA GDKPSR

(B)

002 M AMHAALTPL TNKYRFIDVQ PLTGVLGAEI TGVDLR EPLD DSTWNEILDA

052 FHTYQVIYFP GQAITNEQHI AFSR RFGPVD PVPILKSIEG YPEVQMIRR E

102 ANESSRFIGD DWHTDSTFLD APPAAVVMR A IEVPEYGGDT GFLSMYSAWE

152 TLSPTMQATI EGLNVVHSAT K VFGSLYQAT NWRFSNTSVK VMDVDAGDRE

202 TVHPLVVTHP VTGRRALYCN QVYCQK IQGM TDAESK SLLQ FLYEHATKFD

252 FTCR VRWKK D QVLVWDNLCT MHRAVPDYAG K FRYLTR TTV AGDKPSR

Figure 35.   Peptide Map of the MON 87429-Produced FT_T and *E. coli*-Produced FT_T

(A)   The amino acid sequence of the MON 87429-produced FT_T protein was deduced from the *ft_t* gene, a modified version of the R-2,4-dichlorophenoxypropionate dioxygenase (*Rdpa*) gene, present in MON 87429.   Boxed regions correspond to peptides that were identified from the MON 87429-produced FT_T protein sample using Nano LC-MS/MS.   In total, 97% coverage (288 out of 296 amino acids) of the expected protein sequence was covered by the identified peptides.

(B)   The amino acid sequence of the *E. coli*-produced FT_T protein was deduced from the *ft_t* gene, a modified version of the R-2,4-dichlorophenoxypropionate dioxygenase (*Rdpa*) gene, that is contained on the expression plasmid.   Boxed regions correspond to peptides that were identified from the *E. coli*-produced FT_T protein sample using MALDI-TOF MS.   In total, 65% coverage (194 out of 297 amino acids) of the expected protein sequence was covered by the identified peptides.

B1(c)(iii)   Results of Western blot analysis of the FT_T protein isolated from the grain of MON 87429 and immunoreactivity comparison to *E. coli*-produced FT_T protein

Western blot analysis was conducted using mouse anti-FT_T monoclonal antibody to provide additional confirmation of the identity of the FT_T protein isolated from the grain of MON 87429 and to assess the equivalence of the immunoreactivity of the MON 87429-produced and *E. coli*-produced FT_T proteins.   The results showed that immunoreactive bands with the same electrophoretic mobility were present in all lanes loaded with the MON 87429-produced and *E. coli*-produced FT_T proteins (Figure 36).   For each amount loaded, comparable signal intensity was observed between the MON 87429-produced and *E. coli*-produced FT_T protein bands.   As expected, the signal intensity increased with increasing load amounts of the MON 87429-produced and *E. coli*-produced FT_T proteins, thus, supporting the identity of the MON 87429-produced FT_T protein.

To compare the immunoreactivity of the MON 87429-produced and the *E. coli*-produced FT_T proteins, densitometric analysis was conducted on the bands that migrated at the expected apparent molecular weight (MW) for FT_T proteins (~35 kDa).   The signal intensity (reported in $OD \times mm^2$) of the band of interest in lanes loaded with MON 87429-produced and the *E. coli*-produced FT_T proteins was measured (Table 23).   Because the mean signal intensity of the MON 87429-produced FT_T protein band was within ± 35% of the mean signal of the *E. coli*-produced FT_T protein, the MON 87429-produced FT_T and *E. coli*-produced FT_T proteins were determined to have equivalent immunoreactivity.
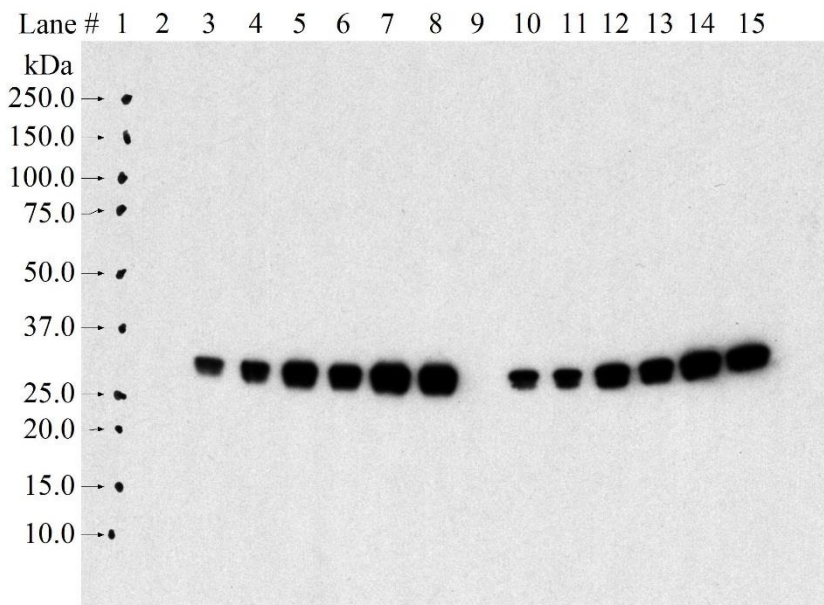
Figure 36. **Western Blot Analysis and Immunoreactivity of MON 87429-Produced and** *E. coli*-**Produced FT_T Proteins**

Aliquots of the MON 87429-produced FT_T protein and the *E. coli*-produced FT_T protein were subjected to SDS-PAGE and electrotransferred to a PVDF membrane. Proteins were detected using mouse anti-FT_T monoclonal antibody and then horse anti-mouse polyclonal antibody conjugated with peroxidase. Immunoreactive bands were visualized using an ECL system. The approximate MW (kDa) of the standards are shown on the left. The 45 second exposure is shown. Lane designations are as follows:

Lane	Sample	Amount (ng)
1	Precision Plus Protein™ Standards	-
2	Blank	-
3	MON 87429-produced FT_T	5
4	MON 87429-produced FT_T	5
5	MON 87429-produced FT_T	10
6	MON 87429-produced FT_T	10
7	MON 87429-produced FT_T	20
8	MON 87429-produced FT_T	20
9	Blank	-
10	*E. coli*-produced FT_T	5
11	*E. coli*-produced FT_T	5
12	*E. coli*-produced FT_T	10
13	*E. coli*-produced FT_T	10
14	*E. coli*-produced FT_T	20
15	*E. coli*-produced FT_T	20

Table 23.   Immunoreactivity of the MON 87429-Produced and *E. coli*-Produced FT_T Proteins

Mean Signal Intensity from MON 87429-Produced FT_T[1] (OD x mm²)	Mean Signal Intensity from *E. coli*-Produced FT_T [1] (OD x mm²)	Acceptance Limits[2] (OD x mm²)
94,017.0	97,454.4	63,345.4 – 131,563.4

[1] Each value represents the mean of six values (n = 6).
[2] The acceptance limits are for the MON 87429-produced FT_T protein and are based on the interval between -35% (97,454.4 x 0.65 = 63,345.4) and +35 % (97,454.4 x 1.35 = 131,563.4) of the mean of the *E. coli*-produced FT_T signal intensity across all loads.

B1(c)(iv)   Results of the MON 87429-produced FT-T protein molecular weight analysis

For apparent MW and purity determination, the MON 87429-produced FT_T and the *E. coli*-produced FT_T proteins were subjected to SDS-PAGE. Following electrophoresis, the gel was stained with Brilliant Blue G-Colloidal stain and analyzed by densitometry. The MON 87429-produced FT_T protein (Figure 37, lanes 3-8) migrated with the same mobility on the gel as the *E. coli*-produced FT_T protein (Figure 37, lane 2) and the apparent MW was calculated to be 36.0 kDa (Table 24). Because the experimentally determined apparent MW of the MON 87429-produced FT_T protein was within the acceptance limits for equivalence (Table 25), the MON 87429-produced FT_T and *E. coli*-produced FT_T proteins were determined to have equivalent apparent molecular weights.
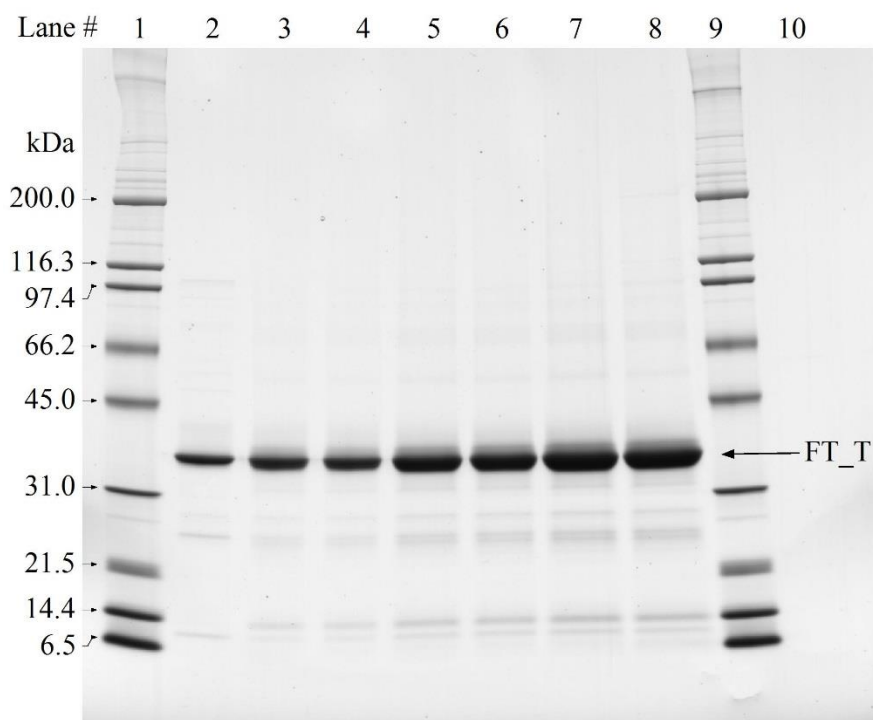
Figure 37. Purity and Apparent Molecular Weight Analysis of the MON 87429-Produced FT_T Protein

Aliquots of the MON 87429-produced and the *E. coli*-produced FT_T proteins were subjected to SDS-PAGE and the gel was stained with Brilliant Blue G-Colloidal stain. The MWs (kDa) are shown on the left and correspond to the standards loaded in lanes 1 and 9. Lane designations are as follows:

Lane	Sample	Amount (µg)
1	Broad Range MW Standard	5.0
2	*E. coli*-produced FT_T	1.0
3	MON 87429-produced FT_T	1.0
4	MON 87429-produced FT_T	1.0
5	MON 87429-produced FT_T	2.0
6	MON 87429-produced FT_T	2.0
7	MON 87429-produced FT_T	3.0
8	MON 87429-produced FT_T	3.0
9	Broad Range MW Standard	5.0
10	Blank	

Table 24. **Apparent Molecular Weight and Purity Analysis of the MON 87429-Produced FT_T Protein**

	Apparent MW[1] (kDa)	Purity[2] (%)
Average (n=6)	36.0	91

[1]Final MW was rounded to one decimal place.
[2]Average % purity was rounded to the nearest whole number.

Table 25. **Apparent Molecular Weight Comparison Between the MON 87429-Produced FT_T and *E. coli*-Produced FT_T Proteins**

Apparent MW of MON 87429-Produced FT_T Protein (kDa)	Apparent MW of *E. coli*-Produced FT_T Protein (kDa)	Acceptance Limits[1] (kDa)
36.0	35.5	34.1 – 36.8

[1] Data obtained from the *E. coli*-produced FT_T protein was used to generate a prediction interval for setting the acceptance limits.

B1(c)(v)   MON 87429 FT_T glycosylation analysis

Some eukaryotic proteins are post-translationally modified by the addition of carbohydrate moieties (Rademacher *et al.*, 1988). To test whether the FT_T protein was glycosylated when expressed in the maize grain of MON 87429, the MON 87429-produced FT_T protein was analyzed using an ECL™ glycoprotein detection method. Transferrin, a glycosylated protein, was used as a positive control in the assay. To assess equivalence of the MON 87429-produced and *E. coli*-produced FT_T proteins, the *E. coli*-produced FT_T protein was also analyzed.

A clear glycosylation signal was observed at the expected molecular weight (~ 80 kDa) in the lanes containing the positive control (transferrin) and the band intensity increased with increasing concentration (Figure 38, panel A). In contrast, no glycosylation signal was observed in the lanes containing the *E. coli*-produced FT_T protein or MON 87429-produced FT_T protein (Figure 38, panel A).

To confirm that MON 87429-produced FT_T and *E. coli*-produced FT_T proteins were appropriately loaded for glycosylation analysis, a second membrane with identical loadings and transfer time was stained with Coomassie Blue R250 for protein detection. Both the MON 87429-produced and *E. coli*-produced FT_T proteins were detected (Figure 38, panel B). These data indicate that the glycosylation status of MON 87429-produced FT_T protein is equivalent to that of the *E. coli*-produced FT_T protein and that neither is glycosylated.
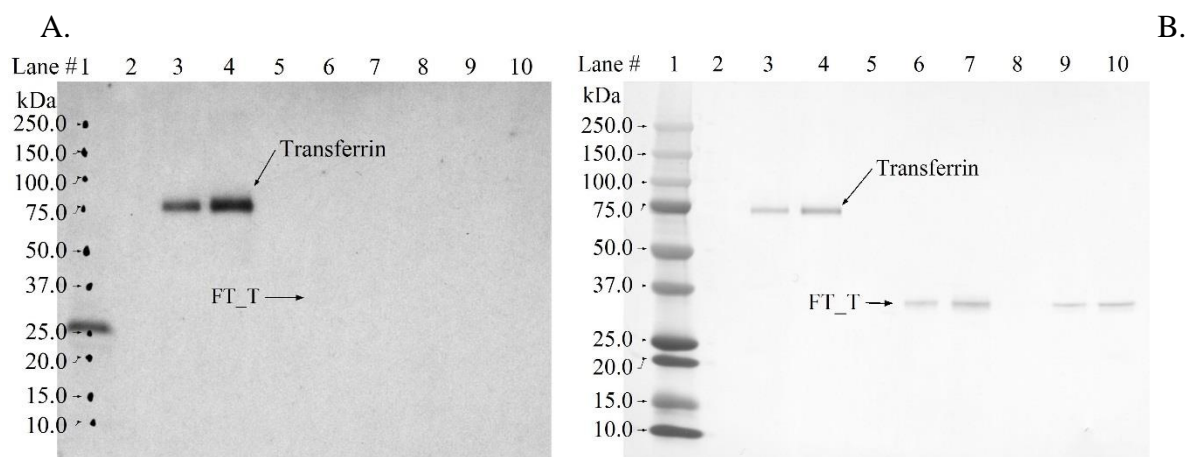
Figure 38. **Glycosylation Analysis of the MON 87429-Produced and *E. coli*-Produced FT_T Proteins**

Aliquots of the transferrin (positive control), *E. coli*-produced FT_T and MON 87429-produced FT_T were subjected to SDS-PAGE and electrotransferred to a PVDF membrane. The MWs (kDa) correspond to the Precision Plus Dual Color Protein™ Standards. The arrows show the expected migration of the MON 87429-produced and *E. coli*-produced FT_T proteins and transferrin. (A) Where present, the labeled carbohydrate moieties were detected by addition of streptavidin conjugated to HRP followed by a luminol-based detection using ECL reagents and exposure to Hyperfilm®. The 30 second exposure is shown. (B) An equivalent blot was stained with Coomassie Blue R250 to confirm the presence of proteins. Lane designations are as follows:

Lane	Sample	Amount (ng)
1	Precision Plus Protein™ Standards	-
2	Blank	-
3	Transferrin (positive control)	100
4	Transferrin (positive control)	200
5	Blank	-
6	MON 87429-produced FT_T	100
7	MON 87429-produced FT_T	200
8	Blank	-
9	*E. coli*-produced MON 87429 FT_T	100
10	*E. coli*-produced MON 87429 FT_T	200

B1(c)(vi)   FT_T functional activity

The functional activities of the MON 87429-produced and *E. coli*-produced FT_T proteins were determined using a colorimetric assay that measures the FT_T catalyzed degradation of 2,4-D to 2,4-DCP.   In this assay, protein-specific activity is expressed as units per milligram of protein (U/mg), where a unit (U) is 1 nmole of 2,4-D to 2,4-DCP per min at 25°C.   The MON 87429-produced and *E. coli*-produced FT_T proteins were considered to have equivalent functional activity if the specific activity of both were within the preset acceptance limits of 183 to 974 U/mg (the prediction interval calculated from a data set of historically determined FT_T protein activity;).

The experimentally determined specific activity for the MON 87429-produced and *E. coli*-produced FT_T proteins are presented in Table 26.   The specific activities of MON 87429-produced and *E. coli*-produced FT_T proteins were 723 U/mg and 720 U/mg of FT_T protein, respectively. Because the specific activities of MON 87429-produced and *E. coli*-produced FT_T proteins fall within the preset acceptance limits (Table 26), the MON 87429-produced FT_T protein was considered to have equivalent functional activity to that of the *E. coli*-produced FT_T protein.

Table 26.   Functional Activity of MON 87429-Produced and *E. coli*-Produced FT_T Proteins

MON 87429-Produced FT_T[1] (U/mg)	*E. coli*-Produced FT_T[1] (U/mg)	Acceptance Limits[2] (U/mg)
723	720	183.4 – 974.0

[1] Value refers to mean calculated based on samples spectrophotometrically read in triplicate plate wells.

[2] Data obtained from two *E. coli*-produced FT_T lots were used to generate a prediction interval for setting the acceptance limits.

B1(c)(vii)   FT_T protein identity and equivalence – Conclusion

The MON 87429-produced FT_T protein was purified from MON 87429 grain, was characterised, and a comparison of the physicochemical and functional properties between the MON 87429-produced and the *E. coli*-produced FT_T proteins was conducted following a panel of analytical tests: 1) N-terminal sequence analysis established the same identity for the MON 87429-produced and *E. coli*-produced FT_T proteins; 2) Nano LC-MS/MS analysis yielded peptide masses consistent with the expected peptide masses from the theoretical trypsin digest of the *ft_t* gene product present in MON 87429; 3) the MON 87429-produced and the *E. coli*-produced FT_T proteins were both detected on a Western blot probed with antibodies specific for FT_T protein and the immunoreactive properties of both proteins was shown to be equivalent; 4) the electrophoretic mobility and apparent molecular weight of the MON 87429-produced and *E. coli*-produced FT_T proteins were shown to be equivalent; 5) the glycosylation status of MON 87429-produced and *E. coli*-produced FT_T proteins was determined to be equivalent; and 6) the functional activity of the MON 87429-produced and *E. coli*-produced FT_T was demonstrated to be equivalent.   These results demonstrate that the MON 87429-produced FT_T protein and the *E. coli*-produced FT_T protein are equivalent.   This demonstration of protein equivalence confirms that the *E. coli*-produced FT_T protein is appropriate for use in the evaluation of the safety of the MON 87429-produced FT_T protein.

B1(d)   Characterisation and equivalence of MON 87429-produced CP4 EPSPS protein

For details, please also refer to ████████ 2018 (MSL0029463).

Identity and Function of the CP4 EPSPS Protein

The 5-enolpyruvylshikimate-3-phosphate synthase (EPSPS) family of enzymes is ubiquitous in plants and microorganisms and their properties have been well studied. Bacterial and plant EPSPS enzymes are mono-functional with molecular mass of 44-48 kD (Kishore *et al.*, 1988).   EPSPS is a key enzyme involved in aromatic amino acid biosynthesis and catalyses the reaction where the enolpyruvyl group from phosphoenol pyruvate (PEP) is transferred to the 5-hydroxyl of shikimate-3-phosphate to form 5-enolpyruvylshikimate-3-phosphate (EPSP) and inorganic phosphate (Alibhai and Stallings, 2001).   The CP4 EPSPS protein expressed in MON 87429 is functionally the same to endogenous plant EPSPS enzymes except it displays a much reduced affinity for glyphosate (Sikorski and Gruys, 1997). Shikimic acid is a substrate for the biosynthesis of the aromatic amino acids phenylalanine, tryptophan and tyrosine, as well as many secondary metabolites, such as tetrahydrofolate, ubiquinone, and vitamin K and the shikimic acid pathway is absent in mammals, fish, birds, reptiles and insects (Alibhai and Stallings, 2001). The CP4 EPSPS protein degrades rapidly in simulated gastric and intestinal fluids and no adverse effects were noted on mice gavaged with a high dose (572 mg/kg bodyweight) of this protein (Harrison *et al.*, 1996). Additionally, the CP4 EPSPS protein does not have significant sequence or structural homology to known toxins or allergens (Harrison *et al.*, 1996; OECD, 1999).   As is documented in this review paper (ILSI-CERA, 2010), regulatory agencies in a number of countries outside the U.S. (*e.g.*, Canada, Mexico, Australia, Japan, Brazil, Argentina) have assessed and verified the food, feed and environmental safety of CP4 EPSPS protein.

Results from the physicochemical and functional characterisation of the CP4 EPSPS protein in MON 87429 indicate that it is similar to CP4 EPSPS protein produced in several other commercially available crops that have been reviewed by the FDA and deregulated by the USDA (*e.g.* Roundup Ready® events of soybean, maize, cotton, sugarbeet, canola, and alfalfa).   The safety and mode-of-action of CP4 EPSPS proteins are well documented and is the subject of numerous publications (Harrison *et al.*, 1996; Hoff *et al.*, 2007; ILSI-CERA, 2010; U.S. EPA, 1996).   Additionally, on August 2, 1996 the U.S. EPA established an exemption from the requirement of a tolerance for residues of the plant pesticide inert ingredient CP4 EPSPS and the genetic material necessary for its production in all plants (40 CFR § 174.523, redesignated from § 180.1174, effective April 25, 2007).

Identity and Equivalence Studies of the CP4 EPSPS Protein

As previously described, the safety assessment of crops derived through biotechnology includes characterisation of the physicochemical and functional properties of and confirmation of the safety of the introduced protein(s). For the safety data generated using *E. coli*-produced CP4 EPSPS protein to be applied to CP4 EPSPS protein produced in MON 87429, the equivalence of the plant- and *E. coli*-produced proteins must be estabilished. To assess the equivalence between MON 87429-produced and *E. coli*-produced CP4 EPSPS protein, a small quantity of the CP4 EPSPS protein was purified from grain of MON 87429

maize. The MON 87429-produced CP4 EPSPS protein was characterised and the equivalence of the physicochemical characteristics and functional activity between the MON 87429-produced and the *E. coli*-produced CP4 EPSPS proteins was assessed using a panel of six analytical tests as shown in Table 27. Taken together, these data provide a detailed characterisation of the MON 87429-produced CP4 EPSPS protein and establish the equivalence of MON 87429-produced CP4 EPSPS and *E. coli*-produced CP4 EPSPS proteins.

Table 27.   Summary of MON 87429 CP4 EPSPS Protein Identity and Equivalence

Analytical Test Assessment	Section Cross Reference	Analytical Test Outcome
1. N-terminal sequence	B1(d)(i)	The expected N-terminal sequence was confirmed
2. Nano LC-MS/MS[1]	B1(d)(ii)	Nano LC-MS/MS[1] analysis yielded peptide masses consistent with the expected peptide masses from the theoretical trypsin digest of the MON 87429-produced CP4 EPSPS sequence
3. Western blot analysis	B1(d)(iii)	MON 87429-produced CP4 EPSPS protein identity was confirmed using a Western blot probed with an antibody specific for CP4 EPSPS proteins Immunoreactive properties of the MON 87429-produced CP4 EPSPS and the *E. coli*-produced CP4 EPSPS proteins were shown to be equivalent
4. Apparent molecular weight (MW)	B1(d)(iv)	Electrophoretic mobility and apparent molecular weight of the MON 87429-produced CP4 EPSPS and the *E. coli*-produced CP4 EPSPS proteins were shown to be equivalent
5. Glycosylation analysis	B1(d)(v)	MON 87429-produced CP4 EPSPS and the *E. coli*-produced CP4 EPSPS proteins were each shown to not be glycosylated
6. Functional activity	B1(d)(vi)	Functional activity of the MON 87429-produced CP4 EPSPS and the *E. coli*-produced CP4 EPSPS proteins were shown to be equivalent

[1] Nano LC-MS/MS = Nanoscale liquid chromatography coupled to tandem mass spectrometry
[2] SDS-PAGE = sodium dodecyl sulfate-polyacrylamide gel electrophoresis

A summary of the data obtained to support a conclusion of protein equivalence is below.

B1(d)(i)   Results of the N-terminal sequencing analysis

The expected N-terminal sequence for the CP4 EPSPS protein deduced from the *cp4 epsps* gene present in maize of MON 87429 was observed by LC-MS/MS (see Experimental Sequence 1, Figure 39). A second N-terminal sequence was also observed, in which N-terminal methionine was cleaved *in vivo* from MON 87429-produced CP4 EPSPS by methionine aminopeptidase and other aminopeptidases (see Experimental Sequence 2, Figure 39).   The cleavage of the N-terminal methionine from proteins *in vivo* by methionine aminopeptidase is common in many organisms (Bradshaw *et al.*, 1998; Wang *et al.*, 2016). The N-terminal sequencing results for MON 87429-produced CP4 EPSPS protein were

consistent with the sequencing results for the *E. coli*-produced CP4 EPSPS protein observed by fifteen-cycles of Edman sequence analysis (Figure 39). Hence, the sequence information confirms the identity of the CP4 EPSPS protein isolated from the grain of MON 87429.

Amino Acids Residue # from the N-terminus	→	1	2	3	4	5	6	7	8	9	10	11	12	13	14	15
E. coli-produced CP4 EPSPS sequence	→	M	L	H	G	A	S	S	R	P	A	T	A	(R)	K	S
		|	|	|	|	|	|	|	|	|	|	|	|	|	|	|
Expected CP4 EPSPS Sequence	→	M	L	H	G	A	S	S	R	P	A	T	A	R	K	S
		|	|	|	|	|	|	|	|	|	|	|	|	|		
MON 87429-produced CP4 EPSPS Experimental Sequence 1	→	*M	L	H	G	A	S	S	R	P	A	T	A	R		
			|	|	|	|	|	|	|	|	|	|	|	|		
MON 87429-produced CP4 EPSPS Experimental Sequence 2	→	-	L	H	G	A	S	S	R	P	A	T	A	R		

Figure 39.   N-Terminal Sequence of the MON 87429-Produced CP4 EPSPS Protein

The experimental sequence obtained from the MON 87429-produced CP4 EPSPS was compared to the expected sequence deduced from the *cp4 epsps* gene present in MON 87429. *E. coli*-produced CP4 EPSPS protein sequence above was derived from the reference substance certificate of analysis (COA) (lot 10000739). The single letter International Union of Pure and Applied Chemistry - International Union of Biochemistry (IUPAC-IUB) amino acid code is M, methionine; L; leucine; H, histidine; G, glycine; A, alanine; S, serine; R, arginine; P, proline; T, threonine; K, lysine; ( ), tenuous designation; *, acetylation and oxidation were observed at the N-terminal methionine.

B1(d)(ii)   Results nano LC-MS/MS mass fingerprint analysis

Peptide mass fingerprint analysis is a standard technique used for confirming the identity of proteins.   The ability to identify a protein using this method is dependent upon matching a sufficient number of observed tryptic peptide fragment masses with predicted tryptic peptide fragment masses.   In general, protein identification made by peptide mapping is considered to be reliable if >40% of the protein sequence was identified by matching experimental masses observed for the tryptic peptide fragments to the expected masses for the fragments (Biron *et al.*, 2006; Krause *et al.*, 1999). The identity of the MON 87429-produced CP4 EPSPS protein was confirmed by LC-MS/MS analysis of peptide fragments produced by the trypsin digestion of the MON 87429-produced CP4 EPSPS protein.

There were 45 unique peptides identified that corresponded to the masses expected to be produced by trypsin digestion of the MON 87429-produced CP4 EPSPS protein (Table 28). The identified masses were used to assemble a coverage map of the entire CP4 EPSPS protein (Figure 40A).   The experimentally determined coverage of the CP4 EPSPS protein was 92% (Figure 40A, 420 out of 455 amino acids).   This analysis further confirms the identity of MON 87429-produced CP4 EPSPS protein.

There were 28 unique peptides identified that corresponded to the masses expected to be produced by trypsin digestion of the *E. coli*-produced CP4 EPSPS protein (Table 29) by MALDI-TOF MS analysis during the protein characterisation.   The identified masses were used to assemble a coverage map of the entire CP4 EPSPS protein (Figure 40B).   The experimentally determined coverage of the *E. coli*-produced CP4 EPSPS protein was 64% (Figure 40B, 291 out of 455 amino acids).   This analysis further confirms the identity of *E. coli*-produced CP4 EPSPS protein.

Table 28. Summary of the Tryptic Masses Identified for the MON 87429-Produced CP4 EPSPS Using Nano LC-MS/MS[1]

Experimental Mass[2]	Calculated Mass[3]	Difference[4]	Fragment[5]	Sequence[6]
1369.6883	1369.6884	-0.0001	1-13	*MLHG…ATAR
1222.6535	1222.6530	0.0005	2 - 13	LHGA…ATAR
990.5455	990.5458	-0.0003	14 - 23	KSSG…GTVR
1500.8235	1500.826	-0.0025	14 - 28	KSSG…PGDK
862.4507	862.4509	-0.0002	15 - 23	SSGL…GTVR
528.2909	528.2908	0.0001	24 - 28	IPGDK
1108.5992	1108.5989	0.0003	24 - 33	IPGD…ISHR
598.3186	598.3187	-0.0001	29 - 33	SISHR
1358.6285	1358.6289	-0.0004	34 - 46	SFMF…GETR
1557.8255	1557.8250	0.0005	47 - 61	ITGL…NTGK
834.3843	834.3840	0.0003	62 - 69	AMQAMGAR
2449.2101	2449.2087	0.0014	105 - 127	LTMG…SLTK
615.3276	615.3275	0.0001	128 - 132	RPMGR
710.4438	710.4439	-0.0001	133 - 138	VLNPLR
789.4054	789.4055	-0.0001	139 - 145	EMGVQVK
677.2611	677.2616	-0.0005	146 - 151	SEDGDR
1356.7024	1356.6997	0.0027	146 - 157	SEDG…VTLR
1638.8715	1638.8689	0.0026	146 - 160	SEDG…RGPK
697.4486	697.4487	-0.0001	152 - 157	LPVTLR
1229.6745	1229.6768	-0.0023	158 - 168	GPKT…ITYR
947.5075	947.5076	-0.0001	161 - 168	TPTPITYR
929.5014	929.5004	0.001	169 - 177	VPMA…AQVK
2366.3270	2366.3243	0.0027	178 - 200	SAVL...IMTR
628.2815	628.2816	-0.0001	201 - 205	DHTEK
1992.9551	1992.9575	-0.0024	206 - 224	MLQG…DGVR
843.4929	843.4926	0.0003	225 - 231	TIRLEGR
4187.2564	4187.2552	0.0012	234 - 274	LTGQ...NPTR
2182.1678	2182.1667	0.0011	275 - 294	TGLI…INPR
1114.5619	1114.5618	0.0001	295 - 305	LAGG...ADLR
1369.7309	1369.7314	-0.0005	295 - 307	LAGG...LRVR
534.3014	534.3013	0.0001	308 - 312	SSTLK
1387.7313	1387.7307	0.0006	308 - 320	SSTL...PEDR
871.4400	871.4400	0	313 - 320	GVTVPEDR
3248.6134	3248.6097	0.0037	321 - 351	APSM…EELR
732.3766	732.3766	0	352 - 357	VKESDR
1585.88	1585.8787	0.0013	352 - 366	VKES…NGLK
1358.7158	1358.7154	0.0004	354 - 366	ESDR…NGLK
871.5127	871.5127	0	358 - 366	LSAV…NGLK

Table 28. Summary of the Tryptic Masses Identified for the MON 87429-Produced CP4 EPSPS Using Nano LC-MS/MS[1] (continued)

Experimental Mass[2]	Calculated Mass[3]	Difference[4]	Fragment[5]	Sequence[6]
1761.8214	1761.8203	0.0011	367 - 382	LNGV...LVVR
628.3296	628.3293	0.0003	383 - 388	GRPDGK
2256.1486	2256.1472	0.0014	383 - 405	GRPD…LDHR
1645.8283	1645.8285	-0.0002	389 - 405	GLGN...LDHR
4319.0954	4319.0948	0.0006	406 - 446	IAMS...LGAK
804.4226	804.4229	-0.0003	447 - 453	IELSDTK
946.4976	946.4971	0.0005	447 - 455	IELS…TKAA

[1] All imported values were rounded to 4 decimal places.

[2] Only experimental masses that matched calculated masses with the highest scores are listed in the table.

[3] The calculated mass is the exact molecular mass calculated from the matched peptide sequence.

[4] The calculated difference = experimental mass – calculated mass.

[5] Position refers to amino acid residues within the predicted MON 87429-produced CP4 EPSPS sequence as depicted in Figure 40A.

[6] For peptide matches greater than nine amino acids in length, the first 4 residues and last 4 residues are show separated by three dots (...).

* acetylation and oxidation observed

Table 29.   Summary of the Tryptic Masses Identified for the *E. coli*-Produced CP4 EPSPS Using MALDI-TOF MS[1]

Experimental Mass[2]	Calculated Mass[3]	Difference[4]	Fragment[5]	Sequence[6]
991.61	991.55	0.06	14 - 23	KSSG…GTVR
863.46	863.46	0.00	15 - 23	SSGL…GTVR
2450.32	2450.23	0.09	24 - 46	IPGD…GETR
599.32	599.33	-0.01	29 - 33	SISHR
1359.65	1359.64	0.01	34 - 46	SFMF…GETR
1558.87	1558.83	0.04	47 - 61	ITGL…NTGK
835.39	835.39	0.00	62 - 69	AMQAMGAR
3244.58	3244.52	0.06	73 - 104	EGDT…TGCR
2450.32	2450.22	0.10	105 - 127	LTMG…SLTK
616.32	616.34	-0.02	128 - 132	RPMGR
711.45	711.45	0.00	133 - 138	VLNPLR
1357.70	1357.71	-0.01	146 - 157	SEDG…VTLR
698.45	698.46	-0.01	152 - 157	LPVTLR
948.51	948.52	-0.01	161 - 168	TPTPITYR
1859.96	1860.01	-0.05	161 - 177	TPTP…AQVK
930.55	930.51	0.04	169 - 177	VPMA…AQVK
2367.28	2367.33	-0.05	178 - 200	SAVL...IMTR
629.34	629.29	0.05	201 - 205	DHTEK
1993.93	1993.97	-0.04	206 - 224	MLQG…DGVR
2183.12	2183.17	-0.05	275 - 294	TGLI…INPR
1115.56	1115.57	-0.01	295 - 305	LAGG...ADLR
872.44	872.45	-0.01	313 - 320	GVTVPEDR
733.47	733.38	0.09	352 - 357	VKESDR
1359.65	1359.72	-0.07	354 - 366	ESDR…NGLK
872.44	872.52	-0.08	358 - 366	LSAV…NGLK
1763.78	1763.81	-0.03	367 - 382	LNGV...LVVR
629.34	629.34	0.00	383 - 388	GRPDGK
1646.81	1646.84	-0.03	389 - 405	GLGN...LDHR

[1] All imported values were rounded to 2 decimal places.

[2] Only experimental masses that matched calculated CP4 EPSPS trypsin digested masses are listed in the table.

[3] The calculated mass is the exact molecular mass calculated from the matched peptide sequence.

[4] The calculated difference = experimental mass - calculated mass.

[5] Position refers to amino acid residues within the predicted *E. coli*-produced CP4 EPSPS sequence as depicted in Figure 40B.

[6] For peptide matches greater than nine amino acids in length, the first 4 residues and last 4 residues are show separated by three dots (...).

(A)

001 MLHGASSRPA TARKSSGLSG TVRIPGDKSI SHRSFMFGGL ASGETRITGL

051 LEGEDVINTG KAMQAMGARI RKEGDTWIID GVGNGGLLAP EAPLDFGNAA

101 TGCRLTMGLV GVYDFDSTFI GDASLTKRPM GRVLNPLREM GVQVKSEDGD

151 RLPVTLRGPK TPTPITYRVP MASAQVKSAV LLAGLNTPGI TTVIEPIMTR

201 DHTEKMLQGF GANLTVETDA DGVRTIRLEG RGKLTGQVID VPGDPSSTAF

251 PLVAALLVPG SDVTILNVLM NPTRTGLILT LQEMGADIEV INPRLAGGED

301 VADLRVRSST LKGVTVPEDR APSMIDEYPI LAVAAAFAEG ATVMNGLEEL

351 RVKESDRLSA VANGLKLNGV DCDEGETSLV VRGRPDGKGL GNASGAAVAT

401 HLDHRIAMSF LVMGLVSENP VTVDDATMIA TSFPEFMDLM AGLGAKIELS

451 DTKAA

(B)

001 MLHGASSRPA TARKSSGLSG TVRIPGDKSI SHRSFMFGGL ASGETRITGL

051 LEGEDVINTG KAMQAMGARI RKEGDTWIID GVGNGGLLAP EAPLDFGNAA

101 TGCRLTMGLV GVYDFDSTFI GDASLTKRPM GRVLNPLREM GVQVKSEDGD

151 RLPVTLRGPK TPTPITYRVP MASAQVKSAV LLAGLNTPGI TTVIEPIMTR

201 DHTEKMLQGF GANLTVETDA DGVRTIRLEG RGKLTGQVID VPGDPSSTAF

251 PLVAALLVPG SDVTILNVLM NPTRTGLILT LQEMGADIEV INPRLAGGED

301 VADLRVRSST LKGVTVPEDR APSMIDEYPI LAVAAAFAEG ATVMNGLEEL

351 RVKESDRLSA VANGLKLNGV DCDEGETSLV VRGRPDGKGL GNASGAAVAT

401 HLDHRIAMSF LVMGLVSENP VTVDDATMIA TSFPEFMDLM AGLGAKIELS

451 DTKAA

Figure 40.   Peptide Map of the MON 87429-Produced CP4 EPSPS and *E. coli*-Produced CP4 EPSPS

(A). The amino acid sequence of the MON 87429-produced CP4 EPSPS protein was deduced from the *cp4 epsps* gene present in MON 87429.   Boxed regions correspond to peptides that were identified from the MON 87429-produced CP4 EPSPS protein sample using Nano LC-MS/MS.   In total, 92% coverage (420 out of 455 amino acids) of the expected protein sequence was covered by the identified peptides.

(B). The amino acid sequence of the *E. coli*-produced CP4 EPSPS protein was deduced from the *cp4 epsps* gene that is contained on the expression plasmid.   Boxed regions correspond to peptides that were identified from the *E. coli*-produced CP4 EPSPS protein sample using MALDI-TOF MS.   In total, 64% coverage (291 out of 455 amino acids) of the expected protein sequence was covered by the identified peptides

B1(d)(iii)   Results of Western blot analysis of the CP4 EPSPS protein isolated from the grain of MON 87429 and immunoreactivity comparison to *E. coli*-produced MON 87429 CP4 EPSPS protein

Western blot analysis was conducted using goat anti-CP4 EPSPS polyclonal antibody as additional means to confirm the identity of the CP4 EPSPS protein isolated from the grain of MON 87429 and to assess the equivalence of the immunoreactivity of the MON 87429-produced and *E. coli*-produced CP4 EPSPS proteins.

The results showed that immunoreactive bands with the same electrophoretic mobility were present in all lanes loaded with the MON 87429-produced and *E. coli*-produced CP4 EPSPS proteins (Figure 41).   For each amount loaded, comparable signal intensity was observed between the MON 87429-produced and *E. coli*-produced CP4 EPSPS protein bands.   As expected, the signal intensity increased with increasing load amounts of the MON 87429-produced and *E. coli*-produced CP4 EPSPS proteins, thus, supporting identification of MON 87429-produced CP4 EPSPS protein.

To compare the immunoreactivity of the MON 87429-produced and the *E. coli*-produced CP4 EPSPS proteins, densitometric analysis was conducted on the bands that migrated at the expected apparent MW for CP4 EPSPS proteins (~ 44 kDa).   The signal intensity (reported in $OD \times mm^2$) of the band of interest in lanes loaded with MON 87429-produced and the *E. coli*-produced CP4 EPSPS proteins was measured (Table 30).   Because the mean signal intensity of the MON 87429-produced CP4 EPSPS protein band was within ± 35% of the mean signal of the *E. coli*-produced CP4 EPSPS protein, the MON 87429-produced CP4 EPSPS and *E. coli*-produced CP4 EPSPS proteins were determined to have equivalent immunoreactivity.
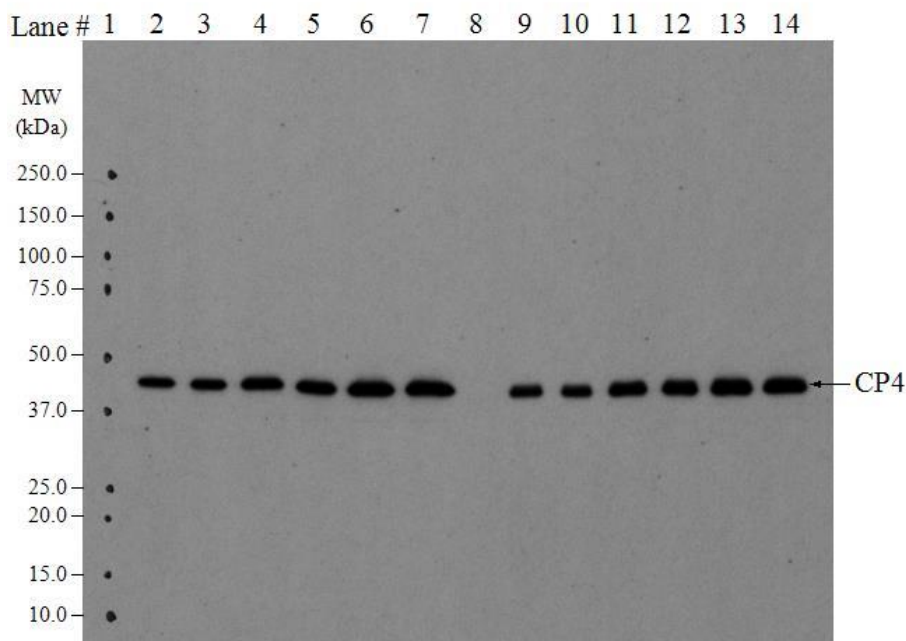
Figure 41.   Western Blot Analysis of MON 87429-Produced and *E. coli*-Produced CP4 EPSPS Proteins

Aliquots of the MON 87429-produced CP4 EPSPS protein and the *E. coli*-produced CP4 EPSPS protein were subjected to SDS-PAGE and electrotransferred to a nitrocellulose membrane.   Proteins were detected using goat anti-CP4 EPSPS polyclonal antibody conjugated with peroxidase. Immunoreactive bands were visualized using an ECL system.   The 1-minute exposure is shown. The approximate MW (kDa) of the standards are shown on the left.   Lane 15 was cropped from the image.   Lane designations are as follows:

Lane	Sample	Amount (ng)
1	Precision Plus Protein™ Standards	-
2	*E. coli*-produced CP4 EPSPS	1
3	*E. coli*-produced CP4 EPSPS	1
4	*E. coli*-produced CP4 EPSPS	2
5	*E. coli*-produced CP4 EPSPS	2
6	*E. coli*-produced CP4 EPSPS	3
7	*E. coli*-produced CP4 EPSPS	3
8	Blank	-
9	MON 87429-produced CP4 EPSPS	1
10	MON 87429-produced CP4 EPSPS	1
11	MON 87429-produced CP4 EPSPS	2
12	MON 87429-produced CP4 EPSPS	2
13	MON 87429-produced CP4 EPSPS	3
14	MON 87429-produced CP4 EPSPS	3
15	Blank	-

Table 30. Immunoreactivity of the MON 87429-Produced and *E. coli*-Produced CP4 EPSPS Proteins

Mean Signal Intensity from MON 87429-Produced CP4 EPSPS [1] ($OD \times mm^2$)	Mean Signal Intensity from *E. coli*-Produced CP4 EPSPS [1] ($OD \times mm^2$)	Acceptance Limits [2] ($OD \times mm^2$)
22773.65	24458.90	15898.29 - 33019.52

[1] Each value represents the mean of six values (n = 6).
[2] The acceptance limits are for the MON 87429-produced CP4 EPSPS protein and are based on the interval between -35% (24458.90 x 0.65 = 15898.29) and +35 % (24458.90 x 1.35 = 33019.52) of the mean of the *E. coli*-produced CP4 EPSPS signal intensity across all loads.

B1(d)(iv)   Results of the MON 87429-produced CP4 EPSPS protein molecular weight analysis and purity analysis

For apparent MW and purity determination, the MON 87429-produced CP4 EPSPS and the *E. coli*-produced CP4 EPSPS proteins were subjected to SDS-PAGE. Following electrophoresis, the gel was stained with Brilliant Blue G-Colloidal stain and analyzed by densitometry. The MON 87429-produced CP4 EPSPS protein (Figure 42, lanes 3-8) migrated to the same position on the gel as the *E. coli*-produced CP4 EPSPS protein (Figure 42, lane 2) and the apparent MW was calculated to be 44.0 kDa (Table 31). Because the experimentally determined apparent MW of the MON 87429-produced CP4 EPSPS protein was within the acceptance limits for equivalence (Table 32), the MON 87429-produced CP4 EPSPS and *E. coli*-produced CP4 EPSPS proteins were determined to have equivalent apparent molecular weights.

The purity of the MON 87429-produced CP4 EPSPS protein was calculated based on the six lanes loaded on the gel (Figure 42, lanes 3-8). The average purity was determined to be 88% (Table 31).
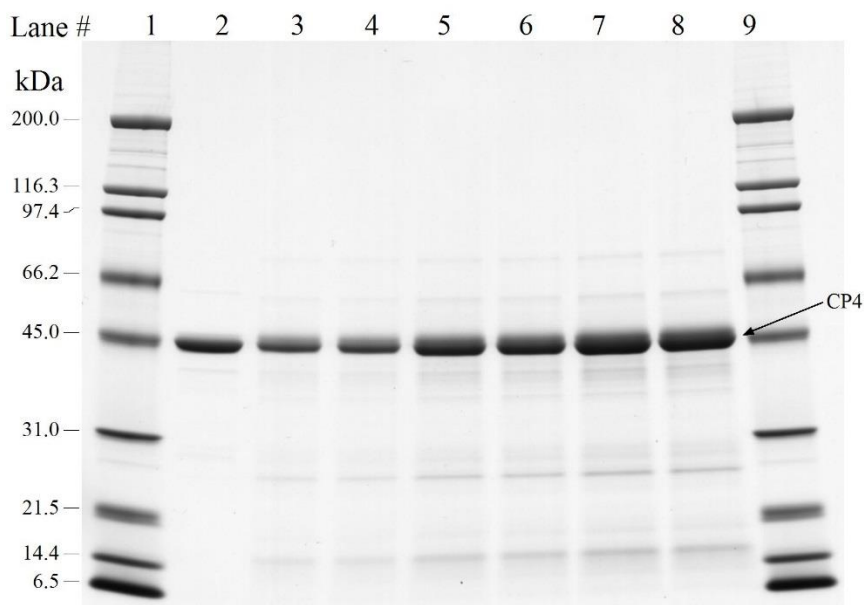
Figure 42.   Purity and Apparent Molecular Weight Analysis of the MON 87429-Produced CP4 EPSPS Protein

Aliquots of the MON 87429-produced and the *E. coli*-produced CP4 EPSPS proteins were subjected to SDS-PAGE and the gel was stained with Brilliant Blue G-Colloidal stain.   The MWs (kDa) are shown on the left and correspond to the standards loaded in lanes 1 and 9.   Lane 10 was cropped from the image.   Lane designations are as follows:

Lane	Sample	Amount (µg)
1	Broad Range MW Standard	5.0
2	*E. coli*-produced CP4 EPSPS	1.0
3	MON 87429-produced CP4 EPSPS	1.0
4	MON 87429-produced CP4 EPSPS	1.0
5	MON 87429-produced CP4 EPSPS	2.0
6	MON 87429-produced CP4 EPSPS	2.0
7	MON 87429-produced CP4 EPSPS	3.0
8	MON 87429-produced CP4 EPSPS	3.0
9	Broad Range MW Standard	5.0
10	Blank	

Table 31. **Apparent Molecular Weight and Purity Analysis of the MON 87429-Produced CP4 EPSPS Protein**

	Apparent MW[1] (kDa)	Purity[2] (%)
Average (n=6)	44.0	88

[1]Final MW was rounded to one decimal place.
[2]Average % purity was rounded to the nearest whole number.

Table 32. **Apparent Molecular Weight Comparison Between the MON 87429-Produced CP4 EPSPS and *E. coli*-Produced CP4 EPSPS Proteins**

Apparent MW of MON 87429-Produced CP4 EPSPS Protein (kDa)	Apparent MW of *E. coli*-Produced CP4 EPSPS Protein (kDa)	Acceptance Limits[1] (kDa)
44.0	43.8	42.6 – 45.1

[1] Data obtained for the *E. coli*-produced CP4 EPSPS protein and several plant-produced CP4 EPSPS proteins was used to generate the prediction interval).

B1(d)(v)   MON 87429 CP4 EPSPS glycosylation analysis

Some eukaryotic proteins are post-translationally modified by the addition of carbohydrate moieties (Rademacher *et al.*, 1988).   To test whether the CP4 EPSPS protein was glycosylated when expressed in the maize grain of MON 87429, the MON 87429-produced CP4 EPSPS protein was analyzed using an ECL™ glycoprotein detection method. Transferrin, a glycosylated protein, was used as a positive control in the assy.   To assess equivalence of the MON 87429-produced and *E. coli*-produced CP4 EPSPS proteins, the *E. coli*-produced CP4 EPSPS protein, previously shown to be free of glycosylation (Harrison *et al.*, 1996), was also analyzed.

A clear glycosylation signal was observed at the expected molecular weight (~ 80 kDa) in the lanes containing the positive control (transferrin) and the band intensity increased with increasing concentration (Figure 43A).   In contrast, no glycosylation signal was observed in the lanes containing the *E. coli*-produced CP4 EPSPS protein or MON 87429-produced CP4 EPSPS protein (Figure 43A).

To confirm that MON 87429-produced CP4 EPSPS and *E. coli*-produced CP4 EPSPS proteins were appropriately loaded for glycosylation analysis, a second membrane with identical loadings and transfer time was stained with Coomassie Blue R250 for protein detection.   Both the MON 87429-produced and *E. coli*-produced CP4 EPSPS proteins were detected (Figure 43B).   These data indicate that the glycosylation status of MON 87429-produced CP4 EPSPS protein is equivalent to that of the *E. coli*-produced CP4 EPSPS protein and that neither is glycosylated.

A.   B.
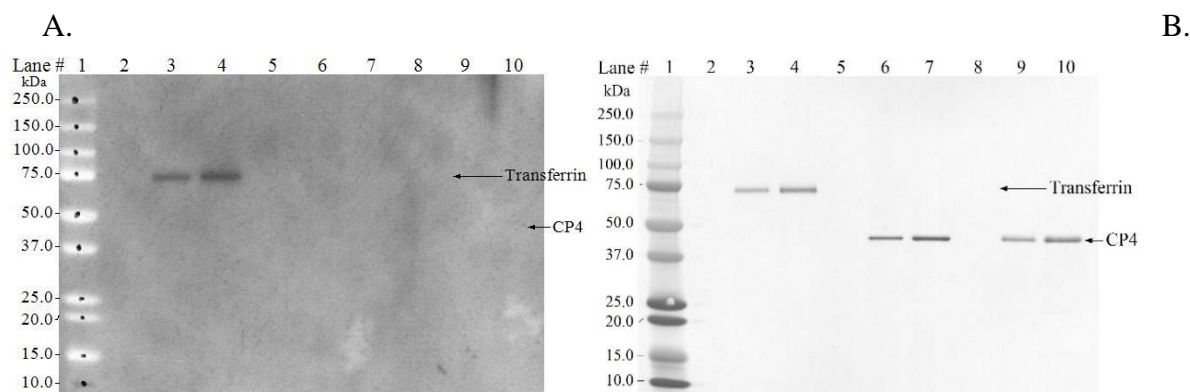
Figure 43.   Glycosylation Analysis of the MON 87429-Produced CP4 EPSPS Protein

Aliquots of the transferrin (positive control), *E. coli*-produced CP4 EPSPS and MON 87429-produced CP4 EPSPS were subjected to SDS-PAGE and electrotransferred to a PVDF membrane.   The MWs (kDa) correspond to the Precision Plus Protein™ Standards.   The arrows show the expected migration of the MON 87429-produced and *E. coli*-produced CP4 EPSPS proteins and transferrin. (A) Where present, the labeled carbohydrate moieties were detected by addition of streptavidin conjugated to HRP followed by a luminol-based the detection using ECL reagents and exposure to Hyperfilm®. The 4-minute exposure is shown. (B) An equivalent blot was stained with Coomassie Blue R250 to confirm the presence of proteins.   Lane designations are as follows:

Lane	Sample	Amount (ng)
1	Precision Plus Protein™ Standards	-
2	Blank	-
3	Transferrin (positive control)	100
4	Transferrin (positive control)	200
5	Blank	-
6	*E. coli*-produced MON 87429 CP4 EPSPS	100
7	*E. coli*-produced MON 87429 CP4 EPSPS	200
8	Blank	-
9	MON 87429-produced CP4 EPSPS	100
10	MON 87429-produced CP4 EPSPS	200

B1(d)(vi)   CP4 EPSPS functional activity

The functional activity of the MON 87429-produced and *E. coli*-produced CP4 EPSPS proteins was determined using a colorimetric assay that measures formation of inorganic phosphate (Pi) from the EPSPS-catalyzed reaction between S-3-P and PEP. In this assay, protein-specific activity is expressed as units per milligram of protein (U/mg), where a unit is defined as one μmole of inorganic phosphate released from PEP per minute at 25°C.   The MON 87429-produced CP4 EPSPS and *E. coli*-produced CP4 EPSPS proteins were considered to have equivalent functional activity if the specific activity of both were within acceptance limits of 1.96 to 7.90 U/mg (the prediction interval calculated from a data set of historically determined CP4 EPSPS protein activity).

The experimentally determined specific activity for the MON 87429-produced and *E. coli*-produced CP4 EPSPS proteins are presented in Table 33.   The specific activities of MON 87429-produced and *E. coli*-produced CP4 EPSPS proteins were 2.46 U/mg and 4.27 U/mg of CP4 EPSPS protein, respectively. Because the specific activities of MON 87429-produced and *E. coli*-produced CP4 EPSPS proteins fall within the preset acceptance limits (Table 33), the MON 87429-produced CP4 EPSPS protein was considered to have equivalent functional activity to that of the *E. coli*-produced CP4 EPSPS protein.

Table 33.   Functional Activity of MON 87429-Produced CP4 EPSPS and *E. coli*-Produced CP4 EPSPS Proteins

MON 87429-Produced CP4 EPSPS [1] (U/mg)	*E. coli*-Produced CP4 EPSPS [1] (U/mg)	Acceptance Limits[2] (U/mg)
2.46	4.27	1.96 – 7.90

[1] Value refers to mean calculated based on n = 6 which includes three replicate assays spectrophotometrically read in duplicate plate wells.
[2] Data obtained for the *E. coli*-produced CP4 EPSPS and several plant-produced CP4 EPSPS were used to generate a prediction interval for setting the acceptance limits   .

B1(d)(vii)   MON 87429 CP4 EPSPS protein identity and equivalence – Conclusion

The CP4 EPSPS protein purified from grain of MON 87429 maize was characterised and the equivalence of the immunoreactive and physicochemical characteristics and functional activity between the MON 87429-produced and the *E. coli*-produced CP4 EPSPS proteins was established using a panel of analytical tests: 1) the N-terminal sequence of the MON 87429-produced CP4 EPSPS protein was confirmed by Nano LC-MS/MS analysis; 2) Nano LC-MS/MS analysis yielded peptide masses consistent with the expected peptide masses from the theoretical tryptic digest of the MON 87429-produced CP4 EPSPS sequence; 3) MON 87429-produced CP4 EPSPS protein was detected on a Western blot probed with antibodies specific for CP4 EPSPS protein and the immunoreactive properties of the MON 87429-produced and *E. coli*-produced CP4 EPSPS proteins were shown to be equivalent; 4) the electrophoretic mobility and apparent molecular weight of the MON 87429-produced and *E. coli*-produced CP4 EPSPS proteins were shown to be equivalent; 5) MON 87429-produced and *E. coli*-produced CP4 EPSPS proteins were determined to not be glycosylated; and 6) functional activities of the MON 87429-produced and *E. coli*-produced CP4 EPSPS proteins were demonstrated to be equivalent.

Taken together, these data provide a detailed characterisation of the MON 87429-produced CP4 EPSPS protein and establish the equivalence of the MON 87429-produced and the *E. coli*-produced CP4 EPSPS proteins. This equivalence justifies the use of the *E. coli*-produced CP4 EPSPS protein in studies to establish the safety of the CP4 EPSPS protein expressed in MON 87429.

B2   Antibiotic Resistance Marker Genes

MON 87429 does not contain genes that encode resistance to antibiotic markers.   Molecular characterisation data presented in Section A demonstrate the absence of antibiotic resistance marker gene in MON 87429.

B2(a)   Clinical importance of antibiotic that GM is resistant to (if any)

Not applicable.

B2(b)   Presence in food of antibiotic resistance protein (if any)

Not applicable.

B2(c)   Safety of antibiotic protein

Not applicable.

B2(d)   If GM organism is micro-organism, is it viable in final food?

Not applicable.

B3   Characterisation of Novel Proteins or Other Novel Substances

B3(a)   Biochemical function and phenotypic effects of novel substances

B3(a)(i)   Description, mode-of-action, and specificity of DMO protein expressed in MON 87429

Description of DMO Protein Expressed in MON 87429

Wild type DMO was initially purified from *Stenotrophomonas maltophilia* (*S. maltophilia*) strain DI-6 (Herman *et al.*, 2005; Palleroni and Bradbury, 1993), isolated from soil at a dicamba manufacturing plant (Krueger *et al.*, 1989).   DMO is targeted to the chloroplast by chloroplast transit peptide (CTP) to allow co-localization with the endogenous reductase and ferredoxin enzymes that supply electrons for the DMO demethylation reaction as described by Behrens *et al.* (2007).   In the construction of the plasmid vector used in the development of MON 87429, PV-ZMHT519224, a CTP coding sequence from *Arabidopsis thaliana* (*APG6*) was joined to the *dmo* coding sequence; this coding sequence results in the production of a precursor protein consisting of the DMO protein and a N-terminal 68 amino acid CTP APG6 that is utilized to target the precursor protein to the chloroplast (Herrmann, 1995; Klee *et al.*, 1987).   Typically, transit peptides are precisely removed from the precursor protein following delivery to the targeted plastid (della-Cioppa *et al.*, 1986) resulting in the full length mature protein.   However, there are examples in the literature of alternatively processed forms of a protein targeted to a plant's chloroplast (Behrens *et al.*, 2007; Clark and Lamppa, 1992).   Such alternative processing is observed with the DMO precursor protein produced in MON 87429.

MON 87429 contains a *dmo* expression cassette that encodes for a single MON 87429 DMO precursor protein that is post-translationally processed into two forms of DMO. The two forms of MON 87429 DMO have been identified by the N-terminal sequencing analysis. One form, referred to as MON 87429 DMO+1 and the other, MON 87429 DMO+0. MON 87429 DMO+0 does not contain the first amino acid of MON 87429 DMO+1. Because the difference in molecular weight between these two forms is beyond the resolution of the SDS-PAGE used, only one single band was observable by Coomassie stain of SDS-PAGE and Western blot analyses with the apparent molecular weight of ~38.4 kDa.   Since the minor differences in the amino acid sequences between MON 87429 DMO+1 and MON 87429 DMO+0 occur at the N-terminus, which are derived from APG6, they are not expected to have an effect on structure of the catalytic site, functional activity, immunoreactivity or specificity because the N-terminus is sterically distant from the catalytic site (D'Ordine *et al.*, 2009; Dumitru *et al.*, 2009).   Therefore, MON 87429 DMO protein will be used to refer to both forms of the protein collectively and distinctions will only be made where necessary.   Except for the single amino acid derived from the APG6 and an additional leucine at position two, the MON 87429 DMO protein has an identical sequence to the wild-type DMO protein from the DI-6 strain of *S. maltophilia* (Herman *et al.*, 2005)).

DMO protein produced in MON 87429 is also present in MON 88701 cotton and MON 87419 maize, which completed FDA consultations in 2013 and in 2016, respectively and approved by FSANZ in 2014 and 2016, respectively.   In 2011, Monsanto also

completed FDA consultation and received approval from FSANZ for MON 87708 soybean A1063 that contains DMO protein.   Under FDA consultation, both the MON 87708 DMO and MON 88701 DMO proteins were assessed following the criteria outlined above, which determined that food and feed products derived from MON 87708 soybean and MON 88701 cotton and its progeny are as safe and nutritious as food and feed derived from conventional soybean and cotton. The safety of these proteins has also been reviewed and approved in numerous other countries (*e.g*., Canada, Colombia, Japan, Korea, Mexico and Taiwan for MON 88701 cotton; Brazil, Canada, China, European Union, Indonesia, Japan, Korea, Mexico, Philippines, Taiwan and Vietnam for MON 87708 soybean)[4].   Except for minor amino acid differences at the N-terminus of MON 87429 expressed DMO protein, the amino acid sequence of MON 87429 DMO protein is identical to the DMO protein expressed in MON 88701 and MON 87419).   Except for minor amino acid differences at the N-terminus of MON 87429 expressed DMO protein, position 2 and 112, the amino acid sequence of MON 87429 DMO protein is identical to the DMO protein expressed in MON 87708. These minor amino acid differences between the DMO proteins expressed in MON 87429, MON 88701, MON 87419 and MON 87708 are not anticipated to have an effect on the structure of the catalytic site, functional activity, immunoreactivity or enzymatic specificity of the protein (D'Ordine *et al.*, 2009; Dumitru *et al.*, 2009).

Mode-of-Action of DMO Expressed in MON 87429

MON 87429 contains a demethylase gene from *S. maltophilia* that expresses a DMO protein. As a mono-oxygenase protein, the DMO protein is part of a the larger oxygenase family of enzymes that incorporate one or two oxygen atoms into substrates and are widely distributed in many universal metabolic pathways (Harayama *et al.*, 1992).   DMO is a Rieske-type non-heme iron oxygenase and is part of a three component system comprised of a reductase, a ferredoxin, and a terminal oxygenase, which in this case is the DMO protein.   In MON 87429 maize, these three proteins work together to catalyses the demethylation of the broadleaf herbicide dicamba to the non-herbicidal compound 3,6-dichlorosalicylic acid (DCSA) and formaldehyde, thus conferring dicamba resistance (Chakraborty *et al.*, 2005). This three-component redox system is presented in Figure 44.

---

[4]   Source Biotechnology Industry Organization BIOTradeStatus database (http://www.biotradestatus.com/).
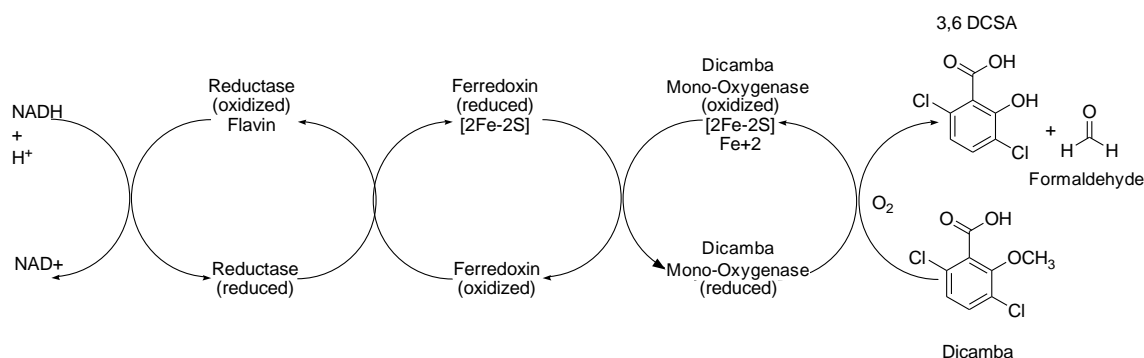
Figure 44.   Three Components of the DMO Oxygenase System

Depicted is the electron transport chain that starts with NADH and ends with DMO resulting in the demethylation of dicamba to form DCSA.

The crystal structure of a C-terminal histidine tagged DMO protein, which is identical to wild-type DMO except for an additional alanine at position two and a C-terminal polyhistidine tag, has been solved (D'Ordine *et al.*, 2009; Dumitru *et al.*, 2009).   The addition of a polyhistidine tag fused to the N- or C-terminus of a protein of interest is commonly used as a tool to aid in protein purification (Hochuli *et al.*, 1988).   The crystal structure of active DMO was determined to be a trimer comprised of three identical DMO monomers (D'Ordine *et al.*, 2009; Dumitru *et al.*, 2009).   Each DMO monomer contains a Rieske [2Fe-2S] cluster domain and a non-heme iron center domain (D'Ordine *et al.*, 2009; Dumitru *et al.*, 2009) that are typical of all Rieske-type mono-oxygenases (Ferraro *et al.*, 2005).   To catalyze the demethylation of dicamba, electrons transferred from NADH are shuttled through endogenous reductase and ferredoxin to the terminal DMO protein.   The electrons are received by the Rieske [2Fe-2S] cluster of one DMO protein molecule in the trimer and transferred to the non-heme iron center at the catalytic site of an adjacent DMO protein molecule in the trimer (D'Ordine *et al.*, 2009; Dumitru *et al.*, 2009), where it reductively activates oxygen to catalyze the final demethylation of dicamba.   Electron transport from the Rieske [2Fe-2S] cluster domain to the non-heme iron center domain cannot occur within a monomer since the distance is too great (D'Ordine *et al.*, 2009; Dumitru *et al.*, 2009).   As a result of the demethylation reaction, the non-herbicidal compound DCSA and formaldehyde are formed from dicamba.   DCSA is a known cotton, soybean, soil, and livestock metabolite whose safety has been evaluated by the FAO-WHO and EPA (FAO-WHO, 2011b; FAO-WHO, 2011a; U.S. EPA, 2009).   The other reaction product, formaldehyde, is found naturally in many plants and edible fungi at levels up to several hundred ppm (Adrian-Romero *et al.*, 1999; Tashkov, 1996).   Thus, neither DCSA nor formaldehyde generated by the action of DMO on dicamba pose a significant food or feed safety risk.   The activity of MON 87429-produced DMO was confirmed during characterisation (Section B1(a)).

Specificity of DMO Expressed in MON 87429

The substrate specificity of DMO expressed in MON 87429 was evaluated to understand potential interactions DMO may have with endogenous compounds structurally similar to dicamba that are found in plant.   The literature indicates the specificity of DMO for dicamba

is due to the specific interactions that occur at the catalytic site between the substrate and the protein (D'Ordine *et al.*, 2009; Dumitru *et al.*, 2009). Dicamba interacts with amino acids in the catalytic site of DMO through - the carboxylate moiety, the ring structure and the chlorine atoms of dicamba, which are primarily involved in orienting the substrate in the catalytic site. These chlorine atoms are required for catalysis to occur (D'Ordine *et al.*, 2009; Dumitru *et al.*, 2009). 2-methoxy benzoic acid (*o*-anisic acid) as a substrate, which is identical in structure to dicamba except for the absence of chlorines was tested by two independent laboratories (D'Ordine *et al.*, 2009; Dumitru *et al.*, 2009). No significant turnover was detected under standard assay conditions using HPLC or through liquid chromatography/mass spectrometry methods where picomole levels of products can be observed. 4-Hydroxy-3-methoxybenzoic acid (vanillic acid) was also tested with similar results. Given the limited existence of chlorinated compounds with structures similar to dicamba in plants and other eukaryotes (Wishart *et al.*, 2009; Wishart, 2010), it is unlikely that DMO produced in MON 87429 will catalyse the conversion of other endogenous compounds.

The potential for DMO to metabolize endogenous plant compounds was evaluated previously through *in vitro* experiments in support of MON 87708 (A1063). A set of potential endogenous substrates was selected for evaluation based on structural similarity of the compounds to dicamba and their presence in cotton, corn, or soybean (Buchanan *et al.*, 2000; Janas *et al.*, 2000; Lege *et al.*, 1995; Schmelz *et al.*, 2003). The potential substrates tested were *o*-anisic acid (2-methoxybenzoic acid), vanillic acid (4-hydroxy-3-methoxybenzoic acid), syringic acid (3,5-dimethoxy-4-hydroxybenzoic acid), ferulic acid [3-(4-hydroxy-3-methoxy-phenyl) prop-2-enoic acid] and sinapic acid [3-(4-hydroxy-3,5-dimethoxyphenyl)prop-2-enoic acid] (Figure 45). The assay mixture included NADH, reductase, ferredoxin and DMO. Dicamba was first used as a positive control to demonstrate that the assay system was functional. The disappearance of potential substrates and the formation of potential oxidation products were monitored using liquid chromatography-ultraviolet (LC-UV) and liquid chromatography-mass spectrometry (LC-MS). None of the tested substrates, except dicamba, were metabolized by the histidine tagged DMO in these *in vitro* experiments.

In order to confirm the specificity of the MON 87429 DMO protein for dicamba, and to demonstrate that the minor differences in amino acid sequences present in the MON 87429 DMO protein relative to the DMO proteins expressed in previous biotechnology-derived crops do not impact the activity or selectivity for dicamba herbicide as compared to potential endogenous substrates, the potential for MON 87429 DMO to catabolize dicamba and *o*-anisic acid was evaluated using the same qualitative assay used to evaluate the selectivity of MON 87708 DMO. Although *o*-anisic acid is not known to be present in corn, this substance was chosen for this confirmatory experiment since, among the five substrates used in the original study, which included ferulic acid, *o*-anisic acid, sinapic acid, syringic acid, and vanillic acid, *o*-anisic acid is the substrate that is most structurally similar to dicamba. The results from this assessment were similar to the previously reported results for MON 87708 DMO in that the DCSA product was observed using dicamba as the substrate whereas no demethylated products were observed with *o*-anisic acid as the substrate,

confirming that the MON 87429 DMO did not catabolize *o*-anisic acid. Thus, MON 87429 DMO is active and has a high specificity for dicamba as a substrate.

Dicamba   o-Anisic Acid   Vanillic Acid   Syringic Acid   Ferulic Acid   Sinapic Acid
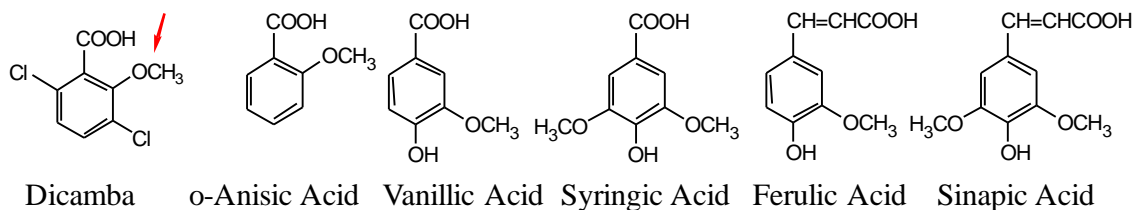
Figure 45. Dicamba and Potential Endogenous Substrates Tested through *in vitro* Experiments with DMO

The arrow indicates methyl group removed by DMO.

B3(a)(ii) Description, mode-of-action, and specificity of PAT (*pat*) protein expressed in MON 87429

Description of PAT (*pat*) Protein

PAT proteins conferring tolerance to glufosinate herbicide (2-amino-4-(hydroxymethylphosphinyl) butanoic acid) have been isolated from two separate species of *Streptomyces*, *S. hygroscopicus* (Thompson *et al.*, 1987) and *S. viridochromogenes* (Wohlleben *et al.*, 1988). The PAT protein isolated from *S. hygroscopicus* is encoded by the *bar* gene, and the PAT protein isolated from *S. viridochromogenes* is encoded by the *pat* gene. For clarity, the PAT protein encoded by the *bar* gene will be referred to as PAT (*bar*) while the PAT protein encoded by the *pat* gene will be referred to as PAT (*pat*). Both PAT (*bar*) and PAT (*pat*) proteins are comprised of 183 amino acids which share 85% identity at the amino acid level (Wehrmann *et al.*, 1996). Based on previous studies (Wehrmann *et al.*, 1996) that have extensively characterised PAT proteins produced from both the *bar* and *pat* genes, OECD recognizes both the proteins to be equivalent with regard to function and safety (OECD, 1999). In addition, the EPA has issued a tolerance exemption for the PAT protein regardless of the encoding gene or crop (U.S. EPA, 1997). The safety of PAT proteins present in biotechnology-derived crops has been extensively assessed (Hérouet *et al.*, 2005; ILSI-CERA, 2011), leading to a conclusion that there is a reasonable certainty of no harm resulting from the consumption of PAT proteins in human food or animal feed (Hérouet *et al.*, 2005).

The PAT protein produced in MON 87429 is from the *pat* gene, referred to as PAT (*pat*), and is identical to the wild type PAT protein encoded by *S. viridochromogenes*, except for the first methionine that is removed due to co-translational processing in MON 87429. N-terminal methionine cleavage is common and naturally occurs in the vast majority of proteins (Meinnel and Giglione, 2008). The resulting MON 87429-produced PAT (*pat*) protein is a single polypeptide of 182 amino acids that has an apparent molecular weight of 25.5 kDa. The PAT (*pat*) protein in MON 87429 is identical to the PAT protein expressed in several commercially available glufosinate tolerant products including T25, TC1507, A5547-127 and

DAS-59122-7 (FSANZ Application A375, A446, A481, A543 respectively) (Hérouet *et al.*, 2005; ILSI-CERA, 2011).

PAT (*pat*) Mode-of-Action

The mode-of-action of the PAT protein has been extensively assessed, as numerous glufosinate-tolerant products including those in cotton, corn, soy, canola, sugar beet and rice have been reviewed by the FDA (U.S. FDA, 1995a; U.S. FDA, 1995b; U.S. FDA, 1997; U.S. FDA, 1998b; U.S. FDA, 1998a; U.S. FDA, 2003; U.S. FDA, 2000; U.S. FDA, 1996) and many other regulatory agencies   (ILSI-CERA, 2011; OECD, 1999; OECD, 2002a).   PAT, including the PAT (*pat*) protein produced in MON 87429, is an enzyme classified as an acetyltransferase that acetylates glufosinate in the presence of acetyl CoA to form the non-herbicidal compound N-acetyl glufosinate.   Glufosinate is a racemic mixture of the D- and L-forms of phosphinothricin.   The herbicidal activity of glufosinate results from the binding of L-phosphinothricin to glutamine synthetase (OECD, 1999; OECD, 2002a).   Glutamine synthetase is responsible for the assimilation of ammonia generated during photorespiration. The binding of L-phosphinothricin to glutamine synthetase results in the inactivation of glutamine synthetase and a subsequent toxic build-up of ammonia within the plant, resulting in death of the plant (Manderscheid and Wild, 1986; OECD, 1999; OECD, 2002a; Wild and Manderscheid, 1984).   Thus, expression of the PAT protein in MON 87429 maize results in the ability to convert L-phosphinothricin to the non-herbicidal N-acetyl glufosinate, thus conferring glufosinate resistance to the crop.

PAT (*pat*) Specificity

The PAT protein expressed in MON 87429 is highly specific for glufosinate.   Enzyme assays   have demonstrated that the PAT protein is unable to acetylate other common L-amino acids that are structurally similar to L-phosphinothricin, and substrate competition assays showed no inhibition of glufosinate acetylation in the presence of high concentrations of L-amino acids that are structurally similar to L-phosphinothricin (including the glufosinate analog L-glutamate) (Wehrmann *et al.*, 1996).   Recent metabolic profiling reported non-specific PAT (*bar*) mediated acetylation of two amino acids (aminoadipate and tryptophan) in senescent leaf extracts from *A. thaliana*, however this observation in maize has not been reported (Christ *et al.*, 2017).   Thus, the PAT protein has high substrate specificity for L-phosphinothricin, the herbicidal component of glufosinate, and it has been shown in other PAT-expressing maize products (e.g. T25, TC1507, and DAS-59122-7) that PAT does not affect maize metabolism.

B3(a)(iii)   Description, mode-of-action, and specificity of FT_T protein expressed in MON 87429

Description of FT_T Protein

The FT_T protein produced in MON 87429 is encoded by the *ft_t* gene that provides tolerance to aryloxyalkanoate herbicides.   Aryloxyalkanoate herbicides include the aryloxyphenoxypropionate acetyl coenzyme A carboxylase (ACCase) inhibitors (so called "FOPs" herbicides such as quizalofop) and some synthetic auxins, such as 2,4-D.   The *ft_t* gene in MON 87429 is a modified version of the R-2,4-dichlorophenoxypropionate dioxygenase (*Rdp*a) gene from a soil bacterium, *Sphingobium herbicidovorans*.   The amino acid sequence of the FT_T protein shares ~89% sequence identity with wild type RdpA protein (Figure 46).   A total of 30 amino acid substitutions throughout the protein sequence resulted in FT_T protein displaying improved enzyme kinetics (increased V_{max}) and substrate affinity (reduced K_m) for 2,4-D, relative to RdpA protein.   The amino acid substitutions also resulted in FT_T protein displaying retained activity at temperatures experienced during the summer months in maize growing areas compared to RdpA protein.

1   AMHAALTPLT NKYRFIDVQP LTGVLGAEIT GVDLREPLDD STWNEILDAF

51   HTYQVIYFPG QAITNEQHIA FSRRFGPVDP VPILKSIEGY PEVQMIRREA

101   NESSRFIGDD WHTDSTFLDA PPAAVVMRAI EVPEYGGDTG FLSMYSAWET

151   LSPTMQATIE GLNVVHSATK VFGSLYQATN WRFSNTSVKV MDVDAGDRET

201   VHPLVVTHPV TGRRALYCNQ VYCQKIQGMT DAESKSLLQF LYEHATKFDF

251   TCRVRWKKDQ VLVWDNLCTM HRAVPDYAGK FRYLTRTTVA GDKPSR

Figure 46.   Amino Acid Sequence Comparison between FT_T and RdpA

The amino acid sequence of the MON 87429 FT_T protein was deduced from the full-length coding nucleotide sequence present in PV-ZMHT519224 (See Table 1 for more detail).   The double underline shows the alanine amino acid from the CTP (MDH) that is the N-terminus of the mature FT_T protein.   The single underline shows the 30 amino acid substitutions in FT_T protein, the number counts start from methionine corresponding to start codon. The substitutions are S6T, S9T, Q10N, R11K, F12Y, E13R, R14F, A16D, L82I, G103S, V105F, D130E, H134Y, T145S, R169K, Q178T, R180W, G209V, S210T, K213R, G214A, V217C, R224K, E226Q, P235S, R246K, G289A, V291D, R292K, and A294S, where the first letter denotes the original amino acids followed by the position and the new amino acid.

FT_T Mode-of-Action

RdpA protein has been characterised as an alpha-ketoglutarate-dependent non-heme iron dioxygenase (Müller *et al.*, 2006), and given their structural similarity, the FT_T protein is also an alpha-ketoglutarate-dependent non-heme iron dioxygenase.   Alpha-ketoglutarate-dependent non-heme iron dioxygenases belong to a diverse superfamily of Fe(II)/alpha-

ketoglutarate dependent hydroxylases that catalyse a range of oxygenation reactions in synthesis and decomposition reactions that include hydroxylation reactions, desaturations, demethylations, ring expansions, ring formations and other oxidative reactions (Hausinger, 2004). This protein superfamily is broadly distributed across the plant, animal and bacterial kingdoms, therefore environmental exposure to Fe(II)/alpha-ketoglutarate dependent hydroxylases is ubiquitous. Members of this superfamily share a common double-stranded, beta-helix protein fold with three metal-binding ligands found in a His^1-X-Asp/Glu-X_n-His^2 motif. In oxygenation reactions, alpha-ketoglutarate (αKG) chelates Fe(II) using its C1-carboxylate and C2-ketone. Decarboxylation of αKG results in the formation of succinate and carbon dioxide, which leads to the generation of an Fe(IV)-oxo or other activated oxygen species that subsequently hydroxylate the primary substrate, e.g., quizalofop (Bugg, 2003; De Carolis and De Luca, 1994; Hausinger, 2004). Thus, the FT_T protein catalyses a dioxygenase reaction in the presence of αKG and oxygen to metabolize quizalofop, a FOP herbicide, into the herbicidally-inactive quizalofop phenol and pyruvate (Figure 47). The FT_T protein also catalyses the dioxygenase reaction that degrades 2,4-dichlorophenoxyacetic acid (2,4-D), a synthetic auxin herbicide, into herbicidally-inactive 2,4-dichlorophenol (2,4-DCP) and glyoxylic acid in the presence of alpha-ketoglutarate and oxygen. Succinate and carbon dioxide are released as products of this reaction. The safety of 2,4-D, quizalofop, and their relevant metabolites have been assessed by US EPA. US EPA concluded that there is a reasonable certainty that no harm will result to the general population, or to infants and children from aggregate exposure to 2,4-D (U.S. EPA, 2017) or quizalofop (U.S. EPA, 2018) residues or their metabolites.
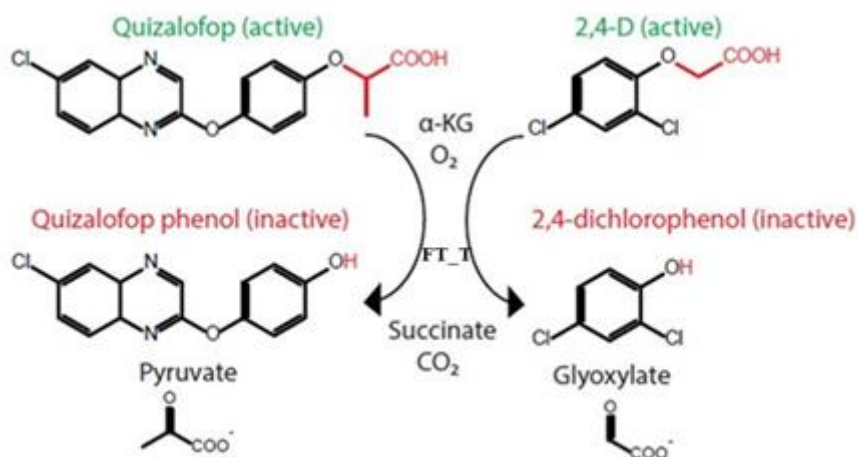
Figure 47. Substrate and Metabolites of FT_T Protein Reaction with Quizalofop (Left) and 2,4-D (Right)

FT_T Specificity

Whereas the amino acid modifications in the FT_T protein, relative to wild type RdpA from *S. herbicidovorans*, improved enzymatic activity, substrate affinity and retained activity at increased temperatures, they did not alter the specificity of the FT_T protein for its substrate. To confirm FT_T protein substrate specificity was not impacted by the optimization, an

endogenous substrate specificity assessment was conducted. Endogenous plant small molecules with similar structures to known FT_T substrates, which are compatible with the FT_T enzymatic active site, were investigated as potential substrates.

The screening approach, described in Figure 48, utilized a three-step process: Step 1, the NAPRALERT[5] database, which includes plant specific small molecule datasets collected from several crop plant species including corn (Bisson *et al.*, 2016), was utilized to identify small molecules with structural similarity to dichlorprop, a synthetic auxin herbicide that has the most basic structure of the herbicidal aryloxyalkanoate compounds. In Step 2, selected compounds were then subjected to *in silico* protein-small molecule docking simulations using the structure of the coordinated FT_T active site that was determined by crystallography. This step resulted in the identification of 38 compounds that showed potential docking to the FT_T active site *in silico*. In Step 3, 32 commercially available compounds out of the 38 compounds identified in Step 2, 11 herbicide control compounds and cinnamate (a compound identified as a marginal substrate in a similar enzyme family (Griffin *et al.*, 2013), were screened as potential substrates *in vitro* by measuring the functional response of purified FT_T protein. The list of compounds assayed, and results can be found in Table 34.
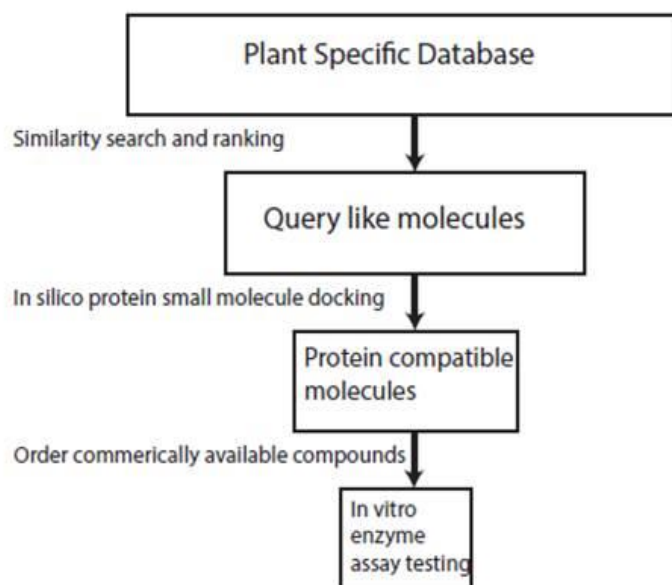
Figure 48. *in silico* and *in vitro* Protocol for FT_T Endogenous Substrate Specificity Screen

Overview of the screening and testing scheme to identify putative endogenous plant small molecules that could act as substrates for the FT_T enzyme.

Table 34. *in vitro* FT_T Enzymatic Activity Assay Compound List

---

[5] https://napralert.org/

Pub Chem ID[1]	Chemical Name[1]	Common Name[1]	Tag[2]	Rel. Activity[3]
5484172	(2R)-2-[4-[(6-chloro-2-quinoxalinyl)oxy]phenoxy]propanoic acid	Quizalofop-P	Herbicide	100%
185588	(2R)-2-(4-chloro-2-methylphenoxy)propanoic acid	Mecoprop-P	Herbicide	69%
91701	2-[4-[[5-(trifluoromethyl)-2-pyridinyl]oxy]phenoxy]propanoic acid	Fluazifop	Herbicide	53%
15118048	(2R)-2-[4-(4-cyano-2-fluorophenoxy)phenoxy]propanoic acid	Cyhalofop	Herbicide	35%
8427	2-(2,4-dichlorophenoxy)propanoic acid	Dichlorprop	Herbicide	21%
1486	2-(2,4-dichlorophenoxy)acetic acid	2,4-D	Herbicide	19%
50895	2-[4-[[3-chloro-5-(trifluoromethyl)-2-pyridinyl]oxy]phenoxy]propanoic acid	Haloxyfop	Herbicide	19%
86134	2-[4-[(6-chloro-1,3-benzoxazol-2-yl)oxy]phenoxy]propanoic acid	Fenoxaprop	Herbicide	15%
7204	2-(4-chloro-2-methylphenoxy)acetic acid	MCPA	Herbicide	15%
50465	2-[(4-amino-3,5-dichloro-6-fluoro-2-pyridinyl)oxy]acetic acid	Fluroxypyr	Herbicide	8%
41428	2-[(3,5,6-trichloro-2-pyridinyl)oxy]acetic acid	Triclopyr	Herbicide	3%
4947	3,4,5-trihydroxybenzoic acid propyl ester	Propyl gallate	Endogenous	1%
637775	(E)-3-(4-hydroxy-3,5-dimethoxyphenyl)-2-propenoic acid	Sinapate	Endogenous	< 1%
7127	1,2-dimethoxy-4-prop-2-enylbenzene	Methyl Eugenol	Endogenous	< 1%
1548883	(Z)-3-(4-hydroxy-3-methoxyphenyl)-2-propenoic acid	Ferulic acid	Endogenous	< 1%
21685	2,6-di(butan-2-yl)phenol	N/A	Endogenous	< 1%
445858	(E)-3-(4-hydroxy-3-methoxyphenyl)-2-propenoic acid	Ferulic acid	Endogenous	< 1%
75318	2-ethoxycarbonylbenzoic acid	Monoethylphalate	Endogenous	< 1%
5281166	2-[(1R,2R)-3-oxo-2-[(Z)-pent-2-enyl]cyclopentyl]acetic acid	Jasmonic acid	Endogenous	< 1%

Pub Chem ID[1]	Chemical Name[1]	Common Name[1]	Tag[2]	Rel. Activity[3]
13988328	8-Hydroxy-2-oxo-1,2-dihydroquinoline-4-carboxylic acid	2,8-dihydroxy-4-quinolinecarboxylic acid	Endogenous	< 1%
6140	(2S)-2-amino-3-phenylpropanoic acid	Phenylalanine	Endogenous	< 1%
736186	(E)-3-(3-hydroxy-4-methoxyphenyl)-2-propenoic acid	Isoferulic acid	Endogenous	< 1%
10742	4-hydroxy-3,5-dimethoxybenzoic acid	Syringic acid	Endogenous	< 1%
802	2-(1H-indol-3-yl)acetic acid	Indole-3-acetic acid	Endogenous	< 1%
637542	(E)-3-(4-hydroxyphenyl)-2-propenoic acid	4-Hydroxycinnamic acid	Endogenous	< 1%
730037	4-(1H-indol-3-yl)-4-oxobutanoic acid	N/A	Endogenous	< 1%
325	(4-propan-2-ylphenyl)methanol	4-Isopropylbenzyl alcohol	Endogenous	< 1%
8554	benzene-1,2-dicarboxylic acid dimethyl ester	Dimethyl phthalate	Endogenous	< 1%
60961	(2R,3R,4S,5R)-2-(6-aminopurin-9-yl)-5-(hydroxymethyl)oxolane-3,4-diol	Adenosine	Endogenous	< 1%
12474015	3-ethyl-5-methoxy-1H-indole	N/A	Endogenous	< 1%
896	N-[2-(5-methoxy-1H-indol-3-yl)ethyl]acetamide	Melatonin	Endogenous	< 1%
13067	2-(1H-indol-3-yl)acetic acid ethyl ester	Ethyl 3-indoleacetate	Endogenous	< 1%
637758	(E)-3-phenyl-2-propenoic acid ethyl ester	Ethyl cinnamate	Endogenous	< 1%
6781	benzene-1,2-dicarboxylic acid diethyl ester	Diethyl phthalate	Endogenous	< 1%
17355	4-phenyl-2-butanone	Benzylacetone	Endogenous	< 1%
3314	2-methoxy-4-prop-2-enylphenol	Eugenol	Endogenous	< 1%
62428	2-(1-naphthalenyl)acetic acid ethyl ester	Ethyl 1-naphthaleneacetate	Endogenous	< 1%

Pub Chem ID[1]	Chemical Name[1]	Common Name[1]	Tag[2]	Rel. Activity[3]
6057	(2S)-2-amino-3-(4-hydroxyphenyl)propanoic acid	Tyrosine	Endogenous	< 1%
10364	2-methyl-5-propan-2-ylphenol	Carvacrol	Endogenous	< 1%
6305	(2S)-2-amino-3-(1H-indol-3-yl)propanoic acid	Tryptophan	Endogenous	< 1%
444539	(E)-3-phenylprop-2-enoic acid	Trans-cinnamate	Literature	< 1%
77021	2,7-dimethoxynaphthalene	N/A	Endogenous	< 1%
689043	(E)-3-(3,4-dihydroxyphenyl)-2-propenoic acid	Caffeic acid	Endogenous	< 1%
3080590	2-(2-oxo-1,3-dihydroindol-3-yl)acetic acid	2-oxoindole-3-acetate	Endogenous	< 1%

[1] The PubChem ID, Chemical Name (IUPAC), Common Name (if available) and Tag are provided (NA is not available). https://pubchem.ncbi.nlm.nih.gov/.

[2] The column "Tag" indicates which compounds are herbicides (Herbicide), endogenous compound (Endogenous) or literature reported (Literature).

[3] The activity of triplicate assays (each with 3 replicates; n= 9) for FT_T activity reported as relative activity, which is the observed activity of the compound relative to quizalofop-P reported as a percentage. Initial velocities were first normalized in each test set against 2,4-D (positive control in each assay) and then across experiments against quizalofop-P.

Eleven herbicide controls were included in the assay. As expected, FT_T protein activity was detected in the presence of the 11 herbicide control compounds. The measured FT_T activity for all 32 endogenous plant compounds and cinnamate was ≤ 1% relative to quizalofop. These data suggest that FT_T protein is specific to substrate molecules with the following structural features: (1) existence of phenoxy group (2) presence of terminal carboxylate, and (3) available site for oxidation between the phenoxy group and terminal carboxylate. Endogenous plant small molecules with all three features did not exist in the NAPRALERT database, including the six compounds identified in the *in silico* Step 2 above that were not commercially available to test *in vitro*. Therefore, the FT_T enzyme is unlikely to metabolize endogenous small molecules in maize plants at biologically relevant activity levels.

B3(a)(iv)   Description, mode-of-action, and specificity of CP4 EPSPS protein expressed in MON 87429

Description of CP4 EPSPS Protein

The *cp4 epsps* coding sequence in MON 87429 encodes a precursor protein of 531 amino acids (455 amino acids encoded by the *cp4 epsps* gene and 76 amino acids encoded by the *CTP2* gene for targeting the CP4 EPSPS protein into chloroplasts). Expression of the *cp4 epsps* gene in MON 87429 results in a single polypeptide chain of 455 amino acids with an apparent molecular weight of ~44 kDa after a complete cleavage of the chloroplast transit peptide (CTP2). The *cp4 epsps* coding sequence is the codon optimized coding sequence of the *aroA* gene from *Agrobacterium* sp. strain CP4 encoding CP4 EPSPS (Barry *et al.*, 2001; Padgette *et al.*, 1996). The CP4 EPSPS protein expressed in MON 87429 is identical in structure and function to the CP4 EPSPS protein expressed in Roundup Ready® products across several crops, including soybeans, maize, canola, cotton, sugar beet, and alfalfa.

CP4 EPSPS Mode-of-Action

The 5-enolpyruvylshikimate-3-phosphate synthase (EPSPS) family of enzymes s ubiquitous in plants and microorganisms and their properties have been well studied. Bacterial and plant EPSPS enzymes are mono-functional with molecular mass of 44-48 kD (Kishore *et al.*, 1988). EPSPS is a key enzyme involved in aromatic amino acid biosynthesis and catalyzes a reaction where the enolpyruvyl group from phosphoenol pyruvate (PEP) is transferred to the 5-hydroxyl of shikimate-3-phosphate (S3P) to form 5-enolpyruvylshikimate-3-phosphate (EPSP) and inorganic phosphate (Alibhai and Stallings, 2001). Shikimic acid is a substrate for the biosynthesis of aromatic amino acids (phenylalanine, tryptophan and tyrosine) and other aromatic molecules that are necessary for plant growth. The shikimic acid pathway and EPSPS enzymes are ubiquitous to plants and microorganisms, but absent in mammals, fish, birds, reptiles, and insects (Alibhai and Stallings, 2001). The CP4 EPSPS protein expressed in MON 87429 is structurally similar and functionally identical to endogenous plant EPSPS enzymes, but has a much reduced affinity for glyphosate, the active ingredient in Roundup® agricultural herbicides, relative to endogenous plant EPSPS (Sikorski and Gruys, 1997). In conventional plants, glyphosate blocks the biosynthesis of EPSP, thereby depriving plants of essential amino acids (Haslam, 1993; Steinrücken and Amrhein, 1980).

In Roundup Ready® plants, which are tolerant to Roundup® agricultural herbicides, requirements for aromatic amino acids and other metabolites are met by the continued action of the CP4 EPSPS enzyme in the presence of glyphosate (Padgette *et al.*, 1996).

CP4 EPSPS Specificity

EPSPS enzymes, including the MON 87429 CP4 EPSPS protein, are highly specific for their substrates. The only known substrates of any biological significance for EPSPS enzymes are S3P and PEP. Glyphosate is not enzymatically modified by EPSPS. Shikimic acid was shown to be a very poor substrate for EPSPS enzyme, requiring much higher concentrations to observe turnover by the enzyme than for S3P (Gruys *et al.*, 1992). Methyl shikimate, quinic acid, and dihydroshikimic acid did not serve as substrates for the EPSPS enzyme (Franz *et al.*, 1997). As with most physiological pathways, there is tight regulation of metabolic flux through the shikimic acid pathway. Pathway flux is regulated both transcriptionally and post-transcriptionally (Maeda and Dudareva, 2012; Tzin *et al.*, 2012). The first enzyme in the pathway, 3-dexoy-D-arabino-heptulosonate 7-phosphate synthase (DAHPS), has been identified as the key regulatory checkpoint for the flux through the pathway, with a possible secondary checkpoints at shikimate kinase and chorismate synthase (Maeda and Dudareva, 2012; Tzin *et al.*, 2012). Plants, therefore, have mechanisms to regulate flux through the shikimate pathway irrespective of EPSPS synthase activity levels. Due to both the high substrate specificity of EPSPS enzymes and lack of a role as a regulatory enzyme in the shikimic acid pathway, there is no likely mechanism for the modification of endogenous plant constituents due to the expression of CP4 EPSPS.

B3(b)   Identification of novel substances (e.g. metabolites), levels and site

Herbicide metabolites are discussed in greater details in Section B6.

For details, please refer to ▓▓▓▓▓▓ 2019 (MSL0030257).

The protein expression levels determined in MON 87429 are used to assess exposure to the introduced proteins via food or feed ingestion and potential environmental exposure. The most appropriate tissues to evaluate DMO, PAT (*pat*), FT_T and CP4 EPSPS protein levels are leaf, root, forage, and grain tissue samples. Levels of the introduced proteins were determined in forage and grain tissue to evaluate food and feed exposure in humans and animals, where the levels are utilized to also calculate margins of exposure for each protein. Leaf and root tissues are distinct above and below ground plant tissues that are important to estimate environmental exposure. To further demonstrate the MON 87429 RHS trait mechanism-of-action, CP4 EPSPS expression in pollen tissue was determined to illustrate the differential expression between vegetative and pollen tissue.   .

MON 87429 DMO, PAT (*pat*), FT_T and CP4 EPSPS protein levels in various tissues of MON 87429 relevant to characterisation and risk assessment were determined by a validated immunoassay. Tissues of MON 87429 were collected from four replicate plots planted in a randomized complete block field design during the 2017 growing season from the following five field sites in the U.S.: Boone County, Indiana (INSH), Audubon County, Iowa (IAAU), Miami County, Ohio (OHTR), York County, Nebraska (NEYO), and Vermilion County,

Illinois (ILCX). The field sites were representative of maize-producing regions suitable for commercial production. Leaf, root, forage, grain and pollen tissue samples were collected from each replicated plot at all field sites treated with dicamba, glufosinate, quizalofop and 2,4-D.

B3(b)(i) Expression levels of DMO protein in MON 87429

MON 87429 DMO protein levels were determined in four tissue types. The results obtained from immunoassays are summarized in Table 35. The mean DMO protein levels were determined across five sites treated with dicamba, glufosinate, quizalofop and 2,4-D. Samples with values determined to be less than the LOD or LOQ were not included in mean determinations. The mean DMO protein level in MON 87429 across all sites was highest in leaf at 35 µg/g dw and lowest in root at 2.3 µg/g dw. The mean DMO protein level in MON 87429 grain was 2.4 µg/g dw.

Table 35. Summary of DMO Protein Levels in Maize Tissues Collected from MON 87429 Produced in United States Field Trials During 2017

Tissue Type[1]	Development Stage[2]	Mean (SE) Range (µg/g dw)[3]	LOQ (µg/g dw)[4]
Forage	R5	21 (1.6) 9.1-32	0.14
Grain	R6	2.4 (0.15) 1.3-3.6	0.14
Leaf	V2-V4	35 (2.3) 16-55	0.14
Root	V2-V4	2.3 (0.27) 1.0-5.2	0.14

[1]The tissue type that was collected.

[2]The crop development stage at which each tissue was collected.

[3]Protein levels are expressed as the arithmetic mean and standard error (SE) as microgram (µg) of protein per gram (g) of tissue on a dry weight basis (dw). The means, SE, and ranges (minimum and maximum values) were calculated for each tissue across all sites (n=20).

[4] LOQ=limit of quantitation.

B3(b)(ii)   Expression levels of PAT (*pat*) protein in MON 87429

MON 87429 PAT (*pat*) protein levels were determined in four tissue types.   The results obtained from immunoassays are summarized in Table 36.   The mean PAT (*pat*) protein levels were determined across five sites treated with dicamba, glufosinate, quizalofop and 2,4-D.   Samples with values determined to be less than the LOD or LOQ were not included in mean determinations.   The mean PAT (*pat*) protein level in MON 87429 across all sites was highest in leaf at 5.8 µg/g dw and lowest in grain at 0.84 µg/g dw.   The mean PAT (*pat*) protein level in MON 87429 grain was 0.84 µg/g dw.

Table 36.   Summary of PAT (*pat*) Protein Levels in Maize Tissues Collected from MON 87429 Produced in United States Field Trials During 2017

Tissue Type[1]	Development Stage[2]	Mean (SE) Range (µg/g dw)[3]	LOQ (µg/g dw)[4]
Forage	R5	1.3 (0.067) 0.71-1.8	0.03
Grain	R6	0.84 (0.066) 0.32-1.5	0.03
Leaf	V2-V4	5.8 (0.40) 2.9-9.8	0.03
Root	V2-V4	2.0 (0.15) 0.40-3.1	0.03

[1] The tissue type that was collected.

[2] The crop development stage at which each tissue was collected.

[3] Protein levels are expressed as the arithmetic mean and standard error (SE) as microgram (µg) of protein per gram (g) of tissue on a dry weight basis (dw). The means, SE, and ranges (minimum and maximum values) were calculated for each tissue across all sites (n=20).

[4] LOQ=limit of quantitation.

B3(b)(iii)   Expression levels of FT_T protein in MON 87429

MON 87429 FT_T protein levels were determined in four tissue types. The results obtained from immunoassays are summarized in Table 37. The mean FT_T protein levels were determined across five sites treated with dicamba, glufosinate, quizalofop and 2,4-D. Samples with values determined to be less than the LOD or LOQ were not included in mean determinations. The mean FT_T protein level in MON 87429 across all sites was the highest in leaf at 440 µg/g dw and lowest in root at 41 µg/g dw. The mean FT_T protein level in MON 87429 grain was 47 µg/g dw.

Table 37.   Summary of FT_T Protein Levels in Maize Tissues Collected from MON 87429 Produced in United States Field Trials During 2017

Tissue Type[1]	Development Stage[2]	Mean (SE) Range (µg/g dw)[3]	LOQ (µg/g dw)[4]
Forage	R5	97 (5.2) 56 - 140	0.036
Grain	R6	47 (3.6) 19 - 79	0.036
Leaf	V2-V4	440 (25) 210 - 670	0.036
Root	V2-V4	41 (4.1) 7.2 - 82	0.036

[1] The tissue type that was collected.

[2] The crop development stage at which each tissue was collected.

[3] Protein levels are expressed as the arithmetic mean and standard error (SE) as microgram (µg) of protein per gram (g) of tissue on a dry weight basis (dw). The means, SE, and ranges (minimum and maximum values) were calculated for each tissue across all sites (n=20).

[4] LOQ=limit of quantitation

B3(b)(iv)   Expression levels of CP4 EPSPS protein in MON 87429

MON 87429 CP4 EPSPS protein levels were determined in four tissue types.   The results obtained from immunoassays are summarized in Table 38.   The mean CP4 EPSPS protein levels were determined across four sites treated with dicamba, glufosinate, quizalofop and 2,4-D.   Samples with values determined to be less than the LOD or LOQ were not included in mean determinations.   The mean CP4 EPSPS protein level in MON 87429 across all sites was the highest in leaf at 54 µg/g dw and lowest in grain at 0.63 µg/g dw.

Table 38.   Summary of CP4 EPSPS Protein Levels in Maize Tissues Collected from MON 87429 Produced in United States Field Trials During 2017

Tissue Type[1]	Development Stage[2]	Mean (SE) Range (µg/g dw)[3]	LOQ (µg/g dw)[4]
Forage	R5	7.6 (0.50) 4.0 - 11	0.30
Grain	R6	0.63 (0.028) 0.41- 0.85	0.34
Leaf	V2-V4	54 (3.2) 30- 82	0.11
Root	V2-V4	10 (1.7) 3.4 - 29	0.11

[1] The tissue type that was collected.
[2] The crop development stage at which each tissue was collected.
[3] Protein levels are expressed as the arithmetic mean and standard error (SE) as microgram (µg) of protein per gram (g) of tissue on a dry weight basis (dw). The means, SE, and ranges (minimum and maximum values) were calculated for each tissue across all sites (n=20).
[4] LOQ=limit of quantitation

B3(c)   Site of expression of all novel substances and levels

Please refer to Section B3(b).

B3(d)   Post-translational modifications to the novel protein(s)

Not applicable.

B3(e)   Evidence of silencing, if silencing is the method of modification

For details, please also refer to ██████2018 (SCR-2018-0601).

MON 87429 maize produces the 5-enolpyruvylshikimate-3-phosphate synthase protein from *Agrobacterium* sp. strain CP4 (CP4 EPSPS) to provide maize lines with tissue-specific glyphosate tolerance to facilitate the production of hybrid maize seed. MON 87429 maize utilizes an endogenous maize regulatory element to target CP4 EPSPS mRNA for degradation in tassel tissues, resulting in reduced CP4 EPSPS protein expression in pollen (Table 39). Appropriately timed glyphosate applications produce a non-viable pollen phenotype and allow for desirable cross pollinations to be made in maize without using mechanical or manual detasseling methods to control self-pollination in female inbred parents. The tissue specific expression of CP4 EPSPS protein allowing for glyphosate induced non-viable pollen phenotype is the second generation of Monsanto's Roundup® Hybridization System (RHS) for hybrid seed production. The first-generation RHS product, MON 87427 maize, completed consultation with FDA in 2012 and received approval from FSANZ in 2012 (A1066).

Table 39.   Summary of CP4 EPSPS Protein Levels in Maize Pollen Tissue Collected from MON 87429 Produced in United States Field Trials During 2017

Tissue Type	Development Stage	Mean (SE) Range (µg/g dw)[1]	LOQ[2] (µg/g dw)
Pollen	R1	<LOQ	0.11

[1]Protein levels are expressed as the arithmetic mean and standard error (SE) as microgram (µg) of protein per gram (g) of tissue on a dry weight basis (dw). The means, SE, and ranges (minimum and maximum values) were calculated for each tissue across all sites (n=20). Over 50% of the samples (12 of 20) were <LOQ and so < LOQ is reported here.
[2]LOQ=limit of quantitation

B3(f)   History of human consumption of novel substances or similarity to substances previously consumed in food

B3(f)(i)   History of safe use of MON 87429 DMO protein

As described below, MON 87429 DMO is homologous to proteins that are common in the environment and in the diets of animals and humans. Given the extensive exposure of humans and animals to these homologous oxygenase proteins, it can be concluded that the oxygenase proteins have a history of safe use.

When determining the homology among proteins, both the linear amino acid sequence of the protein as well as the higher order structure of the proteins should be taken into account. Higher order structures are a relevant measure of homology since structure is more conserved than amino acid sequence (Caetano-Anollés *et al.*, 2009). In general, changes in the amino acid sequence of proteins largely occur through evolutionary mechanisms and are mostly conservative, meaning that such changes do not alter the high order structure of the protein and consequently do not alter the functional activity of the protein (Caetano-Anollés *et al.*, 2009; Illergård *et al.*, 2009). The conservation of high order structure is predominant within important functional and structural domains of proteins in similar classes (Illergård *et al.*, 2009). Therefore, it is necessary to understand the structural similarity shared between DMO and other proteins in order to properly assess their homology and determine if homologues of MON 87429 DMO are widely distributed in nature and/or present in foods or feeds consumed by humans or animals.

As described in Section B1(a), DMO is classified as an oxygenase. Oxygenases are enzymes that incorporate one or two oxygen atoms into their substrates and are widely distributed in many universal metabolic pathways (Harayama *et al.*, 1992). Within this large enzymatic class are mono-oxygenases, which incorporate a single oxygen atom as a hydroxyl group with the concomitant production of water and oxidation of NADH (Harayama *et al.*, 1992). Non-heme iron oxygenases, where iron is involved in the catalytic site, are an important class of oxygenases. Within this class are Rieske non-heme iron oxygenases, which contain a Rieske iron-sulfur [2Fe-2S] cluster. All Rieske non-heme iron oxygenases contain two catalytic domains, a non-heme iron domain (nh-Fe) that is a site of oxygen activation, and a Rieske [2Fe-2S] domain which functions by transporting electrons from ferredoxin to the non-heme iron domain (Ferraro *et al.*, 2005). MON 87429 DMO belongs to this class of oxygenases which are ubiquitous in diverse phyla ranging from bacteria to plants consumed by humans and animals (Ferraro *et al.*, 2005; Schmidt and Shaw, 2001).

The crystal structure of histidine-tagged DMO demonstrated that the quaternary structure of DMO is a trimer, where each individual monomer is in a precise orientation that allows for electron transport between two conserved domains; the Rieske and the non-heme iron domains. Similar to all Rieske non-heme iron oxygenases, DMO monomers contain these two catalytically important and highly conserved domains (D'Ordine *et al.*, 2009; Dumitru *et al.*, 2009; Ferraro *et al.*, 2005). Conservation of these domains ensures that the resulting secondary and tertiary structural domains are in the correct spatial orientation with regard to the non-heme iron and the Rieske [2Fe-2S] domains; which ensures electron transport from ferredoxin and between the monomers of DMO (D'Ordine *et al.*, 2009; Ferraro *et al.*, 2005).

Rieske domains are ubiquitous in numerous bacterial and plant proteins such as the iron-sulfur protein of the cytochrome bc_1 complex, chloroplast cytochrome b_6-f complex in spinach, and choline mono-oxygenases (Breyton, 2000; Darrouzet *et al.*, 2004; Gray *et al.*, 2004; Hibino *et al.*, 2002; Rathinasabapathi *et al.*, 1997; Russell *et al.*, 1998). The presence of two conserved domains, a Rieske [2Fe-2S] domain and a non-heme iron domain, suggests that all Rieske type non-heme iron oxygenases share the same reaction mechanism, by which the Rieske domain transfers electrons from the ferredoxin to the non-heme iron to allow catalysis (Chakraborty *et al.*, 2005; Dumitru *et al.*, 2009; Ferraro *et al.*, 2005). The conservation of these important structural domains required for enzymatic activity is further evidence of the evolutionary relation of all Rieske non-heme iron oxygenases to each other (Nam *et al.*, 2001; Rosche *et al.*, 1997; Werlen *et al.*, 1996). Therefore, enzymes with structural homology and functional similarity to MON 87429 DMO have been described in plants and bacteria and have been extensively consumed by both humans and animals.

B3(f)(ii)   History of safe use of MON 87429 PAT (*pat*) protein

The PAT (*pat*) protein expressed in MON 87429 is 100% homologous to the wild type PAT protein encoded by *S. viridochromogenes*, with the exception of the first methionine that is removed during a co-translational process in MON 87429. N-terminal methionine cleavage occurs naturally in the vast majority of proteins (Meinnel and Giglione, 2008) and has no effect on the physicochemical characteristics, immunoreactivity, functional activity, and/or specificity of the MON 87429-produced PAT (*pat*) protein (Section B1(b).).

Numerous glufosinate-tolerant crops including maize, canola, soybean, sugar beet, rice and cotton have completed consultations with US FDA (U.S. FDA, 1995a; U.S. FDA, 1996; U.S. FDA, 1995b; U.S. FDA, 1997; U.S. FDA, 1998b; U.S. FDA, 1998a; U.S. FDA, 2003; U.S. FDA, 2000), where it was demonstrated that food and feed derived from these crops are not materially different than the respective conventional crops. The safety of PAT proteins has been confirmed following extensive reviews by regulatory agencies in at least 15 different countries for more than 30 biotechnology-derived events in several different crop species (e.g., maize, soybean, cotton, canola and sugarbeet). Additionally, the EPA has issued a tolerance exemption for PAT protein (U.S. EPA, 1997). Prior safety assessments of the PAT proteins expressed in these other biotechnology-derived crops are directly applicable to the MON 87429 PAT (*pat*) protein because the amino acid sequence of the MON 87429 PAT (*pat*) protein is identical to the PAT (*pat*) proteins in these biotechnology-derived crops that are derived from the *pat* gene and because the PAT proteins produced from the *bar* and *pat* are equivalent in terms of function and safety. The PAT proteins have a robust history of safe consumption and safe use in agriculture that is supported by the lack of any documented reports of adverse human or animal affects since the introduction of biotechnology-derived crops expressing PAT proteins in 1995 (Duke, 2005).

B3(f)(iii)   History of safe use of MON 87429 FT_T protein

The FT_T protein is a modified version of RdpA protein, an alpha-ketoglutarate-dependent dioxygenase from the common soil bacterium *Sphingobium herbicidovorans*. As noted in the previous section, FT_T protein shares the common high order structure of alpha-

ketoglutarate-dependent dioxygenases that contains a classical dioxygenase active pocket including an iron atom coordinated by two histidine residues and one aspartic acid or glutamate residue (Hausinger, 2004). These alpha-ketoglutarate-dependent dioxygenases have been identified in a broad range of organisms including bacteria, fungi, plants, and vertebrates, which have been extensively consumed by both humans and animals (Hausinger, 2004; Kundu, 2012) without any reports of adverse effects.

B3(f)(iv)   History of safe use of MON 87429 CP4 EPSPS protein

The safety and mode-of-action of CP4 EPSPS protein is well documented and is the subject of many publications (Harrison *et al.*, 1996; Hoff *et al.*, 2007; ILSI-CERA, 2010; U.S. EPA, 1996). Numerous glyphosate-tolerant, commercially available CP4 EPSPS containing crops have completed consultations with the FSANZ (e.g., MON 87427 A1066 in 2012 and MON 88017 A548 in 2006, where it was demonstrated that food and feed derived from these crops are not materially different than the respective conventional crops. The safety of the CP4 EPSPS proteins has been reviewed by regulatory agencies around the world (ILSI-CERA, 2011; OECD, 1999; OECD, 2002a). Additionally, in 1996 the U.S. EPA established an exemption from the requirement of a tolerance for residues of the plant pesticide inert ingredient CP4 EPSPS and the genetic material necessary for its production in all plants (40 CFR § 174.523, redesignated from § 180.1174, effective April 25, 2007). Prior safety assessments of the CP4 EPSPS protein expressed in these other biotechnology-derived crops are directly applicable to the MON 87429 CP4 EPSPS protein because the amino acid sequence and function of the MON 87429 CP4 EPSPS protein is identical to the CP4 EPSPS proteins in these biotechnology-derived crops. The CP4 EPSPS protein has a robust history of safe consumption and safe use in agriculture that is supported by the lack of any documented reports of adverse human or animal affects since the introduction of Roundup Ready® crops expressing CP4 EPSPS protein.

B4   Assessment of Potential Toxicity

The assessment of the potential toxicity of an introduced protein is based on comparing the biochemical characteristics of the introduced protein to characteristics of known toxins. These biochemical characteristics are assessed by determining: 1) if the protein has structural similarity to known toxins or other biologically-active proteins that could cause adverse effects in humans or animals; 2) if the protein is rapidly degraded by pepsin and pancreatin; 3) if the protein is stable to heat treatment; 4) if the protein exerts any acute toxic effects in mammals.   The MON 87429 DMO, PAT (*pat*), FT_T and CP4 EPSPS proteins in MON 87429 have been assessed for their potential toxicity based on these criteria as explained below.

B4(a)   Bioinformatic comparison (aa) of novel protein(s) to toxins

Structural Similarity of MON 87429 DMO, PAT (*pat*), FT_T and CP4 EPSPS to Known Toxins

For details, please refer to ▮▮▮▮▮▮, 2018 (MSL0029452), ▮▮▮▮▮▮▮▮▮▮▮▮▮▮▮ 2018 (RAR-2018-0231) and ▮▮▮▮▮▮▮▮▮▮▮▮, 2018 (RAR-2018-0126).

The assessment of the potential for protein toxicity includes bioinformatic analysis of the amino acid sequence of the introduced protein.   The goal of the bioinformatic analysis is to ensure that the introduced protein does not share homology to known toxins or anti-nutritional proteins associated with adverse health effects.

Potential structural similarities shared between the MON 87429 DMO, PAT (*pat*), FT_T and CP4 EPSPS proteins with sequences in a protein database were evaluated using the FASTA sequence alignment tool.   The FASTA program directly compares amino acid sequences (*i.e.*, primary, linear protein structure) and the alignment data may be used to infer shared higher order structural similarities between two sequences (*i.e.*, secondary and tertiary protein structures).   Proteins that share a high degree of similarity throughout the entire sequence are often homologous.   Homologous proteins often have common secondary structures, common three-dimensional configuration, and, consequently, may share similar functions (Caetano-Anollés *et al.*, 2009; Illergård *et al.*, 2009).

FASTA bioinformatic alignment searches using the MON 87429 DMO amino acid sequence, PAT amino acid sequence, FT_T amino acid sequence and CP4 EPSPS amino acid sequence were performed with the toxin database to identify possible homology with proteins that may be harmful to human and animal health.   Periodically, the databases used to evaluate proteins are updated. Since the most recent reports were completed, the   toxin (TOX_2018) and protein (PRT_2018) databases have been revised and updated. In order to determine if proteins share significant sequence similarity to new sequences contained in the updated toxin database they were used as a queries for a FASTA searches of the TOX_2018 database. The toxin protein database (TOX_2018) is a subset of sequences derived from the PRT_2018 database that was selected using a keyword search and filtered to remove likely non-toxin proteins.   It is referred to herein as the TOX_2018 database and contains 28,344 sequences.

Using MON 87429 DMO as the query sequence, no alignment with an *E*-score of ≤1e-5 was observed using the TOX_2018 database to run a FASTA search. Using the PAT protein sequence as the query to search the TOX_2018 database resulted in 23 alignments, 18 of which displayed an *E*-score of ≤1e-5. These alignments were with the toxin component of the GNAT (GCN5-related N-acetyltransferase) toxin-antitoxin system of bacteria. As expected, these data show similarities between the PAT (*pat*) protein sequence and the toxin component of the GNAT toxin-antitoxin system of bacteria. Bacterial toxin-antitoxin systems are widespread; they are involved in the maintenance of low copy plasmids (Makarova *et al.*, 2009) and are only toxic when produced intracellularly in bacteria. Alignments with bacterial toxin-antitoxin system proteins do not provide any indication that the PAT protein would adversely impact human or animal health. This is comparable with previously published safety assessments of PAT (*pat*) protein (Hérouet *et al.*, 2005). Using MON 87429 FT_T as the query sequence, no alignment with an *E*-score of ≤1e-5 was observed using the TOX_2018 database to run a FASTA search. Using MON 87429 CP4 EPSPS as the query sequence, no alignment with an *E*-score of ≤1e-5 was observed using the TOX_2018 database to run a FASTA search.

B4(b)   Stability to heat or processing and/or degradation in gastric model

B4(b)(i)   Digestive fate of the MON 87429 DMO, PAT (*pat*), FT_T and CP4 EPSPS proteins

Digestive Fate of the MON 87429 DMO Protein

For details, please also refer to ▮, 2018 (MSL0029822).

Proteins introduced into crops using biotechnology are evaluated for their safety for human and animal consumption. The majority of ingested dietary proteins undergo hydrolytic degradation and/or proteolytic degradation to their constituent amino acids or small peptides, which are then absorbed and used for synthesis of proteins or other glucogenic or ketogenic metabolites by the body (Delaney *et al.*, 2008). Therefore, evaluating a protein's intrinsic sensitivity to proteolytic degradation with enzymes of the gastrointestinal tract is a key aspect to understanding the safety of any introduced proteins in GM crops. One characteristic of protein toxins and many allergens is their ability to withstand proteolytic degradation by enzymes present in the gastrointestinal tract (Astwood *et al.*, 1996; Moreno *et al.*, 2005; Vassilopoulou *et al.*, 2006; Vieths *et al.*, 1999). Allergenic proteins or their fragments, when presented to the intestinal immune system, can lead to a variety of gastrointestinal and systemic manifestations of immune-mediated allergy. The complete enzymatic degradation of an ingested protein by exposure to gastric pepsin and intestinal pancreatic proteases makes it highly unlikely that either the intact protein or protein fragment(s) will reach the absorptive epithelial cells of the small intestine where antigen processing cells reside (Moreno *et al.*, 2005). To reach these cells, protein or protein fragment(s) must first pass through the stomach where they are exposed to pepsin and then the duodenum where they are exposed to pancreatic fluid containing a mixture of enzymes called pancreatin. Therefore, the susceptibility of MON 87429 DMO protein to degradation by pepsin and pancreatin was assessed.

A correlation between the resistance to protein degradation by pepsin and the likelihood of the protein being an allergen has been previously assessed with a group of proteins consisting of both allergens and non-allergens (Astwood *et al.*, 1996; Codex Alimentarius, 2009), but this correlation is not absolute (Fu *et al.*, 2002). A standardized protocol to compare the relative resistance of proteins to degradation by pepsin has been established based on results obtained from an international, multi-laboratory study (Thomas *et al.*, 2004). The multi-laboratory study showed that the results of *in vitro* pepsin degradation assays were reproducible when a standard protocol was followed. Using this standardized *in vitro* pepsin degradation protocol, the susceptibility of DMO protein to pepsin degradation was assessed.

Incubation of test proteins with pancreatin is also used to assess the susceptibility of the protein to proteolytic degradation (Okunuki *et al.*, 2002; Yagami *et al.*, 2000). The relationship between protein allergenicity and susceptibility to pancreatin degradation is limited for several reasons. Namely, the protein has not been first exposed to the acidic, and proteolytic denaturing condition of the stomach, as would be the case *in vivo* (Helm, 2001). Using an established protocol, the susceptibility of DMO protein to pancreatin degradation was assessed.

Degradation of MON 87429 DMO by Pepsin

Degradation of the *E. coli*-produced DMO protein by pepsin was evaluated over time by analyzing digestion mixtures incubated for targeted time intervals following a standardized protocol validated in an international, multi-laboratory ring study (Thomas *et al.*, 2004) collected at targeted incubation time points. The susceptibility of the DMO protein to pepsin degradation was assessed by visual analysis of a Brilliant Blue G Colloidal stained SDS-PAGE gel and by visual analysis of a Western blot probed with an anti-DMO antibody. Both visualization methods were run concurrently with separate SDS-PAGE and Western blot analyses to estimate the limit of detection (LOD) of the DMO protein for each method.

For SDS-PAGE analysis of the digestibility of the DMO protein in pepsin, the gel was loaded with 1 μg of total test protein (based on pre-digestion protein concentrations) for each of the digestion samples (Figure 49A). Because the apparent molecular weights of pepsin (~38 kDa) and the DMO (~38 kDa) proteins are the same, they are difficult to visually distinguish on an SDS-PAGE gel. However. DMO is observed at a slightly higher position and appears darker on a stained gel (see Figure 49A, lanes 2 and 3, respectively). The intensity of the combined bands contained in the Pepsin Treated T0 sample appears as the combination of the intensities of both proteins run separately (Figure 49A, lane 4). After 0.5 min digestion (Pepsin Treated T1 sample), the intensity of the combined bands was reduced to approximately the same level as observed for pepsin alone (0 min No Test Protein Control; Figure 49, compare lanes 2 and 5) suggesting that most of the intact DMO protein was degraded. Peptide fragments of ~3 kDa were observed at the 0.5 and 2 min timepoints but were not observed at the 5 min timepoint or beyond.

No change in the DMO protein band intensity was observed in the absence of pepsin in the 0 min No Pepsin Control and 60 min No Pepsin Control samples (Figure 49A, lanes 3 and 12). This indicates that the degradation of the DMO protein was due to the proteolytic activity of

pepsin and not due to instability of the protein while incubated in the pepsin test system over the course of the experiment.

The 0 min No Test Protein Control and 60 min No Test Protein Control (Figure 49, Panel A, lanes 2 and 13) demonstrated that the pepsin is stable throughout the experimental phase.

A separate SDS PAGE gel to estimate the LOD of the DMO protein was run concurrently with the SDS PAGE for the degradation assessment (Figure 49B).   However, because intact DMO protein and pepsin were not separated in this gel system, the LOD of DMO protein on colloidal Brilliant Blue G stained gel could not be determined.   Therefore, the percent degradation of intact DMO protein was not estimated on colloidal Brilliant Blue G stained gels, but it is reasonable to conclude that DMO was completely degraded by pepsin within 5 minutes.
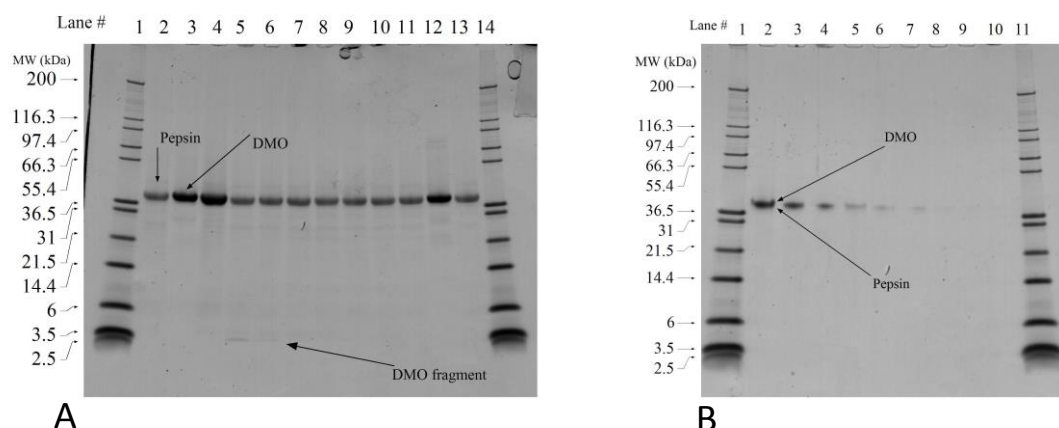
Figure 49.   SDS-PAGE Analysis of the Digestion of DMO Protein by Pepsin

Colloidal Brilliant Blue G stained SDS-PAGE gels were used to assess the degradation of the DMO protein by pepsin.   Approximate molecular weights (kDa) are shown on the left of each gel, and correspond to the protein markers loaded.   Empty lanes were cropped from the images.
A: DMO protein degradation in the presence of pepsin.   Based on pre-reaction protein concentrations, 1 µg of test protein was loaded in each lane containing DMO protein.
B: LOD determination.   Indicated amounts of the test protein from the Pepsin Treated T0 sample were loaded to estimate the LOD of the DMO protein.

Lane	Sample	Incubation Time (min)	Lane	Sample	Amount (ng)
1	Mark 12 MWM	-	1	Mark 12 MWM	-
2	0 min No Test Protein Control	0	2	Pepsin Treated T0	200
3	0 min No Pepsin Control	0	3	Pepsin Treated T0	100
4	Pepsin Treated T0	0	4	Pepsin Treated T0	50
5	Pepsin Treated T1	0.5	5	Pepsin Treated T0	20
6	Pepsin Treated T2	2	6	Pepsin Treated T0	10
7	Pepsin Treated T3	5	7	Pepsin Treated T0	5
8	Pepsin Treated T4	10	8	Pepsin Treated T0	2
9	Pepsin Treated T5	20	9	Pepsin Treated T0	1
10	Pepsin Treated T6	30	10	Pepsin Treated T0	0.5
11	Pepsin Treated T7	60	11	Mark 12 MWM	-
12	60 min No Pepsin Control	60	12	Empty	-
13	60 min No Test Protein Control	60	13	Empty	-
14	Mark 12 MWM	-	14	Empty	-
15	Empty	-	15	Empty	-

For Western blot analysis of DMO pepsin susceptibility, the DMO protein was loaded with approximately 20 ng per lane of total protein (based on pre-reaction total protein concentrations) for each reaction time point examined. The Western blot used to assess the resistance of the DMO protein to pepsin digestion (Figure 50A) was run concurrently with a Western blot to estimate the LOD of the DMO protein (Figure 50B). The LOD of the DMO protein was approximately 0.50 ng (Figure 50B, lane 8). The LOD was used to calculate the maximum relative amount of DMO protein that could remain visually undetected after digestion, which corresponded to approximately 2.5% ($0.5/20 \times 100\% = 2.5\%$) of the total protein loaded.

Western blot analysis demonstrated that the DMO protein was degraded below the LOD within 0.5 min of incubation in the presence of pepsin (Figure 50A, lane 6). Based on the Western blot LOD for the DMO protein, it can be concluded that more than 97.5% (100% - 2.5% = 97.5%) of the intact DMO protein was degraded within 0.5 min. No peptide fragments were detected at any timepoint in pepsin by Western blot.

No apparent change in the DMO protein band intensity was observed in the absence of pepsin in the 0 min No Pepsin Control and 60 min No Pepsin Control samples (Figure 50A, lanes 4 and 13). This indicates that the degradation of the DMO protein was due to the proteolytic activity of pepsin and not due to instability of the protein while incubated in the assay buffer during the course of the experiment.

No immunoreactive bands were observed in the 0 min No Protein Control and 60 min No Protein Control samples (Figure 50A, lanes 3 and 14). This result indicates that there was no non-specific interaction between the pepsin solution and the DMO-specific antibody under these experimental conditions.
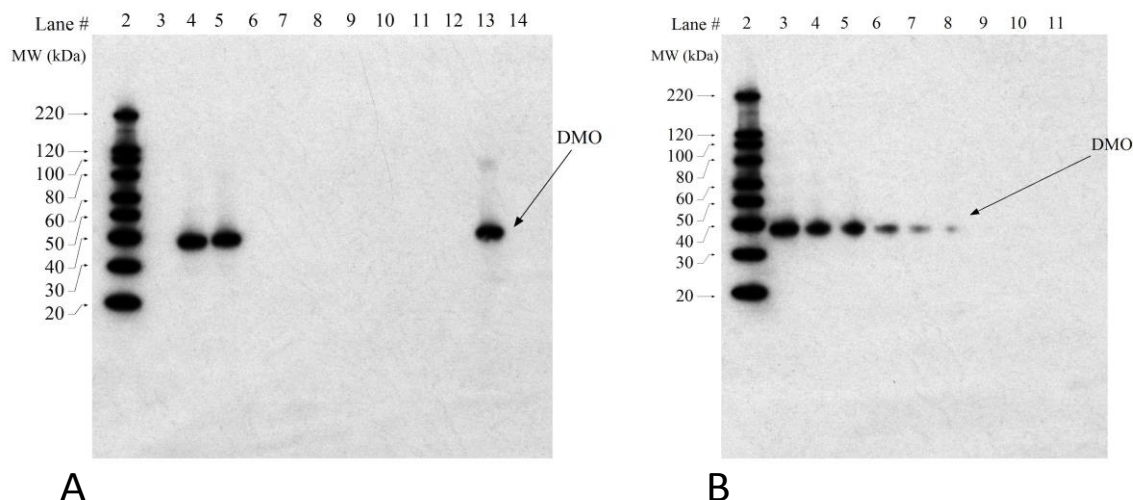
Figure 50.   Western Blot Analysis of the Degradation of DMO Protein by Pepsin

Western blots were conducted using an anti-DMO primary antibody.   Approximate molecular weights (kDa) are shown on the left of each gel, and correspond to the MagicMark XP western protein markers loaded.   Empty lanes were cropped from the images.   A 30 Second exposure is shown.

A: DMO protein degradation by pepsin.   Based on pre-reaction protein concentrations, 20 ng of test protein was loaded in each lane containing DMO protein.

B: LOD determination.   Indicated amounts of the test protein from the Pepsin Treated T0 sample were loaded to estimate the LOD of the DMO protein.

Lane	Sample	Incubation Time (min)	Lane	Sample	Amount (ng)
1	Precision Plus MWM	-	1	Precision Plus MWM	-
2	MagicMark XP	-	2	MagicMark XP	-
3	0 min No Test Protein Control	0	3	Pepsin Treated T0	20
4	0 min No Pepsin Control	0	4	Pepsin Treated T0	10
5	Pepsin Treated T0	0	5	Pepsin Treated T0	5
6	Pepsin Treated T1	0.5	6	Pepsin Treated T0	2.0
7	Pepsin Treated T2	2	7	Pepsin Treated T0	1.0
8	Pepsin Treated T3	5	8	Pepsin Treated T0	0.50
9	Pepsin Treated T4	10	9	Pepsin Treated T0	0.25
10	Pepsin Treated T5	20	10	Pepsin Treated T0	0.10
11	Pepsin Treated T6	30	11	Pepsin Treated T0	0.05
12	Pepsin Treated T7	60	12	Precision Plus MWM	-
13	60 min No Pepsin Control	60	13	Empty	-
14	60 min No Test Protein Control	60	14	Empty	-
15	Precision Plus MWM	-	15	Empty	-

Degradation of MON 87429 DMO Protein by Pancreatin

The degradation of the DMO protein by pancreatin was assessed by Western blot analysis (Figure 51). The total loading of the DMO test protein for each timepoint examined was approximately 20 ng per lane (based on pre-reaction total protein concentrations). The Western blot used to assess the DMO protein degradation (Figure 51A) was run concurrently with the Western blot used to estimate the LOD (Figure 51B) of the DMO protein. The LOD of the DMO protein was observed at approximately the 0.5 ng protein loading (Figure 51A, lane 8). The LOD was used to calculate the maximum relative amount of DMO protein that could remain visually undetected after digestion, which corresponded to approximately 2.5% ($0.5/20 \times 100\% = 2.5\%$) of the total protein loaded.

Western blot analysis demonstrated that a band corresponding to the DMO protein was degraded to a level below the LOD within 5 min of incubation in the presence of pancreatin (Figure 51A, lane 5), the first timepoint assessed. Therefore, based on the LOD, more than 97.5% (100% - 2.5%) of the DMO protein was degraded within 5 min. No peptide fragments were detected at any timepoint in pepsin by Western blot.

No apparent change in the intact DMO band intensity was observed in the absence of pancreatin in the 0 h No Pancreatin Control and 24 h No Pancreatin Control samples (Figure 51A, lanes 3 and 13). This indicates that the degradation of all immunoreactive forms of the DMO protein was due to the proteolytic activity of pancreatin and not due to instability of the protein when incubated in 50 mM KH_2PO_4, pH 7.5 at 37.1ºC over the course of the experiment.

No immunoreactive bands were observed in the 0 h No Test Protein Control and 24 h No Test Protein Control samples (Figure 51A, lanes 2 and 14), demonstrating the absence of non-specific antibody interactions with the pancreatin solution.
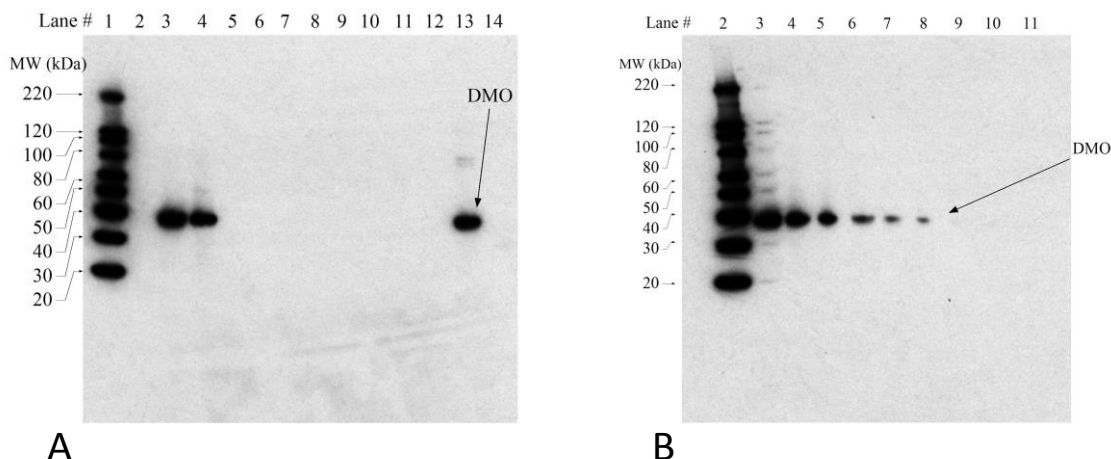
Figure 51.   Western Blot Analysis of the Degradation of DMO Protein by Pancreatin

Western blots were conducted using an anti DMO primary antibody.   Approximate molecular weights (kDa) are shown on the left of each gel, and correspond to the MagicMark XP western protein markers loaded.   Empty lanes were cropped from the images.   A 30 seconds exposure is shown.

A: DMO protein degradation by pancreatin.   Based on pre-reaction protein concentrations, 20 ng of test protein was loaded in each lane containing DMO protein.

B: LOD determination.   Indicated amounts of the test protein from the T0 sample were loaded to estimate the LOD of the DMO protein.

Lane	Sample	Incubation Time	Lane	Sample	Amount (ng)
1	MagicMark XP	-	1	Precision Plus MWM	-
2	0 min No Test Protein Control	0	2	MagicMark XP	-
3	0 min No Pancreatin Control	0	3	Pancreatin Treated T0	20
4	Pancreatin Treated T0	0	4	Pancreatin Treated T0	10
5	Pancreatin Treated T1	5 min	5	Pancreatin Treated T0	5
6	Pancreatin Treated T2	15 min	6	Pancreatin Treated T0	2.0
7	Pancreatin Treated T3	30 min	7	Pancreatin Treated T0	1.0
8	Pancreatin Treated T4	1 h	8	Pancreatin Treated T0	0.50
9	Pancreatin Treated T5	2 h	9	Pancreatin Treated T0	0.25
10	Pancreatin Treated T6	4 h	10	Pancreatin Treated T0	0.10
11	Pancreatin Treated T7	8 h	11	Pancreatin Treated T0	0.05
12	Pancreatin Treated T8	24 h	12	Precision Plus MWM	-
13	24 h No Pancreatin Control	24 h	13	Empty	-
14	24 h No Test Protein Control	24 h	14	Empty	-
15	Precision Plus MWM	-	15	Empty	-

Digestive Fate of the MON 87429 DMO Protein – Conclusions

The ability of the DMO protein to be degraded by pepsin and by pancreatin was evaluated in this study. The results showed that greater than 97.5% of the intact DMO protein was degraded by pepsin within 0.5 min when analyzed by Western blot using a DMO specific antibody. SDS-PAGE gels stained with Brilliant Blue G-colloidal showed that a peptide fragment of ~3 kDa was observed at the 0.5 and 2 min timepoints in the presence of pepsin but was not observed at 5 min timepoint and beyond.

Greater than 97.5% of the intact DMO protein was degraded within 5 min during incubation with pancreatin when analyzed by Western blot. No immunoreactive peptide fragments were observed at any timepoint.

These results show that the intact DMO protein is readily degraded in either pepsin or pancreatin. Rapid degradation of the DMO protein in pepsin and pancreatin indicates that it is highly unlikely that the DMO protein will pose any safety concern to human health.

Degradation of PAT (*pat*) Protein by Pepsin

For details, please also refer to ███████████ 2019 (MSL0030203).

Degradation of the PAT (*pat*) protein by pepsin was evaluated over time by analyzing digestion mixtures incubated for targeted time intervals following a standardized protocol validated in an international, multi-laboratory ring study (Thomas *et al.*, 2004) collected at targeted incubation time points. The susceptibility of PAT (*pat*) protein to pepsin degradation was assessed by visual analysis of a Brilliant Blue G Colloidal stained SDS-PAGE gel and by visual analysis of a Western blot probed with an anti-PAT polyclonal antibody. Both visualization methods were run concurrently with separate SDS-PAGE and Western blot analyses to estimate the limit of detection (LOD) of the PAT (*pat*) protein for each method.

For SDS-PAGE analysis of the digestibility of the PAT (*pat*) protein in pepsin, the gel was loaded with approximately 1 µg of total test protein (based on pre-digestion protein concentrations) for each of the digestion samples (Figure 52A). Visual examination of SDS-PAGE data showed that the intact PAT (*pat*) protein was completely degraded within 0.5 min of incubation in the presence of pepsin (Figure 52A, Lane 5). A peptide fragment of ~3 kDa was observed for the first 5 min of pepsin treatment with the staining intensity decreasing over time and it was completely degraded within 10 min of incubation. This ~3 kDa peptide fragment is likely a result of a partially digested protein. This is comparable with previously published safety assessments of PAT protein (Hérouet *et al.*, 2005).

No change in the PAT (*pat*) protein band intensity was observed in the absence of pepsin in the 0 min No Pepsin Control and 60 min No Pepsin Control samples (Figure 52A, lanes 3 and 12). This indicates that the degradation of the PAT (*pat*) protein was due to the proteolytic activity of pepsin and not due to instability of the protein while incubated in the pepsin test system over the course of the experiment.

The 0 min No Test Protein Control and 60 min No Test Protein Control (Figure 52, Panel A, lanes 2 and 13) demonstrated that the pepsin is stable throughout the experimental phase.

A separate SDS PAGE gel to estimate the LOD of the PAT (*pat*) protein was run concurrently with the SDS PAGE for the degradation assessment (Figure 52B). The LOD of the PAT (*pat*) protein was visually estimated to be approximately 3.6 ng (Figure 52B, Lane 8). This LOD is used to calculate the maximum amount of intact PAT (*pat*) protein that could remain visually undetected after degradation, which corresponded to approximately 0.4% ($3.6/1000 \times 100\% = \sim 0.4\%$) of the total protein loaded. Based on that LOD, more than 99.6% ($100\% - 0.4\% = 99.6\%$) of the intact PAT (*pat*) protein was degraded within 0.5 min of incubation in the presence of pepsin.
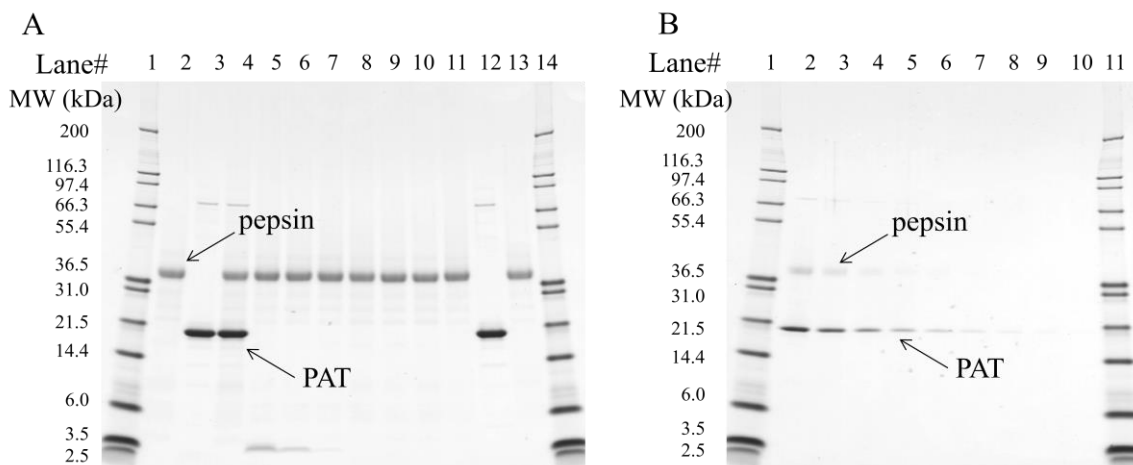
Figure 52.   SDS-PAGE Analysis of the Degradation of PAT (*pat*) Protein by Pepsin

Colloidal Brilliant Blue G stained SDS-PAGE gels were used to assess the degradation of PAT (*pat*) protein by pepsin.   Molecular weights (kDa) are shown on the left of each gel, and correspond to the markers loaded.   In each gel, PAT (*pat*) protein migrated to approximately 21 kDa and pepsin to approximately 38 kDa.   Blank lanes were cropped from the images.
A: PAT (*pat*) protein degradation by Pepsin.   Based on pre-reaction protein concentrations, 1 µg of test protein was loaded in each lane containing PAT (*pat*) protein.
B: LOD determination.   Indicated amounts of the test protein from the Pepsin Treated T0 sample were loaded to estimate the LOD of the PAT (*pat*) protein.

Lane	Sample	Incubation Time (min)
1	Mark 12 MWM	-
2	0 min No Test Protein Control	0
3	T 0 min No Pepsin Control	0
4	Pepsin Treated T0	0
5	Pepsin Treated T1	0.5
6	Pepsin Treated T2	2
7	Pepsin Treated T3	5
8	Pepsin Treated T4	10
9	Pepsin Treated T5	20
10	Pepsin Treated T6	30
11	Pepsin Treated T7	60
12	60 min No Pepsin Control	60
13	60 min No Test Protein Control	60
14	Mark 12 MWM	-

Lane	Sample	Amount (ng)
1	Mark 12 MWM	-
2	Pepsin Treated T0	230
3	Pepsin Treated T0	115
4	Pepsin Treated T0	57.5
5	Pepsin Treated T0	28.8
6	Pepsin Treated T0	14.4
7	Pepsin Treated T0	7.2
8	Pepsin Treated T0	3.6
9	Pepsin Treated T0	1.8
10	Pepsin Treated T0	0.9
11	Mark 12 MWM	

For Western blot analysis of PAT (*pat*) pepsin susceptibility, the PAT (*pat*) protein was loaded with approximately 20 ng per lane of total protein (based on pre-reaction total protein concentrations) for each reaction time point examined. The Western blot used to assess the resistance of the PAT (*pat*) protein to pepsin digestion (Figure 53A) was run concurrently with a Western blot to estimate the LOD of the PAT (*pat*) protein Figure 53B). The LOD of the PAT (*pat*) protein was approximately 0.36 ng (Figure 53, lane 8). The LOD was used to calculate the maximum relative amount of PAT (*pat*) protein that could remain visually undetected after digestion, which corresponded to approximately 1.8% (0.36/20 × 100% = 1.8%) of the total protein loaded.

Western blot analysis demonstrated that the PAT (*pat*) protein was degraded below the LOD within 0.5 min of incubation in the presence of pepsin (Figure 53Figure 53A, lane 5). Based on the Western blot LOD for the PAT (*pat*) protein, it can be concluded that more than 98.2% (100% - 1.8% = 98.2%) of the intact PAT (*pat*) protein was degraded within 0.5 min. No peptide fragments were detected at any timepoint in pepsin by Western blot.

No apparent change in the PAT (*pat*) protein band intensity was observed in the absence of pepsin in the 0 min No Pepsin Control and 60 min No Pepsin Control samples (Figure 53A, lanes 3 and 12). This indicates that the degradation of the PAT (*pat*)protein was due to the proteolytic activity of pepsin and not due to instability of the protein while incubated in the pepsin test system over the course of the experiment.

No immunoreactive bands were observed in the 0 min No Protein Control and 60 min No Protein Control samples (Figure 53A, lanes 2 and 13). This result indicates that there was no non-specific interaction between the pepsin solution and the PAT specific antibody under these experimental conditions.
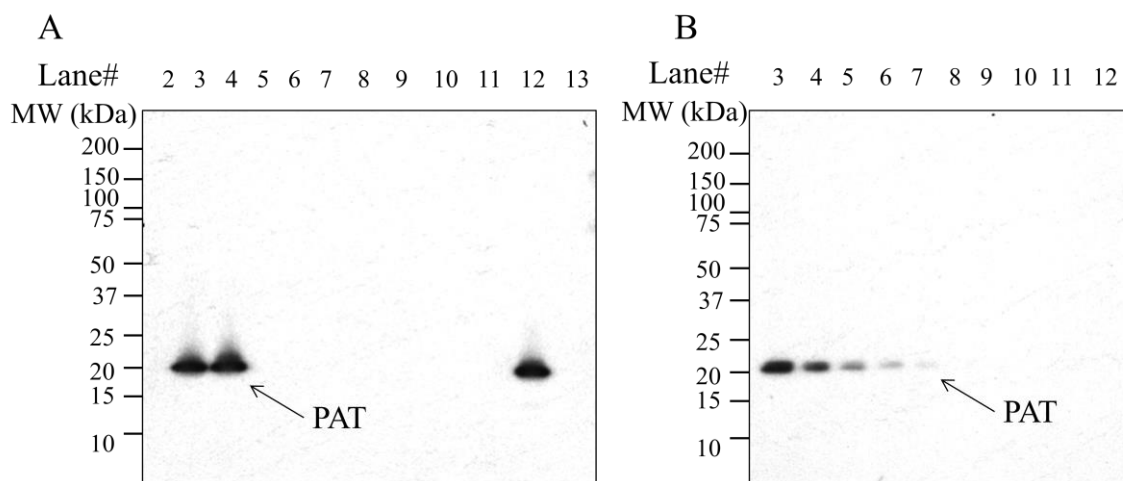
Figure 53.   Western Blot Analysis of the Degradation of PAT (*pat*) Protein by Pepsin

Western blots probed with an anti-PAT antibody were used to assess the degradation of PAT (*pat*) by pepsin.   Molecular weights (kDa) are shown on the left of each gel, and correspond to the markers loaded (cropped from images).   Blank lanes were cropped from the images.   A 20 sec exposure is shown.

A: PAT (*pat*) protein degradation by pepsin.   Based on pre-reaction protein concentrations, 20 ng of test protein was loaded in each lane containing PAT (*pat*) protein.

B: LOD determination.   Indicated amounts of the test protein from the Pepsin Treated T0 sample were loaded to estimate the LOD of the PAT (*pat*) protein.

Lane	Sample	Incubation Time (min)	Lane	Sample	Amount (ng)
1	Precision Plus MWM	-	1	Precision Plus MWM	-
2	0 min No Test Protein Control	0	2	Empty	-
3	0 min No Pepsin Control	0	3	Pepsin Treated T0	5.8
4	Pepsin Treated T0	0	4	Pepsin Treated T0	2.9
5	Pepsin Treated T1	0.5	5	Pepsin Treated T0	1.44
6	Pepsin Treated T2	2	6	Pepsin Treated T0	0.72
7	Pepsin Treated T3	5	7	Pepsin Treated T0	0.36
8	Pepsin Treated T4	10	8	Pepsin Treated T0	0.18
9	Pepsin Treated T5	20	9	Pepsin Treated T0	0.09
10	Pepsin Treated T6	30	10	Pepsin Treated T0	0.045
11	Pepsin Treated T7	60	11	Pepsin Treated T0	0.022
12	60 min No Pepsin Control	60	12	Pepsin Treated T0	0.011
13	60 min No Test Protein Control	60	13	Empty	-
14	Precision Plus MWM	-	14	Precision Plus MWM	-

Degradation of PAT (*pat*) Protein by Pancreatin

The degradation of the PAT (*pat*) protein by pancreatin was assessed by Western blot analysis (Figure 54). The total loading of the PAT (*pat*) test protein for each timepoint examined was approximately 20 ng per lane (based on pre-reaction total protein concentrations). The Western blot used to assess the PAT (*pat*) protein degradation (Figure 54A) was run concurrently with the Western blot used to estimate the LOD (Figure 54B) of the intact PAT (*pat*) protein. The LOD of the PAT (*pat*) protein was observed at approximately the 0.17 ng protein loading (Figure 54A, lane 8). The LOD was used to calculate the maximum relative amount of the PAT (*pat*) protein that could remain visually undetected after digestion, which corresponded to approximately 0.9% (0.17/20 × 100% = ~0.9%) of the total protein loaded.

Western blot analysis demonstrated that a band corresponding to the PAT (*pat*) protein was degraded to a level below the LOD within 5 min of incubation in the presence of pancreatin (Figure 54A, lane 5), the first timepoint assessed. Therefore, based on the LOD, more than 99% (100% - 0.9% = 99.1%) of the PAT (*pat*) protein was degraded within 5 min. No other immunoreactive bands were detected in any other tested specimens. This is comparable with previously published safety assessments of PAT (*pat*) protein (Hérouet *et al.*, 2005).

No apparent change in the intact PAT (*pat*) band intensity was observed in the absence of pancreatin in the 0 h No Pancreatin Control and 24 h No Pancreatin Control samples (Figure 54A, lanes 3 and 13). This indicates that the degradation of all immunoreactive forms of the PAT (*pat*) protein was due to the proteolytic activity of pancreatin and not due to instability of the protein when incubated in the pancreatin test system over the course of the experiment.

No immunoreactive bands were observed in the 0 h No Test Protein Control and 24 h No Test Protein Control samples (Figure 54A, lanes 2 and 14), demonstrating the absence of non-specific antibody interactions with the pancreatin solution.

Figure 54.   Western Blot Analysis of the Degradation of PAT (*pat*) Protein by Pancreatin

Western blots probed with an anti-PAT antibody were used to assess the degradation of PAT (*pat*) by pancreatin.   Molecular weights (kDa) are shown on the left of each gel, and correspond to the markers loaded (cropped from images).   Blank lanes were cropped from the images.   A 15 sec exposure is shown.

A: PAT (*pat*) protein degradation by pancreatin.   Based on pre-reaction protein concentrations, 20 ng of test protein was loaded in each lane containing PAT (*pat*) protein.

B: LOD determination.   Indicated amounts of the test protein from the T0 sample were loaded to estimate the LOD of the PAT (*pat*) protein.

Lane	Sample	Incubation Time
1	Precision Plus MWM	-
2	0 min No Test Protein Control	0
3	0 min No Pancreatin Control	0
4	Pancreatin Treated T0	0
5	Pancreatin Treated T1	5 min
6	Pancreatin Treated T2	15 min
7	Pancreatin Treated T3	30 min
8	Pancreatin Treated T4	1 hr
9	Pancreatin Treated T5	2 hr
10	Pancreatin Treated T6	4 hr
11	Pancreatin Treated T7	8 hr
12	Pancreatin Treated T8	24 hr
13	24 hr No Pancreatin Control	24 hr
14	24 hr No Test Protein Control	24 hr
15	Precision Plus MWM	-

Lane	Sample	Amount (ng)
1	Precision Plus MWM	-
2	Empty	-
3	Pancreatin Treated T0	5.6
4	Pancreatin Treated T0	2.78
5	Pancreatin Treated T0	1.39
6	Pancreatin Treated T0	0.69
7	Pancreatin Treated T0	0.35
8	Pancreatin Treated T0	0.17
9	Pancreatin Treated T0	0.087
10	Pancreatin Treated T0	0.043
11	Pancreatin Treated T0	0.022
12	Pancreatin Treated T0	0.011
13	Empty	-
14	Precision Plus MWM	-

Digestive Fate of PAT (*pat*) Protein – Conclusions

The ability of the PAT (*pat*) protein to be degraded by pepsin and by pancreatin was evaluated in this study. The results of the SDS-PAGE analysis demonstrate that greater than 99.6% of the intact PAT (*pat*) protein was degraded by pepsin within 0.5 min and at least 98.2% of the intact PAT (*pat*) protein was degraded by pepsin within 0.5 min when analyzed by Western blot using a PAT specific antibody. SDS-PAGE analysis showed that a peptide fragment of ~3 kDa was observed in the 0.5 min time points in the presence of pepsin, but was gone by 10 min.

At least 99.1% of the intact PAT (*pat*) protein was degraded within 5 min during incubation with pancreatin when analyzed by Western blot.

These results show that the intact PAT (*pat*) is rapidly degraded by pepsin and pancreatin. Rapid and complete degradation of the PAT (*pat*) protein by pepsin and pancreatin indicates that the PAT (*pat*) protein is highly unlikely to pose any safety concern to human or animal health.

Degradation of FT_T Protein in the Presence of Pepsin

For details, please refer to ███████, 2018 (MSL0029802).

Degradation of the FT_T protein by pepsin was evaluated over time by analyzing digestion mixtures incubated for targeted time intervals following a standardized protocol validated in an international, multi-laboratory ring study (Thomas *et al.*, 2004) collected at targeted incubation time points. The susceptibility of FT_T protein to pepsin degradation was assessed by visual analysis of a Brilliant Blue G Colloidal stained SDS-PAGE gel and by visual analysis of a Western blot probed with an anti-FT_T polyclonal antibody. Both visualization methods were run concurrently with separate SDS-PAGE and Western blot analyses to estimate the limit of detection (LOD) of the FT_T protein for each method.

For SDS-PAGE analysis of the digestibility of the FT_T protein in pepsin, the gel was loaded with 1 µg of total test protein (based on pre-digestion protein concentrations) for each of the digestion samples (Figure 55, Panel A). The SDS-PAGE gel for the digestibility assessment was run concurrently with a separate SDS-PAGE gel to estimate the LOD of the FT_T protein (Figure 55, Panel B). The LOD of intact FT_T protein was approximately 3.1 ng (Figure 55, Panel B, lane 8). Visual examination of SDS-PAGE data showed that the intact FT_T protein was digested within 0.5 min of incubation in pepsin (Figure 55, Panel A, lane 5). Therefore, based on the LOD, more than 99.7% (100% - 0.3% = 99.7%) of the intact FT_T protein was digested within 0.5 -min of incubation in pepsin. Transiently-stable peptide fragments at ~4-kDa were observed throughout the course of the digestion. There is a slight decrease in the intact FT_T protein band intensity and generation of fragments greater than 20 kDa observed in the 60 min No Pepsin Control compared to the 0 min No Pepsin Control (Figure 55, Panel A, lanes 12 and 3, respectively). This likely indicates that a small portion of FT_T protein is unstable possibly due to either the acidic conditions or minor contaminants in the FT_T solution; however, the rapid degradation of the intact FT_T protein

and the subsequent fragments in the pepsin degradation samples was due to the proteolytic activity of pepsin.

The 0 min No Test Protein Control and 60 min No Test Protein Control (Figure 55, Panel A, lanes 2 and 13) demonstrated that the pepsin is stable throughout the experimental phase.
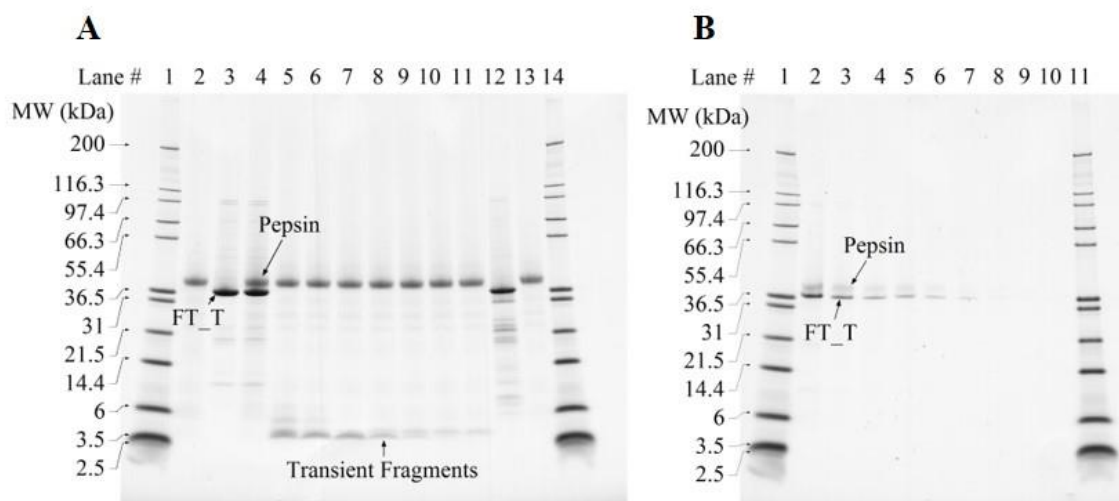
Figure 55. SDS-PAGE Analysis of the Degradation of FT_T Protein by Pepsin

Colloidal Brilliant Blue G stained SDS-PAGE gels were used to assess the degradation of FT_T protein by pepsin. Molecular weights (kDa) are shown on the left of each gel and correspond to the markers loaded. In each gel, the FT_T protein migrated to approximately 35 kDa and pepsin to approximately 38 kDa. Empty lanes and molecular weight markers that were not visible on the film were cropped from the images.

A: FT_T protein degradation in the presence of pepsin. Based on pre-reaction protein concentrations, 1 µg of test protein was loaded in each lane containing FT_T protein.

B: LOD determination. Indicated amounts of the test protein from the Pepsin Treated T0 sample were loaded to estimate the LOD of the FT_T protein.

Lane	Sample	Incubation Time (min)	Lane	Sample	Amount (ng)
1	Mark12 MWM	-	1	Mark12 MWM	-
2	0 min No Test Protein Control	0	2	Pepsin Treated T0	200
3	0 min No Pepsin Control	0	3	Pepsin Treated T0	100
4	Pepsin Treated T0	0	4	Pepsin Treated T0	50
5	Pepsin Treated T1	0.5	5	Pepsin Treated T0	50
6	Pepsin Treated T2	2	6	Pepsin Treated T0	25
7	Pepsin Treated T3	5	7	Pepsin Treated T0	12.5
8	Pepsin Treated T4	10	8	Pepsin Treated T0	3.1
9	Pepsin Treated T5	20	9	Pepsin Treated T0	1.6
10	Pepsin Treated T6	30	10	Pepsin Treated T0	0.8
11	Pepsin Treated T7	60	11	Mark12 MWM	-
12	60 min No Pepsin Control	60	12	Empty	-
13	60 min No Test Protein Control	60	13	Empty	-
14	Mark12 MWM	-	14	Empty	-
15	Empty	-	15	Empty	-

For Western blot analysis of FT_T pepsin susceptibility, the FT_T protein was loaded with approximately 40 ng per lane of total protein (based on pre-reaction total protein concentrations) for each reaction time point examined. The Western blot used to assess FT_T protein degradation (Figure 56, Panel A) was run concurrently with the Western blot used to estimate the LOD (Figure 56, Panel B). The LOD of the FT_T protein was approximately 0.31 ng (Figure 56, Panel B, Lane 10). Western blot analysis demonstrated that the intact FT_T protein was degraded below the LOD within 0.5 min of incubation in the presence of pepsin (Figure 56, Panel A, Lane 6). Based on the Western blot LOD for the FT_T protein, more than 99.2% (100% - 0.8% = 99.2%) of the intact FT_T protein was degraded within 0.5 min. No peptide fragments were detected at the 0.5 min and beyond time points in the Western blot analysis.

No change in the intact FT_T protein band intensity were observed in the 0 min No Pepsin Control and the 60 min No Pepsin Control. There were three antibody-recognized fragments greater than 20 kDa observed in the 60 min No Pepsin Control that were not observed in the 0 min No Pepsin Control (Figure 56, Panel A, lanes 13 and 4, respectively). This indicates that small portion of the FT_T protein is slightly unstable possibly due to either the acidic conditions or minor contaminants in the FT_T solution; however, a majority of the degradation of the intact FT_T protein and the subsequent fragments in the pepsin degradation samples was due to the proteolytic activity of pepsin. The transiently-stable fragments at ~4 kDa that were observed by SDS-PAGE were not recognized by the antibody used in this Western blot.

No immunoreactive bands were observed in 0 min No Protein Control and 60 min No Protein Control (Figure 56, Panel A, lanes 3 and 14). This result indicates that there was no non-specific interaction between the pepsin solution and the FT_T-specific antibody under these experimental conditions.

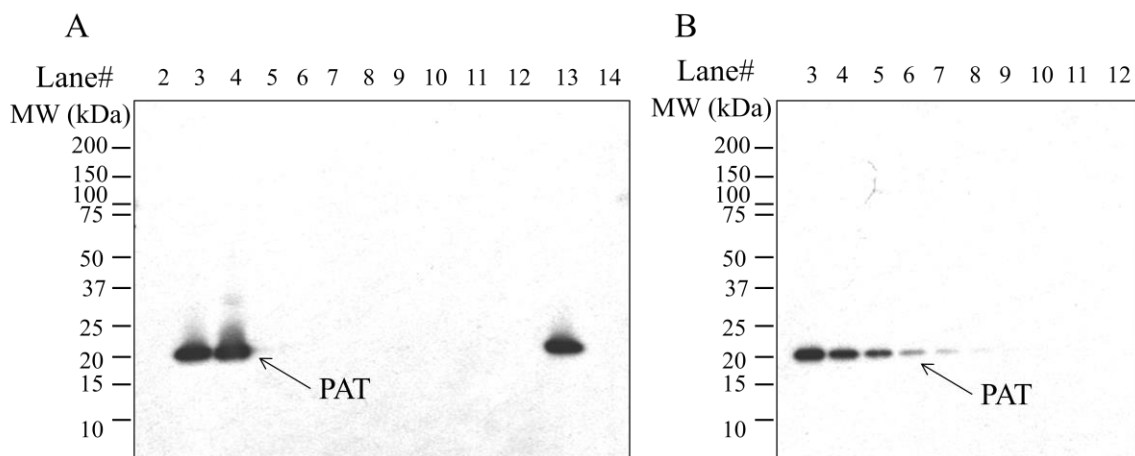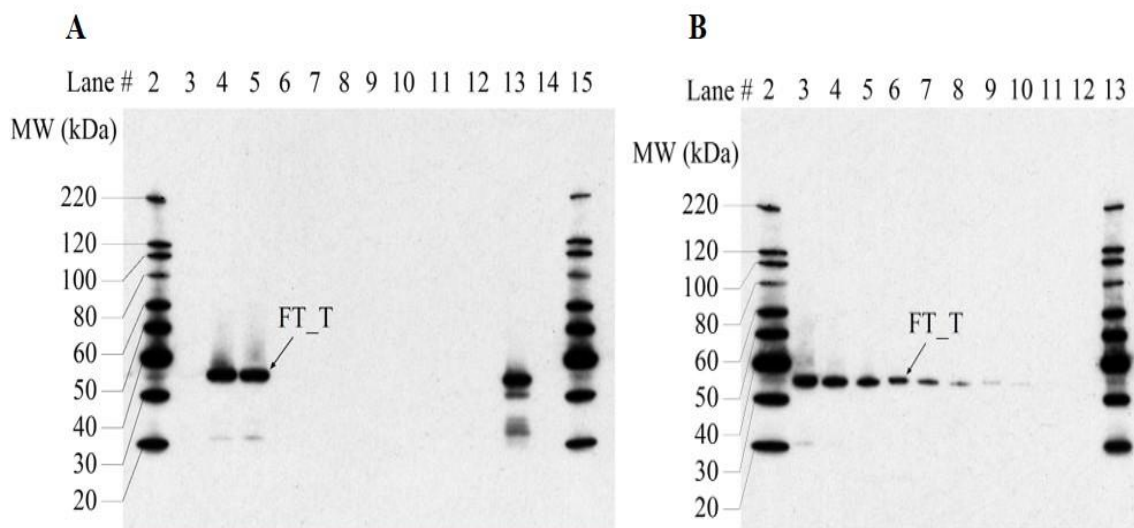**Figure 56.   Western Blot Analysis of the Degradation of FT_T Protein by Pepsin**

Western blots probed with an anti-FT_T antibody were used to assess the degradation of FT_T by pepsin.   Molecular weights (kDa) are shown on the left of each gel and correspond to the MagicMark™ molecular weight marker loaded in two lanes of each gel.   Empty lanes and molecular weight markers that were not visible on the film were cropped from the images.   A 30 sec exposure is shown.

A: FT_T protein degradation by pepsin.   Based on pre-reaction protein concentrations, 40 ng of test protein was loaded in each lane containing FT_T protein.

B: LOD determination.   Indicated amounts of the test protein from the Pepsin Treated T0 sample were loaded to estimate the LOD of the FT_T protein.

Lane	Sample	Incubation Time (min)	Lane	Sample	Amount (ng)
1	Precision Plus MWM	-	1	Precision Plus MWM	-
2	MagicMark MWM	-	2	MagicMark MWM	-
3	0 min No Test Protein Control	0	3	Pepsin Treated T0	40
4	0 min No Pepsin Control	0	4	Pepsin Treated T0	20
5	Pepsin Treated T0	0	5	Pepsin Treated T0	10
6	Pepsin Treated T1	0.5	6	Pepsin Treated T0	5
7	Pepsin Treated T2	2	7	Pepsin Treated T0	2.5
8	Pepsin Treated T3	5	8	Pepsin Treated T0	1.25
9	Pepsin Treated T4	10	9	Pepsin Treated T0	0.63
10	Pepsin Treated T5	20	10	Pepsin Treated T0	0.31
11	Pepsin Treated T6	30	11	Pepsin Treated T0	0.16
12	Pepsin Treated T7	60	12	Pepsin Treated T0	0.08
13	60 min No Pepsin Control	60	13	MagicMark MWM	-
14	60 min No Test Protein Control	60	14	Precision Plus MWM	-
15	MagicMark MWM	-	15	Empty	-

Degradation of FT_T Protein in the Presence of Pancreatin

The degradation of the FT_T protein by pancreatin was assessed by Western blot analysis (Figure 57). The Western blot used to assess the FT_T protein degradation (Figure 57, Panel A) was run concurrently with the Western blot used to estimate the LOD (Figure 57, Panel B) of the FT_T protein. The LOD of the FT_T protein was observed at approximate 0.31 ng protein loading (Figure 57, Panel B, lane 10). The LOD was used to calculate the maximum relative amount of FT_T protein that could remain visually undetected after digestion, which corresponded to approximately 0.8% of the total protein loaded.

The gel used to assess degradation of the FT_T protein by Western blot was loaded with approximately 40 ng per lane of total protein (based on pre-reaction protein concentrations) for each reaction time point examined. Western blot analysis demonstrated that a band corresponding to the FT_T protein was degraded to a level below the LOD within 5 minutes of incubation with pancreatin (Figure 57, Panel A, lane 5), the first time point assessed. Therefore, based on the LOD, more than 99.2% (100% - 0.8% = 99.2%) of the FT_T protein was digested within 5 minutes. No peptide fragments were detected at the 5 min and beyond time points in the Western blot analysis.

No obvious change in the intact FT_T (~35.5 kDa) band intensity was observed in the absence of pancreatin in the 0 min No Pancreatin Control and 24 hour No Pancreatin Control (Figure 57, Panel A, lanes 3 and 13). This indicates that the degradation of all immunoreactive forms of the FT_T protein was due to the proteolytic activity of pancreatin and not due to instability of the protein when incubated in the pancreatin test system over the course of the experiment.

No immunoreactive bands were observed in the 0 min No Test Protein Control and 24 hour No Test Protein Control (Figure 57, Panel A, lanes 2 and 14), demonstrating the absence of non-specific antibody interactions with the pancreatin solution.
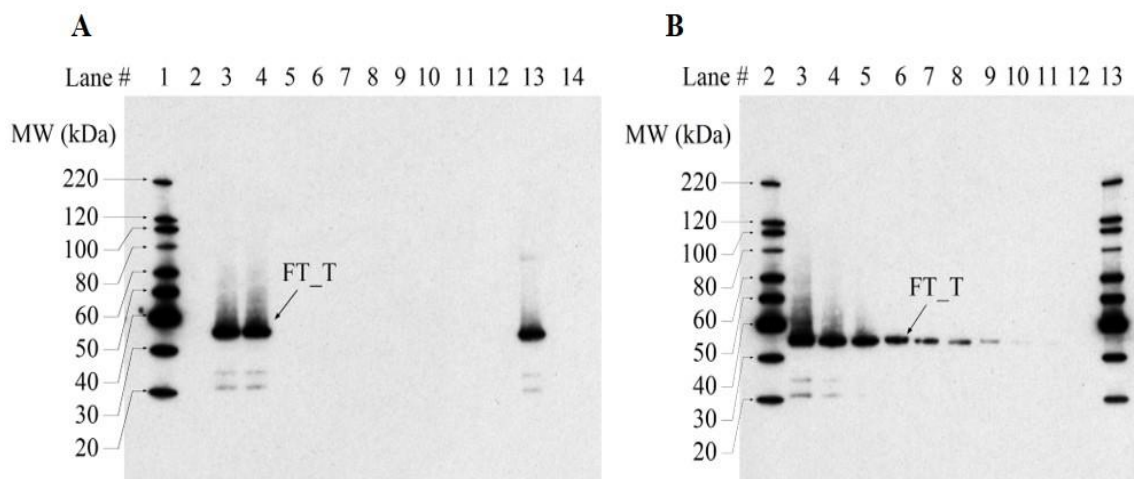
Figure 57.   Western Blot Analysis of the Degradation of FT_T Protein by Pancreatin

Western blots probed with an anti-FT_T antibody were used to assess the degradation of FT_T by pancreatin. Molecular weights (kDa) are shown on the left of each gel and correspond to the MagicMark™ molecular weight marker loaded in each gel. Empty lanes and molecular weight markers that were not visible on the film were cropped from the images. A 60 sec exposure is shown.

A: FT_T protein degradation by pancreatin. Based on pre-reaction protein concentrations, 40 ng of test protein was loaded in each lane containing FT_T protein.

B: LOD determination. Indicated amounts of the test protein from the Pancreatin Treated T0 sample were loaded to estimate the LOD of the FT_T protein.

Lane	Sample	Incubation Time	Lane	Sample	Amount (ng)
1	MagicMark MWM	-	1	Precision Plus MWM	-
2	0 min No Test Protein Control	0	2	MagicMark MWM	-
3	0 min No Pancreatin Control	0	3	Pancreatin Treated T0	40
4	Pancreatin Treated T0	0	4	Pancreatin Treated T0	20
5	Pancreatin Treated T1	5 min	5	Pancreatin Treated T0	10
6	Pancreatin Treated T2	15 min	6	Pancreatin Treated T0	5
7	Pancreatin Treated T3	30 min	7	Pancreatin Treated T0	2.5
8	Pancreatin Treated T4	1 h	8	Pancreatin Treated T0	1.25
9	Pancreatin Treated T5	2 h	9	Pancreatin Treated T0	0.63
10	Pancreatin Treated T6	4 h	10	Pancreatin Treated T0	0.31
11	Pancreatin Treated T7	8 h	11	Pancreatin Treated T0	0.16
12	Pancreatin Treated T8	24 h	12	Pancreatin Treated T0	0.08
13	24 h No Pancreatin Control	24 h	13	MagicMark MWM	-
14	24 h No Test Protein Control	24 h	14	Precision Plus MWM	-
15	Precision Plus MWM	-	15	Empty	-

Degradation of FT_T Protein by Pepsin Followed by Pancreatin

To better understand the fate of the transiently-stable peptide fragments at ~4 -kDa that were observed in the reaction mixtures throughout the course of the pepsin digestion of FT_T, sequential digestibility of the FT_T protein was conducted.   This sequential digestibility was assessed both by visual analysis of a Colloidal Brilliant Blue G stained SDS-PAGE gel, and visual analysis of a Western blot probed with an anti FT_T-polyclonal antibody.

For the sequential degradation assay, the FT_T protein was incubated with pepsin for 2 min, followed by incubation with pancreatin.   For the Colloidal Brilliant Blue G stained SDS-PAGE assessment, the gel was loaded with 1 µg of FT_T protein (based on pre-digestion protein concentrations) for each of the digestion samples.   Examination of SDS-PAGE data showed that the intact FT_T protein was digested within 2 min of incubation in pepsin (Figure 58, Panel A, lane 3) and the small transient fragments at ~4 kDa was completely digested within 0.5 min of pancreatin exposure (Figure 58, Panel A, lane 7).

No change in the fragment band intensities was observed in the absence of pancreatin in the SEQ 0 min No Pancreatin Control and SEQ 2 hour No Pancreatin Control (Figure 58, Panel A, lanes 5 and 14).   This indicates that the digestion of the fragments was due to the proteolytic activity of pancreatin and not due to instability of the fragment when incubated in the test system over the course of the experiment.

The SEQ 0 min No Test Protein Control and SEQ 2 hour No Test Protein Control (Figure 58Panel A, lanes 4 and 15) demonstrated the integrity of the pancreatin over the course of the experiment.   The intensity of some pancreatin bands decreased somewhat during the course of the experiment, most likely due to auto-digestion.   This is not expected to adversely impact the pancreatin degradation results, as the transiently stable fragments were digested within 0.5 min of exposure to pancreatin.

The sequential digestion of the FT_T protein was also assessed by Western blot (Figure 58, Panel B), with 40 ng of the test protein (based on total protein pre-digestion concentrations) loaded per lane.   No bands were detected in the 2 min Pepsin Treated sample (Figure 58, Panel B, lane 3).
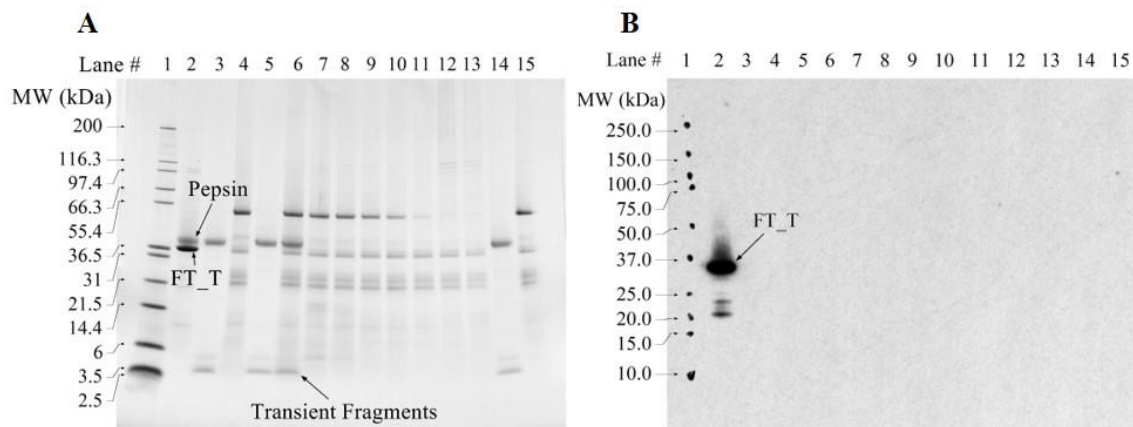
Figure 58.   SDS-PAGE and Western Blot Analysis of the Degradation of FT_T Protein by Sequential Digestion

SDS-PAGE and Western blot analysis were used to assess the degradation of FT_T in sequential digestion.   Molecular weights (kDa) are shown on the left of each gel and correspond to the markers loaded (cropped in panel B).
A: Colloidal Brilliant Blue G stained SDS-PAGE gel analysis of FT_T in sequential digestion. Based on pre-digestion protein concentrations, 1 µg of test protein was loaded in each lane containing FT_T protein.
B: Western blot analysis of FT_T in sequential digestion.   Based on pre-digestion protein concentrations, 40 ng of test protein was loaded in each lane containing FT_T protein.   A 60 sec exposure is shown.

Lane	Sample	Incubation Time	Lane	Sample	Incubation Time
1	Mark12 MWM	-	1	Precision Plus MWM	-
	Pepsin Degradation			**Pepsin Degradation**	
2	0 min Pepsin Treated	0 min	2	0 min Pepsin Treated	0 min
3	2 min Pepsin Treated	2 min	3	2 min Pepsin Treated	2 min
	Pancreatin Degradation			**Pancreatin Degradation**	
4	SEQ 0 min No Test Protein Control	0 min	4	SEQ 0 min No Test Protein Control	0 min
5	SEQ 0 min No Pancreatin Control	0 min	5	SEQ 0 min No Pancreatin Control	0 min
6	SEQ T0	0 min	6	SEQ T0	0 min
7	SEQ T1	0.5 min	7	SEQ T1	0.5 min
8	SEQ T2	2 min	8	SEQ T2	2 min
9	SEQ T3	5 min	9	SEQ T3	5 min
10	SEQ T4	10 min	10	SEQ T4	10 min
11	SEQ T5	30 min	11	SEQ T5	30 min
12	SEQ T6	1 h	12	SEQ T6	1 h
13	SEQ T7	2 h	13	SEQ T7	2 h
14	SEQ 2 h No Pancreatin Control	2 h	14	SEQ 2 h No Pancreatin Control	2 h
15	SEQ 2 h No Test Protein Control	2 h	15	SEQ 2 h No Test Protein Control	2 h

Digestive Fate of the FT_T Protein – Conclusions

The ability of FT_T protein to be degraded by pepsin and by pancreatin was evaluated in this study.   The results showed that at least 99.7% of the intact FT_T protein was degraded by pepsin within 0.5 min when analyzed by SDS-PAGE and at least 99.2% of the intact FT_T was degraded by pepsin within 0.5 min when analyzed by Western blot using a FT_T specific antibody.   SDS-PAGE analysis showed that transient peptide fragments at ~4 kDa were observed throughout the course of the pepsin digestion.   At least 99.2% of the intact FT_T protein was degraded by pancreatin within 5 min when analyzed by Western blot.   These results show that the full-length FT_T is rapidly degraded by pepsin and pancreatin.   The transient fragments at ~4 kDa were rapidly degraded by sequential digestion, indicating that gastrointestinal digestion is sufficient to degrade the intact FT_T protein and any fragments thereof.   Rapid and complete degradation of the FT_T protein by pancreatin alone and pepsin followed by pancreatin indicates that the FT_T protein poses no meaningful risk to human or animal health.

Degradation of CP4 EPSPS by Pepsin

For details, please also refer to ▮▮▮▮▮▮▮▮ 2002 (MSL17566) and ▮▮▮▮▮▮▮▮, 1993 (MSL12949).

Harrison *et al*. (1996) demonstrated that the *E. coli*-produced CP4 EPSPS protein is rapidly degraded in simulated gastric fluids (SGF, i.e.   pepsin solution). Based on Western blot analysis, CP4 EPSPS protein was undetectable within 15 seconds of incubation in the presence of pepsin.

Subsequent digestive fate experiments confirmed the *in vitro* digestibility of the CP4 EPSPS protein in pepsin. For SDS-PAGE analysis of the digestibility of the CP4 EPSPS protein in pepsin, the gel was loaded with 0.5 μg of total test protein (based on pre-digestion protein concentrations) for each of the digestion samples (Figure 59A).   Visual examination of SDS-PAGE data showed that the intact CP4 EPSPS protein was completely degraded within 15 seconds of incubation in the presence of pepsin (Figure 59A, lane 5).

No change in the CP4 EPSPS protein band intensity was observed in the absence of pepsin in the 0 min No Pepsin Control and 60 min No Pepsin Control samples (Figure 59A, lanes 2 and 15).   This indicates that the degradation of the CP4 EPSPS protein was due to the proteolytic activity of pepsin and not due to instability of the protein while incubated in the pepsin test system over the course of the experiment.

The 0 min No Test Protein Control and 60 min No Test Protein Control (Figure 59, Panel A, lanes 2 and 13) demonstrated that the pepsin is stable throughout the experimental phase.

A separate SDS PAGE gel to estimate the LOD of the CP4 EPSPS protein was run concurrently with the SDS PAGE for the degradation assessment (Figure 59B).   The LOD of intact CP4 EPSPS protein was approximately 10 ng (Figure 59B, lane 11), which corresponded to approximately 2% ($10/500 \times 100\% = 2\%$) of the total protein loaded. Therefore, based on the LOD, more than 98% ($100\% - 2\% = 98\%$) of the intact CP4 EPSPS protein was degraded   within 15 seconds of incubation in pepsin, which is similar to the

results reported by Harrison *et al*. (1996).
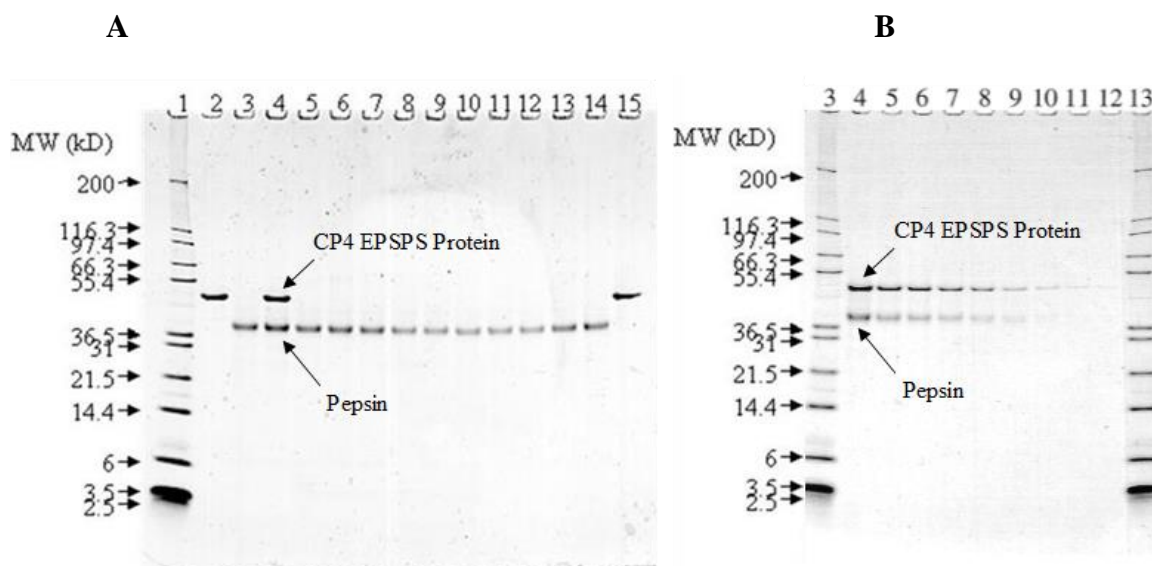
Figure 59.   SDS-PAGE Analysis of the Degradation of CP4 EPSPS Protein by Pepsin

Colloidal Brilliant Blue G stained SDS-PAGE gels were used to assess the degradation of CP4 EPSPS protein by pepsin.   Molecular weights (kDa) are shown on the left of each gel and correspond to the markers loaded.   In each gel, the CP4 EPSPS protein migrated to approximately 44 kDa and pepsin to approximately 38 kDa.   Empty lanes and molecular weight markers that were not visible on the gel were cropped from the images.

Panel A: CP4 EPSPS protein degradation in the presence of pepsin.   Based on pre-reaction protein concentrations, 0.5 µg of test protein was loaded in each lane containing CP4 EPSPS protein.

Panel B: LOD determination.   Indicated amounts of the test protein from the Pepsin Treated T0 sample were loaded to estimate the LOD of the CP4 EPSPS protein.

Lane	Sample	Incubation Time (min)	Lane	Sample	Amount (ng)
1	Molecular Weight Marker	-	1	Empty	-
2	0 min No Pepsin Control	0	2	Empty	-
3	0 min No Test Protein Control	0	3	Molecular Weight Marker	-
4	Pepsin Treated T0	0	4	Pepsin Treated T0	500
5	Pepsin Treated T1	0.25	5	Pepsin Treated T0	250
6	Pepsin Treated T2	0.5	6	Pepsin Treated T0	200
7	Pepsin Treated T3	1	7	Pepsin Treated T0	150
8	Pepsin Treated T4	2	8	Pepsin Treated T0	100
9	Pepsin Treated T5	4	9	Pepsin Treated T0	50
10	Pepsin Treated T6	8	10	Pepsin Treated T0	25
11	Pepsin Treated T7	15	11	Pepsin Treated T0	10
12	Pepsin Treated T8	30		Pepsin Treated T0	5
13	Pepsin Treated T9	60		Molecular Weight Marker	-
14	60 min Test Protein No Control	60	12	Empty	-
15	60 min No Pepsin Control	60	13	Empty	-

For Western blot analysis of CP4 EPSPS pepsin susceptibility, the CP4 EPSPS protein was loaded with approximately 1 ng per lane of total protein (based on pre-reaction total protein concentrations) for each reaction time point examined. The Western blot used to assess the resistance of the CP4 EPSPS protein to pepsin digestion (Figure 60A) was run concurrently with a Western blot to estimate the LOD of the CP4 EPSPS protein (Figure 60B). The LOD of intact CP4 EPSPS protein was approximately 0.05 ng (Figure 60B, lane 10). The LOD was used to calculate the maximum relative amount of CP4 EPSPS protein that could remain visually undetected after digestion, which corresponded to approximately 5% ($0.05/1 \times 100\% = 5\%$) of the total protein loaded.

Western blot analysis demonstrated that the CP4 EPSPS protein was degraded below the LOD within 0.25 min (15 seconds) of incubation in the presence of pepsin (Figure 60A, lane 5). Based on the Western blot LOD for the CP4 EPSPS protein, it can be concluded that more than 95% (100% - 5% = 95%) of the intact CP4 EPSPS protein was degraded within 0.25 min. No peptide fragments were detected at any timepoint in pepsin by Western blot.

No apparent change in the CP4 EPSPS protein band intensity was observed in the absence of pepsin in the 0 min No Pepsin Control and 60 min No Pepsin Control samples (Figure 60A, lanes 2 and 15). This indicates that the degradation of the CP4 EPSPS protein was due to the proteolytic activity of pepsin and not due to instability of the protein while incubated in the test system over the course of the experiment.

No immunoreactive bands were observed in the 0 min No Protein Control and 60 min No Protein Control samples (Figure 60A, lanes 3 and 14). This result indicates that there was no non-specific interaction between the pepsin solution and the CP4 EPSPS-specific antibody under these experimental conditions.
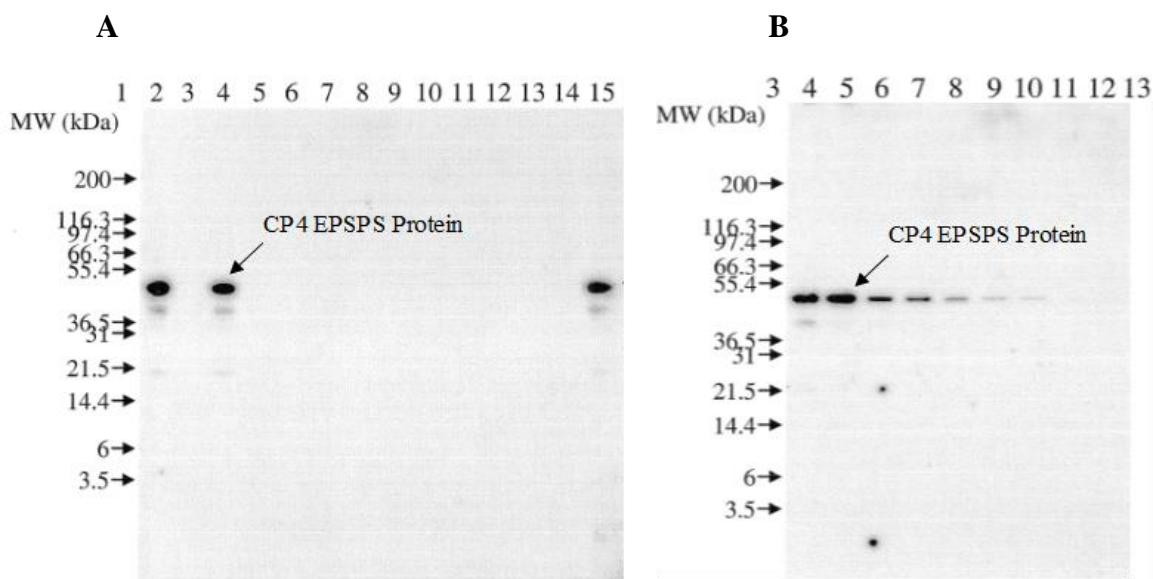
Figure 60.   Western Blot Analysis of the Degradation of the Produced CP4 EPSPS Protein by Pepsin

Western blots probed with an anti-CP4 EPSPS antibody were used to assess the degradation of CP4 EPSPS by pepsin.   Molecular weights (kDa) are shown on the left of each gel, and correspond to the markers loaded (cropped from images).   Blank lanes were cropped from the images.

Panel A: CP4 EPSPS protein degradation by pepsin.   Based on total pre-reaction protein concentrations, 1 ng of test substance was loaded in each lane containing CP4 EPSPS protein.

Panel B: LOD determination.   Indicated amounts of the CP4 EPSPS protein from the Pepsin Treated T0 sample were loaded to estimate the LOD of the CP4 EPSPS protein.   Lane designations are as follows:

Lane	Sample	Incubation Time (min)	Lane	Sample	Amount (ng)
1	Molecular Weight Marker	-	1	Empty	-
2	0 min No Pepsin Control	0	2	Empty	-
3	0 min No Test Protein Control	0	3	Molecular Weight Marker	-
4	Pepsin Treated T0	0	4	Pepsin Treated T0	1
5	Pepsin Treated T1	0.25	5	Pepsin Treated T0	0.5
6	Pepsin Treated T2	0.5	6	Pepsin Treated T0	0.4
7	Pepsin Treated T3	1	7	Pepsin Treated T0	0.3
8	Pepsin Treated T4	2	8	Pepsin Treated T0	0.2
9	Pepsin Treated T5	4	9	Pepsin Treated T0	0.1
10	Pepsin Treated T6	8	10	Pepsin Treated T0	0.05
11	Pepsin Treated T7	15	11	Pepsin Treated T0	0.02
12	Pepsin Treated T8	30		Pepsin Treated T0	0.01
13	Pepsin Treated T9	60		Molecular Weight Marker	-
14	60 min Test Protein No Control	60	12	Empty	-
15	60 min No Pepsin Control	60	13	Empty	-

Degradation of CP4 EPSPS Protein by Pancreatin

The CP4 EPSPS protein degradation in pancreatin was assessed by Western blot analysis. The CP4 EPSPS protein was loaded with approximately 10 ng per lane of total protein (based on pre-reaction total protein concentrations) for each reaction time point examined. CP4 EPSPS protein standard was loaded at 5 ng and 10 ng on the same gel (Figure 61, lane 1 and 2). Greater than 50% of the CP4 EPSPS protein was degraded after a 10 min incubation in pancreatin at 37°C (Figure 61, lane 6) compared to the level detected at time zero (lane 5) and that of 5 ng load of CP4 EPSPS (lane1). No CP4 EPSPS protein was detected after incubation in pepsin for 100 min or longer (lanes 8-10 and 12). This result is similar to the results reported by Harrison et al. (1996).
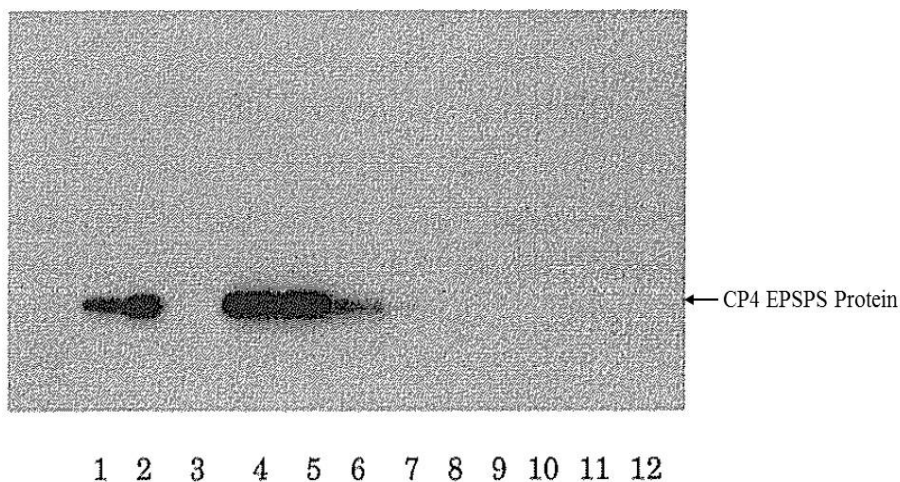
Figure 61.   Western Blot Analysis of the CP4 EPSPS Protein Degradation in Pancreatin

The CP4 EPSPS protein was added to pepsin to a final concentration of 50 μg/ml, and incubated at 37°C for the designated duration as indicated below.   The reactions were terminated by heating at ~100°C for 5 min before analysis by SDS-PAGE followed by Western.

Lane	Sample	Incubation Time (min)
1	CP4 EPSPS (5ng)	0
2	CP4 EPSPS (10ng)	0
3	Pancreatin only	0
4	CP4 EPSPS (10ng)	0
5	Pancreatin Treated T1 (10ng)	0
6	Pancreatin Treated T2 (10ng)	10
7	Pancreatin Treated T3 (10ng)	32
8	Pancreatin Treated T4 (10ng)	100
9	Pancreatin Treated T5 (10ng)	270
10	Pancreatin Treated T6 (10ng)	1181
11	Pancreatin only	1171
12	CP4 EPSPS (10ng) + Pancreatin	1160

Digestive Fate of the CP4 EPSPS Protein – Conclusions

Experiments designed to test the digestibility of the CP4 EPSPS protein by pepsin were performed. Results indicate that the CP4 EPSPS protein was rapidly digested when incubated in pepsin. At least 98% of the full length CP4 EPSPS protein was digested within 15 seconds in pepsin when analyzed using Colloidal Brilliant Blue G stained SDS polyacrylamide gels. At least 95% of the CP4 EPSPS protein was digested within 15 seconds in pepsin when evaluated using Western blot analysis. No proteolytic fragments were observed for samples evaluated using Western blot analysis. The CP4 EPSPS protein was also rapidly digested when incubated in pancreatin. Greater than 50% of the CP4 EPSPS protein was digested within 10 minutes in pancreatin when evaluated using Western blot analysis.

Results from these experiments show that the CP4 EPSPS protein is rapidly degraded by pepsin and pancreatin. Rapid degradation of the CP4 EPSPS protein in the presence of pepsin and pancreatin supports the conclusion that the CP4 EPSPS protein is highly unlikely to pose a safety concern to human and animal health

B4(b)(ii)   Heat stability of the purified MON 87429 DMO, PAT (*pat*) , FT_T and CP4 EPSPS proteins

Heat Susceptibility of the Purified MON 87429 DMO Protein

For details, please also refer to ▮▮▮▮▮▮ 2018 (MSL0029818).

Temperature can have a profound effect on the structure and function of proteins. Heat treatment is widely used in the preparation of foods derived from maize grain (Hammond and Jez, 2011). It is reasonable that such processing will have an effect on the functional activity and structure of DMO protein when consumed in different food products derived from MON 87429, thus reducing any potential safety concerns posed by the protein. Therefore, an assessment of the effect of heating was conducted as a surrogate for the conditions encountered during the preparation of foods from MON 87429 grain.

The effect of heat treatment on the activity of the DMO protein was evaluated using purified protein expressed in *E. coli*. Heat treated samples and an unheated control sample of DMO protein were analyzed: 1) using a functional assay to assess the impact of temperature on the enzymatic activity of the DMO protein; and 2) using SDS-PAGE to assess the impact of temperature on protein integrity.

Aliquots of DMO protein were heated to 25, 37, 55, 75 and 95 ºC for either 15 or 30 minutes, while a separate aliquot of DMO protein was maintained on ice for the duration of the heat treatments to serve as a temperature control. The effect of heat treatment on the activity of DMO was evaluated using a functional activity assay. The effect of heat treatment on the integrity of the DMO protein was evaluated using SDS-PAGE analysis of the heated and temperature control DMO protein samples.

Results of the functional activity assay for the DMO protein incubated for 15 and 30 minutes are listed in Table 40 and Table 41, respectively. The control sample had an activity of 325 and 480 nmol $\times$ minute^{-1} $\times$ mg^{-1} of DMO protein for the 15- and 30-minute incubation

periods, respectively, demonstrating that protein activity was maintained during incubation on ice.   Protein activity was retained when incubated for 15 and 30 minutes at a temperature of 25ºC (100% and 96% of activity compared to the control for 15 and 30 minutes, respectively).   Incubation for 15 and 30 minutes at 37ºC slightly reduced functional activity to 86% and 93% of the control DMO protein activity, respectively.   At temperatures of 55°C and above the functional activity of the DMO protein was reduced to 0% relative to the control DMO protein activity whether heated for 15 or 30 minutes.

The results of the SDS-PAGE analysis of the heat-treated samples incubated for 15- and 30-minutes are illustrated in Figure 62 and Figure 63, respectively.   The control sample loaded on each gel (Figure 62 and Figure 63, lane 2) showed equivalent ~38 kDa band intensity to the 100% reference standard (Figure 62 and Figure 63, lane 8), demonstrating that the DMO protein was stable on wet ice during the incubation period.   No apparent decrease in band intensity of the ~38 kDa DMO protein was observed when heated at temperatures of 25, 37, 55, 75 and 95ºC for 15 minutes (Figure 62, lanes 3-7) or 30 minutes (Figure 63, lanes 3-7). Higher molecular weight species were observed in the DMO protein heated to 75 and 95ºC for 15 and 30 minutes (Figure 62 and Figure 63, lane 7) which may be due to aggregation of the DMO protein when exposed to high temperatures.

These data demonstrate that the DMO protein behaves with a predictable tendency toward protein denaturation and loss of functional activity at elevated temperatures.   Heat treatment is widely used in the preparation of foods containing components derived from maize grain. Therefore, it is reasonable to conclude that DMO protein would not be consumed as an active protein in food products derived from MON 87429 due to standard processing practices that include heat treatment at or above 75 ºC for the majority of foods derived from processed maize (Hammond and Jez, 2011).

Table 40.   Dicamba Monooxygenase Activity Assay of Heat-Treated *E. coli*-produced DMO Protein after 15 Minutes

Treatment	Specific Activity (nmol × minute^{-1} × mg^{-1})[1]	Relative Activity (% of control sample)
Control Treatment (wet ice)	325	100%
25 ℃	324	100%
37 ℃	281	86%
55 ℃	0	0%
75 ℃	0	0%
95 ℃	0	0%

[1] Mean specific activity determined from n=3.
[2] DMO protein activity of control samples was assigned 100 % active.
[3] Relative Activity = [specific activity of sample/specific activity of control sample] x 100

Table 41.   Dicamba Monooxygenase Activity Assay of Heat-Treated *E. coli*-produced DMO Protein After 30 Minutes

Treatment	Specific Activity (nmol × minute^{-1} × mg^{-1})[1]	Relative Activity (% of control sample)
Control Treatment (wet ice)	480	100%
25 ℃	462	96%
37 ℃	446	93%
55 ℃	0	0%
75 ℃	0	0%
95 ℃	0	0%

[1] Mean specific activity determined from n=3.
[2] DMO protein activity of control samples was assigned 100 % active.
[3] Relative Activity = [specific activity of sample/specific activity of control sample] x 100

Figure 62.   SDS-PAGE of DMO Protein Demonstrating the Effect After 15 Minutes at Elevated Temperatures on Protein Structural Stability

Heat-treated samples of *E. coli*-produced DMO (3.0 µg total protein) separated on a Tris-glycine 4-20 % polyacrylamide gel under denaturing and reducing conditions.   The gel was stained with Brilliant Blue G Colloidal.   Approximate molecular weights (kDa) are shown on the left and correspond to molecular weight markers in lanes 1 and 10.

Lane	Description	Total Amount
1	Broad Range Molecular Weight Markers	5 µg
2	*E. coli*-produced DMO Protein Control	3.0 µg
3	*E. coli*-produced DMO Protein 25 ℃	3.0 µg
4	*E. coli*-produced DMO Protein 37 ℃	3.0 µg
5	*E. coli*-produced DMO Protein 55 ℃	3.0 µg
6	*E. coli*-produced DMO Protein 75 ℃	3.0 µg
7	*E. coli*-produced DMO Protein 95 ℃	3.0 µg
8	*E. coli*-produced DMO Protein Reference 100 % Equivalence	3.0 µg
9	*E. coli*-produced DMO Protein Reference 10 % Equivalence	0.3 µg
10	Broad Range Molecular Weight Markers	5 µg

Figure 63.   SDS-PAGE of DMO Protein Demonstrating the Effect After 30 Minutes at Elevated Temperatures on Protein Structural Stability

Heat-treated samples of *E. coli*-produced DMO (3.0 µg total protein) separated on a Tris-glycine 4-20 % polyacrylamide gel under denaturing and reducing conditions.   The gel was stained with Brilliant Blue G Colloidal.   Approximate molecular weights (kDa) are shown on the left and correspond to molecular weight markers in lanes 1 and 10.

Lane	Description	Total Amount
1	Broad Range Molecular Weight Markers	5 µg
2	*E. coli*-produced DMO Protein Control	3.0 µg
3	*E. coli*-produced DMO Protein 25 ºC	3.0 µg
4	*E. coli*-produced DMO Protein 37 ºC	3.0 µg
5	*E. coli*-produced DMO Protein 55 ºC	3.0 µg
6	*E. coli*-produced DMO Protein 75 ºC	3.0 µg
7	*E. coli*-produced DMO Protein 95 ºC	3.0 µg
8	*E. coli*-produced DMO Protein Reference 100 % Equivalence	3.0 µg
9	*E. coli*-produced DMO Protein Reference 10 % Equivalence	0.3 µg
10	Broad Range Molecular Weight Markers	5 µg

Heat Susceptibility of the Purified PAT (*pat*) Protein

For details, please also refer to ▮▮▮▮ 2019 (SCR-2019-0110).

Temperature can have a profound effect on the structure and function of proteins. Heat treatment is widely used in the preparation of foods derived from maize grain (Hammond and Jez, 2011). It is reasonable that such processing will have an effect on the functional activity and structure of PAT (*pat*) protein when consumed in different food products derived from MON 87429, thus reducing any potential safety concerns posed by the protein. Therefore, an assessment of the effect of heating was conducted as a surrogate for the conditions encountered during the preparation of foods from MON 87429 grain.

The effect of heat treatment on the activity of MON 87429-produced PAT (*pat*) protein was evaluated using the *E. coli*-produced PAT (*pat*) protein. Heat-treated samples and an unheated control sample of *E. coli*-produced PAT (*pat*) protein were analyzed: 1) using a functional assay to assess the impact of temperature on the enzymatic activity of PAT (*pat*) protein; and 2) using SDS-PAGE to assess the impact of temperature on protein integrity.

Aliquots of *E. coli*-produced PAT (*pat*) protein were heated to 25, 37, 55, 75, and 95 °C for either 15 or 30 minutes, while a separate aliquot of *E. coli*-produced PAT (*pat*) protein was maintained on ice for the duration of the heat treatments to serve as a temperature control. The effect of heat treatment on the activity of PAT (*pat*) protein was evaluated using a functional activity assay. The effect of heat treatment on the integrity of the PAT (*pat*) protein was evaluated using SDS-PAGE analysis of the heated and temperature control PAT (*pat*) protein samples.

The effects of heating on the functional activity of *E. coli*-produced PAT (*pat*) are presented in Table 42 and Table 43. The functional activity of PAT (*pat*) protein was unaffected at 25 and 37 ℃ for 15 and 30 minutes. The functional activity of the PAT (*pat*) protein was reduced by approximately 90% or greater relative to the activity of control PAT protein whether heated at 55°C and above for 15 or 30 min. These results suggest that temperature has a considerable effect on the functional activity of PAT (*pat*) protein.

Analysis by SDS-PAGE stained with Brilliant Blue G-Colloidal demonstrated that the PAT (*pat*) control treatment and reference standard contain a major band at ~25 kDa, corresponding to the PAT (*pat*) protein (Figure 64 and Figure 65, Lanes 2 and 8). No apparent decrease in the intensity of this band was observed in heat-treated PAT (*pat*) protein at 25, 37, 55, 75 and 95 °C for 15 minutes (Figure 64, Lanes 3-7) or 30 minutes (Figure 65, Lanes 3-7). However, PAT (*pat*) protein heated to 95℃ for 15 and 30 minutes (Figure 64 and Figure 65, Lane 7) showed some appearance of higher molecular weight species, which may be due to slight aggregation of the PAT (*pat*) protein when exposed to high temperatures.

These data demonstrate that PAT (*pat*) protein remains intact, but is deactivated at 55 ℃ and above. This is comparable with what has been previously published on the safety assessment of PAT (*pat*) protein (Hérouet *et al.*, 2005). Therefore, it is reasonable to conclude that PAT (*pat*) protein would not be consumed as an active protein in food or feed products due to standard processing practices that include heat treatment.

Table 42. Functional Activity of PAT (*pat*) Protein after 15 Minutes at Elevated Temperatures

Temperature	Specific Activity (μmol $\times$ minute^{-1} $\times$ mg^{-1}) [1]	Relative Activity (% of control sample) [2,3]
0 ℃ (control)	24.5	100 %
25 ℃	26.7	109 %
37 ℃	26.9	110 %
55 ℃	2.8	11 %
75 ℃	0.9	4 %
95 ℃	1.1	4 %

[1] Mean specific activity determined from n=3.
[2] PAT (*pat*) protein activity of control samples was assigned 100 % active.
[3] Relative Activity = [specific activity of sample/specific activity of control sample] $\times$ 100
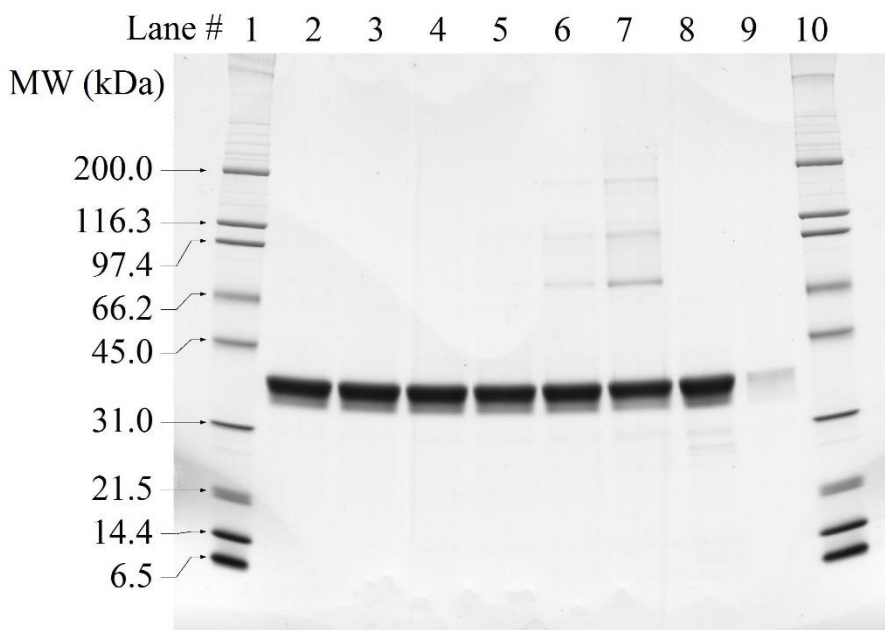
Table 43. Functional Activity of PAT (*pat*) Protein after 30 Minutes at Elevated Temperatures

Temperature	Specific Activity (μmol $\times$ minute^{-1} $\times$ mg^{-1}) [1]	Relative Activity (% of control sample) [2,3]
0 ℃ (control)	24.5	100 %
25 ℃	31.2	127 %
37 ℃	29.8	122 %
55 ℃	1.0	4 %
75 ℃	1.1	4 %
95 ℃	1.3	5 %

[1] Mean specific activity determined from n=3.
[2] PAT (*pat*)   protein activity of control sample was assigned 100 % active.
[3] Relative Activity = [specific activity of sample/specific activity of control sample] $\times$ 100

Figure 64.   SDS-PAGE of *E. coli*-Produced PAT (*pat*) Protein Following Heat Treatment for 15 Minutes

Heat treated samples of *E. coli*-produced PAT (*pat*) (3.0 µg total protein) separated on a Tris-glycine 4-20 % polyacrylamide gel under denaturing and reducing conditions.   The gel was stained with Brilliant Blue G-Colloidal.   Approximate molecular weights (kDa) are shown on the left and correspond to molecular weight markers in lanes 1 and 10.

Lane	Description	Total Amount
1	Broad Range Molecular Weight Markers	4.5
2	*E. coli*-produced PAT *(pat)* Protein Control	3.0
3	*E. coli*-produced PAT *(pat)* Protein 25 ℃	3.0
4	*E. coli*-produced PAT *(pat)* Protein 37 ℃	3.0
5	*E. coli*-produced PAT *(pat)* Protein 55 ℃	3.0
6	*E. coli*-produced PAT *(pat)* Protein 75 ℃	3.0
7	*E. coli*-produced PAT *(pat)* Protein 95 ℃	3.0
8	*E. coli*-produced PAT *(pat)* Protein Reference 100 % Equivalence	3.0
9	*E. coli*-produced PAT *(pat)* Protein Reference 10 % Equivalence	0.3
10	Broad Range Molecular Weight Markers	4.5

Figure 65.   SDS-PAGE of *E. coli*-Produced PAT (*pat*) Protein Following Heat Treatment for 30 Minutes

Heat treated samples of *E. coli*-produced PAT (*pat*) (3.0 µg total protein) separated on a Tris-glycine 4-20 % polyacrylamide gel under denaturing and reducing conditions. The gel was stained with Brilliant Blue G-Colloidal.   Approximate molecular weights (kDa) are shown on the left and correspond to molecular weight markers in lanes 1 and 10.

Lane	Description	Total Amount
1	Broad Range Molecular Weight Markers	4.5
2	*E. coli*-produced PAT (*pat*) Protein Control	3.0
3	*E. coli*-produced PAT (*pat*) Protein 25 ℃	3.0
4	*E. coli*-produced PAT (*pat*) Protein 37 ℃	3.0
5	*E. coli*-produced PAT (*pat*) Protein 55 ℃	3.0
6	*E. coli*-produced PAT (*pat*) Protein 75 ℃	3.0
7	*E. coli*-produced PAT (*pat*) Protein 95 ℃	3.0
8	*E. coli*-produced PAT (*pat*) Protein Reference 100 % Equivalence	3.0
9	*E. coli*-produced PAT (*pat*) Protein Reference 10 % Equivalence	0.3
10	Broad Range Molecular Weight Markers	4.5

Heat Stability of FT_T Protein

For details, please also refer to ▮▮▮▮▮ 2018 (MSL0029688).

Temperature can have a profound effect on the structure and function of proteins. Heat treatment is widely used in the preparation of foods derived from maize grain (Hammond and Jez, 2011). It is reasonable that such processing will have an effect on the functional activity and structure of FT_T protein when consumed in different food products derived from MON 87429, thus reducing any potential safety concerns posed by the protein. Therefore, an assessment of the effect of heating was conducted as a surrogate for the conditions encountered during the preparation of foods from MON 87429 grain.

The effect of heat treatment on the activity of the FT_T protein was evaluated using purified protein. Heat treated samples and an unheated control sample of FT_T protein were analyzed: 1) using a functional assay to assess the impact of temperature on the enzymatic activity of the FT_T protein; and 2) using SDS-PAGE to assess the impact of temperature on protein integrity.

Aliquots of FT_T protein were heated to 25, 37, 55, 75 and 95 ℃ for either 15 or 30 minutes, while a separate aliquot of FT_T protein was maintained on ice for the duration of the heat treatments to serve as a temperature control. The effect of heat treatment on the activity of FT_T was evaluated using a functional activity assay. The effect of heat treatment on the integrity of the FT_T protein was evaluated using SDS-PAGE analysis of the heated and temperature control FT_T protein samples.

The effects of heating on the functional activity of FT_T protein are presented in Table 44 and Table 45. The FT_T protein incubated at 25 ℃ and at 37 ℃ for 15 and 30 minutes was shown to retain functional activity when heated to a temperature of 55 °C for 15 and 30 minutes, the functional activity is reduced to 58 and 35 percent; respectively. At temperatures of 75 °C or greater for 15 and 30 minutes, the functional activity of the FT_T protein was reduced to ≤1 percent relative to the control sample. These results suggest that temperature has a considerable effect on the activity of FT_T.

Analysis by SDS-PAGE stained with Brilliant Blue G Colloidal demonstrated that heat treatment to temperatures of 25, 37, 55, 75 and 95 ℃ for 15 (Figure 66) or 30 minutes (Figure 67) did not result in observable changes in the FT_T protein band intensity. There was a slight visible appearance of higher molecular weight species at heat treatments of 95 ℃ for 15 and 30 minutes, which may be due to slight aggregation of the protein when exposed to high temperatures.

These data demonstrate that the FT_T protein remains largely intact but behaves with a predictable tendency toward protein denaturation and loss of functional activity at elevated temperatures. Heat treatment is widely used in the preparation of foods containing components derived from maize grain. Therefore, it is reasonable to conclude that FT_T protein would not be consumed as an active protein in food products derived from MON 87429 due to standard processing practices that include heat treatment at or above 75 ℃ for the majority of foods derived from processed maize (Hammond and Jez, 2011).

Table 44. Functional Activity Assay of Heat Treated FT_T Protein After 15 Minutes at Elevated Temperatures

Temperature	Specific Activity (nmol $\times$ minute^{-1} $\times$ mg^{-1}) [1]	Relative Activity (% of control sample) [2,3]
0 ℃ (control)	598	100 %
25 ℃	543	91 %
37 ℃	605	101 %
55 ℃	344	58 %
75 ℃	3	<1 %
95 ℃	5	<1 %

[1]Mean specific activity determined from n=3.
[2]FT_T protein activity of control sample was assigned 100 % activity.
[3]Relative Activity = [specific activity of sample/specific activity of control sample] x 100

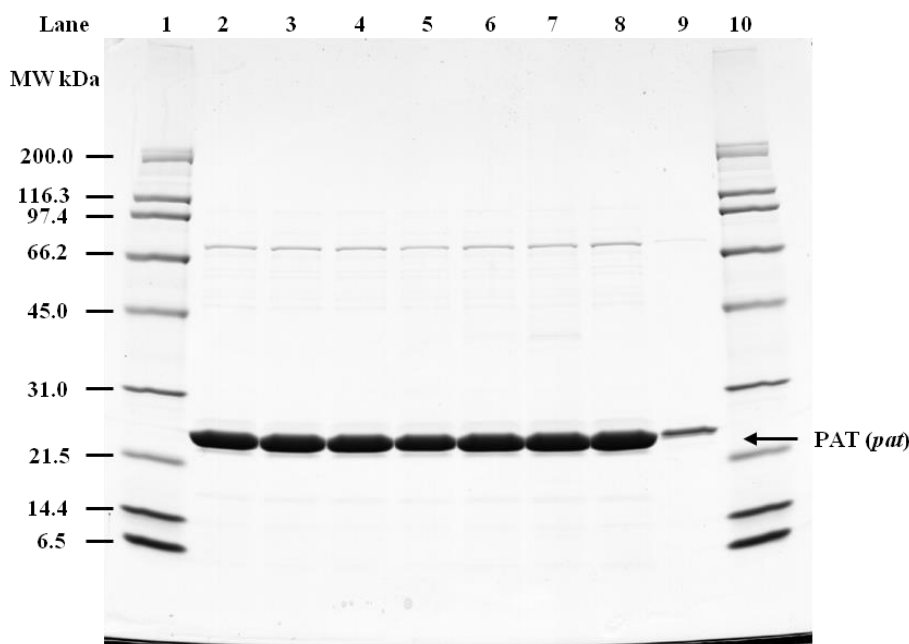**Table 45. Functional Activity Assay of Heat Treated FT_T Protein After 30 Minutes at Elevated Temperatures**

Temperature	Specific Activity (nmol $\times$ minute^{-1} $\times$ mg^{-1}) [1]	Relative Activity (% of control sample) [2,3]
0 ℃ (control)	598	100 %
25 ℃	636	106 %
37 ℃	612	102 %
55 ℃	212	35 %
75 ℃	5	<1 %
95 ℃	7	1 %

[1]Mean specific activity determined from n=3.
[2] FT_T   protein activity of control sample was assigned 100 % activity.
[3]Relative Activity = [specific activity of sample/specific activity of control sample] x 100

Figure 66.   SDS-PAGE of FT_T Protein Demonstrating the Effect After 15 Minutes at Elevated Temperatures on Protein Structural Stability

Heat treated samples of FT_T (3.0 µg total protein) separated on a Tris-glycine 4-20 % polyacrylamide gel under denaturing and reducing conditions.   The gel was stained with Brilliant Blue G Colloidal.   Approximate molecular weights (kDa) are shown on the left and correspond to molecular weight markers in lanes 1 and 10.

Lane	Description	Total Amount
1	Broad Range Molecular Weight Markers	5.0 µg
2	*E. coli*-produced FT_T Protein Control	3.0 µg
3	*E. coli*-produced FT_T Protein 25 ℃	3.0 µg
4	*E. coli*-produced FT_T Protein 37 ℃	3.0 µg
5	*E. coli*-produced FT_T Protein 55 ℃	3.0 µg
6	*E. coli*-produced FT_T Protein 75 ℃	3.0 µg
7	*E. coli*-produced FT_T Protein 95 ℃	3.0 µg
8	*E. coli*-produced FT_T Protein Reference 100 % Equivalence	3.0 µg
9	*E. coli*-produced FT_T Protein Reference 10 % Equivalence	0.3 µg
10	Broad Range Molecular Weight Markers	5.0 µg

Figure 67. SDS-PAGE of FT_T Protein Demonstrating the Effect After 30 Minutes at Elevated Temperatures on Protein Structural Stability

Heat treated samples of FT_T (3.0 µg total protein) separated on a Tris-glycine 4-20 % polyacrylamide gel under denaturing and reducing conditions. The gel was stained with Brilliant Blue G Colloidal. Approximate molecular weights (kDa) are shown on the left and correspond to molecular weight markers in lanes 1 and 10.

Lane	Description	Total Amount
1	Broad Range Molecular Weight Markers	5.0 µg
2	*E. coli*-produced FT_T Protein Control	3.0 µg
3	*E. coli*-produced FT_T Protein 25 °C	3.0 µg
4	*E. coli*-produced FT_T Protein 37 °C	3.0 µg
5	*E. coli*-produced FT_T Protein 55 °C	3.0 µg
6	*E. coli*-produced FT_T Protein 75 °C	3.0 µg
7	*E. coli*-produced FT_T Protein 95 °C	3.0 µg
8	*E. coli*-produced FT_T Protein Reference 100 % Equivalence	3.0 µg
9	*E. coli*-produced FT_T Protein Reference 10 % Equivalence	0.3 µg
10	Broad Range Molecular Weight Markers	5.0 µg

Heat Susceptibility of the CP4 EPSPS Protein

For details, please also refer to ████████, 2011 (MSL0023307).

Temperature can have a profound effect on the structure and function of proteins.   Heat treatment is widely used in the preparation of foods derived from maize grain (Hammond and Jez, 2011).   It is reasonable that such processing will have an effect on the functional activity and structure of CP4 EPSPS protein when consumed in different food products derived from MON 87429, thus reducing any potential safety concerns posed by the protein. Therefore, an assessment of the effect of heating was conducted as a surrogate for the conditions encountered during the preparation of foods from MON 87429 grain.

The effect of heat treatment on the activity of MON 87429-produced CP4 EPSPS protein was evaluated using the *E. coli*-produced CP4 EPSPS protein.   Heat-treated samples and an unheated control sample of *E. coli*-produced CP4 EPSPS protein were analyzed: 1) using a functional assay to assess the impact of temperature on the enzymatic activity of CP4 EPSPS protein; and 2) using SDS-PAGE to assess the impact of temperature on protein integrity.

Aliquots of the *E. coli*-produced CP4 EPSPS protein were heated to 25, 37, 55, 75, and 95 °C for either 15 or 30 minutes, while a single aliquot of the control substance was maintained on wet ice for the duration of the heat treatments.   Heated CP4 EPSPS protein and unheated temperature control substance were analyzed by a CP4 EPSPS activity assay to assess the impact of temperature on the functional activity of CP4 EPSPS protein. Additionally, the protein resulting from each temperature treatment was analyzed by SDS-PAGE to assess CP4 EPSPS degradation.

The effects of heating on the functional activity of *E. coli*-produced CP4 EPSPS protein are presented in Table 46 and Table 47.   When heated at a temperature of 25 ℃, 37 ℃ and 55 ℃ with an incubation time of 15 minutes, a small reduction in CP4 EPSPS activity was observed to 81%, 84 %, and 70% of control respectively. The test substance heated for 30 minutes showed no negative change in CP4 EPSPS activity at 25 ℃ and a small reduction in activity to 88% of control at 37℃.   The test substance heated to 55 ℃ demonstrated a reduction in CP4 EPSPS activity with 25 % activity remaining relative to the control substance after the 30 minute incubation. The level of CP4 EPSPS activity following incubation at temperatures of 75 and 95 ℃ was below the limit of detection for incubations at both time points.

Analysis by SDS-PAGE stained with Brilliant Blue G Colloidal dye (Figure 68 and Figure 69) demonstrated that the reference standard and control substance contain one major band with an apparent molecular weight of approximately 43.8 kDa corresponding to the CP4 EPSPS protein.   Results of the SDS-PAGE data for the heat treatment of the test substances incubated for 15 minutes and 30 minutes are illustrated in Figure 68 and Figure 69, respectively.   The control substance loaded on each respective gel (Figure 68 lane 2 and Figure 69 lane 2) showed equivalent band intensity at 43.8 kDa to the 100 % reference standard (Figure 68 lane 8 and Figure 69 lane 8); demonstrating that the CP4 EPSPS protein was stable on wet ice during the incubation period.   No apparent decrease in band intensity of the 43.8 kDa CP4 EPSPS protein band was observed in the test substance when heated at all temperatures for 15 minutes (Figure 68 lanes 3-7) or 30 minutes (Figure 69 lanes 3-7).

Table 46.   Activity of CP4 EPSPS After 15 Minutes at Elevated Temperatures

Temperature	Specific Activity Units/mg CP4 EPSPS[1]	Relative activity[2]
0 ℃ (control substance)	6.03±0.29	100%
25 ℃	4.88±0.24	81%
37 ℃	5.08±0.33	84%
55 ℃	4.22±0.12	70%
75 ℃	Below LOD[3]	<3%
95 ℃	Below LOD[3]	<3%

[1] Mean specific activity determined from n=2.

[2] CP4 EPSPS activity of control substance was assigned 100 % active.

% CP4 EPSPS activity remaining = [specific activity of sample/specific activity of control substance] x 100

[3] LOD is defined as the value that is three times the assay blank standard deviation plus the mean of the assay blank.

Table 47.   Activity of CP4 EPSPS After 30 Minutes at Elevated Temperatures

Temperature	Specific Activity Units/mg CP4 EPSPS	Relative activity[2]
0 ℃ (control substance)	2.8 ± 0.26	100%
25 ℃	3.1 ± 0.23	110%
37 ℃	2.5 ± 0.05	88%
55 ℃	0.70 ± 0.09	25%
75 ℃	Below LOD[3]	<8%
95 ℃	Below LOD[3]	<8%

[1] Mean specific activity determined from n=2

[2] CP4 EPSPS activity of control substance was assigned 100 % active.

% CP4 EPSPS activity remaining = [specific activity of sample/specific activity of control substance] x 100

[3] LOD is defined as the value that is three times the assay blank standard deviation plus the mean of the assay blank.
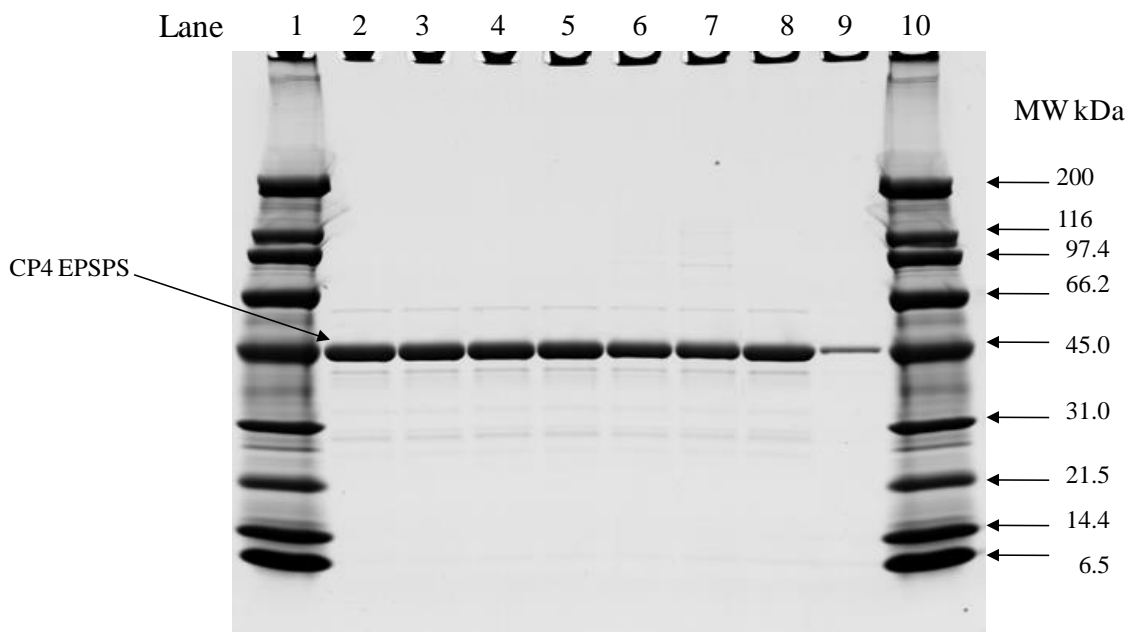
Figure 68. SDS-PAGE of CP4 EPSPS Protein Following Heat Treatment for 15 Minutes

Heated-treated samples of CP4 EPSPS (3.2 µg total protein) separated on a Tris-glycine 4-20% polyacrylamide gel under denaturing and reducing conditions. Gels were stained with Brilliant Blue G Colloidal. Approximate molecular weights (kDa) are shown on the right and correspond to molecular weight markers in lanes 1 and 10.

Lane	Description	Total Amount	
1	Broad Range Molecular Weight Markers	4.5	µ g
2	*E. coli*-produced CP4 EPSPS Protein Control	3.2	µ g
3	*E. coli*-produced CP4 EPSPS Protein 25 ºC	3.2	µ g
4	*E. coli*-produced CP4 EPSPS Protein 37 ºC	3.2	µ g
5	*E. coli*-produced CP4 EPSPS Protein 55 ºC	3.2	µ g
6	*E. coli*-produced CP4 EPSPS Protein 75 ºC	3.2	µ g
7	*E. coli*-produced CP4 EPSPS Protein 95 ºC	3.2	µ g
8	*E. coli*-produced CP4 EPSPS Protein Reference 100 % Equivalence	3.2	µ g
9	*E. coli*-produced CP4 EPSPS Protein Reference 10 % Equivalence	0.32	µ g
10	Broad Range Molecular Weight Markers	4.5	µ g

Figure 69. **SDS-PAGE of CP4 EPSPS Protein Following Heat Treatment for 30 Minutes**

Heated-treated samples of CP4 EPSPS (3.2 µ g total protein) separated on a Tris-glycine 4-20% polyacrylamide gel under denaturing and reducing conditions. Gels were stained with Brilliant Blue G Colloidal. Approximate molecular weights (kDa) are shown on the right and correspond to molecular weight markers in lanes 1 and 10.

Lane	Description	Total Amount	
1	Broad Range Molecular Weight Markers	4.5	µ g
2	*E. coli*-produced CP4 EPSPS Protein Control	3.2	µ g
3	*E. coli*-produced CP4 EPSPS Protein 25 ℃	3.2	µ g
4	*E. coli*-produced CP4 EPSPS Protein 37 ℃	3.2	µ g
5	*E. coli*-produced CP4 EPSPS Protein 55 ℃	3.2	µ g
6	*E. coli*-produced CP4 EPSPS Protein 75 ℃	3.2	µ g
7	*E. coli*-produced CP4 EPSPS Protein 95 ℃	3.2	µ g
8	*E. coli*-produced CP4 EPSPS Protein Reference 100 % Equivalence	3.2	µ g
9	*E. coli*-produced CP4 EPSPS Protein Reference 10 % Equivalence	0.32	µ g
10	Broad Range Molecular Weight Markers	4.5	µ g

B4(b)(iii)   Degradation and heat susceptibility of the MON 87429 DMO, PAT (*pat*), FT_T and CP4 EPSPS proteins - Conclusions

The susceptibility of a protein to heat or its degradation in the presence of pepsin and pancreatin is a factor in the assessment of its potential toxicity.   The degradation of MON 87429 DMO, PAT (*pat*), FT_T and CP4 EPSPS proteins were evaluated by incubation with solutions containing pepsin and pancreatin, and the results show that MON 87429 DMO, PAT (*pat*), FT_T and CP4 EPSPS proteins were readily degraded (Section B4(b)(i)). Exposure to heat during food processing or cooking, and to digestive fluids is likely to have a profound effect on the structure and function of proteins.

The effect of heat treatment on the activity of MON 87429 DMO, PAT (*pat*), FT_T and CP4 EPSPS proteins was evaluated using functional assays to assess the impact of temperature on enzymatic activity, and using SDS-PAGE to assess the impact of temperature on protein integrity.   The results show that MON 87429 DMO protein was completely deactivated by heating at 55 ºC or higher for 15 min or more, PAT (*pat*) protein was substantially deactivated by heating at 75 ºC or above for 15 minutes and at 55°C or above for 30 minutes, FT_T protein was substantially deactivated by heating at 75 ºC or above for 15 minutes and at 55°C or above for 30 minutes, and CP4 EPSPS heated to 55 ºC demonstrated a substantial reduction in activity after the 30 minute incubation and the level of CP4 EPSPS activity following incubation at temperatures of 75 and 95 ºC was below the limit of detection for incubations at both time points (Section B4(b)(ii)).   Therefore, it is anticipated that exposure to functionally active MON 87429 DMO, PAT (*pat*), FT_T or CP4 EPSPS protein from the consumption of MON 87429 or foods derived from MON 87429 is unlikely.

B4(c)   Acute oral toxicity study with the DMO, PAT(*pat*), FT_T and CP4 EPSPS proteins

For details, please refer to ████2018 (MSL0029551), ██████2014 (SA13205), ███████2018 (MSL0029801), ██████ 1993 (MSL13077).

Most known protein toxins act through acute mechanisms to exert toxicity (Hammond and Fuchs, 1998; Pariza and Johnson, 2001; Sjoblad *et al.*, 1992).   The primary exceptions to this rule consist of certain anti-nutritional proteins such as lectins and protease inhibitors, which manifest toxicity in a short term (few weeks) feeding study (Liener, 1994).   The amino acid sequences of the DMO, PAT (*pat*), FT_T and CP4 EPSPS proteins produced in MON 87429 are not similar to any of these anti-nutritional proteins or to any other known protein toxin.   In addition, these proteins are heat labile and readily degraded by gastrointestinal enzymes.   Based on this weight of the evidence and the non-toxic mode of action for these proteins, no further assessment of potential toxicity for these proteins is necessary in accordance with the tiered protein safety assessment paradigm (Codex Alimentarius, 2009; Delaney *et al.*, 2008).   Despite this weight of evidence, acute oral mouse toxicity studies were conducted as confirmatory evidence to support the safety DMO, PAT (*pat*), FT_T and CP4 EPSPS proteins.

E. coli-produced MON 87429 DMO protein was administered by oral gavage   to 10 male and 10 female CD-1 mice at a dose of 1000 mg/kg body wt (bw).   Additional groups of

mice were administered a comparable volume of the buffer or a comparable amount (mg/kg bw) of bovine serum albumin (BSA) to serve as vehicle or protein controls, respectively. Following dosing, all mice were observed daily for mortality or signs of toxicity. Body weights and food consumption were measured weekly. All animals were sacrificed on day 14 and subjected to a gross necropsy. There were no treatment-related effects on survival, clinical observations, body weight gain, food consumption or gross pathology. Therefore, under the conditions of this study, the No Observable Adverse Effect Level (NOAEL) for MON 87429 DMO was considered to be 1000 mg/kg bw.

E. coli-produced PAT (*pat*) protein was administered by oral gavage (as two doses approximately three hours apart) to 10 male and 10 female C57BL/6J mice at a dose of 2000 mg/kg bw. Additionally, 10 male and 10 female mice were administered an equivalent volume of vehicle. Following dosing, all mice were observed daily for mortality or signs of toxicity. Body weights and food consumption were measured weekly. All animals were sacrificed on day 15 and subjected to a gross necropsy. There were no treatment-related effects on survival, clinical observations, body weight gain, food consumption or gross pathology. Therefore, under the conditions of this study, the NOAEL for PAT (*pat*) was considered to be 2000 mg/kg bw.

E. coli-produced FT_T protein was administered by oral gavage to 10 male and 10 female CD-1 mice at a dose of 2000 mg/kg bw. Additional groups of mice were administered comparable volume of the buffer or a comparable amount (mg/kg bw) of bovine serum albumin (BSA) to serve as vehicle or protein controls, respectively. Following dosing, all mice were observed daily for mortality or signs of toxicity. Body weights and food consumption were measured weekly. All animals were sacrificed on day 14 and subjected to a gross necropsy. There were no treatment-related effects on survival, clinical observations, body weight gain, food consumption or gross pathology. Therefore, under the conditions of this study, the NOAEL for FT_T was considered to be 2000 mg/kg bw.

E. coli-produced CP4 EPSPS protein was administered as a single dose by oral gavage to three groups of 10 male and 10 female CD-1 mice at dose levels up to 572 mg/kg bw (Harrison *et al.*, 1996). Additional groups of mice were administered comparable volume of the buffer or a comparable amount (mg/kg bw) of bovine serum albumin (BSA) to serve as vehicle or protein controls, respectively. Following dosing, all mice were observed twice daily for mortality or signs of toxicity. Food consumption was measured daily. Body weights were measured prior to dosing and at study day 7. All animals were sacrificed on day 8 or 9 and subjected to a gross necropsy. There were no treatment-related effects on survival, clinical observations, body weight gain, food consumption or gross pathology. Therefore, under the conditions of this study, the NOAEL for CP4 EPSPS was considered to be 572 mg/kg bw. This acute toxicology study had been reviewed and has completed a consultation with FSANZ under previously submitted application A338, A355, A362, A363, A416, A548, A553, A592, A1049, A1066, A1071, and A1097.

B5   Assessment of Potential Allergenicity

History of safe use of the introduced protein is a key consideration in assessing the potential for allergenicity and toxicity and overall assessment of dietary safety. The history of safe use of DMO, PAT (*pat*), FT_T and CP4 EPSPS proteins have been previously addressed in Section B3(f).

Additionally, following the guidelines adopted by the Codex Alimentarius Commission, an assessment of potential allergenicity of introduced proteins has been conducted by comparing the characteristics of the introduced protein to characteristics of known allergens (Codex Alimentarius, 2009).   A protein is not likely to be associated with allergenicity if: 1) the protein is from a nonallergenic source, 2) the protein represents only a very small portion of the total plant protein, 3) the protein does not share structural similarities to known allergens based on the amino acid sequence, 4) the protein is rapidly degraded in mammalian gastrointestinal systems, and 5) the protein is not stable to heat treatment.   The DMO, PAT (*pat*), FT_T and CP4 EPSPS proteins in MON 87429 have been assessed for their potential allergenicity according to these safety assessment guidelines.

The assessment of the potential toxicity of an introduced protein is based on comparing the biochemical characteristics of the introduced protein to characteristics of known toxins. These biochemical characteristics are assessed by determining: 1) if the protein has structural similarity to known toxins or other biologically-active proteins that could cause adverse effects in humans or animals; 2) if the protein is rapidly degraded by pepsin and pancreatin; 3) if the protein is stable to heat treatment; 4) if the protein exerts any acute toxic effects in mammals; and 5) the anticipated exposure levels for humans and animals.   The DMO, PAT (*pat*), FT_T and CP4 EPSPS proteins in MON 87429 have been assessed for their potential toxicity based on these criteria.

B5(a)   Source of introduced protein

B5(a)(i) DMO protein

As described in Section A2, the *dmo* gene is derived from the bacterium *Stenotrophomonas maltophilia* strain DI-6, isolated from soil at a dicamba manufacturing plant (Krueger *et al.*, 1989).   *S. maltophilia* is ubiquitously present in the environment (Mukherjee and Roy, 2016), including in water and dairy products (An and Berg, 2018; Okuno *et al.*, 2018; Todaro *et al.*, 2011). These bacteria have been used as effective biocontrol agents in plant and animal pathogenesis (Mukherjee and Roy, 2016), and have antibacterial activity against both gram-positive and gram-negative bacteria (Dong *et al.*, 2015).   These bacteria can form biofilms that become resistant to antibiotics (Berg and Martinez, 2015; Brooke *et al.*, 2017).   Several alternative compounds have been shown to be effective against *S. maltophilia* antibiotic resistance, such as immunoglobulin, epigallocatechine-3-gallate from green tea, and essential oils (Mukherjee and Roy, 2016).   *S. maltophilia* has been found in healthy individuals without any hazard to human health (Heller *et al.*, 2016; Lira *et al.*, 2017).   The opportunistic pathogenicity of *S. maltophilia* is mainly associated with hosts with compromised immune systems rather than with any specific virulence genes of these bacteria. Thus, documented

occurrences of *S. maltophilia* infections have been limited to immune-compromised individuals in hospital settings (Lira *et al.*, 2017).

Other than the potential to become an opportunist pathogen in immune-compromised hosts, *S. maltophilia* is not known for human or animal pathogenicity. *S. maltophilia* history of safe use has been extensively reviewed during the evaluation of several dicamba-tolerant events with no safety or allergenicity issues identified by FDA FSANZ (e.g. MON 87419 maize in 2016 (A1118), MON 88701 cotton in 2013 (A1080) and MON 87708 soybean in 2011 (A1063)).

B5(a)(ii) PAT (*pat*) protein

As described in Section A2, the *pat* gene is derived from the bacterium *Streptomyces viridochromogenes* (Wohlleben *et al.*, 1988). *Streptomyces* species are widespread in the environment and present no known allergenic or toxicity issues (Kämpfer, 2006; Kutzner, 1981), though human exposure is quite common (Goodfellow and Williams, 1983). *S. viridochromogenes* is not considered pathogenic to plants, humans or other animals (Cross, 1989; Goodfellow and Williams, 1983; Locci, 1989). *S. viridochromogenes* is widespread in the environment and the history of safe use is discussed in Hérouet *et al.* (2005) and this organism has been extensively reviewed during the evaluation of several glufosinate-tolerant events (e.g., T25, TC1507, A5547-127, DAS-59122-7 and MON 87419) with no safety or allergenicity issues identified by FDA or other regulatory agencies.

B5(a)(iii) FT_T protein

As described in Section A2, MON 87429 contains the *ft_t* gene, a modified version of the *Rdpa* gene from *Sphingobium herbicidovorans*, that expresses the FT_T protein. FT_T is a modified version of the R-2,4-dichlorophenoxypropionate dioxygenase (RdpA) protein (Müller *et al.*, 2006). *S. herbicidovorans* is a common gram-negative, rod-shaped, non-motile, non-spore-forming soil bacterium (Takeuchi *et al.*, 2001; Zipper *et al.*, 1996), which is strictly aerobic and chemo-organotrophic, and not known to be associated with human disease.

Members of the genus *Sphingobium* have been isolated from a wide variety of habitats including soil and freshwater (Chaudhary *et al.*, 2017). *Sphingobium* species have also been isolated from food products such as corn (Rijavec *et al.*, 2007), papaya (Thomas *et al.*, 2007) and tomato (Enya *et al.*, 2007). The biosynthesis and biodegrading properties of this genus have been exploited in the food industry (Fialho *et al.*, 2008; Pozo *et al.*, 2007), bioremediation (Alarcón *et al.*, 2008; Jin *et al.*, 2013), and biofuel industry (Varman *et al.*, 2016). The ubiquitous presence of *Sphingobium* species in the environment has resulted in widespread human and animal exposure without any known adverse safety or allergenicity reports

B5(a)(iv) CP4 EPSPS protein

As described in Section A2, The donor organism for *cp4 epsps* is *Agrobacterium* sp. strain CP4 (Padgette *et al.*, 1996). *Agrobacterium* species are not known for human or animal pathogenicity and are not commonly allergenic (FAO-WHO, 1991; Mehrotra and Goyal, 2012; Nester, 2015). The history of safe use of the CP4 EPSPS protein from *Agrobacterium* sp. strain CP4 has been previously reviewed as a part of consultations with the FDA and FSANZ regarding Roundup Ready® events of soybean (A338, A592, A1049), canola (A363, A1071), maize (A416, A548, A1066, A1097), sugar beet (A378, A525), alfalfa (A575), and cotton (A355, A553).

B5(b)   Bioinformatic comparison (aa) of novel protein(s) to allergens

B5(b)(i)   Structural similarity of MON 87429 DMO to known allergens

For details, please refer to ▮▮▮▮▮, 2018 (MSL0029452).

The Codex guidelines for the evaluation of the allergenicity potential of introduced proteins (Codex Alimentarius, 2009) are based on the comparison of amino acid sequences between introduced proteins and allergens, where allergenic cross-reactivity may exist if the introduced protein is found to have at least 35% amino acid identity with an allergen over any segment of at least 80 amino acids. The Codex guideline also suggests that a sliding window search with a scientifically justified peptide size be used to identify immunologically relevant peptides in otherwise unrelated proteins. Therefore, the extent of sequence similarities between the DMO protein sequence and known allergens, gliadins, and glutenins was assessed using the FASTA sequence alignment tool along with an eight-amino acid sliding window search (Codex Alimentarius, 2009; Thomas *et al.*, 2005). The data generated from these analyses confirm that the DMO protein does not share amino acid sequence similarities with known allergens, gliadins, or glutenins.

Periodically, the databases used to evaluate proteins are updated. Since the most recent reports were completed, the allergen (AD_2018) database has been revised and updated. In order to determine if the DMO protein shares significant sequence similarity to new sequences contained in the updated allergen database, protein sequences were used as a query for a FASTA and Sliding Window search of the AD_2018 database.

The FASTA program directly compares amino acid sequences (i.e., primary, linear protein structure). This alignment data may be used to infer shared higher order structural similarities between two sequences (i.e., secondary and tertiary protein structures). Proteins that share a high degree of similarity throughout the entire sequence are often homologous. By definition, homologous proteins have common secondary structures, and three-dimensional configuration, and, consequently, may share similar functions. The allergen, gliadin, and glutenin protein sequence database (AD_2018) was obtained as the "COMprehensive Protein Allergen REsource" (COMPARE) database from the Health and Environmental Sciences Institute (HESI) and was used for the evaluation of sequence similarities shared between the DMO protein and all proteins in the database. The AD_2018 database contains 2,038 sequences. When used to align the sequence of the introduced protein to each protein in the database, the FASTA algorithm produces an *E*-score

(expectation score) for each alignment.   The *E*-score is a statistical measure of the likelihood that the observed similarity score could have occurred by chance in a search.   A larger *E*-score indicates a low degree of similarity between the query sequence and the sequence from the database.   Typically, alignments between two sequences which have an *E*-score of less than or equal to 1×10^{-5} are considered to have meaningful homology.   Results indicate that the DMO protein sequence does not share meaningful similarity with sequences in the allergen database.   No alignment met or exceeded the threshold of 35% identity over 80 amino acids recommended by Codex Alimentarius (2009) or had an *E*-score of less than or equal to 1×10^{-5}.

A second bioinformatic tool, an eight-amino acid sliding window search, was used to specifically identify short linear polypeptide matches to known allergens.   It is possible that proteins structurally unrelated to allergens, gliadins, and glutenins may contain smaller immunologically meaningful epitopes.   An amino acid sequence may have allergenic potential if it has an exact sequence identity of at least eight linearly contiguous amino acids with a potential allergen epitope (Hileman *et al.*, 2002; Metcalfe *et al.*, 1996).   Using a sliding window of less than eight amino acids can produce matches containing considerable uncertainty depending on the length of the query sequence (Silvanovich *et al.*, 2006), and is not useful to the allergy assessment process (Thomas *et al.*, 2005).   No eight contiguous amino acid identities were detected when the DMO protein sequence was compared to the proteins in the AD_2018 sequence database.

The bioinformatic results demonstrated there were no biologically relevant sequence similarities to allergens when the DMO protein sequence was used as a query for a FASTA search of the AD_2018 database.   Furthermore, no short (eight amino acid) polypeptide matches were shared between the DMO protein sequence and proteins in the allergen database.   These data show that DMO protein sequence lacks both structurally and immunologically relevant similarities to known allergens, gliadins, and glutenins.

B5(b)(ii)   Structural similarity of PAT (*pat*) to known allergens

For details, please refer to ▮▮▮▮▮▮▮▮▮▮ 2018 (RAR-2018-0231).

The Codex guidelines for the evaluation of the allergenicity potential of introduced proteins (Codex Alimentarius, 2009) are based on the comparison of amino acid sequences between introduced proteins and allergens, where allergenic cross-reactivity may exist if the introduced protein is found to have at least 35% amino acid identity with an allergen over any segment of at least 80 amino acids.   The Codex guideline also suggests that a sliding window search with a scientifically justified peptide size be used to identify immunologically relevant peptides in otherwise unrelated proteins.   Therefore, the extent of sequence similarities between the PAT (*pat*) protein sequence and known allergens, gliadins, and glutenins was assessed using the FASTA sequence alignment tool along with an eight-amino acid sliding window search (Codex Alimentarius, 2009; Thomas *et al.*, 2005).   The methods used are summarized in Section B4(a).   The data generated from these analyses confirm that the PAT (*pat*) protein does not share amino acid sequence similarities with known allergens, gliadins, or glutenins.

The bioinformatic evaluation of PAT (*pat*) has been previously conducted throughout the research and development process, with all reports concluding that the PAT protein was not similar to known allergens, toxins, or other biologically active proteins that may adversely affect human or animal health.

B5(b)(iii) Structural similarity of FT_T n to known allergens

For details, please refer to ████████2018 (MSL0029452).

The Codex guidelines for the evaluation of the allergenicity potential of introduced proteins (Codex Alimentarius, 2009) are based on the comparison of amino acid sequences between introduced proteins and allergens, where allergenic cross-reactivity may exist if the introduced protein is found to have at least 35% amino acid identity with an allergen over any segment of at least 80 amino acids.   The Codex guideline also suggests that a sliding window search with a scientifically justified peptide size be used to identify immunologically relevant peptides in otherwise unrelated proteins.   Therefore, the extent of sequence similarities between the FT_T protein sequence and known allergens, gliadins, and glutenins was assessed using the FASTA sequence alignment tool along with an eight-amino acid sliding window search (Codex Alimentarius, 2009; Thomas *et al.*, 2005).   The methods used are summarized in Section B4(a).   The data generated from these analyses confirm that the FT_T protein does not share amino acid sequence similarities with known allergens, gliadins, or glutenins.

The bioinformatic results demonstrated there were no biologically relevant sequence similarities to allergens when the FT_T protein sequence was used as a query for a FASTA search of the AD_2018 database.   Furthermore, no short (eight amino acid) polypeptide matches were shared between the FT_T protein sequence and proteins in the allergen database.   These data show that FT_T protein sequence lacks both structurally and immunologically relevant similarities to known allergens, gliadins, and glutenin.

B5(b)(iv) Structural similarity of CP4 EPSPS to known allergens

For details, please refer to ████████████████ 2018 (RAR-2018-0126).

The Codex guidelines for the evaluation of the allergenicity potential of introduced proteins (Codex Alimentarius, 2009) are based on the comparison of amino acid sequences between introduced proteins and allergens, where allergenic cross-reactivity may exist if the introduced protein is found to have at least 35% amino acid identity with an allergen over any segment of at least 80 amino acids.   The Codex guideline also suggests that a sliding window search with a scientifically justified peptide size be used to identify immunologically relevant peptides in otherwise unrelated proteins.   Therefore, the extent of sequence similarities between the CP4 EPSPS protein sequence and known allergens, gliadins, and glutenins was assessed using the FASTA sequence alignment tool along with an eight-amino acid sliding window search (Codex Alimentarius, 2009; Thomas *et al.*, 2005).   The methods used are summarized in Section B4(a).   The data generated from these analyses confirm that the CP4 EPSPS protein does not share amino acid sequence similarities with known allergens, gliadins, or glutenins.

The bioinformatic evaluation of CP4 EPSPS has been conducted several times throughout the research and development process, with all reports concluding that the CP4 EPSPS protein was not similar to known allergens, toxins, or other biologically active proteins that may adversely affect human or animal health.

B5(c)   Structural properties, including digestion by pepsin, heat treatment

The susceptibility of a protein to heat or its degradation in the presence of pepsin and pancreatin is a factor in the assessment of its potential allergenicity.   The degradation of MON 87429 DMO, PAT (*pat*), FT_T and CP4 EPSPS proteins were evaluated by incubation with solutions containing pepsin and pancreatin, and the results show that MON 87429 DMO, PAT (*pat*), FT_T and CP4 EPSPS proteins were readily degraded (Section B4(b)(i)). Exposure to heat during food processing or cooking, and to digestive fluids is likely to have a profound effect on the structure and function of proteins.

The effect of heat treatment on the activity of MON 87429 DMO, PAT (*pat*), FT_T and CP4 EPSPS proteins was evaluated using functional assays to assess the impact of temperature on enzymatic activity, and using SDS-PAGE to assess the impact of temperature on protein integrity.   The results show that MON 87429 DMO protein was completely deactivated by heating at 55 ℃ or higher for 15 min or more, PAT (*pat*) protein was substantially deactivated by heating at 75 ℃ or above for 15 minutes and at 55°C or above for 30 minutes, FT_T protein was substantially deactivated by heating at 75 ℃ or above for 15 minutes and at 55°C or above for 30 minutes, and CP4 EPSPS heated to 55 ℃ demonstrated a substantial reduction in activity after the 30 minute incubation and the level of CP4 EPSPS activity following incubation at temperatures of 75 and 95 ℃ was below the limit of detection for incubations at both time points (Section B4(b)(ii)).   Therefore, it is anticipated that exposure to functionally active MON 87429 DMO, PAT (*pat*), FT_T or CP4 EPSPS protein from the consumption of MON 87429 or foods derived from MON 87429 is unlikely.

B5(d)   Specific serum screening if protein from allergenic source

Not applicable.

B5(e)   Protein as a proportion of total protein

B5(e)(i)   The DMO protein in MON 87429 as a proportion of total protein

The MON 87429 DMO protein was detected in all plant tissue types assayed (Table 35). Harvested grain is the most relevant tissue analyzed for an allergenicity assessment because foods derived from maize grain can be consumed directly.   The mean level of MON 87429 DMO protein in grain of MON 87429 is 2.4 µg/g dw.   The mean percent dry weight of total protein in grain of MON 87429 is 9.2% (or 92,000 µg/g, Table 52).   The percentage of MON 87429 DMO protein in MON 87429 grain is calculated as follows:

$(2.4\ \mu g/g \div 92{,}000\ \mu g/g) \times 100\% \approx 0.0026\%$ or 26 ppm of total grain protein

Therefore, the MON 87429 DMO protein represents a very small portion of the total protein in the grain of MON 87429.   This low percent of MON 87429 DMO in relation to the total protein reduces the potential risk of allergenicity from this protein.

B5(e)(ii)   The PAT (*pat*) protein in MON 87429 as a proportion of total protein

The PAT (*pat*) protein was detected in all plant tissue types assayed (Table 36).   Harvested grain is the most relevant tissue analyzed for an allergenicity assessment because foods derived from maize grain can be consumed directly.   The mean level of PAT (*pat*) protein in grain of MON 87429 is 0.84 µg/g dw.   The mean percent dry weight of total protein in grain of MON 87429 is 9.2% (or 92,000 µg/g, Table 36).   The percentage of PAT (*pat*) protein in MON 87429 grain is calculated as follows:

(0.84 µg/g ÷ 92,000 µg/g) × 100% ≈ 0.00091% or 9.1 ppm of total grain protein

Therefore, the PAT (*pat*) protein represents a very small portion of the total protein in the grain of MON 87429.   This low percent of PAT (*pat*) in relation to the total protein reduces the potential risk of allergenicity from this protein.

B5(e)(iii)   The FT_T protein in MON 87429 as a proportion of total protein

The FT_T protein was detected in all plant tissue types assayed (Table 37).   Harvested grain is the most relevant tissue analyzed for an allergenicity assessment because foods derived from maize grain can be consumed directly.   The mean level of FT_T protein in grain of MON 87429 is 47 µg/g dw.   The mean percent dry weight of total protein in grain of MON 87429 is 9.2% (or 92,000 µg/g, Table 37).   The percentage of FT_T protein in MON 87429 grain is calculated as follows:

(47 µg/g ÷ 92,000 µg/g) × 100% ≈ 0.051% or 510 ppm of total grain protein

Therefore, the FT_T protein represents a very small portion of the total protein in the grain of MON 87429.   This low percent of FT_T in relation to the total protein reduces the potential risk of allergenicity from this protein.

B5(e)(iv)   The CP4 EPSPS protein in MON 87429 as a proportion of total protein

The CP4 EPSPS protein was detected in all plant tissue types assayed (Table 38) Harvested grain is the most relevant tissue analyzed for an allergenicity assessment because foods derived from maize grain can be consumed directly.   The mean level of CP4 EPSPS protein in grain of MON 87429 is 0.63 µg/g dw.   The mean percent dry weight of total protein in grain of MON 87429 is 9.2% (or 92,000 µg/g, Table 38).   The percentage of CP4 EPSPS protein in MON 87429 grain is calculated as follows:

(0.63 µg/g ÷ 92,000 µg/g) × 100% ≈ 0.00069 % or 6.9 ppm of total grain protein

Therefore, the CP4 EPSPS protein represents a very small portion of the total protein in the grain of MON 87429.   This low percent of CP4 EPSPS in relation to the total protein reduces the potential risk of allergenicity from this protein.

B6   Toxicity of Novel Herbicide Metabolites in GM Herbicide-Tolerant Plants

B6(a)   Novel herbicide use of quizalofop

For details, please refer to ████████, 2019 (MSL0030212).

Monsanto has developed herbicide-tolerant corn, MON 87429, which is tolerant to the herbicides dicamba, glufosinate, aryloxyphenoxypropionate (AOPP) acetyl coenzyme A carboxylase (ACCase) inhibitors ("FOPs" herbicides) and 2,4-D. MON 87429 contains a demethylase gene from *Stenotrophomonas maltophilia* that expresses a dicamba mono-oxygenase (DMO) protein to confer tolerance to dicamba herbicide, the phosphinothricin-N-acetyltransferase (*pat*) gene from *Streptomyces viridochromogenes* that expresses the PAT protein to confer tolerance to glufosinate herbicide and the *ft_t* gene, a modified version of the R-2,4-dichlorophenoxypropionate dioxygenase (*Rdpa*) gene from *Sphingobium herbicidovorans*, that expresses a FOPs and 2,4-D dioxygenase protein (FT_T) that confers tolerance to FOPs and 2,4-D herbicides. MON 87429 also produces the 5-enolpyruvylshikimate-3-phosphate synthase protein from *Agrobacterium* sp. strain CP4 (CP4 EPSPS) to provide maize lines with tissue-specific glyphosate tolerance to facilitate the production of hybrid maize seed. MON 87429 utilizes an endogenous maize regulatory element to target CP4 EPSPS mRNA for degradation in tassel tissues, resulting in reduced CP4 EPSPS protein expression in pollen and tassels. Appropriately timed glyphosate applications produce a non-viable pollen phenotype and allow for specific cross pollinations to be made in maize without using traditional methods to control self-pollination.

A study was conducted in 2018 in the U.S. to determine the magnitude of residues of quizalofop-P-ethyl in MON 87429 raw agricultural commodities (RAC) resulting from the use of a formulation of quizalofop herbicide.

Combined maximum application rate in the U.S. is proposed to be 0.082 lb a.i./A (0.092 kg a.i./ha).   Currently proposed maximum application rates and corresponding application growth stages of quizalofop to MON 87429 in the U.S. are summarized below.   Any combination of application rates and timings may be used within the allowed limits for individual rates and timings as specified on the label.

Maximum Application Rates	
Combined maximum of all applications per year	0.082 lb a.i./A (0.092 kg a.i./kg)
Total in-crop applications from emergence to harvest	0.082 lb a.i./A (0.092 kg a.i./kg)
Maximum single in-crop application	0.041 lb a.i./A (0.046 kg a.i./kg)

The purpose of this summary is to report the residue levels of quizalofop-P-ethyl and its metabolite, quizalofop-P, in MON 87429 maize grain that resulted from applications of MON 54113, an emulsifiable concentrate herbicide containing 0.88 lb a.i. of quizalofop-P-ethyl per gallon.   Use of MON 87429 maize in this study was required to generate data that may be used to support regulatory approval of MON 87429 maize.

The field trials for the study were conducted in the U.S. at six sites in six states: Illinois, Iowa, Kansas, Nebraska, Wisconsin, and Texas.   These states were typical of the major maize producing regions of the U.S. and accounted for approximately 49.1% of the total maize acreage in the U.S. in 2012 (USDA-NASS, 2014). Control and treated plots were established at each site.   Plots measured between 500 and 6,000 square feet in area.   The untreated control plot was a minimum distance of 100 ft from any treated plot.

The same treatment regime was used for all treated plots and consisted of two post-emergent broadcast applications of MON 54113.   The combined rate of both applications was 0.082 lb a.i./acre.

The target application timings and rates are summarized in the following table.

Table 48.   Target Application of Quizalofop-P-Ethyl Formulation MON 54113 to MON 87429 Maize

Treatment	Application Rates*	
	Early Postemergence Application (V2-V4)	**Postemergence Application (V5-V6)**
Control	-	-
Treated	0.041 lb a.i./A (0.046 kg a.i./ha)	0.041 lb a.i./A (0.046 kg a.i./ha)

*Crop oil concentrate (COC) at 1% v/v (1 gal/100 gal spray grade solution) or NIS at 0.25% v/v.

Actual application rates for Application 1 were within ±2% of the target rates for all applications at all sites.   Actual application rates for Application 2 were within ±2% of the target rates for three locations and ±100% (2X) at three locations. The average % of target rate across all applications and all sites was 125%.   Spray volumes ranged from 15.2 to 19.8 gallons per acre (GPA) and were within ±5% of the target spray volumes for all applications at all sites.

Maize samples were collected at full maturity (BBCH 87).   Samples were harvested by hand from each plot, while generally avoiding the outer rows and ends of rows.   For each sample, ears were collected from 12 or more different locations across the entire plot. Corn ears were shelled and the grain was combined to create a composite sample.   In this manner, one sample from the untreated plot was collected first, followed by the two replicate samples from the treated plot.

Metabolism of quizalofop-P-ethyl by MON 87429 was demonstrated in a metabolism study (Lamar, 2018).   The residue of concern is the sum of quizalofop-P-ethyl parent and its metabolite quizalofop-P.

Residue levels of quizalofop-P-ethyl and quizalofop-P were determined by the current version of Monsanto analytical method ME-2170, "Method for Determination of Quizalofop and Quizalofop Ethyl Residues in Crop Matrices Using LC-MS/MS". Analytes were quantitated using LC-MS/MS with electrospray ionization in positive ion mode. The limit of quantitation (LOQ) for each analyte was determined to be 0.010 ppm. The limit of detection (LOD) for quizalofop-P-ethyl and quizalofop-P was determined to be 0.001 ppm and 0.002 ppm, respectively. Both quizalofop-p-ethyl and quizalofop-p residues were below the limit of detection (<LOD), hence there were no measurable residues of quizalofop-p-ethyl and its metabolite quizalofop-p in corn grain. Total residues are expressed as quizalofop-P-ethyl equivalents.

For this study, one untreated control and two treated mature MON 87429 grain samples from each site were analyzed. Additional untreated grain samples were fortified with known amounts of quizalofop-P-ethyl and quizalofop-P and were included in the set for analysis. Untreated samples were fortified at two levels, the LOQ (0.010 ppm) and 10X LOQ (0.100 ppm), with solutions containing both analytes. The average background-corrected recoveries across these two levels were 93.8% and 92.4% for quizalofop-P-ethyl and quizalofop-P, respectively.

The residues in samples collected from Treatment 2 are summarized in the following table:

Table 49.   Quizalofop-P-Ethyl and Quizalofop-P Residues in MON 87429 RAC Grain

Analyte	Treatment 2		
	Median PHI (days)[1]	**Median (ppm)[2,3]**	**Min. – Max. (ppm)[2,3]**
Quizalofop-P-ethyl	99	ND	ND
Quizalofop-P	99	ND	ND
Total[4]	-	ND	ND

[1]PHI - Preharvest Interval - Interval between last application and sampling.
[2]Median of site averaged quizalofop-P-ethyl and quizalofop-P values and range of individual field sample values.
[3]This method has a limit of quantitation (LOQ) of 0.010 ppm (mg/kg). Values below the limit of detection (LOD) are reported as ND (Not Detected).
[4]Calculated as follows: quizalofop-P-ethyl ppm = quizalofop-P-ethyl + (quizalofop-P × 1.08)

The residue results indicate that the existing EPA quizalofop MRL of 0.02 ppm in maize grain (EFSA *et al.*, 2018) is sufficient to account for the use of quizalofop on MON 87429 tolerant maize in the USA. An application to amend Standard 20 of the Food Standards Code is not required due to the absence of any detectable residues.

B6(b)   Novel herbicide use of 2,4-D

For details, please refer to ▮▮▮▮▮▮ 2019 (MSL0030211).

A study was conducted in 2018 in the U.S. to determine the magnitude of residues of 2,4-dichlorophenoxyacetic acid (2,4-D) in MON 87429 raw agricultural commodities (RAC) resulting from the use of a formulation of 2,4-D herbicide.

Combined maximum application rate in the U.S. is proposed to be 2.25 lb a.e./A (2.52 kg a.e./ha).   Currently proposed maximum application rates and corresponding application growth stages of 2,4-D to MON 87429 in the U.S. are summarized below.   Any combination of application rates and timings may be used within the allowed limits for individual rates and timings as specified on the label.

Maximum Application Rates	
Combined maximum of all applications per year	2.25 lb a.e./A (2.52 kg a.e./ha)
Total of all burndown, preplant, at-planting, and preemergence applications	0.75 lb a.e./A (0.84 kg a.e./ha)
Total in-crop applications from emergence up to V8 corn growth stage or 48 inches tall	1.5 lb a.e./A (2 x 0.75 lb a.e./A)* (1.68 kg a.e./ha) (2 x 0.84 kg a.e./ha)*
Maximum single in-crop application	0.75 lb a.e./A (0.84 kg a.e./ha)

*Two applications at 0.75 lb a.e./A (0.84 kg a.e./ha) each

The purpose of this summary is to report the residue levels of 2,4-dichlorophenoxyacetic acid (2,4-D) and its major metabolite, 2,4-dichlorophenol (2,4-DCP), in MON 87429 maize grain that resulted from applications of MON 55642, a water-soluble concentrate herbicide containing 3.8 lb a.e. of 2,4-D per gallon.   Use of MON 87429 maize in this study was required to generate data that may be used to support regulatory approval of MON 87429 maize.

The field trials for the study were conducted in the U.S. at six sites in six states: Illinois, Iowa, Kansas, Nebraska, Wisconsin, and Texas.   These states were typical of the major maize producing regions of the U.S. and accounted for approximately 49.1% of the total maize acreage in the U.S. in 2012 (USDA-NASS, 2014).

Control and treated plots were established at each site.   Plots measured between 500 to 6,000 square feet in area.   The untreated control plot was at a minimum distance of 100 ft from any treated plot.

The same treatment regime was used for all treated plots and consisted of three separate, broadcast applications of MON 55642.   The combined rate of all three MON 55642 applications was 2.25 lb a.e./acre.

The target application timings and rates are summarized in the following table:

Table 50. Target Application of 2,4-D Formulation MON 55642 to MON 87429 Maize

Treatment	Application Rates		
	Preemergence Application	**Early Postemergence Application (V2-V4)**	**Late Postemergence Application (V7-V8)**
Control	-	-	-
Treated	0.75 lb a.e./A (0.84 kg a.e./ha)	0.75 lb a.e./A (0.84 kg a.e./ha)	0.75 lb a.e./A (0.84 kg a.e./ha)

Actual application rates were within ±5% of the target rates for all locations. The average % of target rate across all applications and all sites was 99%. Spray volumes ranged from 12.57 to 14.93 gallons per acre (GPA) and were within ±5% of the target spray volumes for all applications at all sites.

Maize samples were collected at full maturity (BBCH 87). Samples were harvested by hand from each plot, while generally avoiding the outer rows and ends of rows. For each sample, ears were collected from 12 or more different locations across the entire plot. Corn ears were shelled and the grain was combined to create a composite sample. In this manner, one sample from the untreated plot was collected first, followed by the two replicate samples from the treated plot.

Metabolism of 2,4-D by MON 87429 was demonstrated in a metabolism study (Bautista, 2018). The residue of concern is the sum of 2,4-D parent and the metabolite 2,4-DCP.

Residue levels of 2,4-D and 2,4-DCP were determined by the current version of Monsanto analytical method ME-2172, "Method for Determination of 2,4-Dichlorophenoxyacetic Acid (2,4-D) and 2,4-Dichlorophenol (2,4-DCP) Residues in Crop Matrices Using LC-MS/MS.". Analytes were quantitated using LC-MS/MS with atmospheric pressure chemical ionization (APCI) in negative ion mode. The limit of quantitation (LOQ) for each analyte was determined to be 0.010 ppm. The limit of detection (LOD) for 2,4-D and 2,4-DCP was determined to be 0.002 ppm and 0.004 ppm, respectively. Total residues are expressed as 2,4-D acid equivalents.

For this study, one untreated control and two treated grain samples from each site were analyzed. Additional untreated grain samples were fortified with known amounts of 2,4-D and 2,4-DCP and were included in the set for analysis. Untreated samples were fortified at two levels, the LOQ (0.010 ppm) and 10X LOQ (0.100 ppm), with solutions containing both analytes. The average background-corrected recoveries across these two levels were 86.2% and 92.0% for 2,4-D and 2,4-DCP, respectively.

The residues in samples collected from Treatment 2 are summarized in the following table:

Table 51.   2,4-D and 2,4-DCP Residues in MON 87429 RAC Grain

Analyte	Median PHI (days)[1]	Median (ppm)[2,3]	Min. – Max. (ppm)[2,3]
	Treatment 2		
2,4-D	100.5	ND	ND-[0.003]
2,4-DCP	100.5	ND	ND
Total[4]	-	ND	ND-[0.003]

[1]PHI - Preharvest Interval - Interval between last application and sampling.
[2]Median of site averaged 2,4-D and 2,4-DCP values and range of individual field sample values.
[3]This method has a limit of quantitation (LOQ) of 0.010 ppm (mg/kg).   Values below the limit of detection (LOD) are reported as ND (Not Detected). Residues between the LOD and the LOQ are reported in square brackets.
[4]Calculated as follows: 2,4-D ppm = 2,4-D + (2,4-DCP x 1.35)

The residue results indicate that the existing EPA 2,4-D MRL of 0.05 ppm in maize grain (EFSA, 2011) is sufficient to account for the use of 2,4-D on MON 87429 tolerant maize in the USA. An application to amend Standard 20 of the Food Standards Code is not required due to the absence of any quantifiable residues for 2,4-DCP and an "all other foods" default existing for 2,4-D.

B7 Compositional Assessment

Safety assessments of biotechnology-derived crops follow the comparative safety assessment process (Codex Alimentarius, 2009) in which the composition of grain and/or other raw agricultural commodities of the biotechnology-derived crop are compared to the appropriate conventional control that has a history of safe use. For maize, assessments are performed based on the general principles outlined in the OECD consensus document for maize composition (OECD, 2002b).

A recent review of compositional assessments conducted according to OECD guidelines, that encompassed a total of seven biotechnology-derived crop varieties, nine countries, and eleven growing seasons, concluded that incorporation of biotechnology-derived agronomic traits has had little impact on crop composition compared to other sources of variation. Most compositional variation is attributable to growing region, agronomic practices, and genetic background (Harrigan *et al.*, 2010). Numerous scientific publications have further documented the extensive variability in the concentrations of crop components that reflect the influence of environmental and genetic factors as well as extensive conventional breeding efforts to improve nutrition, agronomics, and yield (Harrigan *et al.*, 2010; Harrigan *et al.*, 2009; Ridley *et al.*, 2011; Zhou *et al.*, 2011).

Compositional equivalence between biotechnology-derived and conventional crops supports an "equal or increased assurance of the safety of foods derived from genetically modified plants" (OECD, 2002c). OECD consensus documents on compositional considerations for new crop varieties emphasize quantitative measurements of key nutrients and known anti-nutrients. These quantitative measurements effectively discern any compositional changes that could imply potential nutritional or safety (e.g. antinutritional) concerns. Levels of the components in grain and/or other raw agricultural commodities of the biotechnology-derived crop product are compared to: 1) corresponding levels in a conventional comparator, a genetically similar conventional line, grown concurrently under similar field conditions, and 2) natural ranges from data published in the scientific literature or in publicly-available databases (e.g. ILSI Crop Composition Database). This second comparison places any potential differences between the assessed crop and its comparator in the context of the well-documented variation in the concentrations of crop nutrients and anti-nutrients.

This section provides analyses of concentrations of key nutrients and anti-nutrients in grain and forage of MON 87429 compared to that of a conventional control maize hybrid grown and harvested under similar conditions. The production of materials for compositional analyses used a sufficient variety of field trial sites, reflecting a range of environmental conditions under which MON 87429 is expected to be grown and robust field designs (randomized complete block design with four replicates). Samples were subjected to sensitive analytical methods that allow quantitative and accurate measurements of key components. The information provided in this section addresses relevant factors in Codex Plant Guidelines, Section 4, paragraphs 44 and 45 for compositional analyses (Codex Alimentarius, 2009).

B7(a)   Levels of key nutrients, toxicants and anti-nutrients

For details, please refer to ▮▮▮▮▮▮▮▮▮▮., 2018 (MSL0029410).

Grain and forage samples were harvested from MON 87429 and a conventional control grown at five sites (Audubon County, IA (IAAU); Vermilion County, IL (ILCX); Boone County, Indiana (INSH); York County, Nebraska (NEYO); and Miami County, Ohio (OHTR)) in the United States during 2017.   The field sites were planted in a randomized complete block design with four replicates per site.   MON 87429 and the conventional control were grown under agronomic field conditions typical for each of the different growing regions.   MON 87429 plots were treated with dicamba, glufosinate, quizalofop and 2,4-D to generate samples under conditions of the intended use of the product.   The compositional analysis provided a comprehensive comparative assessment of the levels of key nutrients, anti-nutrients and secondary metabolites in grain and forage of MON 87429 and the conventional control.

The evaluation of MON 87429 followed considerations relevant to the compositional quality of maize as defined by the OECD consensus document (OECD, 2002b). Harvested grain samples were assessed for moisture and levels of nutrients including proximates (protein, total fat and ash), amino acids (18 components), fatty acids (22 components), carbohydrates by calculation, fiber (ADF, NDF and TDF), minerals (calcium, copper, iron, magnesium, manganese, phosphorus, potassium, sodium and zinc) and vitamins (vitamin A, vitamin B_1, vitamin B_2, vitamin B_3, vitamin B_6, vitamin B_9 and vitamin E).   Grain samples were assessed for levels of other components including anti-nutrients (phytic acid and raffinose) and secondary metabolites (ferulic acid, furfural and p-coumaric acid).   Harvested forage samples were assessed for moisture and levels of nutrients including proximates (protein, total fat and ash), carbohydrates by calculation, fiber (ADF and NDF) and minerals (calcium and phosphorus).   In all, 78 different components were analyzed.

Of the 78 measured components, 15 components (caprylic acid, capric acid, lauric acid, myristic acid, myristoleic acid, pentadecanoic acid, pentadecenoic acid, heptadecanoic acid, heptadecenoic acid, gamma linolenic acid, eicosadienoic acid, eicosatrienoic acid, arachidonic acid, sodium and furfural in grain) had more than 50% of the observations fall below the assay limit of quantitation (LOQ) and were excluded from statistical analyses. Moisture values for grain and forage were measured for conversion of components from fresh to dry weight but were not statistically analyzed.   Therefore, 61 components were statistically analyzed (53 in grain and 8 in forage).

The statistical comparison of MON 87429 and the conventional control was based on compositional data combined across all five field sites.   Statistically significant differences were identified at the 5% level (α = 0.05).   A statistically significant difference between MON 87429 and the conventional control does not necessarily imply biological relevance from a food and feed safety perspective.   Therefore, any statistically significant differences observed between MON 87429 and the conventional control were evaluated further to determine whether the detected difference indicated a biologically relevant compositional change or supported a conclusion of compositional equivalence, as follows:

Step 1 – Determination of the Magnitude of Difference between Test (MON 87429) and Conventional Control Means

The difference in means between MON 87429 and the conventional control was determined for use in subsequent steps. For protein and amino acids only, the relative magnitude of the difference (percent change relative to the control) between MON 87429 and the conventional control was determined to allow an assessment of any observed difference in amino acids in relation to the difference in protein.

Step 2 – Assessment of the Difference in the Context of Natural Variation within the Conventional Control across Multiple Sites

The difference between MON 87429 and the conventional control was evaluated in the context of variation within the conventional control germplasm grown across multiple sites (i.e*.,* variation due to environmental influence) by determining the range of replicate values for the conventional control (range value = maximum value minus the minimum value). A mean difference less than the variability seen due to natural environmental variation within the single, closely related germplasm is typically not a food or feed safety concern (Venkatesh *et al.*, 2014).

Step 3 – Assessment of the Difference in the Context of Natural Variation Due to Multiple Sources

The relative impact of MON 87429 on composition was evaluated in the context of sources of natural variation such as environmental and germplasm influences. This assessment determined whether the component mean value of MON 87429 was within the natural variability defined by the literature values or the ILSI Crop Composition Database (ILSI-CCDB) values. This natural variability is important in assessing the biological relevance to food and feed safety of statistically significant differences in composition between MON 87429 and the conventional control.

These evaluations of natural variation are important as crop composition is known to be greatly influenced by environment and variety (Harrigan *et al.*, 2010). Although used in the comparative assessment process, detection of statistically significant differences between MON 87429 and the conventional control mean values does not necessarily imply a meaningful contribution by MON 87429 to compositional variability. Only if the impact of MON 87429 on levels of components is large relative to natural variation inherent to conventional maize would further assessments be required to establish whether the change in composition would have an impact from a food and feed safety and nutritional perspective. Differences between MON 87429 and the conventional control that are within the observed natural variation for maize are not meaningful, therefore the results support a conclusion of compositional equivalence.

B7(a)(i) Compositional equivalence of MON 8729 grain and forage to that of conventional maize

There were no statistically significant differences (p<0.05) for 50 of the 61 components analyzed (Table 52 to Table 58). There were 11 components (total fat, palmitoleic acid, stearic acid, oleic acid, linoleic acid, linolenic acid, behenic acid, copper, iron, magnesium and vitamin E in grain) that showed a statistically significant difference (p<0.05) between MON 87429 and the conventional control.

For total fat, the difference was -0.12% dw (Table 53). For the six fatty acids, the magnitudes of differences ranged from 0.0044 % Total FA (behenic acid) to 0.51% Total FA (oleic acid) (Table 53). As shown in Table 53, the magnitude of differences for total fat and the six fatty acids between MON 87429 and the conventional control were less than the corresponding conventional control range values. This indicates that MON 87429 does not impact levels of these components more than the natural variation within the conventional control grown at multiple locations. The mean levels of total fat and the six fatty acids were within the natural variability of these components as published in the scientific literature on maize composition and/or the ILSI-CCDB (Table 59).

For copper, iron and magnesium, the differences were -0.29 mg/kg dw, -0.85 mg/kg dw and -0.0050% dw, respectively (Table 55). As shown in Table 55, the magnitude of differences for copper, iron and magnesium between MON 87429 and the conventional control were less than the corresponding conventional control range values. This indicates that MON 87429 does not impact levels of these components more than the natural variation within the conventional control grown at multiple locations. The mean levels of copper, iron and magnesium were within the natural variability of these components as published in the scientific literature on maize composition and/or the ILSI-CCDB (Table 59).

For vitamin E, the difference was -0.89 mg/kg dw (Table 56). As shown in Table 56, the magnitude of the difference for vitamin E between MON 87429 and the conventional control was less than the corresponding conventional control range values. This indicates that MON 87429 does not impact levels of this components more than the natural variation within the conventional control grown at multiple locations. The mean level of vitamin E was within the natural variability of this component as published in the scientific literature on maize composition and/or the ILSI-CCDB (Table 59).

These data indicated that the statistically significant differences observed were not biologically meaningful from a food and feed safety perspective. These results support the conclusion that MON 87429 was not a major contributor to variation in component levels in maize grain or forage and confirmed the compositional equivalence of MON 87429 to the conventional control in levels key nutrients and anti-nutrients in grain and forage.

Table 52. Summary of Maize Grain Protein and Amino Acids for MON 87429 and Conventional Control

Component (% dw)[1]	MON 87429 Mean (S.E.)[2] Range	Control Mean (S.E.) Range	Control Range Value[3]	Difference (Test minus Control)		
				Mean (S.E.)	p-Value	% Relative[4]
Protein	9.20 (0.30) 7.95 - 10.99	9.35 (0.30) 8.04 - 11.01	2.96	-0.15 (0.14)	0.289	-1.65
Alanine	0.72 (0.028) 0.63 - 0.91	0.73 (0.028) 0.62 - 0.89	0.27	-0.0082 (0.013)	0.537	-1.12
Arginine	0.45 (0.014) 0.40 - 0.54	0.45 (0.014) 0.38 - 0.51	0.13	0.0047 (0.0068)	0.498	1.05
Aspartic acid	0.61 (0.019) 0.54 - 0.74	0.61 (0.019) 0.53 - 0.71	0.18	0.0021 (0.011)	0.845	0.35
Cystine	0.20 (0.0062) 0.17 - 0.23	0.20 (0.0062) 0.18 - 0.24	0.062	-0.0067 (0.0042)	0.127	-3.27
Glutamic acid	1.77 (0.074) 1.49 - 2.27	1.78 (0.074) 1.50 - 2.18	0.68	-0.014 (0.037)	0.717	-0.76

Table 52. Summary of Maize Grain Protein and Amino Acids for MON 87429 and Conventional Control (continued)

Component (% dw)[1]	MON 87429 Mean (S.E.)[2] Range	Control Mean (S.E.) Range	Control Range Value[3]	Difference (Test minus Control)		
				Mean (S.E.)	p-Value	% Relative[4]
Glycine	0.36 (0.0089) 0.32 - 0.42	0.36 (0.0089) 0.32 - 0.40	0.089	0.00021 (0.0047)	0.964	0.059
Histidine	0.26 (0.0091) 0.22 - 0.31	0.25 (0.0091) 0.22 - 0.30	0.085	0.0018 (0.0053)	0.739	0.70
Isoleucine	0.34 (0.013) 0.30 - 0.43	0.34 (0.013) 0.29 - 0.41	0.12	0.0013 (0.0069)	0.850	0.38
Leucine	1.20 (0.054) 0.98 - 1.56	1.22 (0.054) 1.00 - 1.51	0.52	-0.012 (0.027)	0.672	-0.97
Lysine	0.26 (0.0077) 0.22 - 0.35	0.26 (0.0077) 0.21 - 0.28	0.067	0.0062 (0.0084)	0.499	2.41
Methionine	0.20 (0.0067) 0.17 - 0.25	0.20 (0.0067) 0.17 - 0.24	0.065	-0.0040 (0.0026)	0.135	-1.99

Table 52.   Summary of Maize Grain Protein and Amino Acids for MON 87429 and Conventional Control (continued)

Component (% dw)[1]	MON 87429 Mean (S.E.)[2] Range	Control Mean (S.E.) Range	Control Range Value[3]	Difference (Test minus Control)		
				Mean (S.E.)	p-Value	% Relative[4]
Phenylalanine	0.48 (0.020) 0.40 - 0.59	0.48 (0.020) 0.40 - 0.60	0.20	0.0022 (0.010)	0.845	0.45
Proline	0.88 (0.040) 0.72 - 1.09	0.89 (0.040) 0.71 - 1.03	0.31	-0.010 (0.018)	0.574	-1.14
Serine	0.46 (0.015) 0.38 - 0.58	0.46 (0.015) 0.39 - 0.54	0.15	0.00089 (0.011)	0.939	0.20
Threonine	0.34 (0.0097) 0.30 - 0.42	0.34 (0.0097) 0.30 - 0.39	0.096	0.0010 (0.0056)	0.853	0.31
Tryptophan	0.074 (0.0016) 0.065 - 0.080	0.075 (0.0016) 0.066 - 0.083	0.017	-0.0012 (0.0016)	0.479	-1.65
Tyrosine	0.40 (0.013) 0.35 - 0.47	0.39 (0.013) 0.32 - 0.47	0.15	0.0035 (0.0087)	0.705	0.89
Valine	0.44 (0.015) 0.39 - 0.55	0.44 (0.015) 0.38 - 0.52	0.14	0.0032 (0.0072)	0.656	0.74

[1]dw=dry weight
[2]Mean (S.E.) = least-square mean (standard error)
[3]Maximum value minus minimum value for the control maize hybrid
[4]The relative magnitude of the difference in mean values between MON 87429 (treated with dicamba, glufosinate, quizalofop and 2,4-D) and the control, expressed as a percent of the control.

Table 53.   Summary of Maize Grain Total Fat and Fatty Acids for MON 87429 and Conventional Control

Component	MON 87429 Mean (S.E.)[1] Range	Control Mean (S.E.) Range	Control Range Value[2]	Difference (Test minus Control) Mean (S.E.)	p-Value
Total fat (% dw)[3]	3.76 (0.050) 3.46 - 4.01	3.88 (0.050) 3.58 - 4.16	0.57	-0.12 (0.045)	0.049
Palmitic acid (% Total FA)[4]	12.91 (0.048) 12.68 - 13.21	12.83 (0.048) 12.58 - 13.20	0.62	0.079 (0.043)	0.075
Palmitoleic acid (% Total FA)	0.13 (0.0062) 0.098 - 0.14	0.12 (0.0062) 0.077 - 0.13	0.052	0.0076 (0.0018)	<0.001
Stearic acid (% Total FA)	1.74 (0.054) 1.55 - 2.01	1.66 (0.054) 1.47 - 1.86	0.39	0.074 (0.016)	0.010
Oleic acid (% Total FA)	27.64 (0.52) 25.65 - 29.45	28.15 (0.52) 26.33 - 30.11	3.79	-0.51 (0.12)	<0.001
Linoleic acid (% Total FA)	55.53 (0.63) 53.61 - 57.87	55.21 (0.63) 53.28 - 57.38	4.10	0.32 (0.12)	0.018
Linolenic acid (% Total FA)	1.24 (0.022) 1.13 - 1.33	1.21 (0.022) 1.12 - 1.27	0.15	0.026 (0.0062)	<0.001
Arachidic acid (% Total FA)	0.41 (0.011) 0.37 - 0.45	0.41 (0.011) 0.36 - 0.46	0.10	0.0067 (0.0038)	0.096
Eicosenoic acid (% Total FA)	0.25 (0.0027) 0.24 - 0.28	0.25 (0.0027) 0.23 - 0.27	0.037	-0.0046 (0.0027)	0.154
Behenic acid (% Total FA)	0.16 (0.0053) 0.14 - 0.18	0.15 (0.0053) 0.12 - 0.18	0.062	0.0044 (0.0021)	0.040

[1] Mean (S.E.) = least-square mean (standard error)
[2] Maximum value minus minimum value for the control maize hybrid
[3] dw=dry weight
[4] FA=Fatty Acid
The following components with more than 50% of observations below the assay LOQ were excluded from statistical analysis: caprylic acid, capric acid, lauric acid, myristic acid, myristoleic acid, pentadecanoic acid, pentadecenoic acid, heptadecanoic acid, heptadecenoic acid, gamma linolenic acid, eicosadienoic acid, eicosatrienoic acid and arachidonic acid.

Table 54.   Summary of Maize Grain Carbohydrates by Calculation and Fiber for MON 87429 and Conventional Control

Component (% dw)[1]	MON 87429 Mean (S.E.)[2] Range	Control Mean (S.E.) Range	Control Range Value[3]	Difference (Test minus Control) Mean (S.E.)	p-Value
Carbohydrates by calculation	85.87 (0.38) 83.97 - 87.27	85.61 (0.38) 83.62 - 87.34	3.73	0.25 (0.15)	0.104
ADF	2.63 (0.078) 1.94 - 3.67	2.53 (0.078) 2.28 - 3.03	0.74	0.098 (0.11)	0.378
NDF	7.82 (0.16) 6.97 - 8.63	8.05 (0.16) 6.44 - 9.80	3.36	-0.22 (0.23)	0.339
TDF	11.16 (0.30) 8.83 - 14.84	10.61 (0.30) 9.10 - 11.85	2.74	0.55 (0.39)	0.228

[1]dw=dry weight
[2]Mean (S.E.) = least-square mean (standard error)
[3]Maximum value minus minimum value for the control maize hybrid

Table 55. Summary of Maize Grain Ash and Minerals for MON 87429 and Conventional Control

Component	MON 87429 Mean (S.E.)[1] Range	Control Mean (S.E.) Range	Control Range Value[2]	Difference (Test minus Control) Mean (S.E.)	p-Value
Ash (% dw)[3]	1.15 (0.057) 0.97 - 1.34	1.15 (0.057) 0.91 - 1.41	0.50	-0.0013 (0.024)	0.958
Calcium (% dw)	0.0030 (0.00024) 0.0011 - 0.0041	0.0032 (0.00024) 0.0022 - 0.0040	0.0017	-0.00018 (0.00010)	0.093
Copper (mg/kg dw)	1.36 (0.11) 0.96 - 2.55	1.65 (0.11) 1.11 - 2.93	1.81	-0.29 (0.13)	0.029
Iron (mg/kg dw)	16.55 (0.50) 15.04 - 19.30	17.40 (0.50) 15.43 - 19.77	4.34	-0.85 (0.20)	<0.001
Magnesium (% dw)	0.10 (0.0037) 0.089 - 0.13	0.11 (0.0037) 0.095 - 0.13	0.036	-0.0050 (0.0016)	0.004
Manganese (mg/kg dw)	4.65 (0.48) 3.41 - 7.42	4.77 (0.48) 3.45 - 6.56	3.11	-0.12 (0.11)	0.296
Phosphorus (% dw)	0.28 (0.018) 0.22 - 0.34	0.28 (0.018) 0.21 - 0.34	0.13	-0.0069 (0.0060)	0.312
Potassium (% dw)	0.34 (0.011) 0.30 - 0.39	0.34 (0.011) 0.30 - 0.39	0.086	-0.0043 (0.0042)	0.367
Zinc (mg/kg dw)	16.56 (0.93) 13.16 - 20.77	17.01 (0.93) 13.57 - 20.23	6.65	-0.46 (0.26)	0.100

[1]Mean (S.E.) = least-square mean (standard error)
[2]Maximum value minus minimum value for the control maize hybrid
[3]dw=dry weight
The following components with more than 50% of observations below the assay LOQ were excluded from statistical analysis: sodium.

Table 56.   Summary of Maize Grain Vitamins for MON 87429 and Conventional Control

Component (mg/kg dw)[1]	MON 87429 Mean (S.E.)[2] Range	Control Mean (S.E.) Range	Control Range Value[3]	Difference (Test minus Control) Mean (S.E.)	p-Value
Vitamin A	1.05 (0.038) 0.88 - 1.25	1.02 (0.038) 0.81 - 1.26	0.46	0.023 (0.026)	0.375
Vitamin B_1	4.16 (0.094) 3.63 - 4.57	4.10 (0.094) 3.75 - 4.60	0.85	0.059 (0.067)	0.386
Vitamin B_2	1.70 (0.044) 1.44 - 2.01	1.70 (0.044) 1.40 - 2.20	0.79	0.0032 (0.051)	0.950
Vitamin B_3	20.28 (0.68) 16.25 - 24.94	20.35 (0.68) 17.65 - 26.01	8.36	-0.068 (0.71)	0.928
Vitamin B_6	5.22 (0.16) 4.00 - 5.98	5.31 (0.16) 4.63 - 6.03	1.40	-0.089 (0.13)	0.489
Vitamin B_9	0.61 (0.031) 0.38 - 0.93	0.63 (0.031) 0.39 - 0.85	0.46	-0.022 (0.044)	0.627
Vitamin E	9.84 (0.32) 7.85 - 11.43	10.74 (0.32) 9.50 - 12.56	3.06	-0.89 (0.21)	0.013

[1]dw=dry weight; Common names of vitamins: A=β-Carotene; B1= Thiamine HCl; B2=Riboflavin; B3=Niacin; B6= Pyridoxine HCl; B9=Folic Acid; E=α Tocopherol
[2]Mean (S.E.) = least-square mean (standard error)
[3]Maximum value minus minimum value for the control maize hybrid

Table 57.   Summary of Maize Grain Anti-Nutrients and Secondary Metabolites for MON 87429 and Conventional Control

Component	MON 87429 Mean (S.E.)[1] Range	Control Mean (S.E.) Range	Control Range Value[2]	Difference (Test minus Control) Mean (S.E.)	p-Value
Phytic acid (% dw)[3]	0.64 (0.060) 0.39 - 0.91	0.67 (0.060) 0.44 - 0.91	0.47	-0.033 (0.032)	0.355
Raffinose (% dw)	0.15 (0.020) 0.097 - 0.23	0.16 (0.020) 0.11 - 0.26	0.15	-0.010 (0.0056)	0.083
Ferulic acid (µg/g dw)	1879.28 (25.74) 1733.78 - 2057.47	1871.55 (25.74) 1653.18 - 2071.35	418.17	7.74 (32.71)	0.824
p-coumaric acid (µg/g dw)	133.30 (6.18) 117.78 - 153.05	130.19 (6.18) 108.37 - 210.59	102.22	3.10 (4.87)	0.528

[1]Mean (S.E.) = least-square mean (standard error)
[2]Maximum value minus minimum value for the control maize hybrid
[3]dw=dry weight
The following components with more than 50% of observations below the assay LOQ were excluded from statistical analysis: furfural.

Table 58. Summary of Maize Forage Proximates, Carbohydrates by Calculation, Fiber and Minerals for MON 87429 and Conventional Control

Component (% dw)[1]	MON 87429 Mean (S.E.)[2] Range	Control Mean (S.E.) Range	Control Range Value[3]	Difference (Test minus Control) Mean (S.E.)	p-Value
Protein	7.10 (0.20) 4.57 - 8.93	7.00 (0.20) 6.03 - 8.21	2.18	0.10 (0.22)	0.654
Total fat	2.93 (0.14) 2.20 - 3.54	2.81 (0.14) 1.58 - 3.41	1.83	0.12 (0.17)	0.507
Carbohydrates by calculation	86.32 (0.24) 84.46 - 89.56	86.51 (0.24) 85.04 - 88.11	3.07	-0.19 (0.33)	0.594
ADF	20.59 (0.92) 15.74 - 24.53	21.06 (0.92) 14.63 - 28.26	13.63	-0.47 (0.79)	0.562
NDF	33.63 (1.20) 26.99 - 44.93	34.76 (1.20) 26.95 - 42.49	15.54	-1.13 (1.39)	0.422
Ash	3.65 (0.22) 3.06 - 4.58	3.68 (0.22) 2.80 - 4.72	1.92	-0.034 (0.10)	0.743
Calcium	0.19 (0.013) 0.14 - 0.24	0.21 (0.013) 0.15 - 0.28	0.13	-0.017 (0.0078)	0.089
Phosphorus	0.16 (0.0074) 0.12 - 0.21	0.16 (0.0074) 0.12 - 0.22	0.10	-0.0027 (0.0081)	0.753

[1]dw=dry weight
[2]Mean (S.E.) = least-square mean (standard error)
[3]Maximum value minus minimum value for the control maize hybrid

Table 59. Literature and ILSI-CCDB Database Ranges for Components in Maize Grain and Forage

Tissue Components[1]	Literature Range[2]	ILSI Range[3]
Grain Nutrients		
Proximates		
protein (% dw)	8.27-13.33[a]; 9.17-12.19[b]	5.72-17.26
total fat (% dw)	2.95-4.40[a]; 3.18-4.23[b]	1.363-7.830
ash (% dw)	1.17-2.01[a]; 1.27-1.63[b]	0.616-6.282
Amino Acids		
alanine (% dw)	0.60-1.04[a]; 0.68-0.96[b]	0.44-1.48
arginine (% dw)	0.34-0.52[a]; 0.34-0.50[b]	0.12-0.71
aspartic acid (% dw)	0.52-0.78[a]; 0.59-0.76[b]	0.33-1.21
cystine (% dw)	0.19-0.26[a]; 0.20-0.26[b]	0.12-0.51
glutamic acid (% dw)	1.54-2.67[a]; 1.71-2.44[b]	0.97-3.54
glycine (% dw)	0.33-0.43[a]; 0.33-0.42[b]	0.184-0.685
histidine (% dw)	0.25-0.37[a]; 0.27-0.34[b]	0.14-0.46
isoleucine (% dw)	0.30-0.48[a]; 0.32-0.44[b]	0.18-0.69
leucine (% dw)	1.02-1.87[a]; 1.13-1.65[b]	0.64-2.49
lysine (% dw)	0.26-0.33[a]; 0.28-0.31[b]	0.129-0.668
methionine (% dw)	0.17-0.26[a]; 0.16-0.30[b]	0.11-0.47
phenylalanine (% dw)	0.43-0.72[a]; 0.45-0.63[b]	0.24-0.93
proline (% dw)	0.74-1.21[a]; 0.78-1.11[b]	0.46-1.75
serine (% dw)	0.39-0.67[a]; 0.43-0.6[b]	0.18-0.77
threonine (% dw)	0.29-0.45[a]; 0.31-0.39[b]	0.22-0.67
tryptophan (% dw)	0.047-0.085[a]; 0.042-0.07[b]	0.027-0.215
tyrosine (% dw)	0.13-0.43[a]; 0.12-0.41[b]	0.10-0.73
valine (% dw)	0.42-0.62[a]; 0.45-0.58[b]	0.27-0.86
Fatty Acids		
palmitic acid (% Total FA)	8.80-13.33[a]; 9.84-12.33[b]	6.81-26.55
palmitoleic acid (% Total FA)	0.059-0.23[a]	0.069-0.453
stearic acid (% Total FA)	1.36-2.14[a]; 1.3-2.1[b]	1.02-3.83
oleic acid (% Total FA)	19.50-33.71[a]; 19.59-29.13[b]	16.38-42.81
linoleic acid (% Total FA)	49.31-64.70[a]; 56.51-65.65[b]	34.27-67.68
linolenic acid (% Total FA)	0.89-1.56[a]; 1.03-1.38[b]	0.55-2.33
arachidic acid (% Total FA)	0.30-0.49[a]; 0.30-0.41[b]	0.267-0.993
eicosenoic acid (% Total FA)	0.17-0.29[a]; 0.17-0.27[b]	0.098-1.952
behenic acid (% Total FA)	0.069-0.28[a]; 0.059-0.18[b]	0.098-0.417
Carbohydrates By Calculation		
carbohydrates by calculation (% dw)	81.31-87.06[a]; 82.10-85.98[b]	77.4-89.7
Fiber		
ADF (% dw)	1.82-4.48[a]; 1.83-3.39[b]	1.41-11.34
NDF (% dw)	6.51-12.28[a]; 6.08-10.36[b]	4.28-22.64
TDF (% dw)	10.65-16.26[a]; 10.57-14.56[b]	6.68-35.31
Minerals		
calcium (% dw)	0.0036-0.0068[a]; 0.0035-0.007[b]	0.001-0.101
copper (mg/kg dw)	0.85-3.54[c]	0.55-21.20

Table 59.   Literature and ILSI-CCDB Database Ranges for Components in Maize Grain and Forage (continued)

Tissue Components[1]	Literature Range[2]	ILSI Range[3]
Minerals (cont.)		
iron (mg/kg dw)	14.17-23.40[a]; 15.90-24.66[b]	9.51-191.00
magnesium (% dw)	0.091-0.14[a]; 0.1-0.14[b]	0.06-0.19
manganese (mg/kg dw)	4.83-8.34[a]; 4.78-9.35[b]	1.69-14.30
phosphorus (% dw)	0.24-0.37[a]; 0.27-0.38[b]	0.13-0.55
potassium (% dw)	0.29-0.39[a]; 0.36-0.43[b]	0.18-0.60
zinc (mg/kg dw)	16.78-28.17[a]; 18.25-30.44[b]	6.5-42.6
Vitamins		
vitamin A (mg/kg dw)	0.14-11.27[d]	0.19-49.90
vitamin B$_1$ (mg/kg dw)	2.33-4.17[a]; 2.71-4.33[b]	1.26-40.00
vitamin B$_2$ (mg/kg dw)	0.94-2.42[a]; 1.64-2.81[b]	0.50-7.35
vitamin B$_3$ (mg/kg dw)	15.07-32.38[a]; 13.64-42.06[b]	7.42-46.94
vitamin B$_6$ (mg/kg dw)	4.93-7.53[a]; 4.97-8.27[b]	1.18-12.14
vitamin B$_9$ (mg/kg dw)	0.19-0.35[a]; 0.23-0.42[b]	0.09-3.50
vitamin E (mg/kg dw)	5.96-18.44[a]; 2.84-15.53[b]	0.84-68.67
Grain Other		
Anti-Nutrients		
phytic acid (% dw)	0.69-1.09[a]; 0.60-0.94[b]	0.111-1.940
raffinose (% dw)	0.079-0.22[a]; 0.061-0.15[b]	0.020-0.466
Secondary Metabolites		
ferulic acid (μg/g dw)	1205.75-2873.05[a]; 1011.40-2539.86[b]	291.93-4397.30
p-coumaric acid (μg/g dw)	94.77-327.39[a]; 66.48-259.68[b]	53.4-820.0
Forage Nutrients		
Proximates		
protein (% dw)	5.80-10.24[a]; 5.56-9.14[b]	3.14-16.32
total fat (% dw)	1.28-3.62[a]; 0.20-1.76[b]	0.296-6.755
ash (% dw)	2.67-8.01[a]; 4.59-6.9[b]	0.66-13.20
Carbohydrates By Calculation		
carbohydrates by calculation (% dw)	81.88-89.26[a]; 84.11-87.54[b]	73.3-92.9
Fiber		
ADF (% dw)	19.11-30.49[a]; 20.73-33.39[b]	9.90-47.39
NDF (% dw)	27.73-49.62[a]; 31.81-50.61[b]	20.29-67.80
Minerals		
calcium (% dw)	0.12-0.33[a]; 0.21-0.41[b]	0.06-0.58
phosphorus (% dw)	0.090-0.26[a]; 0.13-0.21[b]	0.07-0.44

[1]dw=dry weight; FA=Fatty Acid; mg/kg/ dw
[2]Literature range references: [a](Harrigan *et al.*, 2009) (see U.S. Field data);[b](Harrigan *et al.*, 2009) (see Chile field data);[c](Ridley *et al.*, 2011);[d](Egesel *et al.*, 2003)
[3]ILSI range is from ILSI Crop Composition Database, 2016 (Accessed February 21, 2017).

B7(a)(ii) Compositional assessment of MON 87429 conclusion

Compositional analysis was conducted on grain and forage of MON 87429 and the conventional control grown at five sites in the United States during the 2017 field season. Of the 61 components statistically assessed from forage and grain, 50 showed no statistically significant differences (p<0.05) between MON 87429 and the conventional control. A total of 11 components (total fat, palmitoleic acid, stearic acid, oleic acid, linoleic acid, linolenic acid, behenic acid, copper, iron, magnesium and vitamin E for grain) showed a statistically significant difference (p<0.05) between MON 87429 and the conventional control. For these components, the mean difference in component values between MON 87429 and the conventional control was less than the range of the conventional control values and the MON 87429 mean component values were within the range of values observed in the literature and/or the ILSI-CCDB.

These results support the overall conclusion that MON 87429 maize was not a major contributor to variation in component levels in grain or forage and confirmed the compositional equivalence of MON 87429 to the conventional control in levels of these components. The statistically significant differences observed were not compositionally meaningful from a food and feed safety perspective.

B7(b)   Levels of other GM-influenced constituents

Not applicable.

B7(c)   Levels of naturally-occurring allergenic proteins

Not applicable.

C.   NUTRITIONAL IMPACT

C1   Data on Nutritional Impact of Compositional Changes

Not Applicable.

C2   Data from an Animal Feeding Study, if Available

The data and information presented in this submission demonstrate that the food and feed derived from MON 87429 are as safe and nutritious as those derived from commercially-available, conventional maize for which there is an established history of safe consumption. Therefore, animal feeding studies do not add value to the safety of MON 87429.

PART 3   STATUTORY DECLARATION – AUSTRALIA

I, Nina McCormick, declare that the information provided in this application fully sets out the matters required and that the same are true to the best of my knowledge and belief, and that no information has been withheld that might prejudice this application.

Signature: _____

Declared before me .... Level 1, 8 Redfern Road, Hawthorn East VIC 3123
An Australian Legal Practitioner within the meaning
of the Legal Profession Uniform Law (Victoria)

This ....24th...................... day of ....October............. 2019.

28th

PART 4   REFERENCES

Adrian-Romero, M., G. Blunden, B.G. Carpenter and E. Tyihák. 1999. HPLC quantification of formaldehyde, as formaldemethone, in plants and plant-like organisms. Chromatographia 50:160-166.

Alarcón, A., F.T. Davies, R.L. Autenrieth and D.A. Zuberer. 2008. Arbuscular mycorrhiza and petroleum-degrading microorganisms enhance phytoremediation of petroleum-contaminated soil. International Journal of Phytoremediation 10:251-263.

Alibhai, M.F. and W.C. Stallings. 2001. Closing down on glyphosate inhibition - With a new structure for drug discovery. Proceedings of the National Academy of Sciences of the United States of America 98:2944-2946.

An, S.-q. and G. Berg. 2018. *Stenotrophomonas maltophilia*. Trends in Microbiology 26:637-638.

Anderson, J.E., J.M. Michno, T.J. Kono, A.O. Stec, B.W. Campbell, S.J. Curtin and R.M. Stupar. 2016. Genomic variation and DNA repair associated with soybean transgenesis: A comparison to cultivars and mutagenized plants. BMC Biotechnology 16:41.

Astwood, J.D., J.N. Leach and R.L. Fuchs. 1996. Stability of food allergens to digestion in vitro. Nature Biotechnology 14:1269-1273.

Barker, R.F., K.B. Idler, D.V. Thompson and J.D. Kemp. 1983. Nucleotide sequence of the T-DNA region from the *Agrobacterium tumefaciens* octopine Ti plasmid pTi15955. Plant Molecular Biology 2:335-350.

Barry, G.F., G.M. Kishore, S.R. Padgette and W.C. Stallings. 2001. Glyphosate-tolerant 5-enolpyruvylshikimate-3-phosphate synthases. Patent 6,248,876, U.S. Patent Office, Washington, D.C.

Bassetti, P. and M.E. Westgate. 1994. Floral asynchrony and kernel set in maize quantified by image analysis. Agronomy Journal 86:699-703.

███████ 2018. Nature of ^{14}C-2,4-Dichlorophenoxyacetic Acid (2,4-D) Residues in/on Corn Raw Agricultural Commodities Following Preemergence or Postemergence Application to Herbicide Tolerant Maize, MON 87429. Monsanto Technical Report MSL0029509. Chesterfield, Missouri.

Behrens, M.R., N. Mutlu, S. Chakraborty, R. Dumitru, W.Z. Jiang, B.J. LaVallee, P.L. Herman, T.E. Clemente and D.P. Weeks. 2007. Dicamba resistance: Enlarging and preserving biotechnology-based weed management strategies. Science 316:1185-1188.

Berg, G., P. Marten and G. Ballin. 1996. *Stenotrophomonas maltophilia* in the rhizosphere of oilseed rape - Occurrence, characterization and interaction with phytopathogenic fungi. Microbiological Research 151:19-27.

Berg, G. and J.L. Martinez. 2015. Friends or foes: Can we make a distinction between beneficial and harmful strains of the *Stenotrophomonas maltophilia* complex? Frontiers in Microbiology 6:241.

Berg, G., N. Roskot and K. Smalla. 1999. Genotypic and phenotypic relationships between clinical and environmental isolates of *Stenotrophomonas maltophilia*. Journal of Clinical Microbiology 37:3594-3600.

Berg, G., N. Roskot, A. Steidle, L. Eberl, A. Zock and K. Smalla. 2002. Plant-dependent genotypic and phenotypic diversity of antagonistic rhizobacteria isolated from different *Verticillium* host plants. Applied and Environmental Microbiology 68:3328-3338.

Berg, R.D. 1996. The indigenous gastrointestinal microflora. Trends in Microbiology 4:430-435.

Biron, D.G., C. Brun, T. Lefevre, C. Lebarbenchon, H.D. Loxdale, F. Chevenet, J.-P. Brizard and F. Thomas. 2006. The pitfalls of proteomics experiments without the correct use of bioinformatics tools. Proteomics 6:5577-5596.

Bisson, J., J. McAlpine, J. Graham and G.F. Pauli. 2016. NAPRALERT, from an historical information silo to a linked resource able to address the new challenges in Natural Products Chemistry and Pharmacognosy. Proceedings of the Joint International Conference on Biological Ontology and BioCreative, Corvallis, Oregon, United States.

Bradshaw, R.A., W.W. Brickey and K.W. Walker. 1998. N-terminal processing: The methionine aminopeptidase and N^α-acetyl transferase families. Trends in Biochemical Sciences 23:263-267.

Breyton, C. 2000. The cytochrome b_6f complex: Structural studies and comparison with the bc_1 complex. Biochimica et Biophysica Acta 1459:467-474.

Brodersen, P. and O. Voinnet. 2006. The diversity of RNA silencing pathways in plants. Trends in Genetics 22:268-280.

Brooke, J.S., G. Di Bonaventura, G. Berg and J.-L. Martinez. 2017. Editorial: A multidisciplinary look at *Stenotrophomonas maltophilia*: An emerging multi-drug-resistant global opportunistic pathogen. Frontiers in Microbiology 8:1511.

Buchanan, B.B., W. Gruissem and R.L. Jones. 2000. Phenylpropanoid and phenylpropanoid-acetate pathway metabolites. Pages 1286-1289 in Biochemistry and Molecular Biology of Plants. American Society of Plant Biologists, Rockville, Maryland.

Bugg, T.D.H. 2003. Dioxygenase enzymes: Catalytic mechanisms and chemical models. Tetrahedron 59:7075-7101.

Caetano-Anollés, G., M. Wang, D. Caetano-Anollés and J.E. Mittenthal. 2009. The origin, evolution and structure of the protein world. Biochemical Journal 417:621-637.

Capehart, T., O. Liefert and D. Olson. 2019. Feed outlook. FDS-19d. U.S. Department of Agriculture, Economic Research Service, Washington, D.C.

https://usda.library.cornell.edu/concern/publications/44558d29f?locale=en [Accessed April 22, 2019].

Carthew, R.W. and E.J. Sontheimer. 2009. Origins and mechanisms of miRNAs and siRNAs. Cell 136:642-655.

Chakraborty, S., M. Behrens, P.L. Herman, A.F. Arendsen, W.R. Hagen, D.L. Carlson, X.-Z. Wang and D.P. Weeks. 2005. A three-component dicamba *O*-demethylase from *Pseudomonas maltophilia*, strain DI-6: Purification and characterization. Archives of Biochemistry and Biophysics 437:20-28.

Chaudhary, D.K., S.-W. Jeong and J. Kim. 2017. *Sphingobium naphthae* sp. nov., with the ability to degrade aliphatic hydrocarbons, isolated from oil-contaminated soil. International Journal of Systematic and Evolutionary Microbiology 67:2986-2993.

Christ, B., R. Hochstrasser, L. Guyer, R. Francisco, S. Aubry, S. Hörtensteiner and J.-K. Weng. 2017. Non-specific activities of the major herbicide-resistance gene *BAR*. Nature Plants 3:937-945.

Clark, S.E. and G.K. Lamppa. 1992. Processing of the precursors for the light-harvesting chlorophyll-binding proteins of photosystem II and photosystem I during import and in an organelle-free assay. Plant Physiology 98:595-601.

Codex Alimentarius. 2009. Foods derived from modern biotechnology. Second Edition. Codex Alimentarius Commission, Joint FAO/WHO Food Standards Programme, Food and Agriculture Organization of the United Nations, Rome, Italy.

Cornejo, M.-J., D. Luth, K.M. Blankenship, O.D. Anderson and A.E. Blechl. 1993. Activity of a maize ubiquitin promoter in transgenic rice. Plant Molecular Biology 23:567-581.

Cross, T. 1989. Other genera. Pages 2586-2615 in Bergey's Manual of Systematic Bacteriology. Volume 4. S.T. Williams and M.E. Sharpe (eds.). Williams & Wilkins, Balitmore, Maryland.

Cunha, B.A. 2009. *Stenotrophomonas maltophilia*. WebMD, LLC, New York, New York. http://www.emedicine.com/med/topic3457.htm [Accessed January 2, 2010].

D'Ordine, R.L., T.J. Rydel, M.J. Storek, E.J. Sturman, F. Moshiri, R.K. Bartlett, G.R. Brown, R.J. Eilers, C. Dart, Y. Qi, S. Flasinski and S.J. Franklin. 2009. Dicamba monooxygenase: Structural insights into a dynamic Rieske oxygenase that catalyzes an exocyclic monooxygenation. Journal of Molecular Biology 392:481-497.

Darrouzet, E., J.W. Cooley and F. Daldal. 2004. The cytochrome bc_1 complex and its homologue the b_6f complex: Similarities and differences. Photosynthesis Research 79:25-44.

De Carolis, E. and V. De Luca. 1994. 2-Oxoglutarate-dependent dioxygenase and related enzymes: Biochemical characterization. Phytochemistry 36:1093-1107.

Delaney, B., J.D. Astwood, H. Cunny, R.E. Conn, C. Herouet-Guicheney, S. MacIntosh, L.S. Meyer, L. Privalle, Y. Gao, J. Mattsson, M. Levine and ILSI. 2008. Evaluation of protein

safety in the context of agricultural biotechnology. Food and Chemical Toxicology 46:S71-S97.

della-Cioppa, G., S.C. Bauer, B.K. Klein, D.M. Shah, R.T. Fraley and G.M. Kishore. 1986. Translocation of the precursor of 5-enolpyruvylshikimate-3-phosphate synthase into chloroplasts of higher plants *in vitro*. Proceedings of the National Academy of Sciences of the United States of America 83:6873-6877.

Denton, M. and K.G. Kerr. 1998. Microbiological and clinical aspects of infection associated with *Stenotrophomonas maltophilia*. Clinical Microbiology Reviews 11:57-80.

Denton, M., N.J. Todd, K.G. Kerr, P.M. Hawkey and J.M. Littlewood. 1998. Molecular epidemiology of *Stenotrophomonas maltophilia* isolated from clinical specimens from patients with cystic fibrosis and associated environmental samples. Journal of Clinical Microbiology 36:1953-1958.

Depicker, A., S. Stachel, P. Dhaese, P. Zambryski and H.M. Goodman. 1982. Nopaline synthase: Transcript mapping and DNA sequence. Journal of Molecular and Applied Genetics 1:561-573.

Dong, H., C. Zhu, J. Chen, X. Ye and Y.-P. Huang. 2015. Antibacterial activity of S*tenotrophomonas maltophilia* endolysin P28 against both gram-positive and gram-negative bacteria. Frontiers in Microbiology 6:1299.

Duke, S.O. 2005. Taking stock of herbicide-resistant crops ten years after introduction. Pest Management Science 61:211-218.

Dumitru, R., W.Z. Jiang, D.P. Weeks and M.A. Wilson. 2009. Crystal structure of dicamba monooxygenase: A Rieske nonheme oxygenase that catalyzes oxidative demethylation. Journal of Molecular Biology 392:498-510.

Duvick, D.N. 2005. The contribution of breeding to yield advances in maize (*Zea mays* L.). Advances in Agronomy 86:83-145.

Echemendia, Y. 2010. Microorganism of the month: *Stenotrophomonas maltophilia*. Environmental Microbiology Laboratory, Inc., Cherry Hill, New Jersey. http://www.emlab.com/s/sampling/env-report-07-2007.html [Accessed August 10, 2010].

Edgerton, M.D. 2009. Increasing crop productivity to meet global needs for feed, food, and fuel. Plant Physiology 149:7-13.

EFSA. 2011. Review of the existing maximum residue levels (MRLs) for 2,4-D according to Article 12 of Regulation (EC) No 396/2005. EFSA Journal 9:2431.

EFSA, A. Brancato, D. Brocca, L. Carrasco Cabrera, C. De Lentdecker, Z. Erdos, L. Ferreira, L. Greco, S. Jarrah, D. Kardassi, R. Leuschner, C. Lythgo, P. Medina, I. Miron, T. Molnar, R. Pedersen, H. Reich, C. Riemenschneider, A. Sacchi, M. Santos, A. Stanek, J. Sturma, J. Tarazona, A. Theobald, B. Vagenende and L. Villamar-Bouza. 2018. Setting of import tolerance for quizalofop-P-ethyl in genetically modified maize. EFSA Journal 16:e05250.

Egesel, C.O., J.C. Wong, R.J. Lambert and T.R. Rocheford. 2003. Gene dosage effects on carotenoid concentration in maize grain. Maydica 48:183-190.

Enya, J., H. Shinohara, S. Yoshida, T. Tsukiboshi, H. Negishi, K. Suyama and S. Tsushima. 2007. Culturable leaf-associated bacteria on tomato plants and their potential as biological control agents. Microbial Ecology 53:524-536.

FAO-WHO. 1991. Strategies for assessing the safety of foods produced by biotechnology. Report of joint FAO/WHO consultation. World Health Organization, Geneva, Switzerland.

FAO-WHO. 2011a. Summary report: Acceptable daily intakes, acute reference doses, short-term and long-term dietary intakes, recommended maximum residue limits and supervised trials median residue values recorded by the 2011 meeting. Food and Agriculture Organization of the United Nations, World Health Organization, Geneva, Switzerland.

FAO-WHO. 2011b. Pesticide residues in food 2010: Joint FAO/WHO meeting on pesticide residues. FAO Plant Production and Protection Paper 200. Food and Agriculture Organization of the United Nations, World Health Organization, Rome, Italy.

Ferraro, D.J., L. Gakhar and S. Ramaswamy. 2005. Rieske business: Structure-function of Rieske non-heme oxygenases. Biochemical and Biophysical Research and Communications 338:175-190.

Fialho, A.M., L.M. Moreira, A.T. Granja, A.O. Popescu, K. Hoffmann and I. Sá-Correia. 2008. Occurrence, production, and applications of gellan: Current state and perspectives. Applied Microbiology and Biotechnology 79:889-900.

Fire, A., S. Xu, M.K. Montgomery, S.A. Kostas, S.E. Driver and C.C. Mello. 1998. Potent and specific genetic interference by double-stranded RNA in *Caenorhabditis elegans*. Nature 391:806-811.

Fling, M.E., J. Kopf and C. Richards. 1985. Nucleotide sequence of the transposon Tn*7* gene encoding an aminoglycoside-modifying enzyme, 3"(9)-*O*-nucleotidyltransferase. Nucleic Acids Research 13:7095-7106.

Franz, J.E., M.K. Mao and J.A. Sikorski. 1997. Glyphosate's molecular mode of action. Pages 521-535 in Glyphosate: A Unique Global Herbicide. American Chemical Society, Washington, D.C.

Frottin, F., A. Martinez, P. Peynot, S. Mitra, R.C. Holz, C. Giglione and T. Meinnel. 2006. The proteomics of N-terminal methionine cleavage. Molecular & Cellular Proteomics 5:2336-2349.

Fu, T.-J., U.R. Abbott and C. Hatzos. 2002. Digestibility of food allergens and nonallergenic proteins in simulated gastric fluid and simulated intestinal fluid - A comparative study. Journal of Agricultural and Food Chemistry 50:7154-7160.

Galinat, W.C. 1988. The origin of corn. Pages 1-31 in Corn and Corn Improvement. Third Edition. G.F. Sprague and J.W. Dudley (eds.). American Society of Agronomy, Inc., Crop

Science Society of America, Inc., Soil Science Society of America, Inc., Madison, Wisconsin.

Giglione, C., A. Boularot and T. Meinnel. 2004. Protein N-terminal methionine excision. Cellular and Molecular Life Sciences 61:1455-1474.

Goodfellow, M. and S.T. Williams. 1983. Ecology of actinomycetes. Annual Review of Microbiology 37:189-216.

Goodman, M.M. 1988. The history and evolution of maize. Critical Reviews in Plant Sciences 7:197-220.

Gorski, S.A., J. Vogel and J.A. Doudna. 2017. RNA-based recognition and targeting: Sowing the seeds of specificity. Nature Reviews Molecular Cell Biology 18:215-228.

Gray, J., E. Wardzala, M. Yang, S. Reinbothe, S. Haller and F. Pauli. 2004. A small family of LLS1-related non-heme oxygenases in plants with an origin amongst oxygenic photosynthesizers. Plant Molecular Biology 54:39-54.

Griffin, S.L., J.A. Godbey, T.J. Oman, S.K. Embrey, A. Karnoup, K. Kuppannan, B.W. Barnett, G. Lin, N.V.J. Harpham, A.N. Juba, B.W. Schafer and R.M. Cicchillo. 2013. Characterization of aryloxyalkanoate dioxygenase-12, a nonheme Fe(II)/α-ketoglutarate-dependent dioxygenase, expressed in transgenic soybean and *Pseudomonas fluorescens*. Journal of Agricultural and Food Chemistry 61:6589-6596.

Gruys, K.J., M.C. Walker and J.A. Sikorski. 1992. Substrate synergism and the steady-state kinetic reaction mechanism for EPSP synthase from *Escherichia coli*. Biochemistry 31:5534-5544.

Hamilton, D.A., M. Roy, J. Rueda, R.K. Sindhu, J. Stanford and J.P. Mascarenhas. 1992. Dissection of a pollen-specific promoter from maize by transient transformation assay. Plant Molecular Biology 18:211-218.

Hammond, B.G. and R.L. Fuchs. 1998. Safety evaluation for new varieties of food crops developed through biotechnology. Pages 61-79 in Biotechnology and Safety Assessment. Second Edition. J.A. Thomas (ed.). Taylor & Francis, Philadelphia, Pennsylvania.

Hammond, B.G. and J.M. Jez. 2011. Impact of food processing on the safety assessment for proteins introduced into biotechnology-derived soybean and corn crops. Food and Chemical Toxicology 49:711-721.

Harayama, S., M. Kok and E.L. Neidle. 1992. Functional and evolutionary relationships among diverse oxygenases. Annual Review of Microbiology 46:565-601.

Harrigan, G.G., D. Lundry, S. Drury, K. Berman, S.G. Riordan, M.A. Nemeth, W.P. Ridley and K.C. Glenn. 2010. Natural variation in crop composition and the impact of transgenesis. Nature Biotechnology 28:402-404.

Harrigan, G.G., W.P. Ridley, K.D. Miller, R. Sorbet, S.G. Riordan, M.A. Nemeth, W. Reeves and T.A. Pester. 2009. The forage and grain of MON 87460, a drought-tolerant corn hybrid,

are compositionally equivalent to that of conventional corn. Journal of Agricultural and Food Chemistry 57:9754-9763.

Harrison, L.A., M.R. Bailey, M.W. Naylor, J.E. Ream, B.G. Hammond, D.L. Nida, B.L. Burnette, T.E. Nickson, T.A. Mitsky, M.L. Taylor, R.L. Fuchs and S.R. Padgette. 1996. The expressed protein in glyphosate-tolerant soybean, 5-enolpyruvylshikimate-3-phosphate synthase from *Agrobacterium* sp. strain CP4, is rapidly digested in vitro and is not toxic to acutely gavaged mice. Journal of Nutrition 126:728-740.

Haslam, E. 1993. Introduction, commentary and overview. Pages 1-16 in Shikimic Acid: Metabolism and Metabolites. John Wiley and Sons, Inc., Chichester, England.

Hausinger, R.P. 2004. Fe(II)/α-Ketoglutarate-dependent hydroxylases and related enzymes. Critical Reviews in Biochemistry and Molecular Biology 39:21-68.

Heck, G.R., C.L. Armstrong, J.D. Astwood, C.F. Behr, J.T. Bookout, S.M. Brown, T.A. Cavato, D.L. DeBoer, M.Y. Deng, C. George, J.R. Hillyard, C.M. Hironaka, A.R. Howe, E.H. Jakse, B.E. Ledesma, T.C. Lee, R.P. Lirette, M.L. Mangano, J.N. Mutz, Y. Qi, R.E. Rodriguez, S.R. Sidhu, A. Silvanovich, M.A. Stoecker, R.A. Yingling and J. You. 2005. Development and characterization of a CP4 EPSPS-based, glyphosate-tolerant corn event. Crop Science 45:329-339.

Heller, D., E.J. Helmerhorst, A.C. Gower, W.L. Siqueira, B.J. Paster and F.G. Oppenheim. 2016. Microbial diversity in the early *in vivo*-formed dental biofilm. Applied and Environmental Microbiology 82:1881-1888.

Helm, R.M. 2001. Topic 5: Stability of known allergens (digestive and heat stability). Joint FAO/WHO expert consultation on foods derived from biotechnology. Food and Agriculture Organization of the United Nations, Rome, Italy.

Herman, P.L., M. Behrens, S. Chakraborty, B.M. Chrastil, J. Barycki and D.P. Weeks. 2005. A three-component dicamba *O*-demethylase from *Pseudomonas maltophilia*, strain DI-6: Gene isolation, characterization, and heterologous expression. Journal of Biological Chemistry 280:24759-24767.

Hérouet, C., D.J. Esdaile, B.A. Mallyon, E. Debruyne, A. Schulz, T. Currier, K. Hendrickx, R.-J. van der Klis and D. Rouan. 2005. Safety evaluation of the phosphinothricin acetyltransferase proteins encoded by the *pat* and *bar* sequences that confer tolerance to glufosinate-ammonium herbicide in transgenic plants. Regulatory Toxicology and Pharmacology 41:134-149.

Herrmann, K.M. 1995. The shikimate pathway: Early steps in the biosynthesis of aromatic compounds. The Plant Cell 7:907-919.

Hibino, T., R. Waditee, E. Araki, H. Ishikawa, K. Aoki, Y. Tanaka and T. Takabe. 2002. Functional characterization of choline monooxygenase, an enzyme for betaine synthesis in plants. Journal of Biological Chemistry 277:41352-41360.

Hileman, R.E., A. Silvanovich, R.E. Goodman, E.A. Rice, G. Holleschak, J.D. Astwood and S.L. Hefle. 2002. Bioinformatic methods for allergenicity assessment using a comprehensive allergen database. International Archives of Allergy and Immunology 128:280-291.

Hochuli, E., W. Bannwarth, H. Döbeli, R. Gentz and D. Stüber. 1988. Genetic approach to facilitate purification of recombinant proteins with a novel metal chelate adsorbent. Nature Biotechnology 6:1321-1325.

Hoff, M., D.-Y. Son, M. Gubesch, K. Ahn, S.-I. Lee, S. Vieths, R.E. Goodman, B.K. Ballmer-Weber and G.A. Bannon. 2007. Serum testing of genetically modified soybeans with special emphasis on potential allergenicity of the heterologous protein CP4 EPSPS. Molecular Nutrition & Food Research 51:946-955.

Holtorf, S., K. Apel and H. Bohlmann. 1995. Comparison of different constitutive and inducible promoters for the overexpression of transgenes in *Arabidopsis thaliana*. Plant Molecular Biology 29:637-646.

Hunt, A.G. 1994. Messenger RNA 3' end formation in plants. Annual Review of Plant Physiology and Plant Molecular Biology 45:47-60.

Illergård, K., D.H. Ardell and A. Elofsson. 2009. Structure is three to ten times more conserved than sequence - A study of structural response in protein cores. Proteins 77:499-508.

ILSI-CERA. 2010. A review of the environmental safety of the CP4 EPSPS protein. International Life Sciences Institute, Center for Environmental Risk Assessment, Washington, D.C.

ILSI-CERA. 2011. A review of the environmental safety of the PAT protein. International Life Sciences Institute, Center for Environmental Risk Assessment, Washington, D.C.

Janas, K.M., M. Cvikrová, A. Palągiewicz and J. Eder. 2000. Alterations in phenylpropanoid content in soybean roots during low temperature acclimation. Plant Physiology and Biochemistry 38:587-593.

Jin, D., X. Kong, B. Cui, Z. Bai and H. Zhang. 2013. Biodegradation of di-n-butyl phthalate by a newly isolated *Halotolerant Sphingobium* sp. International Journal of Molecular Sciences 14:24046-24054.

Jones-Rhoades, M.W., D.P. Bartel and B. Bartel. 2006. MicroRNAs and their regulatory roles in plants. Annual Review of Plant Biology 57:19-53.

Juhnke, M.E. and E. des Jardin. 1989. Selective medium for isolation of *Xanthomonas maltophilia* from soil and rhizosphere environments. Applied and Environmental Microbiology 55:747-750.

Juhnke, M.E., D.E. Mathre and D.C. Sands. 1987. Identification and characterization of rhizosphere-competent bacteria of wheat. Applied and Environmental Microbiology 53:2793-2799.

Kämpfer, P. 2006. The family *Streptomycetaceae*, Part I: Taxonomy. Pages 538-604 in The Prokaryotes. A Handbook on the Biology of Bacteria: Archaea. Bacteria: Firmicutes, Actinomycetes. Volume 3. M.Dworkin, S. Falkow, E. Rosenberg, K.-H. Schleifer, and E. Stackebrandt (eds.). Springer+ Business Media, LLC., New York, New York.

Kiesselbach, T.A. 1949. The structure and reproduction of corn. Research Bulletin 161. University of Nebraska College of Agriculture, Agricultural Experiment Station, Lincoln, NE.

Kishore, G., D. Shah, S. Padgette, G. della-Cioppa, C. Gasser, D. Re, C. Hironaka, M. Taylor, J. Wibbenmeyer, D. Eichholtz, M. Hayford, N. Hoffmann, X. Delannay, R. Horsch, H. Klee, S. Rogers, D. Rochester, L. Brundage, P. Sanders and R.T. Fraley. 1988. 5-enolpyruvylshikimate 3-phosphate synthase. From biochemistry to genetic engineering of gIyphosate tolerance. Pages 37-48 in Biotechnology for Crop Protection. P.A. Hedin, J.J. Menn, and R.M. Hollingworth (eds.). American Chemical Society, Washington, D.C.

Klee, H.J., Y.M. Muskopf and C.S. Gasser. 1987. Cloning of an *Arabidopsis thaliana* gene encoding 5-enolpyruvylshikimate-3-phosphate synthase: Sequence analysis and manipulation to obtain glyphosate-tolerant plants. Molecular and General Genetics 210:437-442.

Kovalic, D., C. Garnaat, L. Guo, Y. Yan, J. Groat, A. Silvanovich, L. Ralston, M. Huang, Q. Tian, A. Christian, N. Cheikh, J. Hjelle, S. Padgette and G. Bannon. 2012. The use of next generation sequencing and junction sequence analysis bioinformatics to achieve molecular characterization of crops improved through modern biotechnology. The Plant Genome 5:149-163.

Krause, E., H. Wenschuh and P.R. Jungblut. 1999. The dominance of arginine-containing peptides in MALDI-derived tryptic mass fingerprints of proteins. Analytical Chemistry 71:4160-4165.

Krueger, J.P., R.G. Butz, Y.H. Atallah and D.J. Cork. 1989. Isolation and identification of microorganisms for the degradation of dicamba. Journal of Agricultural and Food Chemistry 37:534-538.

Kundu, S. 2012. Distribution and prediction of catalytic domains in 2-oxoglutarate dependent dioxygenases. BMC Research Notes 5:410.

Kutzner, H.J. 1981. The family streptomycetaceae. Pages 2028-2090 in The Prokaryotes: A Handbook on Habitats, Isolation, and Identification of Bacteria. Volume 2. M.P. Starr, H. Stolp, H.G. Trüper, A. Balows, and H.G. Schlegel (eds.). Springer-Verlag, Berlin, Germany.

Lambert, B., F. Leyns, L. Van Rooyen, F. Gosselé, Y. Papon and J. Swings. 1987. Rhizobacteria of maize and their antifungal activities. Applied and Environmental Microbiology 53:1866-1871.

Lamppa, G.K., G. Morelli and N.-H. Chua. 1985. Structure and developmental regulation of a wheat gene encoding the major chlorophyll a/b-binding polypeptide. Molecular and Cellular Biology 5:1370-1378.

Leath, M.N. and L.D. Hill. 1987. Economics of production, marketing, and utilization. Pages 210-219 in Corn: Chemistry and Technology. S.A. Watson and P.E. Ramstad (eds.). American Association of Cereal Chemists, St. Paul, Minnesota.

Lege, K.E., J.T. Cothren and C.W. Smith. 1995. Phenolic acid and condensed tannin concentrations of six cotton genotypes. Environmental and Experimental Botany 35:241-249.

Liener, I.E. 1994. Implications of antinutritional components in soybean foods. Critical Reviews in Food Science and Nutrition 34:31-67.

Lira, F., G. Berg and J.L. Martínez. 2017. Double-face meets the bacterial world: The opportunistic pathogen *Stenotrophomonas maltophilia*. Frontiers in Microbiology 8:2190.

Locci, R. 1989. Streptomycetes and related genera. Pages 2451-2508 in Bergey's Manual of Systematic Bacteriology. Volume 4. S.T. Williams and M.E. Sharpe (eds.). Williams & Wilkins, Baltimore, Maryland.

Loy, D.D. and E.L. Lundy. 2019. Nutritional properties and feeding value of corn and its coproducts. Pages 633-659 in Corn: Chemistry and Technology. Third Edition. S.O. Serna-Saldivar (ed.). Woodhead Publishing and AACC International Press.

Maeda, H. and N. Dudareva. 2012. The shikimate pathway and aromatic amino acid biosynthesis in plants. Annual Review of Plant Biology 63:73-105.

Makarova, K.S., Y.I. Wolf and E.V. Koonin. 2009. Comprehensive comparative-genomic analysis of Type 2 toxin-antitoxin systems and related mobile stress response systems in prokaryotes. Biology Direct 4:19.

Manderscheid, R. and A. Wild. 1986. Studies on the mechanism of inhibition by phosphinothricin of glutamine synthetase isolated from *Triticum aestivum* L. Journal of Plant Physiology 123:135-142.

May, J.B. 1987. Wet milling: Process and products. Pages 377-397 in Corn: Chemistry and Technology. S.A. Watson and P.E. Ramstad (eds.). American Association of Cereal Chemists, St. Paul, Minnesota.

McElroy, D., W. Zhang, J. Cao and R. Wu. 1990. Isolation of an efficient actin promoter for use in rice transformation. The Plant Cell 2:163-171.

Mehrotra, S. and V. Goyal. 2012. *Agrobacterium*-mediated gene transfer in plants and biosafety considerations. Applied Biochemistry and Biotechnology 168:1953-1975.

Meinnel, T. and C. Giglione. 2008. Tools for analyzing and predicting N-terminal protein modifications. Proteomics 8:626-649.

Metcalfe, D.D., J.D. Astwood, R. Townsend, H.A. Sampson, S.L. Taylor and R.L. Fuchs. 1996. Assessment of the allergenic potential of foods derived from genetically engineered crop plants. Critical Reviews in Food Science and Nutrition 36:S165-S186.

Moreno, F.J., F.A. Mellon, M.S.J. Wickham, A.R. Bottrill and E.N.C. Mills. 2005. Stability of the major allergen Brazil nut 2S albumin (Ber e 1) to physiologically relevant *in vitro* gastrointestinal digestion. FEBS Journal 272:341-352.

Mukherjee, P. and P. Roy. 2016. Genomic potential of *Stenotrophomonas maltophilia* in bioremediation with an assessment of its multifaceted role in our environment. Frontiers in Microbiology 7:967.

Müller, T.A., M.I. Zavodszky, M. Feig, L.A. Kuhn and R.P. Hausinger. 2006. Structural basis for the enantiospecificities of *R*- and *S*-specific phenoxypropionate/α-ketoglutarate dioxygenases. Protein Science 15:1356-1368.

Nam, J.-W., H. Nojiri, T. Yoshida, H. Habe, H. Yamane and T. Omori. 2001. New classification system for oxygenase components involved in ring-hydroxylating oxygenations. Bioscience, Biotechnology, and Biochemistry 65:254-263.

Nester, E.W. 2015. *Agrobacterium*: Nature's genetic engineer. Frontiers in Plant Science 5:730.

Nunes, F.V. and I.S. de Melo. 2006. Isolation and characterization of endophytic bacteria of coffee plants and their potential in caffeine degradation. Environmental Toxicology 10:293-297.

Odell, J.T., F. Nagy and N.-H. Chua. 1985. Identification of DNA sequences required for activity of the cauliflower mosaic virus 35S promoter. Nature 313:810-812.

OECD. 1999. Consensus document on general information concerning the genes and their enzymes that confer tolerance to phosphinothricin herbicide. ENV/JM/MONO(99)13. Series on Harmonization of Regulatory Oversight in Biotechnology No.11. Organisation for Economic Co-operation and Development, Paris, France.

OECD. 2002a. Module II: Herbicide biochemistry, herbicide metabolism and the residues in glufosinate-ammonium (Phosphinothricin)-tolerant transgenic plants. ENV/JM/MONO(2002)14. Series on Harmonization of Regulatory Oversight in Biotechnology No. 25. Organisation for Economic Co-operation and Development, Paris, France.

OECD. 2002b. Consensus document on compositional considerations for new varieties of maize (*Zea mays*): Key food and feed nutrients, anti-nutrients and secondary plant metabolites. ENV/JM/MONO(2002)25. Series on the Safety of Novel Foods and Feeds, No. 6. Organisation for Economic Co-operation and Development, Paris, France.

OECD. 2002c. Report of the OECD workshop on the toxicological and nutritional testing of novel foods. SG/ICGB(1998)1/FINAL. Organisation for Economic Co-operation and Development, Paris, France.

OECD. 2003. Consensus document on the biology of *Zea mays* subsp. *mays* (maize). ENV/JM/MONO(2003)11. Series on Harmonisation of Regulatory Oversight in Biotechnology No. 27. Organisation for Economic Co-operation and Development, Paris, France.

OGTR. 2008. The biology of *Zea mays* L. ssp *mays* (maize or corn). Version 1, September 2008, Australian Government, Department of Health and Ageing, Office of the Gene Technology Regulator, Canberra, Australia.

Okuno, N.T., I.R. Freire, R.T.R.S. Segundo, C.R. Silva and V.A. Marin. 2018. Polymerase chain reaction assay for detection of *Stenotrophomonas maltophilia* in cheese samples based on the *smeT* gene. Current Microbiology 75:1555-1559.

Okunuki, H., R. Techima, T. Shigeta, J. Sakushima, H. Akiyama, Y. Goda, M. Toyoda and J. Sawada. 2002. Increased digestibility of two products in genetically modified food (CP4 EPSPS and Cry1Ab) after preheating. Journal of the Food Hygienic Society of Japan 43:68-73.

Padgette, S.R., D.B. Re, G.F. Barry, D.E. Eichholtz, X. Delannay, R.L. Fuchs, G.M. Kishore and R.T. Fraley. 1996. New weed control opportunities: Development of soybeans with a Roundup Ready^{TM} gene. Pages 53-84 in Herbicide-Resistant Crops: Agricultural, Environmental, Economic, Regulatory and Technical Aspects. S.O. Duke (ed.). CRC Press, Inc., Boca Raton, Florida.

Palleroni, N.J. and J.F. Bradbury. 1993. *Stenotrophomonas*, a new bacterial genus for *Xanthomonas maltophilia* (Hugh 1980) Swings et al. 1983. International Journal of Systematic Bacteriology 43:606-609.

Pariza, M.W. and E.A. Johnson. 2001. Evaluating the safety of microbial enzyme preparations used in food processing: Update for a new century. Regulatory Toxicology and Pharmacology 33:173-186.

Poehlman, J.M. and D.A. Sleper. 1995. Breeding corn (maize). Pages 321-344 in Breeding Field Crops. Fourth Edition. Iowa State University Press, Ames, Iowa.

Pozo, C., B. Rodelas, M.V. Martínez-Toledo, R. Vílchez and J. González-López. 2007. Removal of organic load from olive washing water by an aerated submerged biofilter and profiling of the bacterial community involved in the process. Journal of Microbiology and Biotechnology 17:784-791.

Prado, J.R., G. Segers, T. Voelker, D. Carson, R. Dobert, J. Phillips, K. Cook, C. Cornejo, J. Monken, L. Grapes, T. Reynolds and S. Martino-Catt. 2014. Genetically engineered crops: From idea to product. Annual Review of Plant Biology 65:769-790.

Rademacher, T.W., R.B. Parekh and R.A. Dwek. 1988. Glycobiology. Annual Review of Biochemistry 57:785-838.

Rathinasabapathi, B., M. Burnet, B.L. Russell, D.A. Gage, P.-C. Liao, G.J. Nye, P. Scott, J.H. Golbeck and A.D. Hanson. 1997. Choline monooxygenase, an unusual iron-sulfur enzyme catalyzing the first step of glycine betaine synthesis in plants: Prosthetic group characterization and cDNA cloning. Proceedings of the National Academy of Sciences of the United States of America 94:3454-3458.

Rausch, K.D., D. Hummel, L.A. Johnson and J.B. May. 2019. Wet milling: The basis for corn biorefineries. Pages 501-535 in Corn: Chemistry and Technology. Third Edition. S.O. Serna-Saldivar (ed.). Woodhead Publishing, Duxford, United Kingdom.

Richter, S. and G.K. Lamppa. 1998. A chloroplast processing enzyme functions as the general stromal processing peptidase. Proceedings of the National Academy of Sciences of the United States of America 95:7463-7468.

Ridley, W.P., G.G. Harrigan, M.L. Breeze, M.A. Nemeth, R.S. Sidhu and K.C. Glenn. 2011. Evaluation of compositional equivalence for multitrait biotechnology crops. Journal of Agricultural and Food Chemistry 59:5865-5876.

Rijavec, T., A. Lapanje, M. Dermastia and M. Rupnik. 2007. Isolation of bacterial endophytes from germinated maize kernels. Canadian Journal of Microbiology 53:802-808.

Rooney, L.W. and S.O. Serna-Saldivar. 2003. Food uses of whole corn and dry-milled fractions. Pages 495-535 in Corn: Chemistry and Technology. Second Edition. P.J. White and L.A. Johnson (eds.). American Association of Cereal Chemists, St. Paul, Minnesota.

Rosche, B., B. Tshisuaka, B. Hauer, F. Lingens and S. Fetzner. 1997. 2-oxo-1,2-dihydroquinoline 8-monooxygenase: Phylogenetic relationship to other multicomponent nonheme iron oxygenases. Journal of Bacteriology 179:3549-3554.

Russell, B.L., B. Rathinasabapathi and A.D. Hanson. 1998. Osmotic stress induces expression of choline monooxygenase in sugar beet and amaranth. Plant Physiology 116:859-865.

Russell, W.A. and A.R. Hallauer. 1980. Corn. Pages 299-312 in Hybridization of Crop Plants. W.R. Fehr and H.H. Hadley (eds.). American Society of Agronomy, Inc., Crop Science Society of America, Inc., Madison, Wisconsin.

Ryan, R.P., S. Monchy, M. Cardinale, S. Taghavi, L. Crossman, M.B. Avison, G. Berg, D. van der Lelie and J.M. Dow. 2009. The versatility and adaptation of bacteria from the genus *Stenotrophomonas*. Nature Reviews Microbiology 7:514-525.

Salomon, S. and H. Puchta. 1998. Capture of genomic and T-DNA sequences during double-strand break repair in somatic plant cells. EMBO Journal 17:6086-6095.

Schmelz, E.A., J. Engelberth, H.T. Alborn, P. O'Donnell, M. Sammons, H. Toshima and J.H. Tumlinson. 2003. Simultaneous analysis of phytohormones, phytotoxins, and volatile organic compounds in plants. Proceedings of the National Academy of Sciences of the United States of America 100:10552-10557.

Schmidt, C.L. and L. Shaw. 2001. A comprehensive phylogenetic analysis of Rieske and Rieske-type iron-sulfur proteins. Journal of Bioenergetics and Biomembranes 33:9-26.

Sidorov, V. and D. Duncan. 2009. *Agrobacterium*-mediated maize transformation: Immature embryos versus callus. Pages 47-58 in Methods in Molecular Biology: Transgenic Maize - Methods and Protocols. M.P. Scott (ed.). Humana Press, Inc, Totowa, New Jersey.

Sikorski, J.A. and K.J. Gruys. 1997. Understanding glyphosate's molecular mode of action with epsp synthase: Evidence favoring an allosteric inhibitor model. Accounts of Chemical Research 30:2-8.

Silvanovich, A., M.A. Nemeth, P. Song, R. Herman, L.Tagliani and G.A. Bannon. 2006. The value of short amino acid sequence matches for prediction of protein allergenicity. Toxicological Sciences 90:252-258.

Sjoblad, R.D., J.T. McClintock and R. Engler. 1992. Toxicological considerations for protein components of biological pesticide products. Regulatory Toxicology and Pharmacology 15:3-9.

Stalker, D.M., C.M. Thomas and D.R. Helinski. 1981. Nucleotide sequence of the region of the origin of replication of the broad host range plasmid RK2. Molecular and General Genetics 181:8-12.

Steinrücken, H.C. and N. Amrhein. 1980. The herbicide glyphosate is a potent inhibitor of 5-enolpyruvylshikimic acid-3-phosphate synthase. Biochemical and Biophysical Research Communications 94:1207-1212.

Sutcliffe, J.G. 1979. Complete nucleotide sequence of the *Escherichia coli* plasmid pBR322. Cold Spring Harbor Symposia on Quantitative Biology 43:77-90.

Swings, J., P. De Vos, M. Van den Mooter and J. De Ley. 1983. Transfer of *Pseudomonas maltophilia* Hugh 1981 to the genus *Xanthomonas* as *Xanthomonas maltophilia* (Hugh 1981) comb. nov. International Journal of Systematic Bacteriology 33:409-413.

Takeuchi, M., K. Hamana and A. Hiraishi. 2001. Proposal of the genus *Sphingomanas sensu stricto* and three new genera, *Sphingobium*, *Novosphingobium* and *Sphingopyxis*, on the basis of phylogenetic and chemotaxonomic analyses. International Journal of Systematic and Evolutionary Microbiology 51:1405-1417.

Tashkov, W. 1996. Determination of formaldehyde in foods, biological media and technological materials by headspace gas chromatography. Chromatographia 43:625-627.

Terada, R. and K. Shimamoto. 1990. Expression of CaMV35S-GUS gene in transgenic rice plants. Molecular and General Genetics 220:389-392.

Thomas, K., M. Aalbers, G.A. Bannon, M. Bartels, R.J. Dearman, D.J. Esdaile, T.J. Fu, C.M. Glatt, N. Hadfield, C. Hatzos, S.L. Hefle, J.R. Heylings, R.E. Goodman, B. Henry, C. Herouet, M. Holsapple, G.S. Ladics, T.D. Landry, S.C. MacIntosh, E.A. Rice, L.S. Privalle, H.Y. Steiner, R. Teshima, R. van Ree, M. Woolhiser and J. Zawodny. 2004. A multi-laboratory evaluation of a common in vitro pepsin digestion assay protocol used in assessing the safety of novel proteins. Regulatory Toxicology and Pharmacology 39:87-98.

Thomas, K., G. Bannon, S. Hefle, C. Herouet, M. Holsapple, G. Ladics, S. MacIntosh and L. Privalle. 2005. In silico methods for evaluating human allergenicity to novel proteins: International Bioinformatics Workshop Meeting Report, 23-24 February 2005. Toxicological Sciences 88:307-310.

Thomas, P., S. Kumari, G.K. Swarna and T.K.S. Gowda. 2007. Papaya shoot tip associated endophytic bacteria isolated from in vitro cultures and host-endophyte interaction in vitro and in vivo. Canadian Journal of Microbiology 53:380-390.

Thompson, C.J., N.R. Movva, R. Tizard, R. Crameri, J.E. Davies, M. Lauwereys and J. Botterman. 1987. Characterization of the herbicide-resistance gene *bar* from *Streptomyces hygroscopicus*. EMBO Journal 6:2519-2523.

Todaro, M., N. Francesca, S. Reale, G. Moschetti, F. Vitale and L. Settanni. 2011. Effect of different salting technologies on the chemical and microbiological characteristics of PDO Pecorino Siciliano cheese. European Food Research and Technology 233:931-940.

Tzin, V., S. Malitsky, M.M.B. Zvi, M. Bedair, L. Sumner, A. Aharoni and G. Galili. 2012. Expression of a bacterial feedback-insensitive 3-deoxy-D-arabino-heptulosonate 7-phosphate synthase of the shikimate pathway in *Arabidopsis* elucidates potential metabolic bottlenecks between primary and secondary metabolism. New Phytologist 194:430-439.

U.S. EPA. 1996. Plant pesticide inert ingredient CP4 enolpyruvylshikimate-3-D and the genetic material necessary for its production in all plants. Federal Register 61:40338-40340.

U.S. EPA. 1997. Phosphinothricin acetyltransferase and the genetic material necessary for its production in all plants; Exemption from the requirement of a tolerance on all raw agricultural commodities. Federal Register 62:17717-17720.

U.S. EPA. 2009. Reregistration eligibility decision for dicamba and associated salts. June 8, 2006, as amended June 17, 2009. U.S. Environmental Protection Agency, Washington, D.C.

U.S. EPA. 2017. 2,4-D; Pesticide tolerances. Federal Register 82:9523-9529.

U.S. EPA. 2018. Quizalofop ethyl; Pesticide tolerances. Federal Register 83:7111-7115.

U.S. FDA. 1995a. AgrEvo BNF No. 23: Oilseed rape: Tolerance to the herbicide glufosinate-ammonium. HCN92. U.S. Food and Drug Administration, Washington, D.C. http://www.accessdata.fda.gov/scripts/fcn/fcnDetailNavigation.cfm?rpt=bioListing&id=8 [Accessed April 2, 2012].

U.S. FDA. 1995b. AgrEvo BNF No. 29: Corn: Tolerance to the herbicide glufosinate-ammonium. T14, T25. U.S. Food and Drug Administration, Washington, D.C. http://www.accessdata.fda.gov/scripts/fcn/fcnDetailNavigation.cfm?rpt=bioListing&id=15 [Accessed April 2, 2012].

U.S. FDA. 1996. Dekalb Genetics BNF No. 28: Corn: Tolerance to the herbicide glufosinate-ammonium. DLL25. U.S. Food and Drug Administration, Washington, D.C. http://www.accessdata.fda.gov/scripts/fcn/fcnDetailNavigation.cfm?rpt=bioListing&id=16 [Accessed April 2, 2012].

U.S. FDA. 1997. AgrEvo BNF No. 46: Canola: Tolerance to the herbicide glufosinate-ammonium. T45. U.S. Food and Drug Administration, Washington, D.C. http://www.accessdata.fda.gov/scripts/fcn/fcnDetailNavigation.cfm?rpt=bioListing&id=30 [Accessed April 2, 2012].

U.S. FDA. 1998a. AgrEvo BNF No. 55: Soybean: Tolerance to the herbicide glufosinate-ammonium. A2704-12, A5547-127. U.S. Food and Drug Administration, Washington, D.C. http://www.accessdata.fda.gov/scripts/fcn/fcnDetailNavigation.cfm?rpt=bioListing&id=38 [Accessed April 2, 2012].

U.S. FDA. 1998b. AgrEvo BNF No. 38: Sugar beet: Tolerance to the herbicide glufosinate-ammonium.   T120-7. http://www.accessdata.fda.gov/scripts/fcn/fcnDetailNavigation.cfm?rpt=bioListing&id=43 [Accessed April 2, 2012].

U.S. FDA. 2000. Aventis BNF No. 63: Rice: Tolerance to the herbicide glufosinate-ammonium. LLRICE E06, LLRICE E62. U.S. Food and Drug Administration, Washington, D.C. http://www.accessdata.fda.gov/scripts/fcn/fcnDetailNavigation.cfm?rpt=bioListing&id=50 [Accessed April 2, 2012].

U.S. FDA. 2003. Bayer CropScience BNF No. 86: Cotton: Tolerance to the herbicide glufosinate-ammonium. LLCotton25. U.S. Food and Drug Administration, Washington, D.C. http://www.accessdata.fda.gov/scripts/fcn/fcnDetailNavigation.cfm?rpt=bioListing&id=56 [Accessed April 2, 2012].

USDA-NASS. 2014. 2012 Census of Agriculture: United States Summary and State Data. U.S. Department of Agriculture, National Agricultural Statistics Service, Washington, D.C. http://www.nass.usda.gov/Publications/AgCensus/2012 [Accessed March 18, 2018].

Varman, A.M., L. He, R. Follenfant, W. Wu, S. Wemmer, S.A. Wrobel, Y.J. Tang and S. Singh. 2016. Decoding how a soil bacterium extracts building blocks and metabolic energy from ligninolysis provides road map for lignin valorization. Proceedings of the National Academy of Sciences of the United States of America 113:pE5802-pE5811.

Vassilopoulou, E., N. Rigby, F.J. Moreno, L. Zuidmeer, J. Akkerdaas, I. Tassios, N.G. Papadopoulos, P. Saxoni-Papageorgiou, R. van Ree and C. Mills. 2006. Effect of *in vitro* gastric and duodenal digestion on the allergenicity of grape lipid transfer protein. Journal of Allergy and Clinical Immunology 118:473-480.

Venkatesh, T.V., M.L. Breeze, K. Liu, G.G. Harrigan and A.H. Culler. 2014. Compositional analysis of grain and forage from MON 87427, an inducible male sterile and tissue selective glyphosate-tolerant maize product for hybrid seed production. Journal of Agricultural and Food Chemistry 62:1964-1973.

Vieths, S., J. Reindl, U. Müller, A. Hoffmann and D. Haustein. 1999. Digestibility of peanut and hazelnut allergens investigated by a simple in vitro procedure. European Food Research and Technology 209:379-388.

Waksman, S.A. and A.T. Henrici. 1943. The nomenclature and classification of the actinomycetes. Journal of Bacteriology 46:337-341.

Wang, C., K.C. Glenn, C. Kessenich, E. Bell, L.A. Burzio, M.S. Koch, B. Li and A. Silvanovich. 2016. Safety assessment of dicamba mono-oxygenases that confer dicamba tolerance to various crops. Regulatory Toxicology and Pharmacology 81:171-182.

Wang, X.-Z., B. Li, P.L. Herman and D.P. Weeks. 1997. A three-component enzyme system catalyzes the O demethylation of the herbicide dicamba in *Pseudomonas maltophilia* DI-6. Applied and Environmental Microbiology 63:1623-1626.

Watson, S.A. 1988. Corn marketing, processing, and utilization. Pages 881-940 in Corn and Corn Improvement. Third Edition. G.F. Sprague and J.W. Dudley (eds.). American Society of Agronomy, Inc., Crop Science Society of America, Inc., Soil Science Society of America, Inc., Madison, Wisconsin.

Wehrmann, A., A.V. Vliet, C. Opsomer, J. Botterman and A. Schulz. 1996. The similarities of *bar* and *pat* gene products make them equally applicable for plant engineers. Nature Biotechnology 14:1274-1278.

Werlen, C., H.-P.E. Kohler and J.R. van der Meer. 1996. The broad substrate chlorobenzene dioxygenase and *cis*-chlorobenzene dihydrodiol dehydrogenase of *Pseudomonas* sp. strain P51 are linked evolutionarily to the enzymes for benzene and toluene degradation. Journal of Biological Chemistry 271:4009-4016.

Wild, A. and R. Manderscheid. 1984. The effect of phosphinothricin on the assimilation of ammonia in plants. Zeitschrift für Naturforschung C 39:500-504.

Wishart, D.S. 2010. Human metabolome database. www.hmdb.ca [Accessed June 2, 2010].

Wishart, D.S., C. Knox, A.C. Guo, R. Eisner, N. Young, B. Gautam, D.D. Hau, N. Psychogios, E. Dong, S. Bouatra, R. Mandal, I. Sinelnikov, J. Xia, L. Jia, J.A. Cruz, E. Lim, C.A. Sobsey, S. Shrivastava, P. Huang, P. Liu, L. Fang, J. Peng, R. Fradette, D. Cheng, D. Tzur, M. Clements, A. Lewis, A. De Souza, A. Zuniga, M. Dawe, Y. Xiong, D. Clive, R. Greiner, A. Nazyrova, R. Shaykhutdinov, L. Li, H.J. Vogel and I. Forsythe. 2009. HMDB: A knowledgebase for the human metabolome. Nucleic Acids Research 37:D603-D610.

Wohlleben, W., W. Arnold, I. Broer, D. Hillemann, E. Strauch and A. Pühler. 1988. Nucleotide sequence of the phosphinothricin *N*-acetyltransferase gene from *Streptomyces viridochromogenes* Tü494 and its expression in *Nicotiana tabacum*. Gene 70:25-37.

Yagami, T., Y. Haishima, A. Nakamura, H. Osuna and Z. Ikezawa. 2000. Digestibility of allergens extracted from natural rubber latex and vegetable foods. Journal of Allergy and Clinical Immunology 106:752-762.

Yang, H., Y. Qi, M.E. Goley, J. Huang, S. Ivashuta, Y. Zhang, O.C. Sparks, J. Ma, B.M. van Scoyoc, A.L. Caruano-Yzermans, J. King-Sitzes, X. Li, A. Pan, M.A. Stoecker, B.E. Wiggins and M.J. Varagona. 2018. Endogenous tassel-specific small RNAs-mediated RNA interference enables a novel glyphosate-inducible male sterility system for commercial production of hybrid seed in *Zea mays* L. PLoS ONE 13:e0202921.

Zambryski, P., A. Depicker, K. Kruger and H.M. Goodman. 1982. Tumor induction by *Agrobacterium tumefaciens*: Analysis of the boundaries of T-DNA. Journal of Molecular and Applied Genetics 1:361-370.

Zhou, J., G.G. Harrigan, K.H. Berman, E.G. Webb, T.H. Klusmeyer and M.A. Nemeth. 2011. Stability in the composition equivalence of grain from insect-protected maize and seed from glyphosate-tolerant soybean to conventional counterparts over multiple seasons, locations, and breeding germplasms. Journal of Agricultural and Food Chemistry 59:8822-8828.

Zipper, C., K. Nickel, W. Angst and H.-P.E. Kohler. 1996. Complete microbial degradation of both enantiomers of the chiral herbicide mecoprop [(RS)-2-(4-chloro-2-methylphenoxy)propionic acid] in an enantioselective manner by *Sphingomonas herbicidovorans* sp. nov. Applied and Environmental Microbiology 62:4318-4322.